Molecular asymmetries governing the nuclear positioning in the oocyte of Drosophila melanogaster

Maëlys Loh

Université Paris Cité
École doctorale Bio Sorbonne Paris Cité (BioSPC, ED562)

Institut Jacques Monod, UMR 7592
Equipe Polarité et Morphogenèse

Molecular asymmetries governing the nuclear positioning in the oocyte of *Drosophila melanogaster*

Présentée par **Maëlys LOH**

Thèse de Doctorat en Développement

Dirigée par Antoine GUICHET
Présentée et soutenue publiquement à Paris, le 25 Janvier 2023

Composition du jury de thèse:

Alexandre BAFFET CR, Institut Curie, Paris, Université PSL	Rapporteur
Marie-Emilie TERRET DR, Collège de France, Paris, Université PSL	Rapporteur
Susana GODINHO Group leader, PhD, Barts Cancer Institute, London	Examinateur
Anne-Marie PRET PU, I2BC, Université de Versailles Saint-Quentin-en-Yvelines	Examinateur
Antoine GUICHET DR, Institut Jacques Monod, Paris, Université Paris Cité	Directeur de thèse
Fred BERNARD MCU, HDR, Institut Jacques Monod, Paris, Université Paris Cité	Membre invité

ABSTRACT

Cellular polarity establishment requires symmetry-breaking events. The oocyte of *Drosophila melanogaster* is a fitting model to study nuclear positioning and molecular asymmetries. During oogenesis, the nucleus migrates within the oocyte to adopt an asymmetrical position. In contact with the adjacent follicular cells of the egg chamber, the correct localization of the nucleus and the associated mRNA, *gurken*, induces local translation of the protein and subsequent establishment of oocyte dorso-ventral axis. Two actors have been identified in the regulation of microtubule-dependent nuclear migration: the centrosomes and the protein Mud. The aim of this project was to better characterize and understand the mechanisms by which Mud and the centrosomes regulate trajectories of the nucleus during its displacement. These players display asymmetrical and dynamic distributions along oogenesis, and regulate two distinct nuclear routes. During my PhD, using microscopy techniques and genetic tools that allow *in vivo* imaging, I investigated the close relationship between the centrosomes and the nucleus in the *Drosophila* oocyte, and discovered a mechanism dependent on Kinesin-1 which affects both centrosome behavior and nucleus positioning. Moreover, I studied the patterning of Mud asymmetrical nuclear localization and its importance in nuclear migration regulation. We identified two nuclear localization sequences for Mud and showed the requirement of Importin-β/Fs(2)Ket for its nuclear localization.

Key words: Cellular biology, Drosophila, oocyte, nucleus positioning, nuclear migration, centrosomes, Mud, Kinesin-1.

RÉSUMÉ

La mise en place de la polarité cellulaire requiert des évènements de brisure de symétrie. L'ovocyte de *Drosophila melanogaster* est un modèle extrêmement puissant dans l'étude de l'établissement d'asymétrie moléculaire et notamment du positionnement nucléaire. Au cours de l'ovogenèse, le noyau migre afin d'adopter une position asymétrique au sein de l'ovocyte. En contact avec les cellules folliculaires adjacentes au follicule ovarien, le localisation correcte du noyau et de l'ARNm *gurken* associé induit la traduction locale de la protéine et la mise en place subséquente de l'axe dorso-ventral de l'ovocyte. Deux acteurs régulant cette migration nucléaire, dépendante des microtubules, ont été identifiés: les centrosomes et la protéine Mud. Ce travail de thèse a pour but d'appréhender et caractériser les mécanismes moléculaires par lesquels Mud et les centrosomes régulent les trajectoires du noyau au cours de son déplacement. Tous les deux ont la particularité d'être distribués de manière asymétrique et dynamique au cours de l'ovogenèse. Au cours de ces recherches, par des approches de microscopie reposant sur l'utilisation d'outils génétiques qui permettent l'imagerie *in vivo*, je me suis intéressée à la relation qui s'exerce entre les centrosomes et le noyau de l'ovocyte chez la drosophile, et nous avons mis en évidence un mécanisme dépendant de la Kinésine-1 qui affecte le comportement des centrosomes ainsi que la position du noyau. De plus, j'ai étudié la mise en place de la distribution asymétrique de Mud à l'enveloppe nucléaire par une analyse structure/fonction, ainsi que son importance dans la régulation de la trajectoire du noyau au cours de l'ovogenèse. Nous avons identifié deux séquences de localisation nucléaire pour Mud et montré que l'Importin-β/Fs(2)Ket était requise pour sa localisation nucléaire.

Titre : Asymétries moléculaires régissant le positionnement du noyau de l'ovocyte chez *Drosophila melanogaster*

Mots-clés: Biologie cellulaire, Drosophile, ovocyte, positionnement nucléaire, migration nucléaire, centrosomes, Mud, Kinésine-1.

RÉSUMÉ SUBSTANTIEL EN FRANÇAIS

La polarité cellulaire est une caractéristique fondamentale des cellules eucaryotes. Elle gouverne l'intégrité et la fonction de la cellule qui s'intègre dans un tissu en favorisant des processus migratoires, de différenciation et de développement. Typiquement, le positionnement du noyau au sein de la cellule est extrêmement régulé, notamment parce qu'il positionne le matériel génétique en amont de la division cellulaire, comme c'est observé dans les neurones par exemple. En effet, la migration intercinétique des noyaux des progéniteurs neuronaux est un évènement en deux temps qui requiert le moteur Dynéine d'une part, et le moteur Kinésine d'autre part (Hu et al., 2013). Egalement, au cours du développement des muscles striés squelettiques, les noyaux des myotubes migrent du centre de la cellule vers la périphérie afin d'assurer la fonction du muscle (Cadot et al., 2015). Des défauts de positionnement nucléaires sont souvent associés à des pathologies, telles que les myopathies, lissencéphalies, cardiomyopathies (Gundersen and Worman, 2013).

Au cours de l'ovogenèse chez *Drosophila melanogaster*, le noyau de l'ovocyte adopte une positon asymétrique au sein de la cellule, résultant en la mise en place de l'axe de polarité dorso-ventral. La particularité du développement chez la mouche réside en partie dans l'établissement des axes de polarité au cours de l'ovogenèse et non pas au moment de l'embryogenèse, comme c'est le cas dans la majorité des espèces. De ce fait, l'inhibition du mouvement nucléaire est létal pour l'embryon. La mouche du vinaigre possède une paire d'ovaires, chacun constitué d'une vingtaine d'ovarioles. Les ovarioles peuvent être décrites comme des suites longilignes de follicule ovariens à différents stades de maturation qui se développent le long d'un axe antéro-postérieur. Ainsi, le germarium à l'extrémité antérieure, par opposition au vitellarium qui s'étend du germarium jusqu'à l'extrémité postérieure de l'ovariole, abrite les cellules souches folliculaires. La division asymétrique de ces cellules génère une cellule souche fille qui maintient le stock de cellules souches, et une cellule qui se différencie et est nommée le cystoblaste. Cette cellule effectue 4 mitoses incomplètes, dépourvues de cytokinèse, pour former le cyste. Le cyste se compose alors de 16 cellules germinales interconnectées par des ponts cytoplasmiques faits d'actine, nommés canaux annulaires. Par l'accumulation d'organelles et de facteurs protéiques, l'une de ces 16 cellules se différencie et devient dès lors l'ovocyte, tandis que les 15 cellules restantes deviennent les cellules nourricières du gamète femelle et veillent à lui fournir tous les nutriments et ARNm nécessaires à sa croissance. A l'extrémité postérieure du germarium, le cyste est recouvert d'une couche de cellules somatiques folliculaires, formant ainsi le follicule ovarien. Le follicule ovarien poursuit sa croissance dans le vitellarium, et subit de nombreuses étapes de développement avant d'aboutir au gamète femelle prêt à être fécondé par le spermatozoïde. Historiquement, l'ovogenèse a été catégorisée en 14 stades de développement (King et al., 1956). Au milieu de l'ovogenèse, au stade 6, le noyau de l'ovocyte migre pour passer d'une position centrale à une position asymétrique au stade 7. En effet, au stade 7, le noyau atteint le cortex antéro-latéral qui correspond aux intersections des membranes plasmiques antérieures et latérales.

A cet endroit spécifique, où il est en contact avec les cellules folliculaires adjacentes, le noyau apporte l'ARNm *gurken*, dont la traduction locale induit la signalisation de Gurken, homologue du TGF-α (Transforming Growth Factor α) via le récepteur EGFR (Epidermal Growth Factor Receptor) exprimé à la surface des cellules somatiques. Cette signalisation, médiée par Gurken, induit la dorsalisation des cellules adjacentes. En l'absence de cette signalisation, les cellules opposées empruntent un destin ventral par défaut. Ainsi, l'axe dorso-ventral est mis en place. La migration du noyau de l'ovocyte est un événement dépendant des microtubules (Koch and Spitzer, 1983). En effet, l'utilisation de drogue dépolymérisante des microtubules, telle que la Colchicine ou son dérivé Colcémide, abolit le mouvement du noyau qui maintient une position centrale dans la cellule. L'ovocyte de la mouche du vinaigre comprend trois sous-réseaux de microtubules nucléés à partir des centrosomes, de l'enveloppe nucléaire, et de la membrane plasmique. Cet ovocyte comporte 16 à 32 centrosomes qui se regroupent au postérieur de la cellule entre le noyau et la membrane plasmique. Au début de l'ovogenèse, les 16 cellules germinales sont en prophase I de méiose et ont alors dupliqué leurs centrioles. Chaque cellule possède donc deux centrosomes. Les centrosomes des cellules nourricières migrent et s'accumulent dans l'ovocyte, ce qui contribue notamment à sa spécification. Au cours de la migration du noyau de l'ovocyte, il a été montré que les microtubules exercent principalement des forces de poussée sur le noyau (Zhao et al., 2012). De plus, le laboratoire a mis en évidence qu'au cours de sa migration, le noyau pouvait emprunter trois trajectoires différentes: une trajectoire longeant la membrane plasmique antérieure de l'ovocyte, une trajectoire longeant la membrane postérieure, et une trajectoire cytoplasmique s'effectuant sans contact au cours du mouvement (Tissot et al., 2017). Des analyses génétiques combinées à la mise au point de microscopie « live imaging » révèlent que les centrosomes et la protéine associée aux microtubules Mud régulent respectivement les voies antérieure et postérieure. De plus, la protéine Mud a la particularité d'être distribuée de manière asymétrique autour du noyau de l'ovocyte, avec un enrichissement sur l'hémisphère nucléaire faisant face à la membrane plasmique postérieure. De manière intéressante, la nucléation de microtubules associée à l'enveloppe nucléaire de l'ovocyte est également asymétrique et enrichie sur le même hémisphère que la protéine Mud.

L'objectif de cette thèse est donc de comprendre par quels mécanismes moléculaires les centrosomes et Mud régulent les trajectoires de migration du noyau de l'ovocyte au cours de l'ovogenèse chez la drosophile. Ce travail m'a permis de redéfinir les critères de sélection et d'identification des stades de l'ovogenèse étudiés, et en particulier ceux qui précèdent la migration du noyau de l'ovocyte. Ainsi, sur la base de l'aspect ratio du follicule ovarien, de la morphologie de l'ovocyte, et du diamètre des cellules nourricières adjacentes à l'ovocyte, j'ai caractérisé les stades 5, 6A, 6B, et 7, et mis en évidence qu'un positionnement nucléaire spécifique était associé à chacun de ces stades. De ce fait, le noyau est positionné à l'antérieur au stade 5 et 6A, en contact avec la membrane plasmique antérieure de l'ovocyte. L'ovocyte, quant à lui, s'arrondit de plus en plus du stade 5 au stade 6A. Au stade 6B, qui précède la migration nucléaire, le noyau est centré dans un ovocyte de forme ovale. Au stade 7, le noyau a migré et a atteint le cortex antéro-latéral où il est en contact avec les cellules folliculaires adjacentes.

De manière concomitante au centrage du noyau au stade 6B, les centrosomes de l'ovocyte s'agrègent entre eux. Dans la plupart des espèces, les centrosomes sont transmis à la descendance par le père. De ce fait, les centrosomes du gamète femelle sont généralement dégradés avant la fécondation et les premières divisions du zygote. Chez la *Drosophile*, les centrosomes sont progressivement inactivés jusqu'à leur désintégration totale avant la fin de l'ovogenèse (Pimenta-Marques et al., 2016). Le laboratoire a mis en évidence que les centrosomes étaient actifs pendant la migration nucléaire, qu'ils restaient groupés et suivaient le mouvement du noyau (Tissot et al., 2017). A partir des ces résultats, nous avons émis l'hypothèse que les centrosomes pouvaient voir leur activité diminuer dès le stade 6B, où ils sont regroupés de manière similaire à des stades plus tardifs. L'utilisation d'une souche transgénique de drosophile, surexprimant la kinase Polo/PLK1 adressée aux centrosomes de l'ovocyte et qui maintient les centrosomes dans un état actif (Pimenta-Marques et al., 2016), induit un défaut de regroupement des centrosomes au stade 6B ainsi qu'un défaut de migration nucléaire au stade 7. Ce résultat permet donc d'établir un lien entre l'activité et le regroupement des centrosomes, de telle sorte que des centrosomes espacés entre eux correspondent à des centrosomes actifs.

De plus, nous avons mis en évidence le rôle de la Kinésine-1 dans le regroupement des centrosomes, affectant également le positionnement nucléaire avant la migration, ainsi que la migration du noyau de l'ovocyte même. Nos résultats montrent en effet que la chaîne lourde de la Kinésine (Khc) est nécessaire pour ces mécanismes, tandis que l'effet de la délétion de la chaîne légère (Klc) est compensé plus tard dans l'ovogenèse, sauvant ainsi le positionnement asymétrique du noyau dans l'ovocyte et l'établissement de l'axe dorso-ventral. Par l'inactivation des centrosomes, nous avons pu rétablir la migration du noyau dans les contextes Khc-délétés. Ce résultat suggère la nécessité d'une régulation très fine de la balance des forces exercées par les microtubules sur le noyau. Une hypothèse pouvant expliquer le rôle de la Kinésine-1 sur le regroupement des centrosomes viendrait de sa capacité à organiser les microtubules anti-parallèles en faisceaux et ainsi les rapprocher en les faisant coulisser les uns par rapport aux autres. En effet, j'ai montré que Khc localise à la fois autour du noyau de l'ovocyte et aux centrosomes. La délétion du domaine d'interaction avec les microtubules responsable de ce mécanisme de coulissement des microtubules de la Kinésine-1 (k*hc*^{mutA}) montre un défaut de positionnement nucléaire au stade 7. Ce résultat indique que le rôle de Khc dans le positionnement du noyau de l'ovocyte de *Drosophile* implique sa fonction de coulissement des microtubules afin de les organiser et pourrait expliquer en partie le regroupement des centrosomes. Une autre hypothèse serait que Kinésine-1, par sa fonction cargo, participe au désassemblage des centrosomes et notamment des composants de la matrice péricentriolaire qui assurent l'activité de ces derniers. Le moteur pourrait alors transloquer ces protéines centriolaires des centrosomes vers d'autres centres organisateurs de microtubules acentrosomaux, à savoir: l'enveloppe nucléaire et la membrane plasmique. Ainsi, j'ai pu montrer que Khc affectait particulièrement Asterless, qui est impliquée dans le recrutement des autres protéines de la matrice péricentriolaire.

Enfin, je me suis intéressée à déterminer le rôle de la protéine Mud dans la régulation de la migration du noyau de l'ovocyte chez la *Drosophile*. Mud (Mushroom body Defect) est l'homologue de NuMA (Nuclear Mitotic Apparatus) chez les vertébrés et Lin-5 chez *C. elegans.* Ces protéines sont connues pour leur rôle dans l'orientation des fuseaux mitotiques et méiotiques au cours des divisions cellulaires et dans le rassemblement des bouts moins des microtubules. A l'interphase, NuMA est détectée au noyau de la cellule, où elle y est séquestrée afin de ne pas interférer avec le réseau de microtubules, mais également dans un but stratégique de la maintenir au plus proche du matériel génétique à la rupture de l'enveloppe nucléaire pour l'organisation du faisceau (Kiyomitsu and Boerner, 2021). Après l'identification de deux séquences de localisation nucléaire par des analyses *in silico*, j'ai pu confirmer l'interaction entre Mud et l'Importine-β/Fs(2)Ket ainsi qu'avec la nucléporine Nup358/RanBP2 dans l'ovocyte de la *Drosophile*. Nos résultats montrent que la localisation de Mud à l'enveloppe nucléaire dans l'ovocyte est dépendante de Fs(2)Ket. Une analyse structure/fonction révèle que l'asymétrie de Mud n'est pas dépendante des microtubules, et qu'elle n'est pas nécessaire dans la régulation des trajectoires du noyau de l'ovocyte par Mud. La délétion des domaines putatifs de localisation nucléaire induit une délocalisation périnucléaire de Mud vers les centrosomes. Ces résultats montrent que ces domaines sont impliqués dans la restriction de Mud à l'enveloppe nucléaire.

ACKNOWLEDGMENTS

Il me parait étrange de manquer soudainement de mots alors que j'entame la rédaction de ces remerciements qui me sont pourtant si chers. Dans les quelques pages précédant ses découvertes éclairées d'Astrophysique, mon frère m'écrivait en 2016: « Je te souhaite tout le meilleur pour ta prometteuse carrière en biologie et te souhaite également d'être aussi bien entourée que moi pour franchir toutes les étapes à venir […]. ». Le sens et la portée de ces mots me paraissent bien différents aujourd'hui qu'à lors de leur première lecture il y a six ans. Il me semble difficile de retranscrire la gratitude que j'éprouve désormais autant à l'égard des chercheurs qui ont façonné mon parcours et que j'admire pour leur dévotion scientifique, que pour mon entourage sans qui l'aboutissement de cette thèse n'aurait pas été possible. C'est donc avec beaucoup d'émotions et d'humilité que je souhaite ici remercier toutes les personnes qui m'ont accompagnée et soutenue tout au long de cette aventure.

First, I would like to sincerely thank the members of my PhD jury, who honor me for having accepted to judge and discuss this work, but also for their availability and benevolence. Thank you to Marie-Emilie Terret, Alexandre Baffet, Susana Godinho, and Anne-Marie Pret.

Je remercie Michel Werner, Géraldine Thouvay et Eric Valdenaire, pour leur disponibilité, aide et enthousiasme, et pour avoir fait de l'Institut un lieu si accueillant pour y réaliser sa thèse. Merci à Martine Malet et Sylvie Boulet, pour votre aide précieuse et si efficace. Merci à Norry Baouz et Jonathan Lopez Arnaiz de faciliter nos expériences et d'avoir rendu les visites au magasin si joyeuses. Merci à la plateforme de protéomique de l'Institut Jacques Monod, ainsi qu'à la plateforme d'imagerie et en particulier à Xavier Baudin, Nicolas Moisan, Vincent Contremoulins, et Paul Lambert, pour votre aide et patience. Merci à Rosine Haguenauer-Tsapis de m'avoir fait découvrir les Apprentis-Chercheurs et de nous avoir accompagnés pendant ces quelques mois.

Je remercie l'équipe de Yohanns Bellaiche pour les mouches transgéniques Mud. Merci à la Société Française de Génétique de m'avoir récompensée d'un prix qui m'a permis d'assister au symposium Microtubules à l'EMBL, Heidelberg. Merci à Gilliane Maton, Isabelle Becam, Eulalie Buffin, et Clément Carré de m'avoir aidée dans la préparation du concours de l'Ecole Doctorale et en particulier à Clément pour nous avoir recommandé cet appartement de thésards !

J'en viens aux remerciements destinés à mes directeurs de thèse Fred Bernard et Antoine Guichet. Antoine, merci de m'avoir accueillie chaleureusement dans ton équipe il y a quatre ans, de ta disponibilité quotidienne pour parler des observations les plus fraîches comme des articles les plus lointains, de ton éternel enthousiasme scientifique pour les expériences et les conférences, de ta confiance et ton écoute, mais aussi pour ton humour. J'espère avoir réussi à apporter une petite part de connaissance à ce système auquel tu es si dévoué. Fred, merci de m'avoir confié ce projet que j'ai tant considéré comme ma plus grande responsabilité et que je te remets aujourd'hui, non sans difficulté émotive. Merci de ton incroyable investissement au cours du stage de M2 et pour la liberté que tu m'as ensuite accordée pendant ces années de thèse. Merci de tes relectures pertinentes, de ta vue aiguisée lors de l'alignement des figures, et de ta disponibilité malgré toutes tes autres responsabilités. J'espère que ces souvenirs de premier encadrement de thésard te resteront positifs.

Un grand merci aux membres de mon équipe. À Véronique Brodu, merci pour ton soutien scientifique et émotionnel, pour ton aide bibliographique et moléculaire, pour tes encouragements répétés, ta disponibilité, ainsi que ton attention bienveillante et parfois chocolatée. À Jean-Antoine Lepesant, merci pour ces discussions enrichissantes scientifiques ou philosophiques, mais aussi pour ton humour et ta répartie qui ont nourri les moments les plus plaisants dans la pièce à mouches, et enfin pour tes conseils professionnels comme agricoles. À Sandra Claret, merci pour toutes ces questions-réponses derrière nos ordis, tes suggestions, ton écoute, ton humour salvateur et le partage de ta créativité scientifique et décoratrice. Merci d'avoir à maintes reprises, tenté de susciter, à mes côtés, l'enthousiasme et l'optimisme de Fred pour les résultats les plus prometteurs, et de ton éternelle bonne humeur. À Sylvain Brun, merci pour tes suggestions et encouragements. À Fanny Roland-Gosselin, merci pour ton soutien à l'Institut comme en dehors, de m'avoir fait quitter les pauses déjeuners/analyses pour des pauses plus champêtres et ensoleillées, d'avoir mis des confettis dans les claviers d'ordinateurs et dans ma tête lorsque les journées manquaient de couleurs, pour le partage de nombreuses pintes de café, de recettes et de session décoration d'intérieur. Il me reste à dégoter le trophée du thésard à te remettre, que tu sauras brillamment honorer j'en suis sûre. À Sandra Carvalho, merci pour ton soutien et ta gentillesse constante, pour ces discussions tardives encourageantes, et ces délicieuses chouquettes qui m'ont aidée à finir les manips qui n'en finissaient plus. Ça a été un vrai plaisir de te voir réussir, et de voir que tu fais déjà une merveilleuse thésarde, je te souhaite le meilleur pour ces années si importantes au sein du labo. Merci à tous les stagiaires qui ont fait partie de l'équipe et qui ont vivifié mes journées, notamment merci à Maxime Klein d'avoir mis du baume dans mon coeur et de la musique dans mes oreilles, à Axel Gosseye, à Fanny Wodrascka, à Lola Wargnier d'avoir été si enthousiaste pendant les quelques jours passés à nos côtés. Un merci spécial est réservé à Déborah Dauvet avec qui j'ai découvert les drosophiles et l'horreur de leur génétique, mais aussi avec qui j'ai passé un merveilleux stage et début de thèse. Un merci méditerranéen et à l'huile d'olive est adressé à Flora Ambroise, ultime stagiaire de l'équipe, dont l'humilité, le sérieux et la générosité ont inspiré de fabuleux moments. Merci pour toutes ces sessions enflammées et explosives dans la pièce à mouches, ces danses et dialogues exotiques partagés dans le bureau, et tes sourires qui à eux-seuls ensoleillaient mes journées. Merci à mes propres stagiaires, à Nicolas Glonti, à Thierry Tran pour ta persévérance, ta reconnaissance et ton enthousiasme qui m'ont fait adorer l'expérience d'Apprentis Chercheurs, je te souhaite le meilleur pour tes études brillantes, et à Amaury Beuzelin pour ton intérêt et ta curiosité, je te souhaite de pouvoir un jour, à ton tour, encadrer un étudiant au cours de ta propre thèse ! Merci à Amina Zemouri de m'avoir accueillie et accompagnée dans mes débuts à l'Institut, pour tes conseils, et ces derniers moments d'analyse sur fond sonore d'Epica. Merci à Alain Debec, camarade de bureau regretté autant pour les pauses déjeuners animées que pour les partages d'acquisitions fluorescentes. Merci d'avoir égaillé mes journées par la démonstration d'arts martiaux contraints, ou par tes photos ensoleillées. Enfin, je dois un long merci à l'ensemble des membres de cette équipe pour avoir toléré mon craquage émotionnel sur la porte commune 428B, qui s'est étendu sur mon bureau et celui de Fanny avec l'arrivée du Sapin fin Janvier 2022, et jusque dans les couloirs avec les anniversaires de Flora.

Je tiens ensuite à remercier mon labo d'adoption et tous les membres de l'équipe Pintard. Merci tout d'abord à Lionel Pintard, pour ton investissement dans mon comité de thèse, ton écoute, ta disponibilité et tes précieux conseils. Merci à Nicolas Joly, pour ces discussions tardives aussi honnêtes que rassurantes qui m'ont beaucoup donné à réfléchir, et puis pour cette lame en acier qui a aidé de nombreuses sessions live. Merci à Batool Ossareh-Nazari, Lucie Van Hove, Ludivine Roumbo, Anaïs Pillan, Philippine Ormancey, et Griselda Velez Aguilera, pour votre gentillesse et soutien. Enfin, un merci tout particulier à Eva Beaumale et Sylvia Nkombo Nkoula, tout d'abord pour avoir gardé votre calme lorsque je suis arrivée en M2 en pensant que mes sessions au Spinning étaient plus importantes que tout autre activité dans le monde, et ensuite pour votre sincère amitié et soutien tout au long de ma thèse. Merci d'avoir toujours été présentes dans les épisodes joyeux, mais aussi dans les moins drôles, et pour tous vos conseils.

I would like to thank Paul Conduit, for the investment you put into your role as my PhD committee member, your suggestions for the project but also for your refreshing vision of research in general, thank you for your kindness and your benevolence, and for having introduced me to Susana in Heidelberg.

Merci à Manon Monier, pour ton amitié, ton soutien et ta bonne humeur permanente. Merci pour toutes ces discussions joyeuses ou malheureuses qui m'ont apporté beaucoup de soleil dans les couloirs du 4ème. Merci à Bénédicte Lefevre, pour ta présence qui semblait déjà si familière lorsque je suis arrivée, ton honnêteté et ta bonne humeur constante, merci à toi et à Amélie pour votre affection et soutien. Merci à Lina-Marie Briu pour ta douce et chaleureuse bienveillance malgré les deux étages qui nous éloignent. À Chrystelle Maric-Antoinat, pour ta bonne humeur contagieuse et tes encouragements depuis le M2. Merci à Akila Merah pour ta chaleur, ton honnêteté et ton aide très appréciée. J'espère que nous aurons de nouvelles occasions de trinquer avec une bière allemande en l'hommage de tes talents de photographe. Thank you to Adria Chorro and Konstantina Filippopoulou for your support. Merci à Aurélien Perrier pour les pauses cafés que nous n'aurons jamais réussi à prendre, et pour les samedis escalades et triathlon que je ne pourrai jamais suivre, mais surtout merci pour tes chaleureux encouragements. Merci à Mélanie Aubry, à Layla El-Mossadeq, et à Thadshagine Ganeswaran pour les regards encourageants et les sourires compatissants à chaque croisements dans les couloirs. Merci à Tien Nguyen pour ta bienveillance, ton empathie et ta générosité. Thank you to Lakshmi Balasubramaniam and Surabhi Sonam, for your warm welcome when I arrived in the institute, your advice, and all the lunch breaks complaining about the Spinning. Merci à Charlou-tout-doux, appelé aussi Charles Le Ciclé, camarade bien-pensant de déjeuners frisquets ou de pauses humoristiques requinquantes. Merci pour tes salutations revigorantes et pour ton aide sérieuse à avoir extrait Fanny du labo plus d'une fois ! À Carine Auguste, merci pour toutes ces émotions et pour avoir ensoleillé la laverie et nos coeurs. À Téo Bitaille, merci pour ton aide et ta compréhension, mais aussi pour ton humour unique. À Clarisse Picard, merci pour ta gentillesse et ton aide ces derniers mois. Et finalement, merci à Jean-Louis Babibel, Christophe, Clothilde, Guillaume, Hubert, Camille, Christian, Patrick, Murielle, et à l'occasion Vincent Maupu, pour la variété de nos discussions faites de philosophie pétillante, de réflexions apocalyptiques, ou encore de décoration d'intérieur, bien éloignées de la vie du labo mais qui m'ont aidée à surmonter avec plus de légèreté ces derniers mois de thèse.

Je veux maintenant remercier mes proches, sans qui je n'aurais pu espérer écrire ces mots.
Un énième merci à Arthur Charles-Orszag, qui a joué un rôle déterminant tout au long de mon cursus universitaire depuis les tous premiers TP passionnants de biologie cellulaire en L1, suivis de ce premier stage si enrichissant à l'Institut Pasteur dans l'équipe de Guillaume Duménil où tu m'as fait découvrir les joies de la culture cellulaire et du microscope confocal spinning disk. Merci de m'avoir fait rêver du Master BDC, de l'expérience de la thèse, et du monde de la recherche, de ton enthousiasme et ta passion communicative, et d'être toujours présent depuis. Merci à Guillaume, Daria Bonazzi, Paul Kennouche, Sylvie Goussard, Pierre Nivoit, Jean-Philippe Corre, Hebert Echenique-Rivera, et Valeria Manriquez d'avoir rendu ce stage si riche.
Ce qui m'amène à remercier mes compagnons de route d'Orsay où j'ai réalisé mon stage de M1 dans l'équipe de Jacques Ghysdael, sous l'encadrement de Christine Tran Quang. Un grand merci à Benedetta Zaniboni, Kanokporn Faguier, Chiara Giudiceandrea, Romain Humeau, et Grégoire Huré pour toute votre aide et votre soutien. Un tendre merci à ma Caro pour m'avoir accueillie dans la plus joyeuse des maisons pendant ce stage à Orsay, de m'avoir aidée à renfort de saucisson à la noisette, de fondants au chocolat et de cafés à la belle étoile, et ensuite de ton amitié et de ton soutien pendant ces années de thèse. J'en viens à remercier mes colloques extraordinaires, Mahaut, Pauline, Mado, Vicky et en particulier à Anaïs, Delphine et Aurélie.
Un chaleureux merci à Maeva Vallucci, pour m'avoir guidée dès le lycée vers la Biologie, pour tous tes généreux conseils et réponses apportées, tes encouragements bienveillants et ton amitié sincère et constante.
Un merci plein d'amour à mes compagnons chéris, Leya Ghostine, Samuel Olivier, et Johan Ludot, avec qui j'ai vécu les premières heures palpitantes sur les bancs de Paris Diderot, découvert l'horreur de la thermodynamique et l'enzymologie, et avec qui je partage aujourd'hui les plus tendres apéros. Les mots me manquent pour vous dire ma gratitude pour votre soutien et votre amitié qui m'est si précieuse. Merci à Clayre Grumiaux, Sujith Sritharan, et Sebastian Castro de compléter cette joyeuse troupe.
Un merci plein d'affection à mes chers amis de L3, collègues des TP les plus mémorables, partenaires de sorties inoubliables ou presque, et depuis toujours membres actifs du comité de recueil d'excuses de Ruru, merci à Julie Lopes, Anjoline Tran, Dr. Juliette Dochez-Arnault, Ruben Laskar, Célia Tendero, Céline Pereira, Laura Saban, Margot Mureau, Nataël Sorel, et Déborah Neto.
Un merci à l'absinthe, au martini, et à la framboise à Mathilde DiMarco (et Ian Debeerst), Morgane Djebar, Barbara Trifault et Ismahan Abdirizak, pour votre présence si importante, le partage rassurant des expériences ratées, des CSI, des conférences, et des discussions terrifiantes d'après-thèse. Je nous souhaite le meilleur, plein de voyages, une multitude de concerts de Ian autour de bols de frites tardifs et plus festifs.
Un merci affectueux à Pierrette Bourduge, pour ton attention si précieuse depuis bientôt 20 ans, doublée de tes encouragements aimants.
A Simone et Suzanne Deschamps, à qui j'avais promis « les bulles » pour vous remercier de m'avoir toujours accompagnée, de la maternelle jusqu'à ma troisième année de thèse. Merci de votre amour et de vos encouragements alors que vous faisiez face à la plus difficile des épreuves.

Un chaleureux merci à Anthony, Florian, Quentin, Lucas et Clara, et en particulier à Vanessa, pour m'avoir toujours soutenue même après la lecture de mes missives collégiennes dramatiques qui parlaient orientation, d'avoir été là dans tous les moments de vie, et pour tes encouragements motivants que je chéris.
Some raspberries and many thanks are addressed to Janet & Richard, Luke & Laura, and Mary & Pat. Thank you for your loving and warm support and to bring us the joy and virtual cuddles we need every week to head back into the new one.

Un merci à la carotte et au céleri
Pour mon poussin tout gris,
Qui apaise mes journées et illumine mes nuits.
La thèse aurait été bien pourrie,
Sans le réconfort de tes petits mimis.
Et la vie bien nulle,
Sans toi ma crapule.
A Pinou, Penny Poppy Bertille,
Ma toute petite pomme dauphine.

Enfin, je termine par les remerciements qui sont dédiés à ma famille, qui a vécu aussi intensément que moi ces quatre dernières années et qui me soutient inconditionnellement.
Merci à mon grand frère Alan, qui joue depuis toujours un rôle prépondérant dans mon parcours de vie, scolaire puis universitaire. Qui a éveillé ma curiosité scientifique et m'a encouragée à chaque instant à me diriger vers la recherche en Biologie en m'accompagnant notamment dès la seconde, à ma première conférence tenue dans l'amphithéâtre Buffon de l'Institut Jacques Monod, en me faisant rêver de l'Université Paris Diderot et du monde de la recherche. Merci de m'avoir toujours guidée, motivée et soutenue, et encore plus particulièrement ces dernières années. Je ne pensais pas pouvoir t'admirer davantage, mais la réalisation de ma propre thèse n'a fait qu'amplifier ce sentiment. Merci aussi bien-sûr à Natacha, pour ton regard chaleureux, ton attention et tes conseils bienveillants, pour tous ces bons moments et les cannelés réconfortants.
Merci à mes parents qui depuis toujours m'encouragent à suivre une voie de passion et qui me portent à tous les instants. Merci en particulier de nous avoir fourni, à Nate et moi, le meilleur des cadres pour réaliser notre M2 et de nous avoir aidés autant que possible pendant la thèse, de vous être adaptés à notre rythme de vie plutôt chaotique, de nous avoir conduits au labo les weekends, de vous intéresser aux microtubules ou à la culture cellulaire, de votre soutien infaillible dans les moments de doutes mais aussi d'avoir célébré avec nous les joies scientifiques, et finalement d'avoir été à mes côtés pour la rédaction des pages qui suivent.
Finally, I want to dearly thank my partner Nate, who brings me unconditional support since the first day of our M2 internship, who still finds patience after a 14h work day to reassure my doubts, listen to my complains, and motivate me, who is always willing to help and suggest ideas and improvements for my project, who taught me molecular biology techniques by distance and always shows interest for my results, and who is finally editing the English and structure of this manuscript. Thank you for your tremendous and loving support during these years. The researcher you have become impresses and inspires me every day, and I am beyond thankful that we are living this PhD journey together.

TABLE OF CONTENT

ABBREVIATIONS

APEX : Ascorbate Peroxydase
Asl : Asterless
Asp / ASPM-1 : Abnormal Spindle
BAC : Bacterial Artificial Chromosome
BAF : Barrier to Autointegration Factor
Bocks : Bocksbeutel
Cam / CMD-1 : Calmodulin
ChFP : Cherry Fluorescent Protein
Cnn : Centrosomin
CRISPR : Clustered Regularly Interspaced Short Palindromic Repeats
C-terminal : Carboxyl-terminal
DAB : 3,3'-Diaminobenzidine
DLic : Dynein Light Intermediate Chain
Dmn : Dynamitin
DNA : Desoxyribonucleo amino acid
EB1 : End binding protein 1
EGFR : Epidermal Growth Factor Receptor
EtOH : Ethanol
Fs(2)Ket : Female Sterile 2 Ketel
ɣ-TuRC : ɣ-tubulin ring complex
ɣ-TuSC : ɣ-tubulin small complex
GBP : GFP Binding Protein
GDP : Guanosine Diphosphate
GFP : Green Fluorescent Protein
GTP : Guanosine Triphosphate
KASH : Klarsicht, ANC1, Syne homology
Ket (Fs(2)Ket) : Ketel
Khc : Kinesin Heavy Chain
Klc : Kinesin Light Chain
LEM : LAP2, Emerin, MAN1
mRNA : messenger Ribonucleic Acid
MTOC : Microtubule Organizing Center
Mud : Mushroom body Defect
N-terminal : Amino-terminal
NC : Nurse Cell
ncMTOC : non centrosomal Microtubule Organizing Center
NE : Nuclear Envelope
NES : Nuclear Export Signal
Nesprin : Nuclear envelope spectrin-repeat proteins
NLS : Nuclear Localization Signal
NPC : Nuclear Pore Complex
NuMA : Nuclear Mitotic Apparatus
Nup : Nucleoporin
Ote : Otefin
PCM : Pericentriolar Material
PH : Pleckstrin Homology domain
Plk1 : Polo-like kinase 1
Ran-GAP : Ran GTPase Activating Protein
RanGEF : Ran Guanine nucleotide Exchange Factor
RFP : Red Fluorescent Protein
RNA : Ribonucleic acid
RNAi : interferent RNA
Shot : Short Stop
SUN : Sad1 and Unc84 homology
TGF-α : Transforming Growth Factor α
WT : Wild Type

INTRODUCTION

FOREWORD

My PhD work aimed to elucidate the molecular mechanisms regulated by the centrosomes and the microtubule-associated protein Mushroom body Defect (Mud) in the migratory trajectories of the oocyte nucleus during oogenesis in *Drosophila melanogaster*.

During fruit fly oogenesis, asymmetrical positioning of the oocyte nucleus is required for the establishment of the dorso-ventral axis, which polarizes the future embryo and the subsequent adult fly (Neuman-Silberberg and Schupbach, 1994). The oocyte nuclear migration is a microtubule-dependent process (Koch and Spitzer, 1983), and relies mainly on microtubule pushing forces (Zhao et al., 2012). My lab has shown that during its migration the nucleus can follow three distinct trajectories within the oocyte (Tissot et al., 2017). Furthermore, they provided evidence that the centrosomes and Mud regulate anterior and posterior trajectories respectively.

A particularity of our model system is that on one hand, the oocyte contains 16 to 32 centrosomes that gather and form a Microtubule Organizing Center (MTOC) at the posterior of the oocyte between the nucleus and plasma membrane. These centrosomes are eliminated before oogenesis completion, as the centrosomes are paternally contributed in the *Drosophila*, like in most metazoan (Pimenta-Marques et al., 2016). On the other hand, two other sources of non-centrosomal MTOC (ncMTOC) are described in the oocyte; at the plasma membrane and the nucleus where the distribution of microtubule nucleation is polarized with an enrichment of nucleation sites on the posterior nuclear hemisphere (Tissot et al., 2017). The protein Mud is also distributed in an asymmetrical manner on the posterior nuclear hemisphere of the oocyte nucleus and is closely associated with the nuclear envelope, as it co-localizes with the nucleoporin Nup107 (Tissot et al., 2017). Mud is known for its role to orientate the spindles and focus microtubule minus ends (Bowman et al., 2006). Therefore, its localization is generally observed at the cortex or spindles. However, in interphase Mud is detected at the nuclear rim in *Drosophila* syncytial embryos (Yu et al., 2006). Moreover, the Mud vertebrate homolog is named NuMA, which stands for Nuclear Mitotic Apparatus, as this microtubule-associated protein is detected at the spindle during mitosis and within the nucleus during interphase (Compton et al., 1992). Using mostly microscopy and live-imaging technique, I investigated the regulation of Mud localization and asymmetry at the oocyte nucleus and the importance for its regulation of nuclear trajectories. We identified protein partners and Nuclear Localization Signals (NLS) on Mud. By refining the oogenesis stages, I studied centrosome behavior prior to and during migration and I identified the involvement of Kinesin-1 in their clustering, which influences both the nuclear positioning and the migration.

In the following introduction, I first aim to review the importance of nuclear positioning within the cell and the role played by its cytoskeleton. I will introduce *Drosophila* oocyte development, focusing on the contribution of microtubules. Then, the final two chapters are dedicated to the centrosomes and protein Mud.

CHAPTER I : NUCLEUS POSITIONING WITHIN THE CELL

Contrary to prokaryotes, eukaryotic cells have the particularity to be compartmentalized by membranes that define distinct organelles. Organelles are host of specific functions and metabolic activities, which differ temporally and spatially, and maintain cellular function and integrity. Organelle spatial organization within the cell defines cellular polarity. Notably, the position of the nucleus within the cell is tightly controlled as it is critical for development, but also in different cellular processes like cellular migration or differentiation. In this first chapter, I aim to discuss the importance of nuclear positioning within the cell. I first focus on the nucleus and review the characteristics of its nuclear envelope and the nucleocytoplasmic transport of proteins. Then, I review the role played by the cytoskeleton, and particularly the microtubules, on nuclear positioning.

1. The nucleus

a) The nuclear envelope

In eukaryotic cells, genetic material is compartmentalized and protected within the nucleus. The nucleus is the largest organelle of the cell, constructed from a double membrane named the nuclear envelope (NE). The inner nuclear membrane and the outer nuclear membrane are separated by the perinuclear space, which are fused at regions containing the nuclear pore complex (NPC) (Lyakhovetsky and Gruenbaum, 2014). The NE relies on a dense fibrillar network, the nuclear lamina, which is composed of intermediate filaments the lamins and associated proteins. The proteins of the outer and inner nuclear membranes participate in linking the lamina and cytoskeleton. Through these interactions and the transmission of mechanical forces, the NE acts as a protective barrier and gives the nucleus the resistance to compression and deformation.
On one hand some proteins of the outer nuclear membrane bind cytoskeleton elements (*reviewed later in I 3.b*), and on the other hand, the interaction of different inner nuclear membrane proteins with the lamins have been identified. Among these lamin-binding proteins, there are the LEM (LAP2, Emerin, MAN1) domain proteins which mediate the attachment of the lamina to the NE (Zheng et al., 2000).
The NE has also an important role in the regulation of molecule exchange between the two compartments: the nucleoplasm and cytoplasm. This exchange requires a selective transport that occurs through the NPCs, which are embedded in the NE and act as molecular gateways (fig I. 1.A). NPC is a large (125 MDa) multimeric structure made of a central channel, cytoplasmic ring, cytoplasmic filaments, and nuclear ring, and nuclear basket (Hetzer, 2010; Strambio-De-Castillia et al., 2010). The number of NPCs on each nucleus varies depending on organism, cell type, and growth conditions (Nguyen Ba et al., 2009). The functional units of the NPC are proteins called the nucleoporins (Nup), and one single NPC contains different Nups that are represented in different populations (Brohawn et al., 2009).

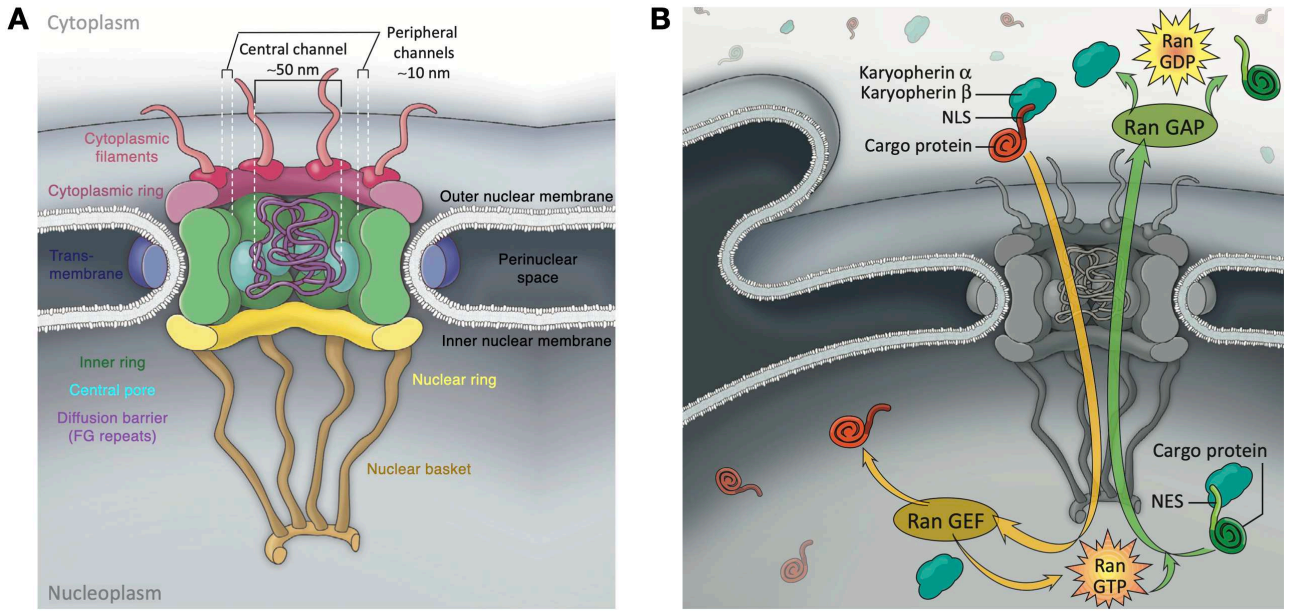

Figure I. 1 : Scheme of the nuclear envelope and the nucleocytoplasmic transport adapted from (Katta et al., 2014)**.** (A) The nuclear envelope (NE) separates the nucleoplasm from the cytoplasm. The NE is composed of an outer nuclear membrane and an inner nuclear membrane, separated by the perinuclear space. These two membranes fused at the nuclear pore complexes (NPCs) which are embedded in the NE. The NPC is composed of nucleoporins which assemble into different structures: the cytoplasmic ring and the cytoplasmic filaments, the inner ring and central pore containing nucleoporins enriched in phenylalanine-glycine (FG) repeats, and the nuclear ring and nuclear basket. (B) The NPC acts as a molecular barrier controlling the exchange between the nucleoplasm and the cytoplasm. Nuclear localization signal (NLS)-containing proteins are recognized by Importins α and β. Importins carry NLS-containing proteins inside the nucleus. The dissociation of the complex is mediated by RanGEF. Similarly, nuclear export signal (NES)-containing proteins are exported from the nucleus to the cytoplasm as they are recognized and carried by Exportins. This transport is mediated by the enzymes RanGAP and RanGEF which establish a gradient of Ran-GDP and Ran-GTP regulating the association and dissociation between cargo and karyopherins.

b) The nucleocytoplasmic transport

There are two types of nucleocytoplasmic transport through the NPC: passive diffusion and facilitated translocation. Small molecules (<40 kDa) can passively diffuse through the NPC, whereas larger molecules require selectively bound partners which ferry them through the NPC (Nguyen Ba et al., 2009). To do so, these nuclear proteins have a specific sequence that is recognized by nuclear transporters; named karyopherins. To enter the nucleoplasm, proteins expose a nuclear localization signal (NLS) that is recognized by Importins. Respectively, to exit the nucleus, proteins expose a nuclear export signal (NES) that is recognized by Exportins. This facilitated translocation through the NPC involving Importins-Exportins is rapid with an estimated speed of 0,5µm.s^{-1} for the translocating material to cross the NPC central channel (Ribbeck and Görlich, 2001).

The first identification of an NLS was *via* the analysis of simian virus 40 (SV40) mutants, whose NLS was composed of 7 amino acids: Pro-Lys-Lys-Lys-Arg-Lys-Val (PKKKRKV) (Adam et al., 1989). Since then, many types of NLS have been identified and according to their residue composition, we distinguish the classical NLS from non-classical NLS. NLS can be located at almost any part of protein sequence (Lu et al., 2021). Classical NLS are categorized into monopartite and bipartite NLS. Monopartite NLS are a single cluster of 4-8 basic amino acids. The typical motif of monopartite NLS is the following: K(K/R)X(K/R), where K is a lysine residue, R

an arginine residue, and X can be any residue (Nguyen Ba et al., 2009). Bipartite NLS are characterized by two clusters of 2-3 positively charged amino acids that are separated by a 9-12 amino-acid linker region, containing several prolines (P), and their typical motif can be R/K(X)$_{10-12}$KRXK (Nguyen Ba et al., 2009). While some NLS-containing proteins can directly be bound by Importin-β, independently of Importin-α (Pollard et al., 1996), the classical mechanism involves first, recognition of the NLS by Importin-α (fig I. 1.B). Following Importin-α recognition of the NLS, Importin-α binds to Importin-β. The complex NLS-containing protein, Importin-α and Importin-β is then imported to the nucleus after a series of enzymatic steps involving the guanine nucleotide-binding protein, Ran. Ran is the most abundant member of the small Ras superfamily of GTPases. Its function relies on the conformational change induced by its GDP or GTP-bound state, which is mediated by the guanine nucleotide exchange factor (RanGEF) and the GTPase-activating protein (RanGAP). For this system to ensure the transport of molecules between the nucleus and cytoplasm, Ran-GTP and Ran-GDP forms are asymmetrically distributed in the ¢. While Ran-GTP is enriched inside of the nucleus, Ran-GDP is enriched in the cytoplasm. The release of NLS-containing protein into the nucleoplasm requires the import complex dissociation that occurs via the interaction between Importin-β and Ran-GTP. After dissociation, Importin-α is exported from the nucleus by nuclear export factors in conjunction with Ran-GTP. The complex Importin-β-Ran-GTP returns to the cytoplasm where GTP is hydrolyzed which releases Ran-GDP from Importin-β.

There are multiple homologs of Importin-α (8 in humans, 5 in the fly) and Importin-β (more than 20 in humans, 16 in the fly) (Chen et al., 2015; Nguyen Ba et al., 2009; Quan et al., 2008). Depending on isoforms, affinity with the NLS-NES varies, which provides additional layer of nuclear import-export regulation. Other mechanisms are used in the cell to regulate the nucleocytoplasmic transport, like phosphorylation-dephosphorylation of signaling molecules or intramolecular masking of the NLS or NES. Intramolecular masking occurs when the signal of import-export is not accessible to karyopherins due to conformational changes of the proteins or competitive interaction with other proteins (Nguyen Ba et al., 2009).

c) The nucleoskeleton

The integrity, rigidity, and architecture of the nucleus relies on its nucleoskeleton termed the nuclear matrix (Cau et al., 2014; Razin et al., 2014). The nuclear matrix is composed of the nuclear lamina, and of NPC nucleoplasmic domains, inner nuclear membrane proteins, and peripheral chromatin (Razin et al., 2014). Actin, lamins, and the Nuclear Mitotic Apparatus (NuMA) protein were some of the first protagonists to be reported as components of the nuclear matrix (Clark and Rosenbaum, 1979; Gueth-Hallonet et al., 1998; Zeng et al., 1994). The lamina is made of type V intermediate filaments proteins, the lamins. They polymerize into fibrils that assemble and form a filamentous meshwork within the inner nuclear membrane. Therefore, the lamina provides a structural network for the NE, and anchoring sites for NPCs and chromatin (Pałka et al., 2018; Peter and Stick, 2012). While in mammals, four lamins have been distinguished into A-type lamins (Lamin A and C) and B-type lamins (Lamins B1 and B2), in *Drosophila*, the two majors types of lamins are called Dm$_0$ (corresponding to B-type Lamin) and Lamin C (corresponding to A-type

Lamin) (Lyakhovetsky and Gruenbaum, 2014; Smith et al., 1987). Like in vertebrates, Lamin Dm_0/B-type is expressed in all cells, whereas Lamin C/A-type is expressed only in some tissues (Prokocimer et al., 2009). They are also involved in the anchoring of NPCs and they possess even distribution across the NE. Furthermore, it has been shown by different groups that lamins play a role in chromatin function and gene expression as they can bind chromatin via lamin-binding proteins and maintain its organization near the nuclear periphery (Dechat et al., 2008; Gruenbaum et al., 2005; Lyakhovetsky and Gruenbaum, 2014). Moreover, Lamin A/B and Emerin have been shown to bind actin *in vitro* and provide nucleation sites for nuclear actin, where actin regulates the transcription through chromatin organization, and participates in the NE integrity (Holaska and Wilson, 2007; Serebryannyy and de Lanerolle, 2020; Simon and Wilson, 2011; Simon et al., 2010). This evidence highlights that lamins and their associated proteins are key players in the maintenance of the NE mechanical integrity and chromatin maintenance. Nucleus positioning involves specific connections between the NE and cytoskeleton elements, and relies on molecular mechanisms that are finely regulated and controlled.

2. Nuclear positioning and the importance of the cytoskeleton

Nuclear positioning depends on the cell type, but also on different processes that the cell goes through, such as cellular division, migration and differentiation. Controlling the nuclear position is therefore critical for the cell. Furthermore, dysregulation of nuclear positioning have been associated with pathologies, such as myopathies, lissencephaly, cardiomyopathies (Gundersen and Worman, 2013). Indeed, defects in nuclear positioning caused by mutations in genes encoding proteins involved in microtubule function, Linker of Nucleoskeleton and Cytoskeleton (LINC) complex, and the nuclear lamina have been linked to human diseases.

a) Cytoskeleton elements : intermediate filaments, actin and microtubules

The cytoskeleton is a dynamic interconnected network of polymers and proteins which structures the shape of the cell. The cytoskeleton allows resistance to external and internal mechanical forces, mediating signaling cascades, and is crucial for the distribution of cellular components and therefore cellular polarity (Fletcher and Mullins, 2010). There are three types of cytoskeleton polymers: intermediate filaments, actin, and microtubules. All three of these elements interact with the NE and mediate the displacement of nucleus in different cell types. In some cases, one cytoskeleton element is sufficient to drive nuclear movements, and in others, they work together to ensure nuclear positioning. More and more studies show that the cytoskeleton elements functionally interact together and loss of one component can perturb the others (Huber et al., 2015). Typically, cytolinkers are proteins that establish links and junctions between the cytoskeleton subtypes. We can cite the plakin protein family which proteins often possess a coiled-coil domain and domains of interactions with the different cytoskeleton elements (Goryunov et al., 2004).

Intermediate filaments are non polar polymers. In terms of their mechanical properties, the intermediate filament network is weak, but can stiffen in response to microenvironment stress without breaking, which confers elastic properties to the cell (Charrier and Janmey, 2016; Guo et al., 2013). There are different type of intermediate filaments, among them, lamins are nuclear type V intermediate filaments that ensure the rigidity and elasticity of the NE (Peter and Stick, 2012), and vimentin is a type III intermediate filament which extends from the nuclear surface through the cytoplasm and has been shown to provide structural strength to the cytoplasm (Patteson et al., 2020). Notably, in several cell types like human mesenchymal stem cells, endothelial cells, and mouse fibroblasts, vimentin establishes a cage around the nucleus (Murray et al., 2014), which indirectly connects the outer nuclear membrane of the NE through interactions with the LINC complex (Ketema et al., 2013). Furthermore, vimentin can interact with actin and microtubules *via* the cytolinker plectin, and thus participates in the connection between the cell surface and NE and transmit the mechanical stress to the nucleus (Esue et al., 2006; Schoumacher et al., 2010; Serres et al., 2020). Interestingly, apart from lamins, insects like *Drosophila* lack cytoplasmic intermediate filaments (Goldstein and Gunawardena, 2000; Herrmann and Strelkov, 2011; Rubin et al., 2000). Although it remains controversial, recent studies have identified proteins that have similar properties than intermediate filaments, such as an atypical Tropomyosin in *Drosophila* (Cho et al., 2016) and Isomin in *Isotomurus maculatus* (Mencarelli et al., 2011). In addition of force transmission and nuclear shape ans stiffness regulation (Patteson et al., 2019), intermediate filaments have been shown to mediate actin-dependent positioning of the astrocyte nuclei (Dupin et al., 2011).

The actin filament is a double helix of 5 to 8nm diameter and is composed of globular actin monomers (G actin) which polymerize and form fibrillar actin (F actin). As the monomers are polarized, the growing actin microfilaments are polarized as well. Actin microfilaments regulate many processes of nuclear positioning, either by anchoring it to the cell cortex, or by actively ensuring its displacement (Starr and Han, 2003). Notably, during mouse oocyte growth, preceding meiotic divisions, the nucleus moves from an asymmetrical position within the cell to a centered position (Almonacid et al., 2018). This movement, independent of microtubules nor centrosomes, requires the actin cytoskeleton and its associated motor Myosin V. A gradient of actin is established from the cortex to the center of the oocyte, which generates propulsion forces that center the nucleus (Almonacid et al., 2019a; Almonacid et al., 2019b). This actin-mediated nuclear movement correlates with further meiotic division success. An example in which actin microfilaments anchor the nuclei occurs within the *Drosophila* oocyte. At the end of oogenesis, the nurse cells expel their cytoplasmic content through connecting tunnels, the ring canals. During this cytoplasmic dumping, the nurse cell nuclei have to remain away from the ring canals to prevent a flux blockage. This retention process of nuclei in the center of the cell is actin-dependent (Bernard et al., 2018; Guild et al., 1997).

Microtubules are the largest elements of the cytoskeleton as their diameter reaches 25nm. Heterodimers of tubulin α and β assemble to form a protofilament. Subsequently, 13 protofilaments assemble laterally and parallel to each other to form a microtubule. There are different ways to form new microtubules. 1) They can spontaneously form in the presence of GTP. 2) They can also nucleate *de novo* using the ɣTubulin ring complex (ɣTuRC) as a template which helps the assembly and orientation of tubulin dimers (fig I. 2). 3) Via severing proteins and minus end-stabilizing proteins, they can be branched on pre-existing microtubules and pursue polymerization (Akhmanova and Kapitein, 2022). Microtubules are relatively long and rigid, but their elastic properties allow their deformation caused by motors or their own growth. By exerting pushing or pulling forces, depending on the associated molecular motor, microtubules are often involved in nucleus positioning and displacement (Gundersen and Worman, 2013). During muscle development, nuclei migrate from the center to periphery of the myotube in a microtubule-dependent manner (Metzger et al., 2012). Moreover, abnormal aggregation or mispositioning of these nuclei are associated with muscle disease and are correlated with muscle weakness and dysfunction in model organisms. In *S. pombe*, growing microtubules interact with the cell periphery and generate pushing forces that maintain the nucleus in the cell center (Tran et al., 2001). Generally, microtubule pulling forces involve cortically anchored dynein (the minus end microtubule motor) and are observed in centrosome movements in *C. elegans* for example (Grill et al., 2003). Microtubules, actin, and intermediate filaments interact with the LINC complex which directly connects the nucleus to cytoskeleton and plays a key role in nuclear positioning of many cell types.

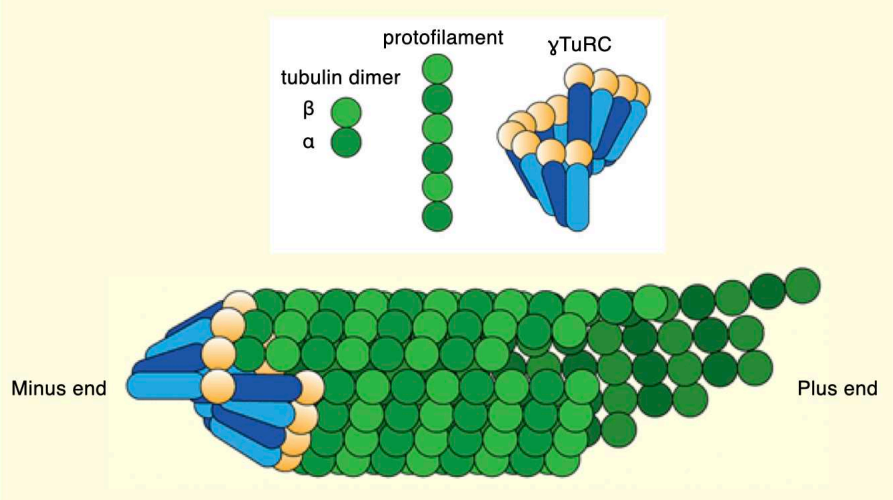

Figure I. 2 : Microtubule nucleation, adapted from (Tovey and Conduit, 2018)**.** The ɣ-TuRC, composed of ɣ-tubulin (yellow) and Gamma-tubulin complex component protein proteins (blue), serves as template for microtubule nucleation. α- and β-tubulin dimers bind ɣ-tubulin and assemble into protofilaments. Polymerization progresses towards the dynamic plus end of the microtubule, conversely to the anchoring minus end which stabilizes the microtubule.

b) Linker of Nucleoskeleton and cytoskeleton (LINC) complex

The LINC complex links the lamina and cytoskeleton (Crisp et al., 2006). It is composed of proteins that are transmembrane proteins of the NE and interact in the perinuclear space: on one hand the outer nuclear membrane KASH (Klarsicht, ANC1, Syne homology) proteins, and on the other hand the inner nuclear membrane SUN (Sad1, Unc) proteins (fig I. 3). SUN proteins are composed of a conserved SUN domain that localizes in the perinuclear space, a coiled-coil region directed toward the inner nuclear membrane and a transmembrane and nucleoplasmic domain (Bone et al., 2014; Liu et al., 2007; Sosa et al., 2013). SUN proteins interact with KASH proteins in the perinuclear space linking them to nucleoskeleton. KASH proteins link SUN proteins with cytoskeleton elements. Three KASH proteins bind to a SUN trimer (Sosa et al., 2012). Six KASH-domain proteins have been identified in mammals: a family of four Nesprins (Nuclear envelope spectrin-repeat proteins), KASH5, and LRMP (Lymphocyte-restricted membrane protein) (Lindeman and Pelegri, 2012; Morimoto et al., 2012).

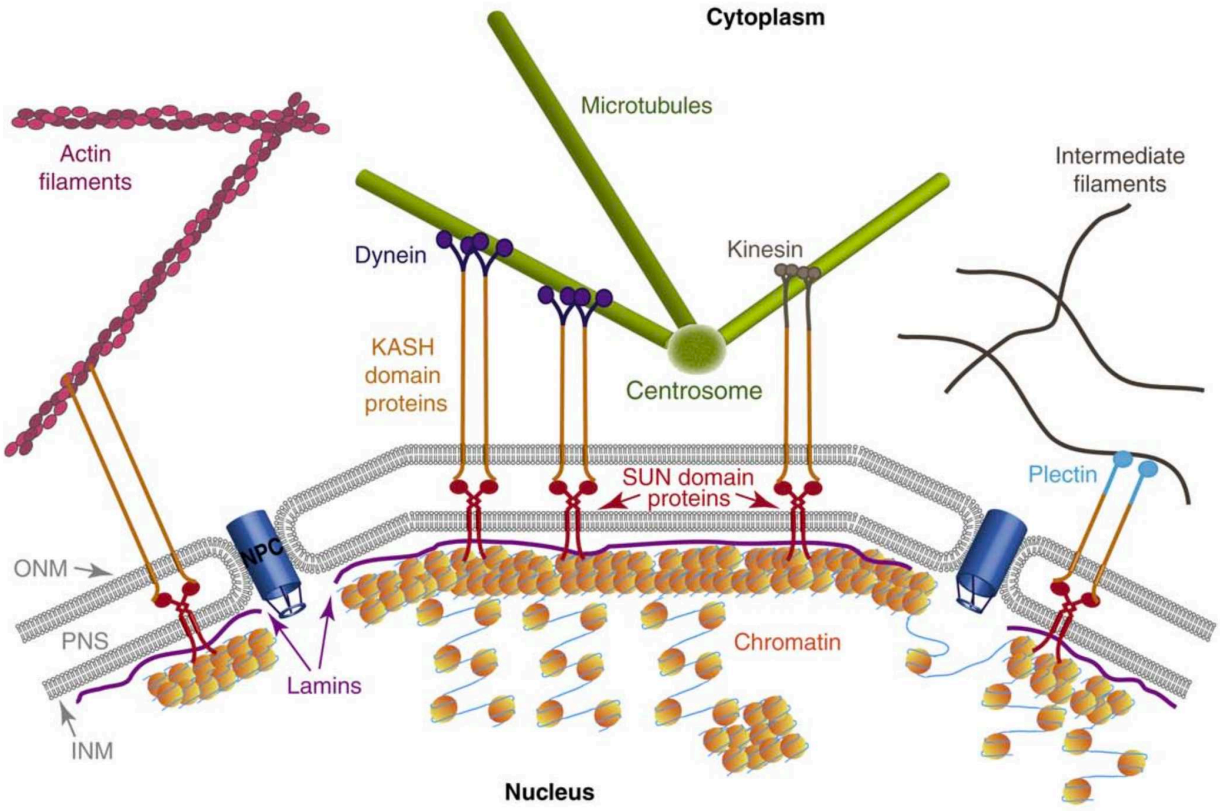

Figure I. 3 : The LINC complex links the nucleoskeleton and cytoskeleton, scheme from (Gerlitz and Bustin, 2011)**.** The two membranes of the NE (gray) are fused at the NPCs (dark blue) and separate the nucleoplasm from the cytoplasm. Within the inner nuclear membrane, lamins assemble and constitute the lamina which interacts with chromatin. The SUN and KASH proteins interact in the perinuclear space. While SUN proteins interact with the lamins, KASH proteins interact with cytoskeleton elements but also with microtubule-associated motors.

The affinity of LINC complexes for one of the cytoskeleton elements is given by the N-terminal of KASH proteins, which vary depending on the proteins. Nesprin proteins interact with actin through a calponin homology domain (Sosa et al., 2013). Nesprins 1, 2, 4, and KASH5 interact with microtubules through kinesins and Dynein (Morimoto et al., 2012; Roux et al., 2009). Nesprin 3 associates with intermediate filaments through plectin (Wilhelmsen et al., 2005). The LINC complex can therefore play an important role in nucleus positioning by connecting the different cytoskeleton element or associated molecular motors to the NE. In *C. elegans*, LINC complex KASH protein Unc-83 recruits Dynein and Kinesin-1 to the NE, where Kinesin-1 is required to move the nucleus while Dynein is involved in its directionality (Fridolfsson and Starr, 2010). In mammalian cells, KASH5 recruits dynein to the NE and acts as an activating adaptor for the molecular motor (Agrawal et al., 2022).

While there are 6 KASH proteins in mammals, there are only two KASH proteins in *Drosophila* : Msp-300 and Klarsicht. The *Drosophila* SUN proteins are Sperm-associated antigen 4 (Spag-4), only expressed in the males, and Klaroid (Technau and Roth, 2008). Klaroid has been shown to be necessary for perinuclear localization and function of Klarsicht in the eye imaginal disc (Kracklauer et al., 2007), where Klarsicht is involved in nuclear migration during eye development (Patterson et al., 2004). Surprisingly, it has been shown that neither *msp-300* single mutant or *msp-300 ; klarsicht* double mutant affect the nuclear positioning in the *Drosophila* oocyte. Although Klaroid depletion prevented Msp-300 and Klarsicht localization at the NE, nucleus positioning was not altered. Therefore, Msp-300, Klarsicht, and Klaroid were reported as dispensable for nuclear morphology and positioning in the oocyte of *Drosophila* (Technau and Roth, 2008). However, preliminary results in my lab suggest a role of the LINC complex in *Drosophila* oocyte nuclear positioning, as the depletion of Klaroid or Klarsicht in association with Mud depletion prevents the correct position of the nucleus (data from Jean-Antoine Lepesant).

In addition to the transmission of mechanical signals to the nucleus, the LINC complex is involved in different processes like NPC assembly and NPC distribution across the NE (D'Angelo et al., 2006; Liu et al., 2007), nuclei anchoring (Lei et al., 2009), DNA damage response (Lei et al., 2012), centrosome-nucleus coupling (Zhang et al., 2009).

c) Microtubule associated motors

To position organelles, microtubules and their associated motors Dynein and Kinesin play a critical role. The motors can use microtubules as routes to transport the nucleus as a cargo, or can reorganize microtubule network favoring nuclear displacement (Akhmanova and Kapitein, 2022). Cytoplasmic Dynein, here after named Dynein, is a motor that drives cargo motility and moves towards microtubule minus end. Dynein is a large multi-subunit complex of 6 polypeptides (Canty et al., 2021) (fig I. 4). It is composed of two dynein heavy chains, two intermediate light chains, and three light chains. Dynein activity requires dynactin complex and their interaction and motility are mediated by Bicaudal D (BicD) (Allan, 2014; McKenney et al., 2014; Splinter et al., 2012). Dynein and dynactin also interact with lissencephaly-1 (Lis1) and nuclear distribution protein E (NudE) complex, which regulate the motor functions (Reck-Peterson et al., 2018; Trokter et al., 2012). Dynein is involved in mechanisms that focus the microtubule minus ends for the meiotic and mitotic spindles; pull the microtubule plus ends; and promote centrosome motility or microtubule sliding (Allan, 2011; Gros et al., 2021; Merdes et al., 1996).

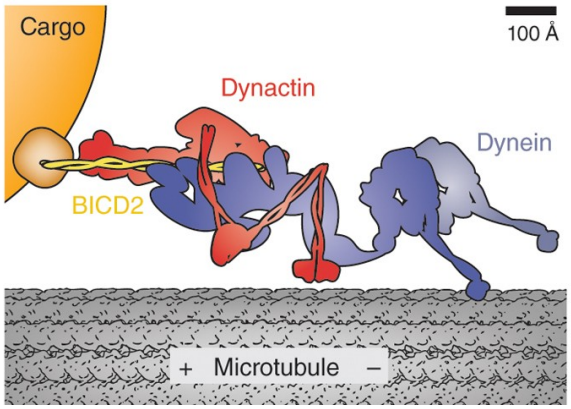

Figure I. 4: Structure of cytoplasmic Dynein complex, from (Allan, 2014). Scheme representing Dynein complex showing Dynein (in purple) which is composed of two Dynein Heavy Chains, two intermediate light chains, and three light chains. Dynein interacts with Dynactin (in red) via BICD2 (in yellow) which also serves as a cargo adaptor.

The Kinesin superfamily is constituted of 15 kinesin families that can be categorized into three subgroups: N-kinesins whose motor domain is in amino-terminal (N-terminal) region; M-kinesins whose motor domain is in middle and the C-kinesins whose motor domain is in carboxyl-terminal (C-terminal) region (Hirokawa et al., 2009). While the N-kinesins regulate microtubule plus-end motility, the C-kinesins drive the microtubule minus-end motility, and the M-kinesins have a microtubule depolymerizing activity (Dagenbach and Endow, 2004). Kinesin-1, a N-kinesins, is the most abundant kinesin and is referred as the classic Kinesin. It is a hetero-tetramer composed of two heavy chains (Khc) and two light chains (Klc) (fig I. 5) (Verhey et al., 2011).

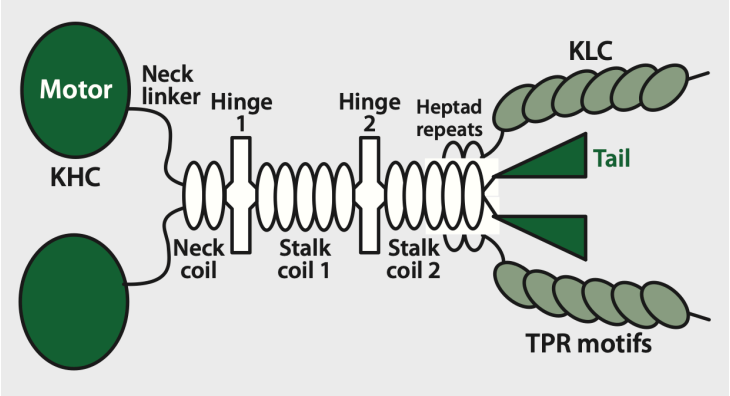

Figure I. 5: Structure of Kinesin-1, from (Verhey et al., 2011). Kinesin-1 is composed of a dimer of Khc subunits and two Klc. Khc displays a motor domain, followed by a neck linker and a neck coil that are involved in homodimerization and the functionality of the motor. Khc contains two Hinge domains, and finally a globular tail domain involved in the regulation of the motor activity and the cargo binding. Hinge domains are domains that allow the folding of Kinesin-1, by the interaction of the C-terminal with the N-terminal, and the subsequent auto-inhibition of the motor.
Klc subunits are composed of repeated TPR motifs that constitute domains of cargo binding.

Dynein and Kinesin motors are involved in different processes and notably in cytoskeleton organization. They can act as cross-linkers by binding two microtubules and linking them together (Guha et al., 2021). Relying on the attachment of two microtubules by an associated motor, microtubules can slide which allows the movement of two microtubules apart, either with the plus-end leading or the minus-end leading depending on the associated motor (plus-end directed or minus-end directed). In the case where the motor binds a non-motile structure, such as the plasma membrane, the microtubule that it binds can glide along the cortex. Khc can drive microtubule motility by either cross-linking microtubules or promoting microtubule sliding/gliding. In *Drosophila* oocytes, Khc-mediated gliding and sliding are required for cytoplasmic streaming (Ganguly et al., 2012; Jolly and Gelfand, 2010; Palacios and St Johnston, 2002; Winding et al., 2016). In skeletal muscles, Kinesin-1/Kif5-B has also been shown to be associated with the NE via Nesprin-dependent anchoring and to regulate nuclear migration (Wilson and Holzbaur, 2015). In *C. elegans* oocytes that lack centrosomes, nuclear migration is dependent on Kinesin-1 and allows correct positioning of the nucleus. This defines the attachment of the subsequent spindle upon meiosis at the anterior cortex and therefore consolidates the antero-posterior axis of the future embryo (McNally et al., 2010). The interkinetic nuclear migration is a fitting model which requires both motors Dynein and Kinesin. The migration occurs in the radial glial progenitors which give rise to neurons, glia, and neural stem cells during brain development. The nuclei of these cells migrate twice during the cell cycle: in G2 phase towards the apical side in a Dynein-dependent manner, and in G1 phase towards the basal side in a Kinesin-3-dependent manner (Tsai et al., 2010). These migrations are centrosome-independent, suggesting the requirement of the molecular motors on the nuclear surface. Interestingly, it was shown that prior to G2-migration, Dynein is recruited at the NE either by nucleoporin RanBP2/Nup358 or by Nup133/Cenp-F (Baffet et al., 2015; Hu et al., 2013).

d) MTOC and ncMTOC

In dividing animal cells, centrosomes are the main Microtubule Organizing Center (MTOC) and have a key role in spindle orientation leading to correct segregation of chromosomes; preserving the integrity of the daughter cell genome. However, in differentiated cells, microtubule minus ends are not always anchored or nucleated by centrosomes, but rather on organelles such as the Golgi apparatus, nucleus, endoplasmic reticulum, plasma membrane, and chromosomes (Akhmanova and Kapitein, 2022; Petry and Vale, 2015; Wu and Akhmanova, 2017). The Golgi apparatus can act as an ncMTOC in the cell and is capable of nucleating and anchoring microtubules (Wu and Akhmanova, 2017). Conversely to centrosomes which form symmetric arrays of microtubules, the Golgi-associated MTOC nucleates and organizes microtubules in a polarized manner. These arrays can be used for asymmetric vesicular transport and therefore participate in cellular polarity (Vinogradova et al., 2009). Nuclear ncMTOC is particularly well described in skeletal muscle cells which lack active centrosomes, and in which ɣ-tubulin and centrosomal components are redistributed to the NE upon differentiation (Bugnard et al., 2005; Tassin et al., 1985). Notably, the LINC complex is required for recruitment of nucleating components at the NE (Meinke et al., 2014), and the microtubule minus ends associate directly with the NE via molecular factors.

Furthermore, along the NE-associated microtubule network, Dynein-mediated pulling and microtubule Kinesin-1-mediated sliding coordinate with microtubule-associated proteins (MAP) to position nuclei near the center of syncytial myotubes (Cadot et al., 2012; Folker et al., 2012; Metzger et al., 2012). In plant cells, lacking centrosomes, the NE nucleates and anchors microtubules (Wu and Akhmanova, 2017). Studies suggest that this microtubule network influence the shape of the nuclei and the distribution of NPCs (Batzenschlager et al., 2014; Batzenschlager et al., 2013). In some epithelial cells, the plasma membrane ncMTOC can organize parallel microtubules which are important for asymmetric transport. For example, in differentiated epithelial cells of the tracheal system, centrosomal microtubules are severed and relocalized at the plasma membrane whilst structural platforms promoting microtubule nucleation ɣ-TuRC are redistributed and anchored at the plasma membrane (Brodu et al., 2010). Another alternative in cortical ncMTOC establishment that does not require ɣ-tubulin, is the presence of anchoring proteins such as the spectraplakin Short Stop (Shot). Shot interacts with cortical actin and recruits Patronin which binds microtubule minus ends in the oocyte of *Drosophila melanogaster* (Nashchekin et al., 2016). Altogether, these different centrosomal and non-centrosomal MTOCs participate in cellular polarity by controlling protein transport or organelle positioning. They act together, such that the activity of one is dependent on the activity of another (Wu and Akhmanova, 2017). In some differentiated cells, centrosomes undergo a downregulation and their protein components are redistributed to benefit ncMTOCs (Muroyama et al., 2016). For example, upon cellular differentiation, centrosomes can lose their MTOC nucleating function for the benefit of non-centrosomal MTOC (ncMTOC) (Brodu et al., 2010). It has been shown in epithelial cells, that despite a reduced nucleation activity, the centrosomes still nucleate microtubules but their anchoring capacity is defective (Muroyama et al., 2016).

CHAPTER II : NUCLEAR POSITIONING IN THE *DROSOPHILA* OOCYTE

To study cellular polarity and cytoskeleton involvement, *Drosophila* oocyte is a very suitable model. Cell polarity is essential along fruit fly oogenesis, from oocyte specification, to polarity axis establishment, as well as the position of the oocyte nucleus. Throughout these events, microtubule cytoskeleton plays an essential role to ensure oocyte polarity. In this chapter, I will review the oocyte specification and polarization during oogenesis, and the establishment of the two polarity axis: antero-posterior and dorso-ventral. Interestingly, the determination of the dorso-ventral axis relies on asymmetrical positioning of the oocyte nucleus; which is microtubule-dependent, and requires centrosomes and the microtubule-associated protein, Mud.

1. Oogenesis in *Drosophila melanogaster*

a) The *Drosophila* egg chamber

The internal reproductive organs of female *Drosophila melanogaster* are composed of a pair of ovaries, an oviduct, a uterus, a seminal receptacle, and a pair of spermathecae. The spermathecae and the seminal receptacle are sperm-storage organs and are also required for the maintenance of sperm viability (McDonough-Goldstein et al., 2021). Ovaries are the structures containing the developing egg chambers (fig II. 1). Each ovary is constituted of 20 ovarioles which are the functional units of ovaries. An ovariole is a polarized and autonomous continuity of egg chambers at different stages of maturation along the antero-posterior axis (Koch et al., 1967). At the end of oogenesis, the mature egg chamber, which is ready to be fertilized, goes through the oviduct; the canal connecting the ovaries and the spermathecae.

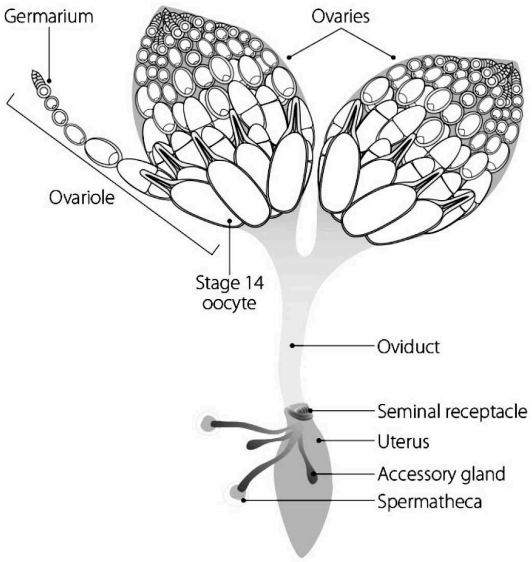

Figure II. 1: The internal reproductive organs of the female fruit fly. A pair of ovaries containing the developing female gamete, an oviduct which connects the ovaries with the seminal receptacle, spermatheca, and the uterus. Each ovary is composed of ovarioles that are continuities of egg chambers at different stage of maturation. The most mature egg chambers are localized to the posterior side of the ovary, close to the oviduct, the canal by which the egg chambers go through to be further fertilized by the sperm. The most immature egg chambers are at the anterior side of the ovariole, close to the germarium.

Regarding morphological features, oogenesis has been distinguished in 14 stages of developed egg chambers (King et al., 1956). Ovarioles are structured as such that germarium, at the anterior, is followed by vitellarium which contains progressively matured egg chambers (fig II. 2).

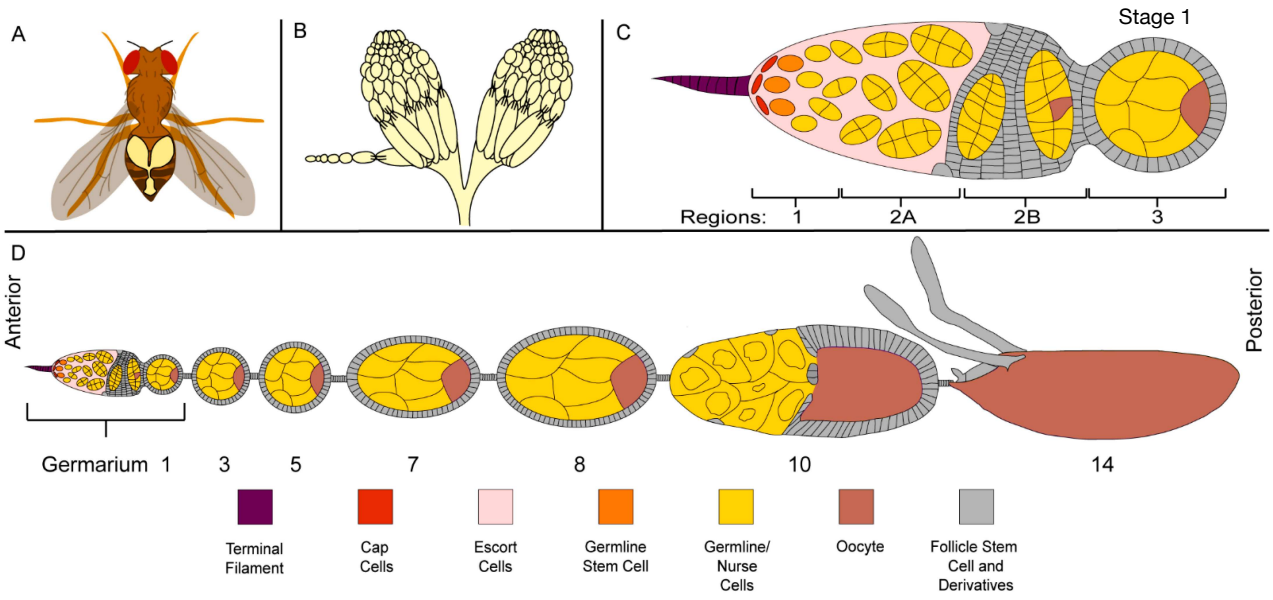

Figure II. 2 : Drosophila oogenesis, from (Lebo and McCall, 2021)**.** (A) The internal reproductive organs are shown in yellow in the fly abdomen. (B) Zoom on an ovary pair, each composed of ovarioles. (C) Detail of the germarium, which contains the stem cells, and in which the oocyte is specified. The germarium is composed of 4 regions: 1, 2A, 2B, 3. In region 3, the newly egg chamber is formed and composed of a monolayer of follicular cells (gray) surrounding the germ cells: the nurse cells (yellow) and the oocyte (brown). The egg chamber in region 3 corresponds to Stage 1 of oogenesis. (D) Scheme of different stages of oogenesis along the antero-posterior axis. At the end of oogenesis, the oocyte is ready to be reactivated in order to complete meiosis and be fertilized by the sperm.

Oogenesis starts in the germarium (fig II. 2.C). The more mature the egg chamber is, the most posteriorly the egg chamber localizes in the ovariole. The germarium is a specialized structure containing germline stem cells (GSC), organized in 4 regions: 1, 2a, 2b, and 3 (Koch and King, 1966). The GSC divide in an asymmetrical manner along the antero-posterior axis of the germarium. These divisions give rise to new GSC, one maintains the GSC pool at the anterior of the ovariole, while the other GSC goes through differentiation. This differentiating event produces the cystoblast. The cystoblast goes through 4 rounds of incomplete mitosis without cytokinesis. This gives rise to a cyst of 16 germinal cells interconnected by cytoplasmic bridges, namely the ring canals. Among these cells, the two oldest are connected by 4 ring canals, while the others are connected through 1, 2, or 3 ring canals (Brown and King, 1964). These two cells are the pro-oocytes. Only one of these two differentiates into the oocyte, remains diploid, and begins its meiotic program (Theurkauf et al., 1993). The 15 remaining germ cells of the cyst start endoreplication cycles and become polyploid. By accumulating more proteins, RNA, and organelles as they endoreplicate, they become the 15 nurse cells of the egg chamber. Their function is to ensure the growth of the oocyte, with which they are connected via the ring canals. Therefore, they provide nutrients, mRNAs, and cytoplasmic components like Golgi apparatus, mitochondria, endoplasmic reticulum, and centrosomes to the oocyte. The cyst pursues its development and progresses towards the posterior of the germarium, where it is surrounded by a protective layer of somatic follicular cells. On the germarium extremity, between regions 2a and 2b, some follicular cells establish a close link with the cyst to finally embed it (Mahowald and Strassheim, 1970). In region 3 at the posterior of the germarium, the cyst becomes round and is completely enveloped by follicular cells. Thus, the cyst becomes the egg chamber composed of germ cells: 15 nurse cells and one oocyte, surrounded by a monolayer of somatic follicular cells.

In between regions 2b and 3, some FSC differentiate into stalk cells linking the newly formed egg chamber with the following younger cyst (Roth and Lynch, 2009). The egg chamber can exit the germarium and pursue its development in the vitellarium, linked with a more mature egg chamber at the posterior and a younger one at the anterior side. Therefore, the egg chambers are organized in a progressive manner within the ovariole. Each ovariole is independent and autonomous and carries an average of 8 egg chambers. The oocyte is the only cell within the egg chamber that persists into meiosis. Furthermore, at the exit of the germarium, meiosis is arrested in prophase I (Megraw and Kaufman, 2000). The oocyte nucleus is transcriptionally inactive at mid-oogenesis (Navarro-Costa et al., 2016). Meiosis will restart, independently of fertilization, when the egg chamber is activated within the oviduct (Bastock and St Johnston, 2008). While, in most species, polarity axes are acquired during embryogenesis, in *Drosophila* it occurs during oogenesis.

b) Polarity axis establishment

The specific localization of three maternal factors specifies the antero-posterior and dorso-ventral axes (Megraw and Kaufman, 2000). These mRNAs are *bicoid* (*bcd*), *oskar* (*osk*) and *gurken* (*grk*). The antero-posterior axis of the cyst is determined in the germarium and guides the polarized maturation of the egg chamber along the ovariole. The patterning of this axis relies on the specification of the oocyte which is positioned at the posterior of the cyst and accumulates specific factors (*reviewed later in II 2.a*) (González-Reyes and St Johnston, 1994). This asymmetry establishes the antero-posterior axis of the cyst which is later translated into the antero-posterior axis of the oocyte itself. *Gurken* (*grk*) is required for the establishment of both axes during oogenesis. It encodes the *Drosophila* homolog of transforming growth factor α (TGF-α). Gurken is the ligand of receptor Torpedo, the *Drosophila* homolog of epidermal growth factor receptor (EGFR). Like other mRNAs, *grk* accumulates at the posterior of the oocyte, in the germarium, where it is locally translated. Grk signals to the adjacent follicular cells of the cyst which therefore take a posterior fate (González-Reyes et al., 1995; Huynh and St Johnston, 2004; Riechmann and Ephrussi, 2001). By default and in absence of Grk signaling, the opposite side of the cyst takes an anterior fate. Furthermore, Grk stimulation of posterior follicular cells induce their answer as an « unknown feedback signal », later on around the stage 6-7. This unknown signal generates the reorganization of the microtubule network allowing the transport of *bcd* mRNA towards the anterior and *osk* towards the posterior which patterns the antero-posterior axis of the oocyte (Berleth et al., 1988; Ephrussi et al., 1991; González-Reyes and St Johnston, 1994; Nüsslein-Volhard et al., 1987; Peri and Roth, 2000). *Bcd* and *osk* localization will be maintained throughout oogenesis, but also during embryogenesis, during which they will be the main actors of embryo polarization (Januschke et al., 2002; Roth and Lynch, 2009). *Bcd* determines the future head and thorax and *osk* determines the future abdomen and primordial germ cells (Roth, 2003).

The dorso-ventral axis is dependent on another local translation of *grk* mRNA which relies on the migration of the oocyte nucleus occurring at mid-oogenesis (fig II. 3) (Guichet et al., 2001; Neuman-Silberberg and Schupbach, 1994). Indeed, as *grk* mRNA is associated with the oocyte nucleus, the oocyte nuclear migration positions the nucleus in an asymmetric manner within the cell. Thus, the oocyte nucleus moves from the cell center to the antero-lateral cortex in contact with the adjacent lateral follicular cells. These follicular cells, which express Grk receptor, are capable of receiving the signaling cascade induced by *grk* local translation. Therefore, these cells take a dorsal fate, while the oocyte opposite follicular cells take a ventral fate in absence of Gurken signaling (Neuman-Silberberg and Schupbach, 1994; Schüpbach, 1987).
The oocyte axis establishment relies on signaling pathways between the different cell types of the egg chamber, and on the asymmetrical localization of cytoplasmic determinants within the oocyte that is provided by local translations of mRNAs. The mRNAs are transported from the nurse cells to the oocyte and their spatial distribution is dependent on the microtubules and their associated motors (Januschke et al., 2002; Riechmann and Ephrussi, 2001).

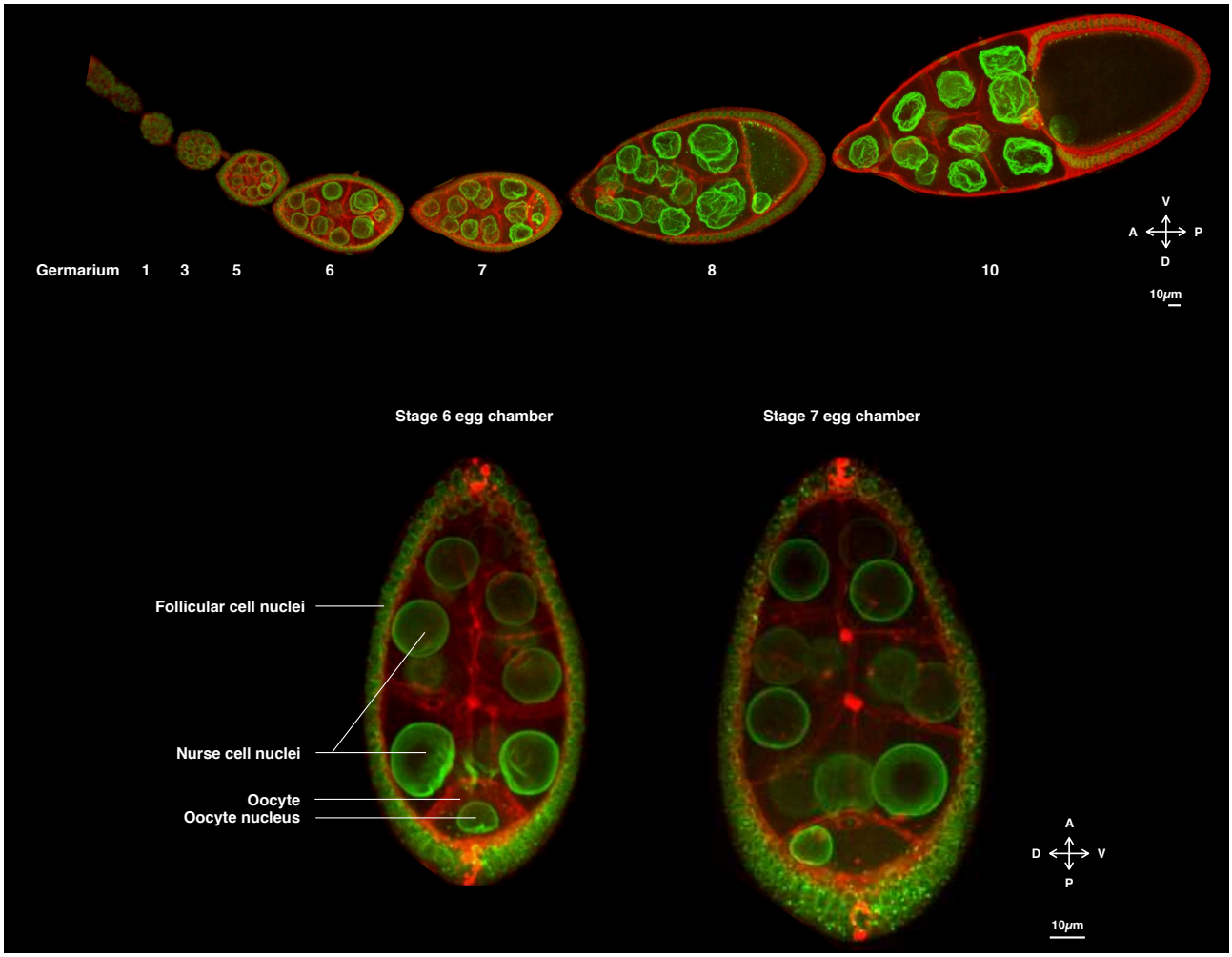

Figure II. 3: The asymmetrical oocyte nuclear positioning at mid-oogenesis, from (Loh et al., 2021)**.** (Top) Fixed ovariole, along the antero-posterior axis (A-P), in which the nuclei are in green and the plasma membrane in red. (Bottom) At stage 6 of oogenesis (left), the nucleus is centered in the oocyte. At stage 7 (right), the nucleus is asymmetrically positioned in the oocyte after the completion of its migration. It is therefore in contact with the antero-lateral cortex, corresponding to the intersection between the anterior and posterior plasma membranes. This specific position, in contact with the adjacent follicular cells, establishes the second polarity axis; dorso-ventral (D-V) axis.

2. The role of the microtubules in the polarization of the oocyte

In this section, I will review the importance of the microtubules throughout the early oogenesis stages, from the oocyte specification to nuclear migration.

a) Sources of microtubules in the oocyte

Apart from the ncMTOC organized by the fusome in the germarium, three sources of nucleation sites have been identified in the fruit fly oocyte. Oogenesis is inhibited under colchicine treatment (Koch and Spitzer, 1983), indicating a fundamental role of microtubules along oocyte development. The first nucleation site is provided by the centriole-containing centrosomes that cluster into an MTOC at the posterior of the oocyte nucleus (*see Chapter III 2.*) (Mahowald and Strassheim, 1970; Megraw and Kaufman, 2000). The second site is the oocyte nucleus, where ɣ-tubulin localizes, and on which NE-associated microtubule regrow after depolymerization induced by colchicine treatment (Januschke et al., 2006). Furthermore, nuclear microtubule nucleation, as well as ɣ-tubulin distribution, are asymmetric with enrichment on the posterior nuclear hemisphere (Januschke et al., 2006; Tissot et al., 2017). Finally, the third site of microtubule nucleation has been described at the oocyte cortex, where microtubules nucleate from the plasma membrane and project into the cytoplasm creating a microtubule density gradient along the posterior-lateral cortex (Khuc Trong et al., 2015; Nashchekin et al., 2016; Parton et al., 2011; Theurkauf et al., 1992). This cortical ncMTOC is described at a late-oogenesis stages around stage 9 and is involved in cytoplasmic streaming that occurs at this stage, where the microtubules are re-arranged in a spiral shape surrounding the ooplasmic flux. Oocyte cytoplasmic streaming is Khc-dependent and contributes to the asymmetrical distribution of nutrient vesicles and organelles (Ganguly et al., 2012; Gutzeit and Koppa, 1982; Jolly and Gelfand, 2010; Palacios and St Johnston, 2002).

Furthermore, it appears that the activity of the different MTOCs could temporarily differ, as the centrosomes go through an elimination process after the nuclear migration (*see Chapter III 2.b*) and the cortical ncMTOC has only been described at later stages of oogenesis.

b) The microtubule-dependent oocyte specification

Over the years, different mechanisms have been proposed to explain oocyte specification from the other cells of the cyst. It appears that the hypothesis of the specification of one random cell among the cyst is not suitable, but this specification rather relies on asymmetrical events involving the microtubule cytoskeleton. Many events and proteins are required in the specification of the oocyte (Huynh and St Johnston, 2004), however, in this section, I will only review those linked with the microtubule cytoskeleton. Generally, oocyte specification requires a polar transport of cytoplasmic determinants, which is microtubule-dependent as it is driven by the minus-end microtubule motor Dynein (Palacios and St Johnston, 2001). Furthermore, microtubule depolymerization induced by a colchicine treatment results in egg chambers of 16 nurse cells (Koch and Spitzer, 1983).

Specification of the future oocyte depends on the formation of an ncMTOC, which extends microtubules through the ring canals and connect the oocyte to nurse cells (Theurkauf et al., 1993). The formation of this ncMTOC is dependent on the spectraplakin protein Short Stop (Shot) which recruits Patronin orthologue of CAMSAP (Calmodulin-regulated spectrin-associated protein) in the vertebrates (Nashchekin et al., 2021). Patronin accumulates in the future oocyte, and together with Shot, stabilizes microtubule minus ends and anchor them to the fusome. The fusome is a membranous organelle which polarizes and organizes the microtubule network emanating from the oocyte ncMTOC (Grieder et al., 2000). This polarized microtubule network serves as a track for Dynein-dependent transport of the pro-oocytes determinants by establishing connections with the future oocyte and the other germ cells through ring canals (Bolívar et al., 2001; McGrail and Hays, 1997). The fusome is unequally distributed among these cells, as the future oocyte contains the most fusome material (Bolívar et al., 2001; Lin and Spradling, 1995). Therefore, in a Dynein-dependent manner, the future oocyte accumulates factors like Orb, mRNAs, mitochondria, and centrioles from the other germ cells and specifies into the oocyte (Huynh and St Johnston, 2004; Lantz et al., 1994; Mahowald and Strassheim, 1970; Riparbelli et al., 2021; Stevens et al., 2007).

In addition to the specification steps, differentiation has to be maintained. The position of cytoplasmic determinants and organelles at the posterior is maintained in a PAR-1-dependent manner (Huynh et al., 2001). Indeed, in absence of PAR-1, Orb and the centrosomes do not correctly migrate from nurse cells to oocyte, and therefore the oocyte exits its meiotic program and becomes a nurse cell. This maintenance occurs also through microtubules which cross the ring canals of the differentiated oocyte to reach and contact nurse cell cytoplasm establishing routes for the continuous transport of components and nutrients needed for its growth and development (Theurkauf et al., 1993).

c) Oocyte nuclear migration is microtubule-dependent

Oocyte nuclear migration is a major symmetry-breaking event during oogenesis in *Drosophila* as it specifies the dorso-ventral axis. The absence of dorso-ventral polarity is lethal for the embryo, making nucleus positioning a critical process during oocyte development. From early stages until mid-oogenesis, it is described that the nucleus is centered or posteriorly positioned before migrating towards the antero-lateral cortex of the oocyte where it stays anchored until the end of oogenesis (Guichet et al., 2001; Roth, 2003; Roth et al., 1999). This migration is dependent on microtubules as the nucleus is still centered at later stages in colcemid-treated egg chambers and the dorso-ventral axis is not specified (fig II. 4) (Januschke et al., 2002; Koch and Spitzer, 1983). Colcemid is a synthetic equivalent of colchicine which depolymerizes microtubules. Furthermore, the microtubule forces exerted on the nucleus are pushing forces coming from the posterior of the oocyte where the centrosomes gather (Tissot et al., 2017; Zhao et al., 2012).

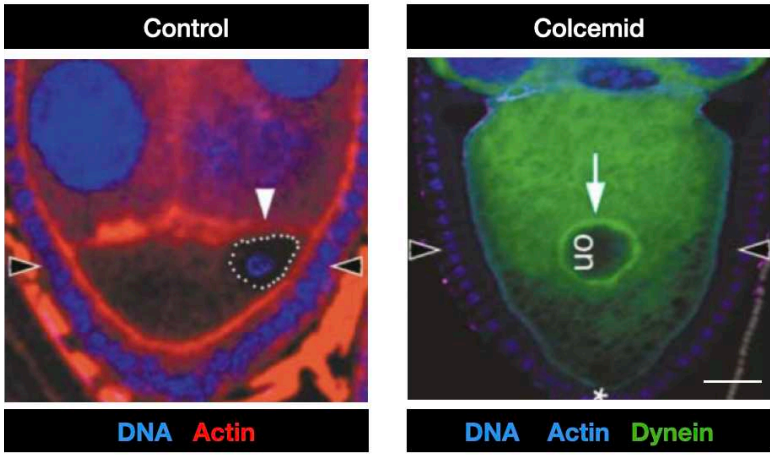

Figure II. 4: The oocyte nuclear migration is microtubule-dependent, adapted from (Januschke et al., 2002). (Left) In the control condition, at stage 7-8, the nucleus is asymmetrically positioned within the oocyte after its migration. (Right) Under Colcemid treatment, which depolymerizes the microtubules, the nucleus did not migrate as it is still centered at later stage of oogenesis. The arrows show the oocyte nuclei. Bar, 10µm. The egg chambers are oriented in the way that the oocyte (which is at the posterior of the egg chamber) faces the bottom of the figure, while the nurse cells (anterior) face the top of the figure.

In the identification of the actors involved in the oocyte nuclear migration, the role of the microtubule associated motors has been investigated as well. It was shown that Kinesin-1 and Dynein are required for the maintenance of nucleus position at the antero-lateral cortex after its migration (Brendza et al., 2002; Januschke et al., 2002). More precisely, only the heavy chain of Kinesin-1, but not its light chain has been reported to be important for this process (Palacios and St Johnston, 2002). However, neither Dynein nor Kinesin-1 have been reported as necessary for proper nuclear migration during mid-oogenesis (Januschke et al., 2002; Zhao et al., 2012). More recently, live-imaging experiments have made it possible to analyze oocyte migration in real-time and revealed that the oocyte nuclear migration is a three-hour event that occurs through different trajectories (Tissot et al., 2017; Zhao et al., 2012). Henceforth, nuclei can migrate along the anterior plasma membrane, or the posterior plasma membrane or take an intermediate route through the cytoplasm without contacting the anterior or posterior membranes before reaching the cortex (fig II. 5.A).

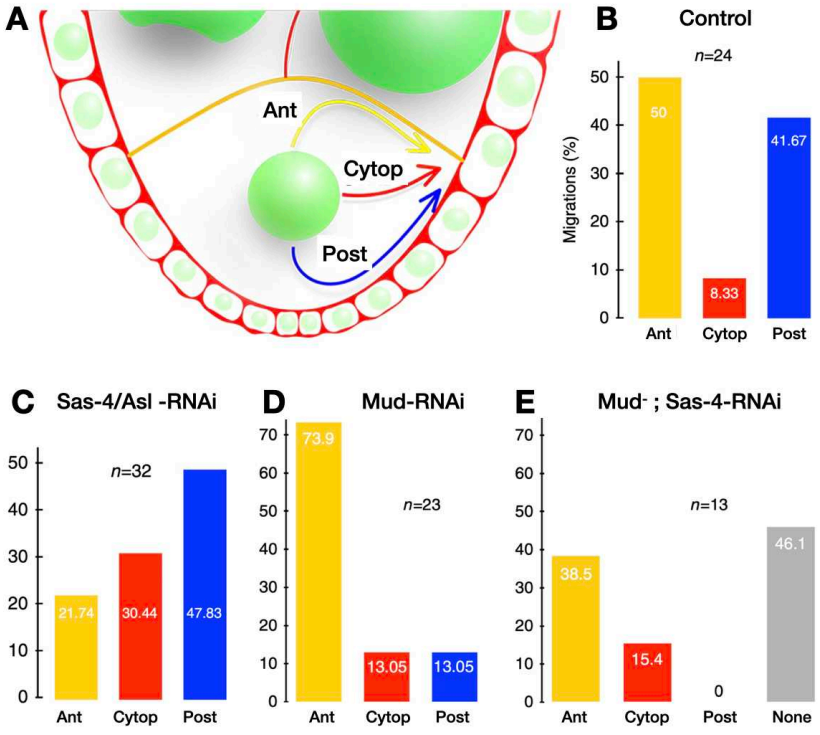

Figure II. 5: The oocyte nuclear migration trajectories, adapted from (Tissot et al., 2017). (A) Scheme of the oocyte showing the three trajectories that can be taken by the nucleus during its migration: along the anterior plasma membrane (Ant), along the posterior plasma membrane (Post), or in between (Cytop).
(B) In the control condition, the quantification of the proportions of trajectories show that the Ant and Post paths are the main. (C) When the centrosomes are affected (either in Sas-4 RNAi or in Asl-RNAi contexts), the trajectories are different with a decrease of the Ant path. (D) In Mud-RNAi context, the posterior trajectory proportion is reduced. (E) In the double mutant affecting both Mud and the centrosomes (*mud* mutant and Sas-4 RNAi), 46,1% of the observed nuclei do not migrate, suggesting an important role of their in the regulation of this movement.

Quantification of the trajectory proportions shows that the anterior and posterior are the principle routes taken by the nuclei (fig II. 5.B). Moreover, Guichet and colleagues have shown that the centrosomes and the microtubule-associated protein (MAP) Mud were two important actors regulating the oocyte nucleus migration (Tissot et al., 2017). On one hand, disruption of centrosomes by the depletion of the Pericentriolar Material (PCM) components Sas-4 or Asl (*see Chapter III 1.a*) revealed that while the migration was not abolished, the nuclear trajectory proportions varied; with a decrease of anterior frequency (fig II. 5.C). On the other hand, depletion of Mud did not inhibit the migration, but induced a decrease of the posterior trajectory frequency (fig II. 5.D). Finally, depletion of both centrosomes and Mud caused an inhibition of the oocyte nuclear migration in 50% of the cases (fig II. 5.E). Altogether, these results indicate that the centrosomes and Mud participate in the regulation of nuclear migration, and that the centrosomes promote an anterior trajectory, while Mud favors a posterior trajectory.
In order to better characterize the nuclear positioning mechanisms, I have investigated the role and behavior of Mud and the centrosomes to understand their precise involvement in the regulation of the nuclear trajectories during the oocyte nucleus migration, during my PhD.

CHAPTER III : CENTROSOMES DURING OOGENESIS

Centrosomes are the most well-described Microtubule Organizing Center (MTOC). They are non-membranous organelles that govern mitotic spindle orientation, cellular trafficking, and cellular motility and have a central role in cellular organization and polarity (Bornens, 2008). Centrosomes are paternally contributed, and therefore have to go through an elimination process during oogenesis prior to fertilization. In the *Drosophila* oocyte, there are 16 to 32 centrosomes that cluster into an MTOC and regulate the anterior trajectory of the nuclear migration by exerting pushing forces, as seen in the previous chapter. In this chapter, I will first review centrosome formation and maturation, then centrosome behavior and elimination during fruit fly oogenesis. Finally, I will discuss centrosome-nucleus coupling in regard to nuclear positioning within the cell.

1. Centrosome biogenesis

a) Centrioles and the Pericentriolar Material

A centrosome is composed of two centrioles and the PCM that surrounds the centrioles (fig III. 1). The centrioles are microtubule-based structures organized in barrel-shape of nine microtubule triplet cylinders that surround a lumen (Avidor-Reiss and Fishman, 2019; Bettencourt-Dias et al., 2011; Doxsey, 2001). One of the two centrioles is an immature daughter centriole and the other is a mature mother centriole that carries appendages; notably involved in microtubule anchoring and centriole positioning (Marthiens and Basto, 2020). These two asymmetric centrioles are linked together by a matrix composed of large coiled-coil proteins of the pericentrin family. Interestingly, the *Drosophila* centrioles do not display distal or subdistal appendages (Callaini et al., 1997).
The PCM is a dynamic matrix indispensable for centriole biogenesis. It ensures stability and function of centrosomes. Indeed, PCM provides anchoring sites for the ɣTuRC which stabilizes, nucleates microtubule minus end, and serves as a platform for further polymerization (Azimzadeh and Bornens, 2007; Marthiens and Basto, 2020; Pimenta-Marques and Bettencourt-Dias, 2020).

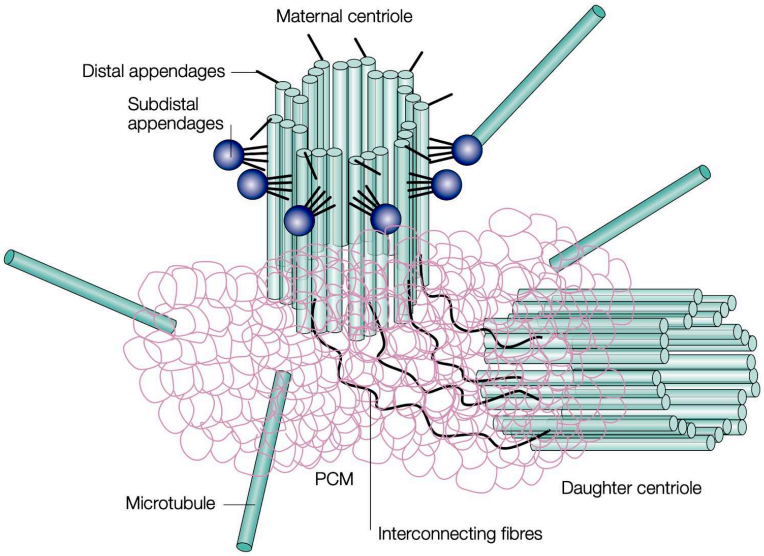

Figure III. 1: Centrosome structure in mammalian cells, from (Doxsey, 2001). Centrosome consists of a pair of centrioles: an immature daughter centriole and a mature mother centriole. Centrioles are barrel-shape structures composed of 9 microtubule triplets. Only mother centriole displays distal and subdistal appendages, which serve as anchoring sites for the microtubules. The two centrioles are linked together trough interconnecting fibers (in black), and are surrounded by PCM (in pink). The PCM is dynamic matrix made of interconnected fibers and proteins which also provides anchoring sites for the ɣ-TuRC and therefore nucleation sites for the microtubules.

In addition to ɣ-tubulin, PCM is composed of proteins such as Asterless/Cep152 (Asl) (*Drosophila*/human), Centrosomin/CDK5RAP2 (Cnn), D-PLP/Pericentrin and Spd2/Cep192, Sas-4/CPAP/CENPJ (Pimenta-Marques and Bettencourt-Dias, 2020). Furthermore, Sas-4 is required for centriole replication (Basto et al., 2006). Two ɣ-tubulin genes exist in *Drosophila*: ɣ*Tub23C* and ɣ*Tub37C* (Zheng et al., 1991). ɣTub37C encodes for the maternal form of ɣ-tubulin and is expressed in nurse cells and oocyte during oogenesis (Tavosanis et al., 1997; Wilson et al., 1997). ɣ-tubulin localizes at centrosomes in the germarium (Bolívar et al., 2001), around the oocyte nucleus, enriched at the posterior pole (Januschke et al., 2006), and possibly along the entire oocyte cortex between stages 8 and 10 (Cha et al., 2002; Nashchekin et al., 2016).

b) Centrosome maturation and activity

Centrosome maturation is distinct from centriole maturation which consists of acquiring distal and subdistal appendages on the mother centriole (Marthiens and Basto, 2020). On the other hand, centrosome maturation corresponds to PCM expansion that occurs through the recruitment of many core scaffolding proteins, microtubule-associated proteins (MAP), and microtubule nucleating complexes (Pimenta-Marques and Bettencourt-Dias, 2020). Therefore, the PCM considerably increases in size during mitosis and gives centrosomes their capacity to nucleate microtubules (Bornens, 2021). Centrosome size varies as it is influenced by the amount of Cnn incorporated into PCM (fig III. 2) (Conduit et al., 2010).

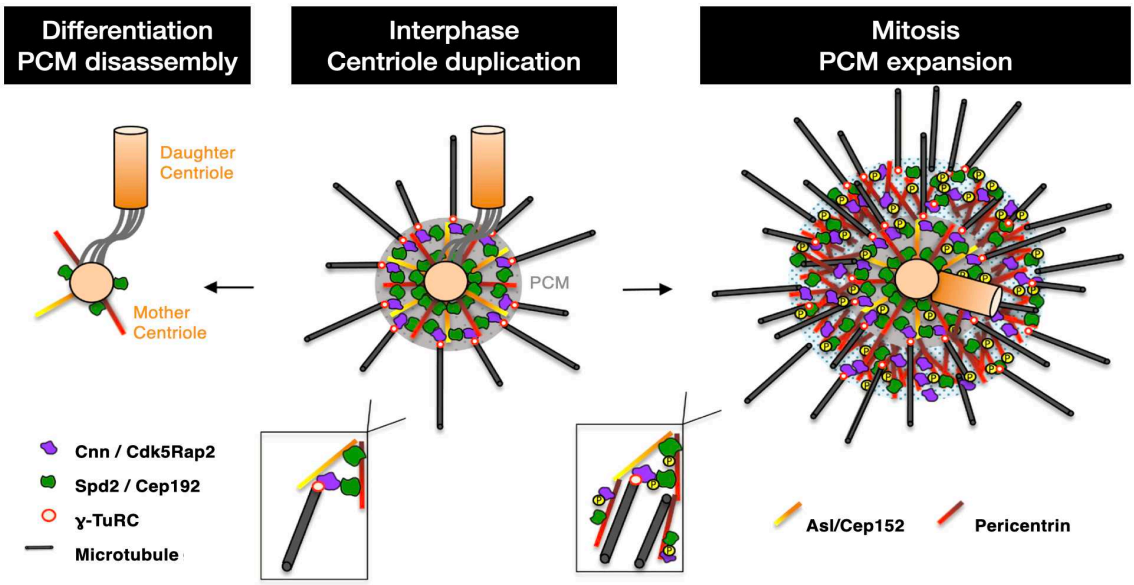

Figure III. 2: Centrosome maturation and disassembly upon mitotic division and cellular differentiation, adapted from (Fry et al., 2017)**.** (Left) During cell differentiation, centrosomes are often inactivated and therefore the PCM surrounding the two centrioles is disassembled. (Center) During interphase, the centrioles duplicate and the original daughter centriole will become a mother centriole that will also recruit PCM components upon mitosis. (Here the representation shows unduplicated centrioles). The PCM size is influenced by the recruitment of Cnn/Cdk5Rap2, Pericentrin and Spd2/Cep152. These proteins extend from the centriole to the outside and therefore generate a matrix on which more proteins can be recruited providing anchoring sites for ɣ-TuRC. (Right) During mitosis, the PCM expands as the centrosome matures, which requires phosphorylation of PCM components by Polo/Plk1. This phosphorylation is necessary to recruit more proteins to induce the nucleation capacity of the centrosomes.

During mitosis in *Drosophila* syncytial embryos, Asl initiates the recruitment of Spd2 and Cnn to mother centrioles. Asl and Spd2 assemble into a scaffold-like structure which promotes the recruitment of other proteins. Cnn molecules are continuously recruited in the center of the PCM close to centrioles, then moves slowly outward to form a scaffold that recruits more PCM components. While Spd2 recruits Cnn, Cnn in return maintains Spd2 within the PCM, creating a positive-feedback loop that maintains the PCM expansion (Conduit et al., 2014b).
Centrosome maturation is mainly regulated by the kinase Polo/PLK1 (Polo-like kinase 1), which recruits and phosphorylates PCM components such as D-PLP/Pericentrin, Spd2/Cep192, Cnn/CDK5RAP2 and maintain the PCM integrity (Conduit et al., 2014a) (Pimenta-Marques and Bettencourt-Dias, 2020). Polo contributes to the accumulation of ɣ-tubulin in the centrosomes as well. The role of Polo and PCM on centriole integrity depend both on a protein of the centriole wall, ANA1/CEP295 (Pimenta-Marques et al., 2022). The recruitment and phosphorylation of these PCM components ensure centrosome integrity and activity. In the next part, I will discuss how centrosomal activity can be down-regulated.

2. Centrosome migration and elimination during *Drosophila* oogenesis

a) Centrosome elimination or down-regulation

The activity and number of centrosomes are regulated along developmental processes and in post-mitotic differentiated cells, such as in muscles, neurons, and epithelial cells, in which centrosomes lose nucleation capacity to benefit other ncMTOC activities (Muroyama and Lechler, 2017). In interphase of *Drosophila* neuroblasts, prior to asymmetric division in which the mother and daughter centrioles are separated, mother centriole loses its microtubule-nucleation capacity, while daughter centriole remains active. The daughter centriole activity maintenance occurs via PCM retention in a Polo-dependent manner (Januschke et al., 2013). Conversely, mother centriole activity is down-regulated. These activity regulations can occur through different processes such as transcriptional changes affecting genes that encode centrosomal proteins; post-translational modifications of MAPs that interfere with the capacity to stabilize, anchor, or nucleate microtubules; or PCM components relocalization to other microtubule nucleation sites (Muroyama and Lechler, 2017). Studies have shown that decreased level or activity of specific proteins involved in centrosomal maintenance and function induces PCM component removal from the centrosomes. For example in the *Drosophila* oocyte, decreased levels of the main regulator of centrosomal activity, Polo/PLK1, is associated with a decrease of centrosomal activity (Pimenta-Marques et al., 2016). In *C. elegans* embryos, PCM component Spd2/Cep192 and the cell-cycle-dependent kinase (CDK) levels are decreased which leads to defective centrosomes (Yang and Feldman, 2015). During oogenesis of most metazoans, including human, fly, frog, and worm zygotes, maternal centrosomes go through a degenerescence phenomenon as centrosomes are inherited not from the egg but the sperm. Centriole elimination is a fundamental process which ensures the correct number of centrosomes and subsequent correct mitosis upon fertilization (Schoborg and Rusan, 2016). While the assembly and maturation of centrosomes are very well described, the mechanisms regulating their elimination or disassembly are less clear.

b) Centrosome accumulation in the *Drosophila* oocyte

The *Drosophila* oocyte is a fitting model to study centrosomes. In early oogenesis, each germ cell of the cyst comports two centrosomes as the cells are in the G2 phase and have duplicated their materials. In region 2b of the germarium, the centrosomes travel *via* the ring canals in a Dynein-dependent manner from the nurse cells to the posterior of the oocyte where they cluster into an MTOC (Bolívar et al., 2001; Mahowald and Strassheim, 1970). Variation of centrosome numbers from one oocyte to another is often seen, as in some cases the duplication is delayed or incorrect; some mother/daughter centrioles lose their reciprocal orientation and are distant from one another (Riparbelli et al., 2021). Therefore, the oocyte contains 16 to 32 centrosomes.
At stages 4-5 of oogenesis, centrosomes form compact clusters in the oocyte at the posterior of the nucleus. Their centriole length highly varies from 125nm to 217nm where Cnn accumulates (Bolívar et al., 2001; Megraw and Kaufman, 2000). The Cnn-stained MTOC remains in the vicinity of the nucleus until completion of its migration, after which, the morphology of the MTOC changes. Indeed, Cnn labeling reveals that MTOC disassembles from nucleus-associated bodies before migration, and reassembles into punctate at the anterior cortex after the migration (Megraw and Kaufman, 2000). Although centrosomes are required for early embryogenesis, it has been shown that centrosomes are not necessary for microtubule reorganization or mRNA localization and are therefore dispensable for oogenesis. This holds true as *Sas-4* mutants lacking centrioles and centrosomes go through normal oogenesis (Stevens et al., 2007). Moreover, in this context, the oocyte nuclear migration is not abolished either (Zhao et al., 2012), but the trajectories taken by nuclei are different (Tissot et al., 2017) (*see Chapter II 2.b*).

c) Centrosome elimination during *Drosophila* oogenesis

Recently, studies on centrosome elimination in *Drosophila* oocytes revealed that it occurs in a two-step process: PCM loss occurs first, and loss of centriolar proteins occurs at later stages until a complete elimination before the end of oogenesis (Pimenta-Marques et al., 2016). While all PCM components are detectable from the germarium until stage 6, a shift among these components seems to appear after completion of the nuclear migration stage. At this stage, some PCM components, notably Spd2, start to disappear and their loss is more important at later stages (Pimenta-Marques et al., 2016). The kinase Polo plays a key role in the maintenance of the oocyte centrosomes and its function is dependent on ANA1, a centriolar wall protein. While ANA1 is critical for centriole activity, Polo and the PCM are indispensable for centriole structure and centrosome function. Along oogenesis, PCM loss is associated with a decrease in Polo levels. Depletion of Polo in oogenesis induces a premature centriole elimination and an ectopic centrosome-targeted expression of Polo prevents PCM loss as well as centrosome elimination (Pimenta-Marques et al., 2016; Pimenta-Marques et al., 2022).

3. Relationship between the centrosomes and the nucleus

In several cell types, the nucleus and centrosomes are coupled and remain in close vicinity. Moreover, under specific processes like differentiation, cell migration, or cell polarization, the position of centrosomes in relation to the nucleus participates in the polarization of the cell (de Anda et al., 2005; Schliwa et al., 1999; Siegrist and Doe, 2006). The nucleus-centrosome coupling relies on mechanisms that involve the cytoskeleton. For example, in fibroblasts (Salpingidou et al., 2007) and astrocytes (Dupin et al., 2009), the distance separating centrosomes from the nucleus is increased under treatment with a microtubule inactivating drug such as nocodazole or taxol. In migrating neurons, a cage of microtubules surrounds the nucleus and links it to the centrosome via Dynein (Tsai and Gleeson, 2005). In these neurons, it has been described that the movement of centrosomes precedes the displacement of nucleus. Nesprins and the LINC complex are obvious actors connecting the nucleus and centrosome and in mediating force transmission between their respective components. In mammalian cells, Emerin, which interacts with the lamina and some Nesprins (Mislow et al., 2002; Zhang et al., 2005), has been shown to interact with β-tubulin and centrosomal microtubules. In this case, Emerin localizes on the outer nuclear membrane or on the endoplasmic reticulum and anchors centrosomal microtubules to the outer nuclear membrane (Salpingidou et al., 2007). Therefore, loss of Emerin in these cells induced the separation between the nucleus and centrosomes. Microtubule-associated motors are also highly involved in nucleus-centrosomes coupling. Dynein localizes at the nucleus of dividing cells, in G2 phase, thanks to an interaction with Bicaudal2, which binds to RanBP2, a nucleoporin of the NPC cytoplasmic face (Splinter et al., 2010). Dynein can therefore bring and maintain closer the centrosomes to the nucleus as it is associated with the nucleus and pulls on the centrosomes-associated microtubules (Salina et al., 2002). In neural stem cells, Dynein is recruited to the NPC via Nup133/Cenp-F and maintains its association between the nucleus and centrosomes during apical migration of the interkinetic nuclear migration (Baffet et al., 2015; Hu et al., 2013). While Dynein is often described to maintain centrosomes in close vicinity of the nucleus by exerting pulling forces on microtubules, Kinesin-1 has been described in mechanisms that mediate the separation of nucleus-centrosomes. For example, in epithelial cells, Kinesin-1/KIF5 is recruited to the NE via an interaction with Nesprin4, and promotes nucleus-centrosomes separation (Roux et al., 2009). This mechanism could be involved in the polarization of epithelial cells by driving centrosomal migration to the apical and positioning the nucleus on the basal side. However, in some cases, kinesins ensure nucleus-centrosome coupling. In Dictyostelium, Kif9 localizes at the NE where it is anchored and interacts with Sun1, and its cytoplasmic motor domain binds the microtubules. Kif9 is M-type kinesin and is capable of microtubule depolymerization activity. Therefore, by depolymerizing centrosome-associated microtubules, Kif9 pulls on the centrosomes bringing them close to the nucleus (Tikhonenko et al., 2013). Furthermore, Kif9 depletion causes a generation of supernumerary centrosomes and subsequently altered mitosis.

The importance of nucleus-centrosome association is required for their respective positioning and their position contribute to cell polarity. Additionally, the need for centrosomes to be close to the genetic material at the onset of mitosis facilitates the attachment of centrosomes to the chromosomes (Bornens, 2008). In the *Drosophila* oocyte, nucleus-centrosome coupling seems to be microtubule-dependent as the nucleus and centrosomes were significantly separated under microtubule depolymerization using colchicine (Januschke et al., 2006). Furthermore, the oocyte NE often displays an indentation and this nuclear deformation has been correlated with centrosomal microtubules that exert pushing forces on the nuclear surface, indicative of a close relation along the nuclear migration (Zhao et al., 2012). Although, altering centrosomes did not affect nucleus asymmetrical positioning, it did affect nuclear trajectories (Tissot et al., 2017).

CHAPTER IV : MUD IN CELLULAR POLARITY

Mud has been identified as one of the key proteins involved in the oocyte nucleus migration during oogenesis in *Drosophila* (Tissot et al., 2017). Mud is the acronym of Mushroom body Defect. The Mushroom Body is a structure in the fly brain that is notably responsible for olfactory memory. *Mud* gene was identified for its importance in the development of this structure, and its mutation is known to induce an abnormal proliferation of neuroblasts, an odor learning deficit in the subsequent mutant flies, and sterility only in the female fly (de Belle and Heisenberg, 1996; Yu et al., 2006). In this final chapter, I will review the characteristics of this MAP, from its homologs and their functions to its association with the nucleus. Finally, I will discuss what is known about the role of Mud in the fruit fly oogenesis.

1. Mud/NuMA/LIN-5

a) Homology

The *Drosophila* protein Mud is the functional homolog of Nuclear Mitotic Apparatus (NuMA) in vertebrates and abnormal cell LINeage 5 (LIN-5) in *C. elegans* (Bowman et al., 2006). Although their sequence homology is not identical, these three proteins share a similar molecular architecture and functions. The *NuMA* gene encodes several isoforms that differ due to alternative splicing (Compton et al., 1992; Tang et al., 1993; Yang et al., 1992; Zeng, 2000). These isoforms have been classified into two groups: the first one consists of two isoforms of approximatively 240kDa and not functionally different. The second group contains two other isoforms of 190kDa that differ in their C-terminal region. Furthermore, the second group is particular as they lack NLS. NuMA is composed of two globular domains in the amino-terminal (N-terminal) and carboxyl-terminal (C-terminal) regions that are separated by a long coiled-coil domain forming an α-helix. The N-terminal region has Calponin Homology (CH) domains, and a Dynein interaction domain. The C-terminal region is capable of binding the protein LGN and the microtubules, but also contains an NLS and chromatin interaction motifs (fig IV. 1) (Du et al., 2001; Gueth-Hallonet et al., 1996; Haren and Merdes, 2002; Kiyomitsu and Boerner, 2021).

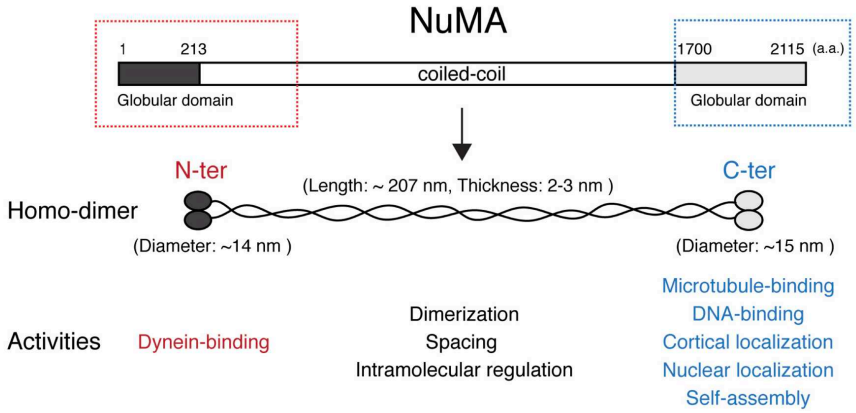

Figure IV. 1: Representation of NuMA's protein domains, adapted from (Kiyomitsu and Boerner, 2021). NuMA can homodimerize via its central coiled-coil region. N-terminal and C-terminal globular structures allow interactions with factors, such as Dynein and microtubules, DNA, and importins respectively.

Although the N-terminal similarity between Mud and human NuMA sequences is low, this region is predicted to adopt a similar CH structure (fig IV. 2). Like NuMA, Mud N- and C-terminals are separated by a long coiled-coil domain (Guan et al., 2000). The coiled-coil domain favors protein interactions but also homodimerization. The C-terminal sequence is more conserved, with the highest similarity in the Pins domain (Partner of Inscuteable, the *Drosophila* homolog of LGN) and microtubule binding region, with a conserved motif called NuMA/LIN-5/Mud (NLM) homology domain (Bowman et al., 2006; Siller et al., 2006).

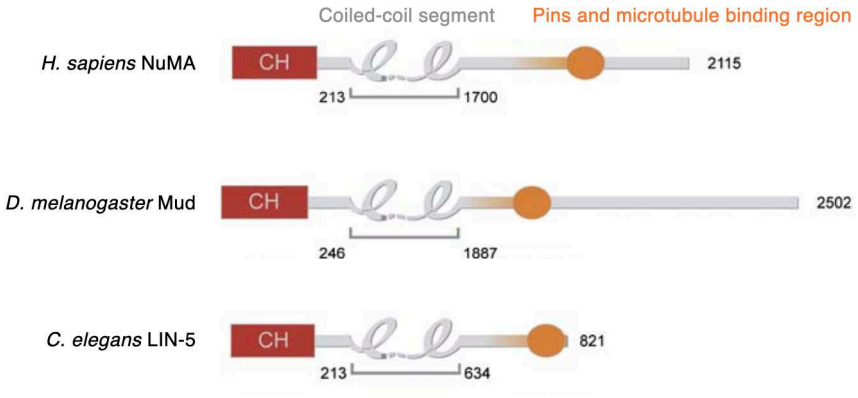

Figure IV. 2: Structural similarities between NuMA, Mud and LIN-5, adapted from (Bowman et al., 2006). Shared molecular architecture of the NuMA sequence homologs in human (*H. sapiens*), fly (*D. melanogaster*), and worm (*C. elegans*). In their N-terminal, the proteins have Calponin Homology (CH) domains followed by long coiled-coil segments, and a highly conserved region that binds the Pins protein and the microtubules at their C-terminal.

The *Drosophila mud* gene encodes for 7 splicing variants (Bosveld et al., 2016; Guan et al., 2000; Zeng, 2000). Like NuMA, Mud has an α-helix core that separates the N-terminal and the C-terminal regions to form globular domains. The N-terminal and core regions are encoded by exons 1-6 and are common to all Mud isoforms, while most differences are observed in the C-terminal region encoded by exons 7-12. The N-terminal region is characterized by the presence of CH domains that are known to interact with microtubules and actin (Yin et al., 2020) (fig IV. 3).
The C-terminal region display two putative transmembrane domains, suggesting that Mud can be associated with membranes. While NuMA bipartite NLS has been characterized, the literature does not describe NLS for Mud nor LIN-5 (Bowman et al., 2006; Gueth-Hallonet et al., 1996).

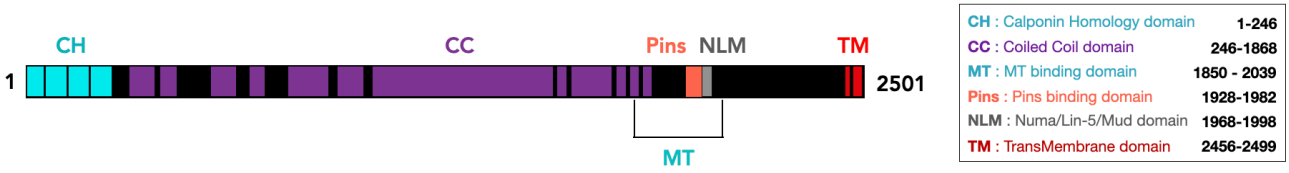

Figure IV. 3: Scheme representing Mud protein domains. In N-terminal region, Mud displays four Calponin Homology (CH) domains, followed by a long coiled-coil domain. A microtubule-binding domain (MT) in C-terminal overlaps with a conserved motif between NuMA/Lin-5/Mud (NLM) and a domain of interaction with the Partner of Inscuteable protein (Pins), the *Drosophila* homolog of LGN. Two putative transmembrane domains have been identified by *in silico* analysis.

b) Cellular localization

NuMA cellular distribution is cell cycle-dependent and regulated by phosphorylations (Compton and Luo, 1995). NuMA displays two different localizations: at the spindles during mitosis and within or around the nucleus during interphase (Lydersen and Pettijohn, 1980). At the onset of mitosis/meiosis, NuMA translocates to the spindles where it is required to focus microtubules and orientate the spindle to ensure correct divisions (Zeng, 2000). In *Drosophila* neuroblasts, during asymmetric cell division, Mud localizes at the cellular cortex in a Pins-dependent manner and also orientates the mitotic spindles (Bowman et al., 2006). The dual localization is also observed for Mud in the *Drosophila* syncytial embryos (fig IV. 4) (Yu et al., 2006).

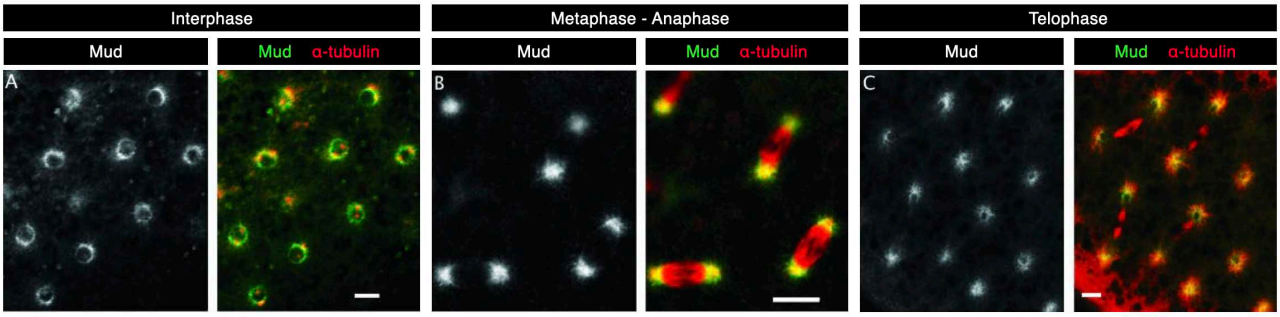

Figure IV. 4: Evolution of Mud distribution along the cell cycle of wild-type *Drosophila* syncytial embryos, adapted from (Yu et al., 2006)**.** Immunofluorescence against Mud and α-tubulin during interphase (A), where Mud localizes around the NE while the α-tubulin is found on the two centrosomes. (B) During metaphase and anaphase, Mud localizes at the spindle poles and on astral microtubules. (C) At the end of mitosis, in telophase, Mud returns to the nascent NE. Bars, 10 µm.

2. Mud/NuMA/LIN-5 associated with the microtubules

Like NuMA, Mud interacts with α-tubulin, stabilizes minus ends of microtubules, and enhances their polymerization (Bowman et al., 2006; Du et al., 2002). Interaction with the microtubule minus end directed motor Dynein is also conserved from NuMA to Mud, and requires the homodimerization feature of the MAP. Together with Dynein, NuMA/Mud can then cross-link microtubules which allows the orientation and organization of the spindles (Forth et al., 2014).
Mud is required for spindle positioning and orientation (Bowman et al., 2006; van der Voet et al., 2009; Yu et al., 2006). In *mud* mutants missegregation of cell fate determinants and defective asymmetric divisions are observed (Bowman et al., 2006). The positioning of the spindle involves an evolutionarily conserved mechanism that requires both cytoplasmic Dynein and a ternary complex composed of NuMA-LGN-Gα in humans, LIN-5-GPR-1/2-Gα in *C. elegans* and Mud-Pins-Gαi in *D. melanogaster* (Dammermann et al., 2003; Du et al., 2001; Galli and van den Heuvel, 2008; Kotak, 2019; Merdes et al., 1996; Srinivasan et al., 2003). This apical complex attaches the spindle astral microtubules to the plasma membrane and exerts pulling forces on it, due to the minus end motor Dynein and therefore orientates the spindle (fig IV. 5). Indeed, Gαi is anchored to plasma membrane and binds LGN/GPR-1/2/Pins, which interacts with NuMA/LIN-5/Mud, which in turn interacts with Dynein (Bergstralh et al., 2017; Bowman et al., 2006; Du et al., 2001).

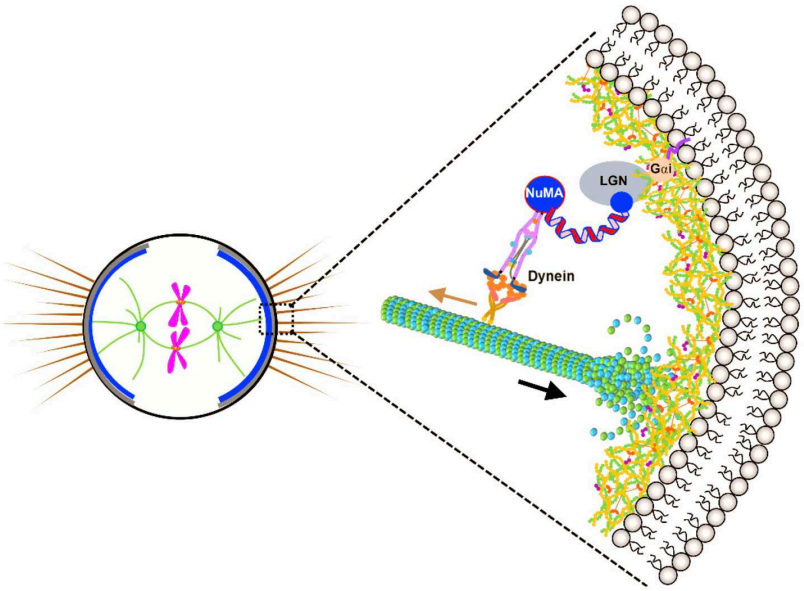

Figure IV. 5 : NuMA spindle orientation and positioning, from (Kotak, 2019)**.** In the meiotic or mitotic cell, thanks to LGN/Pins, NuMA/Mud localizes at the spindle poles and at spindle cortex (represented in blue on the left part of the scheme). LGN/Pins is attached to the cortex as it interacts with the Gαi small proteins. In turn, NuMA/Mud interacts with Dynein which directly bind the free astral microtubules and exert pulling forces on it. The microtubules are therefore pulled towards the cortex, where their plus ends depolymerize. Altogether, this mechanism is required to position and orientate the spindle which in turn correctly position the chromosomes before their segregation.

It has been shown in *C. elegans* that the rotation of the meiotic spindle requiring LIN-5 and Dynein can occur independently of the complex that they form with GPR and Gα, but with Abnormal spindle-like microcephaly associated (ASPM-1) and Calmodulin (CMD-1) (van der Voet et al., 2009). Although cortex localization of LIN-5 is independent of CMD-1 and ASPM-1, its localization at the spindle requires them. Indeed, CMD-1 interacts ASPM-1 and recruits LIN-5 at the meiotic and mitotic spindle poles. The ternary complex recruits Dynein which controls spindle rotation.

3. NuMA/LIN-5/Mud associated with the nucleus

During interphase, NuMA/LIN-5/Mud localize in the nucleus or at the NE rim. While the role of Mud at the nucleus in *Drosophila* has not been investigated, different studies on its human homolog NuMA proposed that this controlled localization is an alternative mechanism to regulate spindle-associated functionality by sequestering it within the nucleus. Studies also suggest important nuclear roles of NuMA, notably in its nuclear integrity, assembly, and architecture. Moreover, nuclear roles of NuMA are independent of its spindle functions (Serra-Marques et al., 2020). NuMA is critical during mitosis and interphase, notably in reformation of the NE, and maintenance of the nuclear shape (Compton and Cleveland, 1993; Merdes and Cleveland, 1998). The nuclear MAP has been also shown to be involved in chromatin organization in the nucleus (Abad et al., 2007; Kivinen et al., 2010). At mitotic exit, NuMA ensures that the genetic material is decondensed and enclosed in a single and spherical nucleus (Rajeevan et al., 2020). The C-terminal region of NuMA not only contains an NLS but also some DNA binding sites, which were shown to regulate the interaction between NuMA and chromatin (Kiyomitsu and Boerner, 2021; Serra-Marques et al., 2020).

4. Mud during oogenesis in *D. melanogaster*

Generally, the spindle associated function of the MAP is conserved in *Drosophila* and is particularly necessary for oocyte meiosis. The sterility induced by *mud* depletion only affects the females (de Belle and Heisenberg, 1996; Yu et al., 2006). It has been proposed that Mud is necessary in the female meiosis II which lacks centrosomes, for its role in the focusing of the meiotic spindle microtubules and for meiosis completion (Yu et al., 2006). In the germarium, Mud is detected at the oocyte NE (Yu et al., 2006) and has been shown to be required for synaptonemal complex assembly, which guides the pairing of homologous chromosomes at the onset of meiosis (Christophorou et al., 2015). During mid-oogenesis, Mud localizes asymmetrically around the nucleus and co-localizes with Cam (Calmodulin), Asp (Abnormal Spindle) and Dynein Light Intermediate Chain (Dlic) (Tissot et al., 2017; Yu et al., 2006; Zhao et al., 2012). These proteins together with Mud display an asymmetric distribution with an enrichment on the nuclear posterior hemisphere before and during nuclear migration. ASP/ASPM-1 interacts with NuMA/Lin-5 and is required for meiotic and mitotic spindle focusing and organization, nuclear migration in the neuroepithelium (van der Voet et al., 2009). Interestingly, in the *Drosophila* oocyte, Asp (homolog of ASP and ASPM-1) is asymmetrically distributed around the NE similarly to Mud (Tissot et al., 2017). Moreover, under Asp depletion in the germ cells, Mud is no longer asymmetrically distributed around the oocyte NE, but isotropically (Tissot et al., 2017). Finally, the oocyte nuclear trajectory proportions are similar in depleted Asp and depleted Mud contexts, with a decrease of the posterior route. Altogether, these results suggest an importance of Mud asymmetry in the regulation of oocyte nuclear trajectory. Guichet and colleagues have shown by high resolution Structure Illumination Microscopy (SIM) that Mud is closely associated with the oocyte NE as it co-localizes with nucleoporin Nup-107 (fig IV. 6 A,A') (Tissot et al., 2017). More recently, they achieved higher precision using electronic microscopy. They observed that Mud is associated with the outer nuclear membrane of the oocyte nucleus (Bernard et al., 2021). Moreover, in addition of its asymmetry, Mud detection reveals a patchy signal at the NE and co-localizes with NPCs (fig IV. 6 B-C').

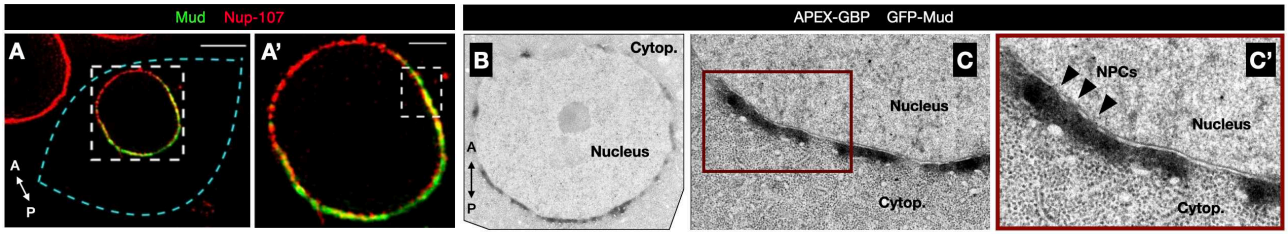

Figure IV. 6 : Mud association with the oocyte nucleus, adapted from (Bernard et al., 2021; Tissot et al., 2017)**.** (A, A') Structured Illumination Microscopy showing a co-localization between Mud and Nup-107 at the oocyte NE (Bar A, 1µm. Bar A', 500nm. Orientation of the oocyte is indicated with A (anterior) and P (posterior). (B,C,C') Electron microscopy of GFP-Mud using APEX-GBP (Ascorbate Peroxydase - GFP Binding Protein) reveals that Mud localizes at the outer nuclear membrane of the oocyte NE, in close association with the Nuclear Pore Complexes (NPCs) indicated by the arrows. Moreover, Mud signal is absent in the NE regions devoid of NPCs.

Investigating how Mud asymmetry is regulated, Guichet and colleagues have shown that it is independent of the oocyte centrosomes which accumulate at the posterior of oocyte in between the plasma membrane and the nucleus, where Mud is enriched (*see Chapter III 2.1*) (Tissot et al., 2017). Interestingly, the microtubule nucleation sites at the oocyte NE is asymmetrical as well. Indeed, the nucleation asters were enriched on the posterior hemisphere two fold more than on the anterior hemisphere (Tissot et al., 2017).

Although no NLS sequences have been described for Mud, it has been shown by co-immunoprecipitation that the protein interact with the Importin β (Wee et al., 2011). Moreover, the authors proposed that this interaction is also a way to sequester Mud as it prevents the interaction between Mud and Pins. Interestingly, the Importin β, named Fs(2)Ket in the fly, localizes mainly to the NE during the cell cycle of the early embryo (Trieselmann and Wilde, 2002), and studies have shown its capacity to bind microtubules (Hughes et al., 2008; Tirián et al., 2003). Given the properties of NuMA/Mud to enhance the microtubule polymerization (Bowman et al., 2006), I developed an exciting hypothesis that Mud is involved in the establishment of the ncMTOC at the oocyte nucleus. I sought to more specifically understand the mechanisms by which Mud regulates the nuclear migration in the oocyte of *Drosophila*.

RESULTS

AIM OF THE PHD PROJECT

Tissot et al., have shown that both oocyte centrosomes and the protein Mud are involved in the trajectory regulation of nuclear migration during oogenesis (*see Introduction Chapter II. 2.b*) (Tissot et al., 2017). These experiments show that centrosomes preferentially control the trajectory along the anterior plasma membrane, while Mud favors the trajectory along the posterior plasma membrane of the oocyte. The depletion of Mud combined with centrosome inactivation causes an inhibition of nuclear migration in 50% of egg chambers. The aim of my PhD project was to characterize the molecular mechanisms by which both centrosomes and Mud contribute to control of oocyte nuclear migration at mid-oogenesis in *Drosophila melanogaster*. Several questions were raised and constituted different axes of the research plan.

As Asp depletion induces a loss of Mud asymmetry and a phenocopy of *mud* mutant nuclear trajectories (Tissot et al., 2017), we hypothesized that Mud asymmetry was necessary for the regulation of nuclear migration. Therefore, I aimed to understand how asymmetry of Mud is established. How does Mud localize at the oocyte NE? Are Mud localization and asymmetry important for its function in the nuclear posterior trajectory regulation? What are Mud protein partners involved in this process? Finally, as the nucleation sites of the oocyte NE display an asymmetry around the nucleus and are enriched where Mud is enriched, we wondered if Mud acts as a scaffolding protein and recruits the complexes necessary to establish a ncMTOC at the NE that participates in nuclear trajectory control.

As the oocyte centrosomes have been shown to be active during the nuclear migration (Tissot et al., 2017), an important question is: How do centrosomes coordinate together to favor a unique migratory route for the oocyte nucleus displacement? What is their behavior prior to and along nucleus migration? Preliminary data of the lab suggested an effect of the microtubule associated motor Kinesin-1 on centrosome clustering. Moreover, its heavy chain subunit (Khc) has been shown to be necessary for the maintenance of the asymmetrical position of the oocyte nucleus after its migration (Januschke et al., 2002; Palacios and St Johnston, 2002). However, the role of Kinesin-1 on nuclear positioning prior to migration and for the migration has not been investigated yet. Therefore, I also aimed to assess the role of Kinesin-1 on the oocyte nucleus migration and characterize the mechanisms regulated by Kinesin-1 regarding centrosome behavior.

PART 1 : MUD IN THE OOCYTE NUCLEAR MIGRATION

In this part, I will present the results I obtained to investigate by which mechanisms Mud regulates the oocyte nuclear posterior trajectory.

CHAPTER I : MUD ASYMMETRY IMPORTANCE

Our lab has described Mud asymmetry at the NE with an enrichment on the nuclear hemisphere facing the oocyte posterior plasma membrane, which remains along nuclear migration (Tissot et al., 2017). They showed that Asp depletion affects Mud asymmetry, and phenocopies the nuclear trajectory proportions observed in the *mud* mutant (Tissot et al., 2017). Like Mud, Asp is asymmetrically distributed around the oocyte NE and enriched on the posterior nuclear hemisphere. I hypothesized that Mud asymmetry was required for its function in nuclear trajectories regulation during migration. Therefore, I aimed to investigate how Mud asymmetry is established and if this feature is important for the control of nuclear trajectories.

1) Genetic tools to study Mud in the *Drosophila* oocyte

a) Genetic tools

In order to study Mud localization at the oocyte NE, I used different transgenic fly strains that were generated by the Bellaiche lab (Bosveld et al., 2016). These strains express GFP-tagged Mud deleted for different permutations of its domains. The constructs have been generated by recombineering transgenesis using a Bacterial Artificial Chromosome (BAC) which allows site specific insertion of large DNA fragments in *Drosophila* genome (Venken and Bellen, 2007). These transgenes were inserted either on the second chromosome at locus 50E1 or on the third chromosome at locus 65B2, under the control of the *mud* endogenous promoter. In order to avoid over expression of Mud, these transgenesis have been realized in a *mud* null context (mud^4). The CRISPR-Cas9 system (Gratz et al., 2013), which allows precise genomic modifications, has been used at the endogenous *mud* locus to generate a construct deleted of MT and Pins domains ($Mud^{\Delta C}$ called here after $Mud^{\Delta MT}$) (Bosveld et al., 2016). Conversely to all these transgenic strains, $mud^{\Delta CH}$ and $mud^{\Delta MT}$ are not tagged with GFP. As GFP tag has been placed in N-terminal before the CH domains which are common to all the isoforms, all the isoforms expressed in the fly ovary should be detectable. Therefore, we have the following forms of Mud in our toolbox (fig I. 1).
First, I validated the use and the function of these GFP-Mud forms as they rescued the female sterility induced in the *mud* null mutant. All the strains are fertile, except $GFP\text{-}mud^{\Delta CC}$. The CC domain corresponds to a large deletion of Mud coiled-coil domain which is known to be important for the structure of the protein and interactions with partner. This observation indicates the importance of the CC domain for Mud functionality.

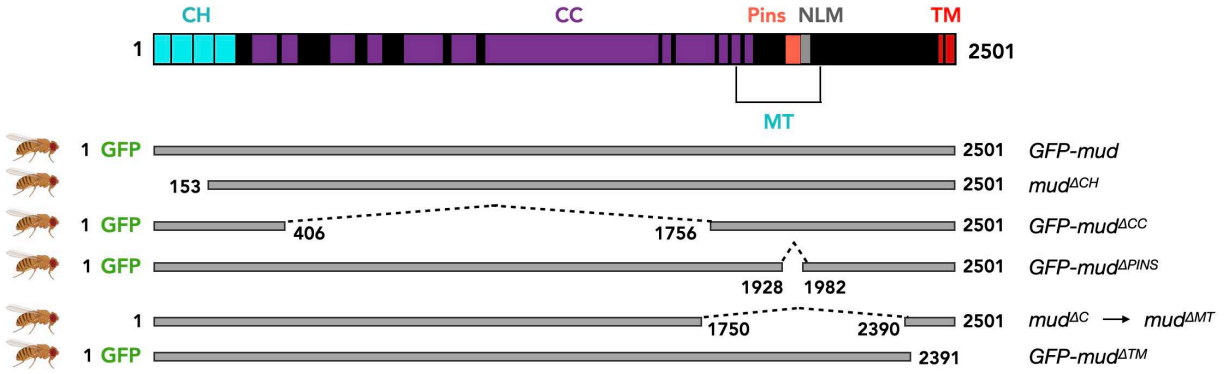

Figure I. 1: Scheme representing the deleted domain of the transgenic flies expressing the respective versions of GFP-Mud. The scheme is based on the longest isoform of Mud. (Top) Mud is a 2501 amino acid (aa) protein and is composed of Calponin Homology (CH) domains (1-246) in N-terminal region, a long Coiled-Coil (CC) domain (246-1868), a Pins binding domain (Pins) (1928-1982), a microtubule binding domain (MT) (1850-2039), a conserved motif NuMA/Lin5/Mud (NLM) (1968-1998), and of putative transmembrane domains (TM) (2456-2499) in C-terminal. (Bottom) Scheme of the different versions of Mud tagged GFP in N-terminal, except for the *mud*$^{\Delta CH}$ and *mud*$^{\Delta MT}$ strains which are not GFP-tagged. All these transgenes were generated by recombineering BAC transgenesis, except *mud*$^{\Delta MT}$ (originally called *mud*$^{\Delta C}$) which has been generated using CRISPR-Cas9 system (Bosveld et al., 2016).

b) Mud asymmetry measurement method

Under the constrains of microtubule pushing forces, it was shown that the oocyte NE can display an indentation on its posterior nuclear hemisphere (fig I. 2.A^1-A^2) (Tissot et al., 2017; Zhao et al., 2012). I wanted to verify that Mud asymmetry was not biased by the nuclear indentation on the posterior hemisphere. To do so, I measured the fluorescence levels on the oocyte nuclear contour of Fs(2)Ket-GFP (Female sterile 2 Ketel) as control, corresponding to Importin-β in the fly which localizes around the oocyte NE, and compared it to the GFP-Mud^{65B2} profile (fig I. 2.B-C). While the Fs(2)Ket-GFP curve displays almost no variation between the two hemispheres, the profile of GFP-Mud^{65B2} fluorescence intensity per pixel shows an increase at the posterior and a decrease at the anterior nuclear hemisphere. These results show that nuclear indentation does not create an artifact regarding Mud asymmetry at the oocyte NE.

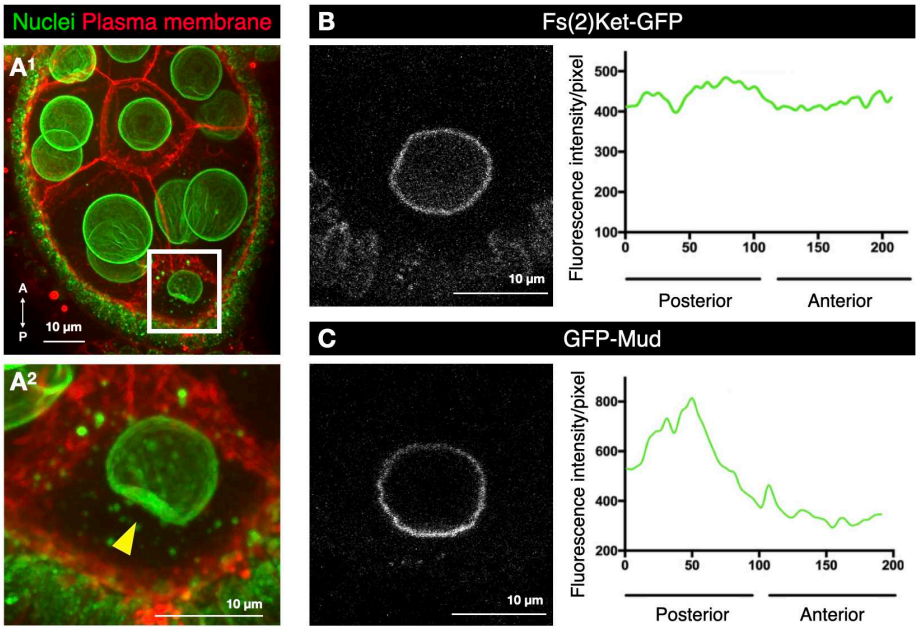

Figure I. 2: Mud asymmetry is not biased by the nuclear indentation. (A^1) Z-projection of WT egg chamber expressing the transgenes Fs(2)Ket-GFP and PH-RFP to label the nuclei and plasma membranes, showing the oocyte nucleus indentation indicated by the yellow arrow in corresponding magnification (A^2). The orientation of the egg chamber is indicated by the arrow A (anterior), P (posterior). Bars, 10µm. (B-C) Representative images of Fs(2)Ket-GFP (B) and GFP-Mud^{65B2} (C) signal and respective graphs representing the intensity per pixel at the contour of the nucleus, distinguishing posterior and anterior hemispheres.

To analyze Mud asymmetry precisely, I wanted to detect Mud on the whole nuclear surface. To do so, I used a semi-automated macro developed in the lab using Fiji software. The macro consists of precisely defining the oocyte anterior and posterior nuclear hemispheres, and measuring Mud signal intensity on each hemisphere. To measure the signal on the whole nucleus, this macro requires a Z-projection of the acquired image stacks (fig I. 3). The percentage of Mud asymmetry on the posterior nuclear hemisphere corresponds to the ratio of fluorescent signal intensity measured on the posterior hemisphere regarding total signal intensity.

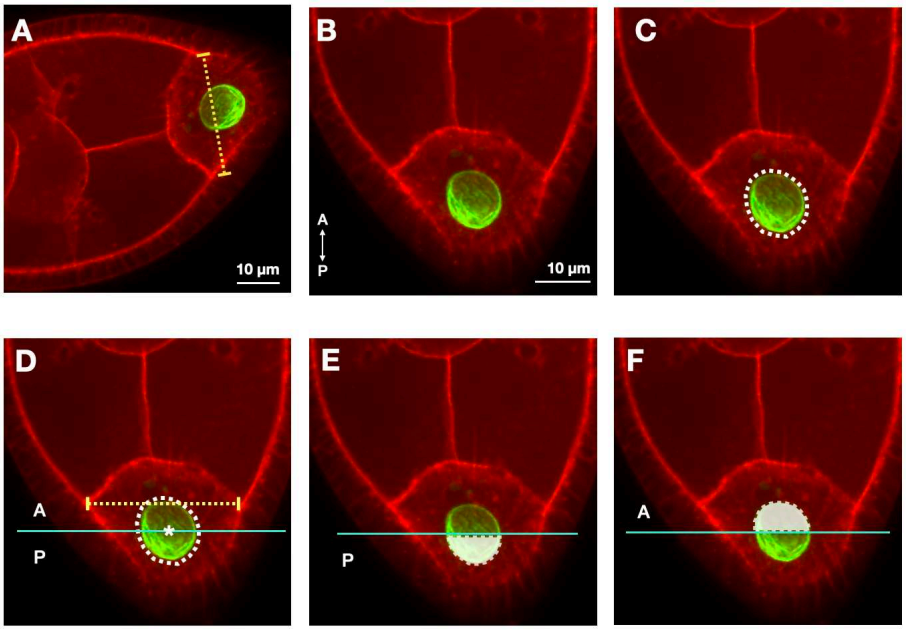

Figure I. 3: Mud asymmetry macro steps. (A) Definition of the axis crossing the anterior and posterior plasma membrane intersections. (B) Egg chamber orientation along the antero-posterior (A-P) axis. (C) Definition of the oocyte nucleus outlines. (D) From nucleus outlines, the macro determines the nuclear centroid (*) and automatically defines the A-P axis crossing the nucleus centroid and parallel to the first axis. This axis delimitates two equal nuclear hemispheres. (E-F) Definition of the outline of the posterior (E) and anterior (F) nuclear hemispheres. The macro measures the intensity of the pixels detected on each hemisphere.

c) Mud asymmetry at the oocyte nuclear envelope

Next, I aimed to compare transgenic GFP-Mud with WT Mud. To do so, I performed immunofluorescence on reference WT strain *w*^{1118} and *GFP-mud*^{65B2} using an anti-Mud antibody (fig I. 4). Mud antibody recognized a sequence in the CC domain that is common to the different isoforms (Izumi et al., 2006). First, these results indicate that Mud posterior asymmetry levels are similar between *w*^{1118} and *GFP-mud*^{65B2} when detecting the antibody signal. Second, these results show that Mud asymmetry was similar when measuring GFP-Mud or anti-Mud antibody signals. Therefore, I validated Mud detection by either GFP signal or antibody.

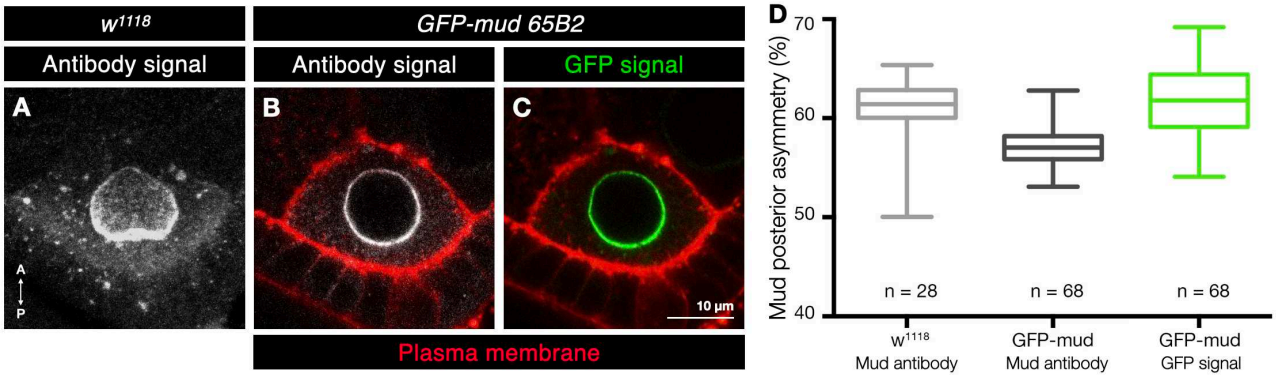

Figure I. 4: Validation of the genetic tools. (A-C) Immunofluorescence against Mud in a WT strain *w*^{1118} (A), and in *GFP-mud*^{65B2} strain detecting the antibody signal (B) or the GFP signal (C). (D) Corresponding quantifications of Mud posterior asymmetry at the oocyte NE. n indicates the number of analyzed egg chamber.

Then, I aimed to compare Mud asymmetry in either strain of locus 50E1 or locus 65B2 *GFP-mud* insertion (fig I. 5.A). The results show that Mud asymmetry level in *GFP-mud*^{50E1} was lower than observed in *GFP-mud*^{65B2} and *w*^{1118}. In order to verify the intensity levels of GFP-Mud in the transgenic strains, I measured the GFP intensity on the whole surface of the oocyte nucleus and observed a significant reduction in *GFP-mud*^{50E1} compared to *GFP-mud*^{65B2} (fig I. 5.B). Thus, 1) as GFP-Mud^{65B2} asymmetry level was closer to WT Mud asymmetry detected by the anti-Mud antibody, and 2) as the GFP intensity level in *GFP-mud*^{65B2} was higher than in *GFP-mud*^{50E1}, I decided to work with the strain expressing the constructs inserted on the third chromosome at locus 65B2 for the asymmetry analysis.

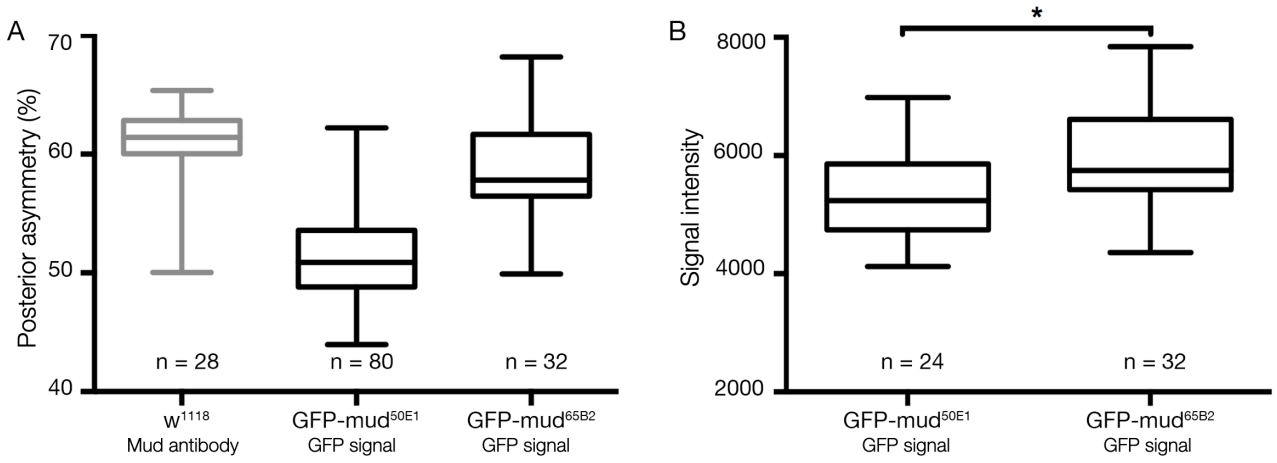

Figure I. 5: Difference of signal intensity between GFP-Mud^{50E1} and GFP-Mud^{65B2}. (A) Graph representing the quantification of Mud posterior asymmetry at the oocyte NE in control *w*^{1118} (detected by immunofluorescence using an antibody against Mud), in *GFP-mud*^{50E1} (detected by the GFP signal), or in *GFP-mud*^{65B2} (detected by the GFP signal). 50% of asymmetry corresponds to no difference of signal intensity on both hemispheres. Under 50%: anterior asymmetry. Above 50%: posterior asymmetry. (B) Graph represents the signal intensity of Mud detected on the nuclear surface of *GFP-mud*^{50E1} or *GFP-mud*^{65B2}. Mann-Whitney test, *$p < 0.05$.

2) Contribution of the Mud domains in its asymmetry

In a first approach to investigate how asymmetry of Mud is established, I assessed the contribution of each protein domain on Mud asymmetry. As mud$^{\Delta CH}$ and mud$^{\Delta MT}$ strains lacked a GFP tag, we generated the *GFP-mud*$^{\Delta CH}$ and *GFP-mud*$^{\Delta MT}$, as well as *GFP-mud* for a control, by CRISPR-Cas9 system at *mud* locus. I observed Mud asymmetry in the respective strains in either fixed egg chambers by immunofluorescence using anti-Mud antibody (except for GFP-Mud$^{\Delta CC}$ for which GFP is detected) (fig I. 6.A) or in living egg chambers detecting the GFP-Mud (fig I. 6.B). These observations show that the deletion of CH domain affects the asymmetry of Mud at the oocyte NE. Deletion of the CC domain phenocopies CH deletion as it is isotropically distributed around the NE in this contexts. Additionally, CC domain deletion induces a delocalization of Mud in the oocyte cytoplasm, as well as around the NE of the nurse cells adjacent to the oocyte. Pins domain deletion does not affect Mud asymmetry. Although the observation of Mud$^{\Delta MT}$ suggest that the protein is still asymmetric, it also displays a partial delocalization of Mud in the perinuclear region at the posterior of the nucleus. Moreover, in *mud*$^{\Delta CC}$ and *mud*$^{\Delta TM}$ contexts (fig I. 6.B), I observed partial delocalization of Mud in the cytoplasm of the oocyte, which is different to what was observed in *mud*$^{\Delta MT}$ condition.

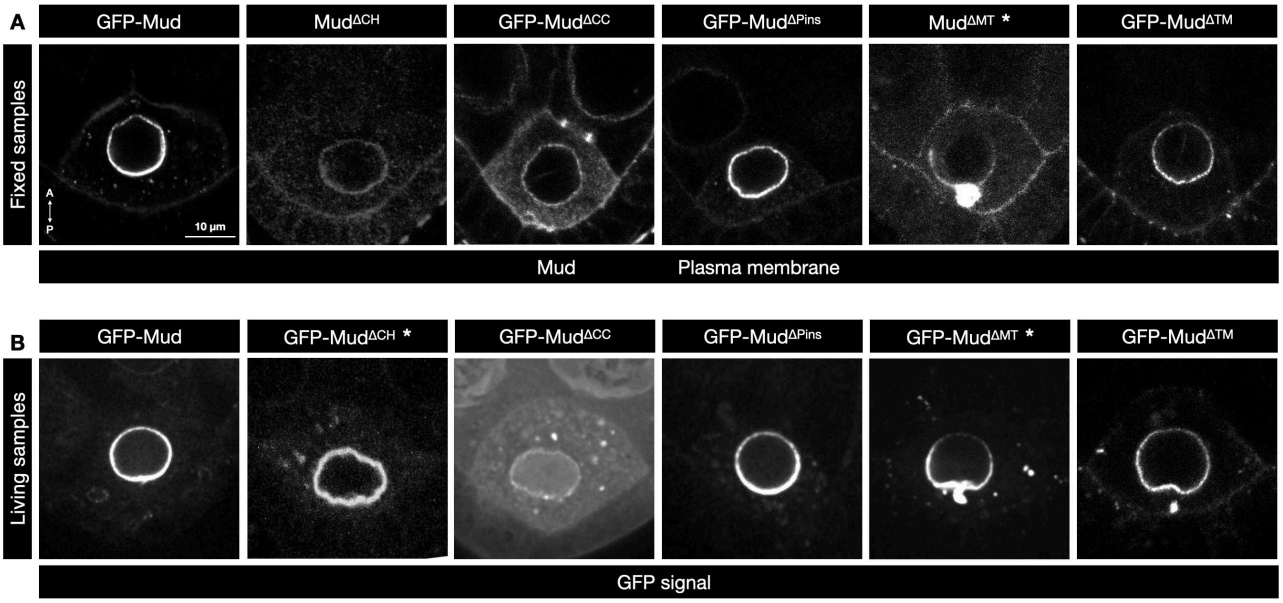

Figure I. 6: CH, CC, MT and TM domains are involved in Mud asymmetry. (A) Mud is detected by immunofluorescence using anti-Mud antibody, except for GFP-Mud$^{\Delta CC}$ for which the detected signal corresponds to GFP. The plasma membrane is labeled using phalloidin. (B) GFP signal detection in living egg chambers of the different strains. (*) Indication of the strains that have been generated by CRISPR-Cas9 technique, all the others strains have been generated by BAC. The orientation of the egg chamber is indicated by the arrow A (anterior), P (posterior). Bars, 10µm.

Next, I quantified Mud asymmetry in these strains, detecting either anti-Mud antibody (fig I. 7.A) or GFP-Mud (fig I. 7.B). As our anti-Mud antibody recognizes a sequence in the CC domain, I did not measure GFP-Mud$^{\Delta CC}$ asymmetry in fixed samples. As the deletion of MT domain causes a strong delocalization of Mud in contact with the NE, which would have interfere with the quantification, I did not quantify the asymmetry in this condition. These results confirm that the deletion of CH, CC and TM domains significantly affect Mud asymmetry compared to the control GFP-Mud. Further data indicate decreased intensity of Mud levels on the whole nuclear surface in *GFP-mud$^{\Delta CC}$* and *GFP-mud$^{\Delta TM}$* compared to *GFP-mud* (fig I. 8). These results reinforce CC and TM domain importance in Mud localization. I validated the use of CRISPR *GFP-Mud* and *GFP-mud$^{\Delta CH}$* and I observed the same asymmetry of Mud compared to the BAC strain *GFP-mud* and *mud$^{\Delta CH}$* (fig I. 9). Altogether, these experiments highlight the contribution of CH, CC, and TM domains in Mud asymmetry, and the contribution of MT domain in Mud localization at the oocyte NE.

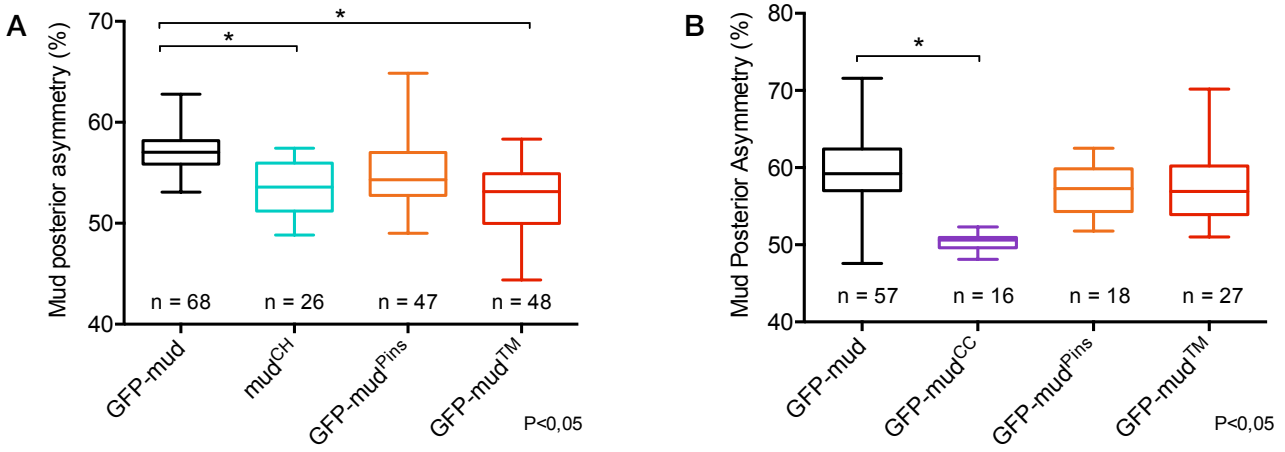

Figure I. 7: The domains CH, CC and TM are involved in Mud asymmetry. Quantifications of Mud posterior asymmetry at the oocyte NE measuring the antibody signal following an immunofluorescence against Mud (A), or the GFP signal of Mud in living egg chambers (B). Mann-Whitney test, *p < 0.05.

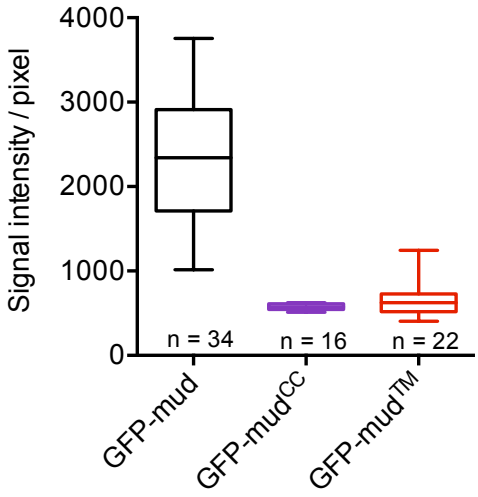

Figure I. 8: Deletion of CC and TM domains affecte Mud levels at the oocyte nucleus. Graph representing the signal intensity of Mud detected on the nuclear surface of *GFP-mud*, *GFP-mud$^{\Delta CC}$* and *GFP-mud$^{\Delta TM}$*.

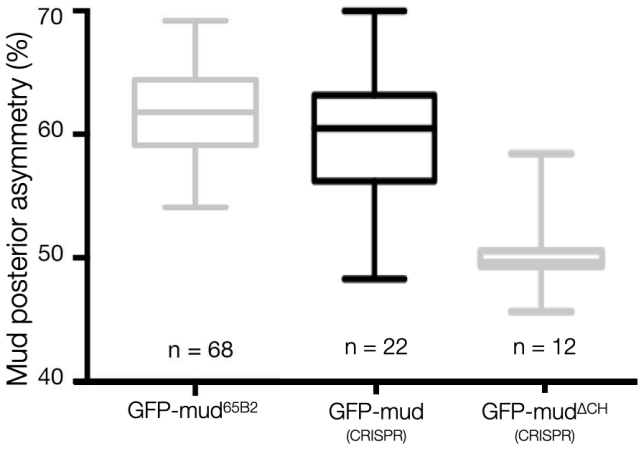

Figure I. 9: GFP-mud and GFP-mud$^{\Delta CH}$ generated by CRISPR Cas9 reproduce similar levels of asymmetry. Quantifications of Mud posterior asymmetry at the oocyte NE measuring GFP signal in *GFP-mud^{65B2}*, *GFP-mud* (CRISPR), and *GFP-mud$^{\Delta CH}$* (CRISPR).

3) Contribution of the microtubules in Mud asymmetry

a) Experimental condition settings

The CH and MT domains are involved in Mud asymmetry and localization at the oocyte NE. They are domains of interaction with the cytoskeleton elements or microtubules. Therefore, I aimed to investigate the direct role of microtubules on Mud asymmetry. To depolymerize microtubules in the *Drosophila* oocyte, I optimized experimental conditions for two Colcemid treatment protocols : ovary incubation with the drug or fly feeding with the drug (fig I. 10.A).

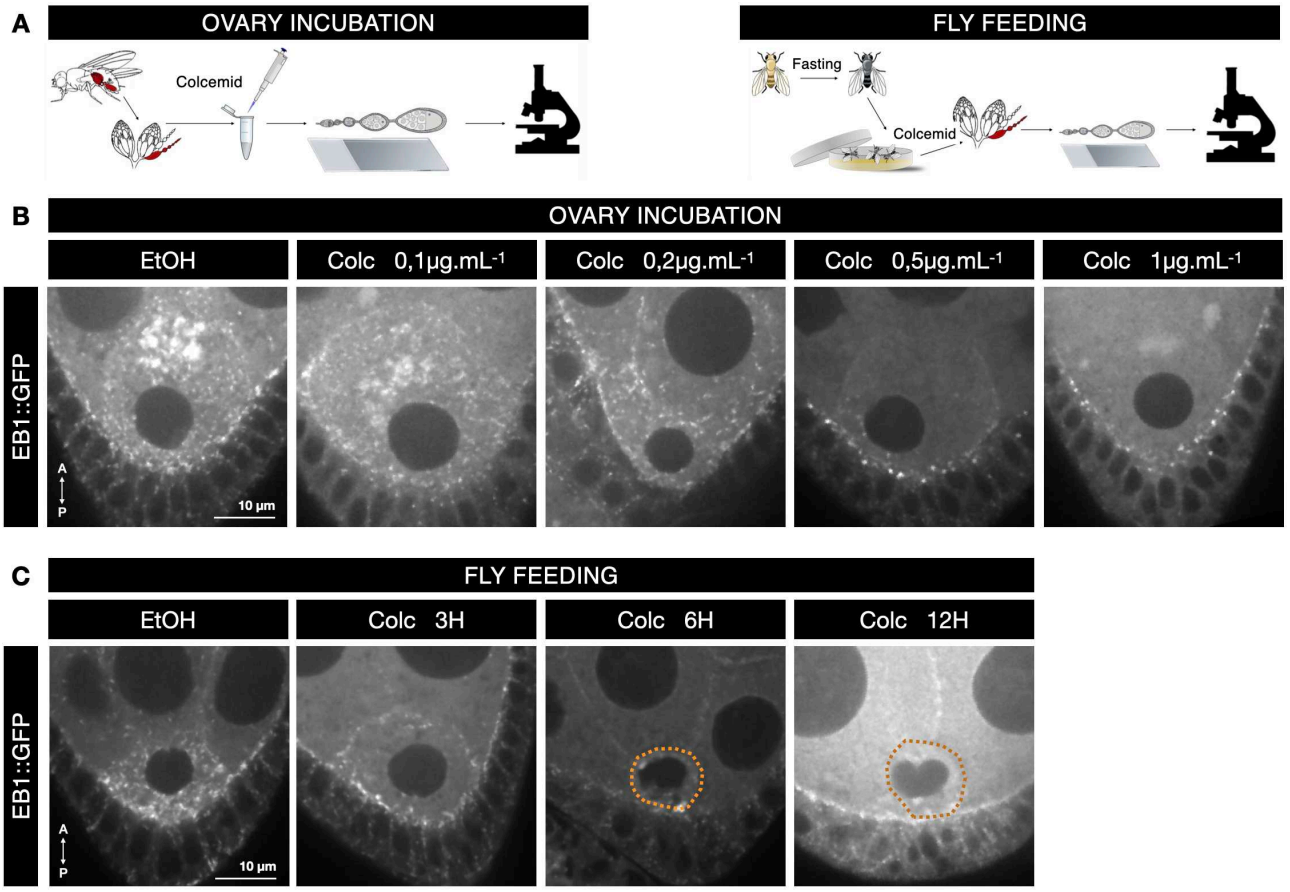

Figure I. 10: Experimental conditions for microtubule depolymerizing. (A left) Protocol of ovary incubation with Colcemid or Ethanol (EtOH). Dissected ovaries are incubated with Colcemid-containing media for 1 hour at 25°C. Then, living ovarioles are mounted on a coverslide and acquisitions are taken at the microscope. (A right) Protocol of fly feeding with Colcemid or EtOH. The flies are starved for 12 hours, then introduced in a cage containing Colcemid-containing food for 3h, 6h or 12h, then dissected living ovaries are mounted on a coverslide and acquisitions are taken at the microscope. (B-C) These condition were performed on flies expressing EB1::GFP in order to follow microtubule depolymerization state. (B) Different Colcemid-containing media concentrations and (C) different exposition times to the drug-containing food were tested. (C) Dotted line represents the anterior plasma membrane of the oocyte. The orientation of the egg chamber is indicated by the arrow A (anterior), P (posterior). Bars, 10µm.

As a control, I treated flies or ovaries with ethanol (EtOH), in which Colcemid is dissolved. To determine Colcemid concentration, I performed a dose-response experiment on flies expressing EB1::GFP, a microtubule plus end protein (fig I. 10.B) and I determined that 1µg.mL^{-1} Colcemid was the optimal condition to efficiently depolymerize the egg chamber microtubules without affecting its development and oocyte growth. Indeed, effects on oocyte growth would not be suitable for further quantifications and analysis on the nucleus. I noticed that 15 to 20 minutes after treatment, microtubules began to re-polymerize. This might be due to drug dilution when the egg chambers are mounted in the observation mounting oil. Therefore, I restrained the experimental window for the acquisitions to 15min after the mounting of the egg chamber in the oil. For the feeding protocol, I starved the flies 12h prior to the experiment, then incubate them with 1µg.mL^{-1} Colcemid-containing food for 3h, 6h or 12h. I determined that 3h of re-feeding with Colcemid food was the optimal condition to correctly depolymerize the oocyte microtubules, without affecting drastically oocyte growth and morphology as it is the case in the 6h and 12h conditions (fig I. 10.C).

b) Mud asymmetry maintenance is independent of microtubules

After optimizing my experimental conditions, I treated *GFP-mud* flies or their ovaries by feeding protocol or incubation protocol respectively, and measured Mud asymmetry at the oocyte NE. Quantifications show that microtubule depolymerization, either by ovary incubation or by fly feeding, does not affect Mud asymmetry, compared to the control (fig I. 11). Therefore, these results show that microtubules were not involved in Mud asymmetry. It is important to note that egg chamber development takes 6 days from GSC to stage 6 (He et al., 2011). Therefore, in our conditions, we did not impair the establishment of Mud asymmetry at the oocyte NE, but we assessed the role of microtubules in its maintenance.

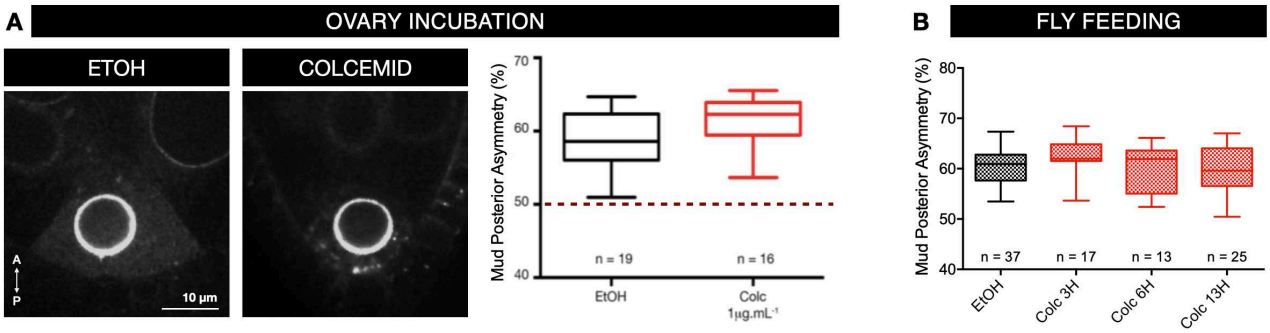

Figure I. 11: Mud asymmetry maintenance is independent of microtubules. (A Left) Acquisitions of GFP-Mud in ovaries treated with EtOH or 1µg.mL^{-1} Colcemid. Quantifications of Mud asymmetry at the oocyte NE under microtubule depolymerization either by (A) incubating the ovaries in Colcemid (red box plots) and EtOH for the control (black box plots), or by (B) feeding the flies with the drug.

These results indicate that microtubules are not necessary for the maintenance of Mud asymmetry at the NE. Microtubule's role in Mud asymmetry establishment remains to be investigated. One hypothesis is that the interaction between partner proteins and Mud, via its CH and MT domains, could regulate Mud distribution at the oocyte NE. Moreover, observations of the partial delocalization of Mud, when CC, MT or TM domains are deleted, suggest a role in Mud restriction at the oocyte NE.

4) Importance of Mud asymmetry in the nuclear trajectory regulation

To assess the importance of Mud asymmetry, I recorded the nuclear migration event on living egg chambers in our different Mud strains. To do so, I performed live imaging microscopy following an original protocol developed in the lab, which allows us to maintain dissected egg chambers alive for 12 hours (Loh et al., 2021; Tissot et al., 2017).

a) Method review - Live Imaging to study the nuclear migration trajectories

jove

Nuclear Migration in the *Drosophila* Oocyte

Maëlys Loh[1], **Antoine Guichet**[1], **Fred Bernard**[1]

[1] Université de Paris, CNRS, Institut Jacques Monod

Corresponding Authors

Antoine Guichet
antoine.guichet@ijm.fr
Fred Bernard
frederic.bernard@ijm.fr

Citation

Loh, M., Guichet, A., Bernard, F. Nuclear Migration in the *Drosophila* Oocyte. *J. Vis. Exp.* (171), e62688, doi:10.3791/62688 (2021).

Date Published

May 13, 2021

DOI

10.3791/62688

URL

jove.com/t/62688

Abstract

Live cell imaging is particularly necessary to understand the cellular and molecular mechanisms that regulate organelle movements, cytoskeleton rearrangements, or polarity patterning within the cells. When studying oocyte nucleus positioning, live-imaging techniques are essential to capture the dynamic events of this process. The *Drosophila* egg chamber is a multicellular structure and an excellent model system to study this phenomenon because of its large size and availability of numerous genetic tools. During *Drosophila* mid-oogenesis, the nucleus migrates from a central position within the oocyte to adopt an asymmetric position mediated by microtubule-generated forces. This migration and positioning of the nucleus are necessary to determine the polarity axes of the embryo and the subsequent adult fly. One characteristic of this migration is that it occurs in three dimensions (3D), creating a necessity for live imaging. Thus, to study the mechanisms that regulate nuclear migration, we have developed a protocol to culture the dissected egg chambers and perform live imaging for 12 h by time-lapse acquisitions using spinning-disk confocal microscopy. Overall, our conditions allow us to preserve *Drosophila* egg chambers alive for a long period of time, thereby enabling the completion of nuclear migration to be visualized in a large number of samples in 3D.

Introduction

For several years, the *Drosophila* oocyte has emerged as a model system to study nuclear migration. The *Drosophila* oocyte develops in a multicellular structure called the egg chamber. Egg chambers encompass 16 germ cells (15 nurse cells and the oocyte) surrounded by an epithelial layer of follicular somatic cells. Egg chamber development has been subdivided into 14 stages (**Figure 1A**), during which the oocyte will grow and accumulate reserves necessary for the early development of the embryo. During the development, upon microtubule reorganization and asymmetric transport of maternal determinants, the oocyte polarizes along the antero-dorsal and dorso-ventral axes. These axes determine the subsequent polarity axes of the embryo and the adult arising from the fertilization of this oocyte[1]. During oogenesis, the nucleus adopts an asymmetric position in the oocyte. In stage 6, the nucleus is centered in the cell. Upon a yet to

be identified signal emitted by the posterior follicular cells which is received by the oocyte, the nucleus migrates toward the intersection between the anterior and lateral plasma membranes in stage 7 (**Figure 1B**)[2,3]. This asymmetric position is required to induce the determination of the dorso-ventral axis.

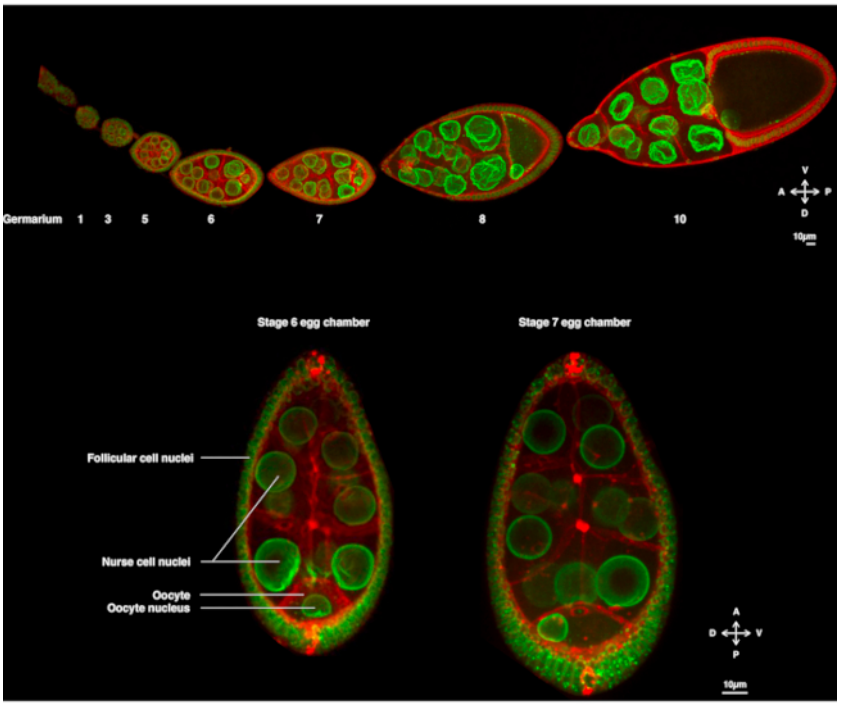

Figure 1: *Drosophila melanogaster* egg chambers. (**A**) Fixed ovariole from transgenic flies expressing *Fs(2)Ket-GFP* that labels the nuclear envelopes and *ubi-PH-RFP* that labels the plasma membranes. The ovariole is composed of developing egg chambers at different stages. Maturation increases along the antero-posterior axis with the germarium at the anterior tip (left) where the germ stem cell resides and the older stage at the posterior tip (right). (**B**) Z-projection of living egg chamber by spinning disk confocal microscopy at stage 6 of oogenesis (left), in which the nucleus is centered in the oocyte. The nucleus will migrate to adopt an asymmetrical position at stage 7 (right) in contact with the anterior plasma membrane (between the oocyte and the nurse cell) and the lateral plasma membrane (between the oocyte and the follicular cells). This position will induce the determination of the dorsal side and, thus, the dorso-ventral axis of the egg chamber. Please click here to view a larger version of this figure.

For many decades, this nuclear migration has been studied on fixed tissues by immunostaining. This approach has notably made it possible to demonstrate that this process depends on a dense network of microtubules[4,5]. More recently, we developed a protocol offering conditions compatible with live imaging of the oocyte during several hours making it possible to study this process dynamically[6].

Hence, for the first time, we have been able to describe that the nucleus has preferential and characteristic trajectories

during its migration, one along the anterior plasma membrane (APM) and another along the lateral plasma membrane (LPM) of the oocyte (**Figure 2**). These latest results underline the importance of live-imaging protocols when studying dynamic processes such as nuclear migration.

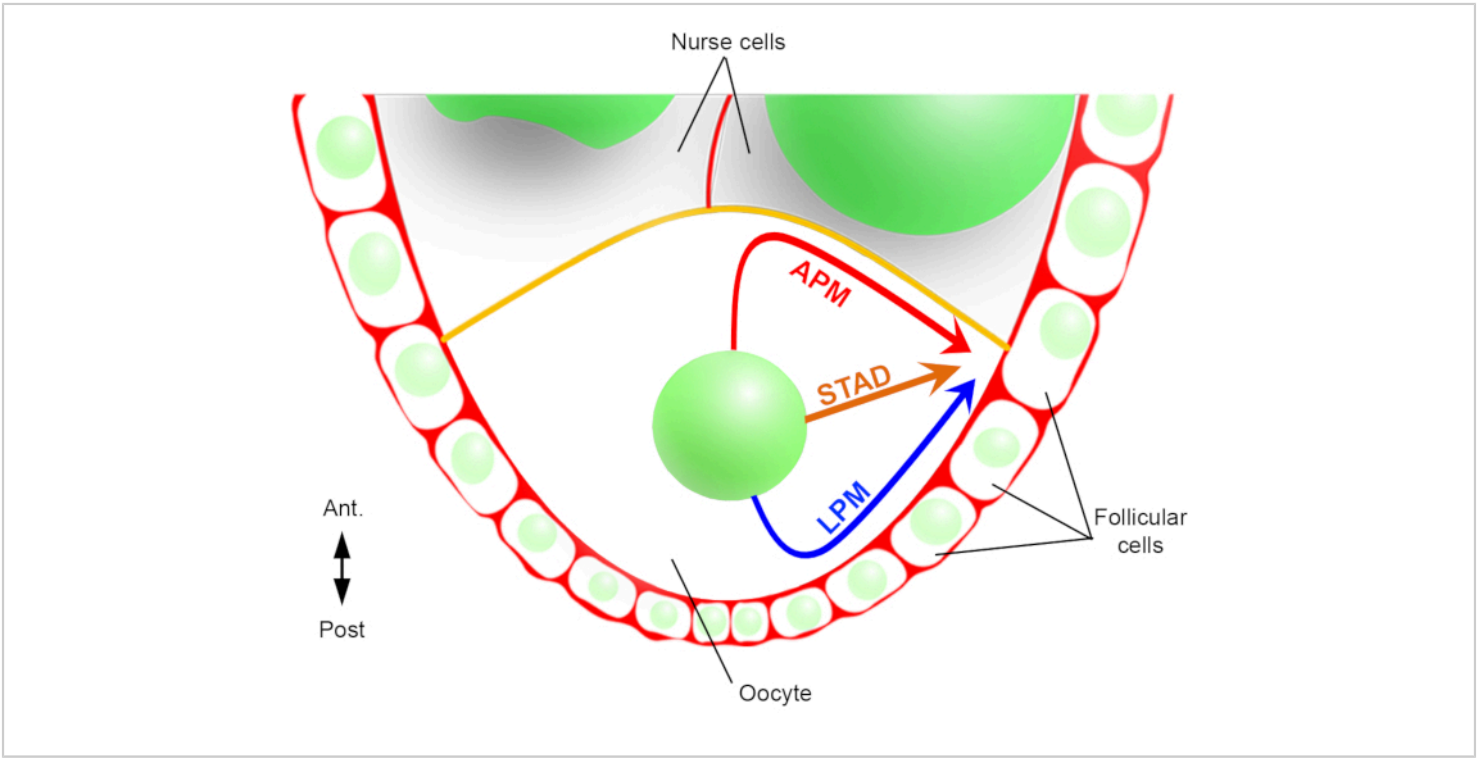

Figure 2: Schematic representation of the different migration paths of the nucleus. At stage 6 of the oogenesis, the oocyte is a large cell with a central nucleus. At this stage, the antero-posterior polarity axis is set with a posterior/lateral plasma membrane of the oocyte in contact with the follicular cells and the anterior plasma membrane (in yellow) is in contact with the nurse cells[2]. We have previously reported that the nucleus could migrate either along the anterior plasma membrane (APM), along the lateral plasma membrane (LPM), or through the cytoplasm (STAD, straight to the antero-dorsal cortex)[6]. Please click here to view a larger version of this figure.

The oocyte nucleus migration is a phenomenon of about 3 h[6], and so far, the event triggering the start of the actual migration is unknown. The start of the migration can also be delayed by protein mutants used to study this mechanism. These unknown variables motivated us to acquire images over long time periods (10-12 h). It is, therefore, important to ensure that the oocytes remain alive. As the egg chamber develops, it elongates along the antero-posterior axis from a spherical to an elliptical shape. This elongation is driven by the rotation of follicular cells, which occurs from stage 1 to stage 8, perpendicular to the antero-posterior axis[7]. In addition, a tubular sheath of muscle with pulsatile property surrounds the egg chambers. Its physiological function is to push the developing follicles toward the oviduct continuously[8]. In order to limit the movements that induce oscillations of the egg chambers after their dissection, we designed an observation micro-chamber measuring 150 µm in height (**Figure 3A**). This height is marginally higher than the size of a follicle at stages

10 and 11. It considerably limits the vertical movements of the sample while preserving the rotation of the egg chamber, thereby resulting in limited defects in follicle development. We then perform live imaging for 12 h on dissected egg chambers by multi-position time-lapse acquisitions using a spinning-disk confocal microscope. Here we describe our protocol for studying the oocyte nuclear migration between stages 6 and 7.

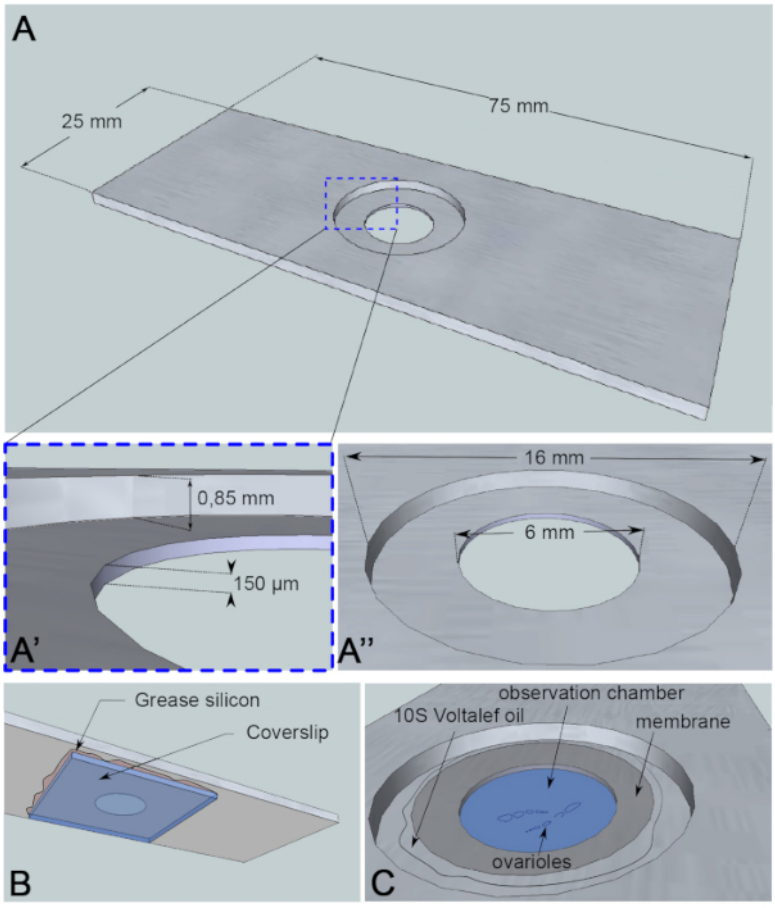

Figure 3: Schematic representation of the observation chamber. (**A**) (Top view) Precise dimensions of the aluminum slide with the heights (A') and circumferences (A'') of the well drilled in the middle of the slide. (**B**) (Bottom view) A coverslip blocking the well is sealed to the slide with silicon grease. (**C**) (Top view) Dissected ovarioles develop in an imaging medium that is covered by a gas permeable membrane. Halocarbon oil is used to stabilize the membrane. Please click here to view a larger version of this figure.

In order to follow the nuclear migration and precisely assess trajectories in the oocyte, markers for both the nuclear envelope and plasma membrane are needed. With this aim, two transgenes that have a high signal/noise ratio and do not fade over the course of live imaging have been selected. To label the plasma membrane, the use of a *P[ubi-PH-RFP]* that encodes the Pleckstrin Homology (PH) domain of the Human Phospholipase C ∂1 (PLC∂1) fused to RFP is recommended.

This PH domain binds to the phosphoinositide PI(4,5)P2 distributed along the plasma membrane of the oocyte[9]. For the nuclear envelope, the *P[PPT-un1]Fs(2)Ket-GFP* protein-trap strain where GFP is inserted within the gene encoding the *Drosophila* ß-importin displays a homogeneous and an intense signal[10]. Young flies (1-2 days old) are placed in fresh vials containing dry yeast 24-48 h prior to ovary dissection.

For this live-imaging assay, a 1 mm thick piece of aluminum, which is nonreactive for the sample, has been cut into the dimensions of a microscopy slide. It has a 16 mm diameter hole in the center of the slide that has been counterbored to 0.85 mm. This counterbore has an additional 6 mm diameter hole with a depth of 150 µm (**Figure 3A**). A coverslip is glued with silicone grease (inert for the sample) at the bottom of the aluminum chamber (**Figure 3B**). After placing the samples in the medium-filled well, a membrane permeable to O_2/CO_2 exchange is placed over the medium and surrounded by halocarbon oil (**Figure 3C**).

For the dissection, it is recommended to use stainless steel forceps with a tip dimension of 0.05 x 0.02 mm, and 0.20 mm diameter needles for the separation of the ovarioles (**Figure 4B,C**). The migrating nuclei are imaged on a spinning-disk confocal inverted microscope CSU-X1 equipped with a camera. Multi-position images were acquired by time-lapse every 15 min at 24 °C. A 15 min interval allows performing multi-position acquisitions with limited photobleaching of the fluorescent proteins and phototoxicity for the samples. Furthermore, a shorter interval would not provide much more informative data to follow the nuclear trajectories. The movies are processed and analyzed *via* Fiji software[11].

Protocol

1. Imaging medium preparation

1. Prepare fresh media on the day of use. Pipette 200 µL of Schneider medium (containing L-Glutamine and 0.40 g/L of $NaHCO_3$ complemented with 10% heat-inactivated fetal calf serum, 100 U/mL of penicillin, and 100 mg/mL of streptomycin).
2. Supplement with 30 µL of insulin 10 mg/mL.
3. Add 4 µL of heat-inactivated fetal calf serum.

2. Observation-chamber preparation

1. With a pipette tip, apply a small amount of silicone grease all around the hole on the underside of the punctured slide (**Figure 4D**).
2. Position a 24 x 50 mm coverslip of 0.13-0.16 mm thickness.
3. With the wide end of a pipette tip, apply pressure on the coverslip to flatten the silicone in order to seal the coverslip and create a silicone ring interior to the slide (**Figure 4F,G**).

3. Ovary dissection

1. Anesthetize a female fly of the desired phenotype on a CO_2 pad.
2. Transfer the female in 150 µL of the imaging medium in a dissecting well (**Figure 4H**).
3. Open one female by grabbing its thorax with forceps and pinching the dorsal abdomen cuticle with a second pair of forceps.

4. Isolate and detach the pair of ovaries, which should be readily visible upon cuticle opening.
5. Carefully remove the uterus, oviduct, and muscle sheath (**Figure 4I**).
6. Place a drop of 10-15 µL of the imaging medium and transfer one ovary in the imaging chamber (**Figure 4J,K**).

4. Egg chamber isolation

1. To separate the ovarioles, hold the posterior end of the ovary (toward the older stages) with the needle. Tease apart the ovarioles by carefully pulling on the germarium with another needle.
2. Remove the remaining muscle sheath on the egg chambers; one needle holding the sheath and the other pulling on the ovariole through the larger chambers (stage 9 or older).
3. Allow the unsheathed ovariole to sink and contact the coverslip.
4. Remove late stages and the rest of the ovaries from the micro-chamber with the help of forceps. Carefully distance the ovarioles from the others with needles to facilitate the acquisition (**Figure 4L**).

5. Observation chamber closing

1. Cut a small square (10 x 10 mm) of permeable membrane (**Figure 4M,N**).
2. Carefully apply the membrane on top of the imaging medium to expel any air bubbles (**Figure 4O**).
3. Hermetically seal the chamber with a thin layer of halocarbon oil around the well on the contour of the membrane (**Figure 4P,Q**).

6. Imaging

1. Place the imaging set-up on the slide holder of the inverted microscope using a 40x objective (HCX PL Apo, 1.25NA, oil immersion).
2. Locate and save positions of different stage 6 oocytes in which the nucleus is ready to migrate.
3. Set-up the 488 and 561 nm lasers. With a measured output laser power of 150 mW, use 30% of the laser power and 300 ms and 500 ms exposure, respectively.
4. Set-up the experiment. Take a time-lapse of 12 h with the interval of 15 min-41 sections with an interval of 1 µm centered on the nucleus.

   NOTE: According to the exposure time described above, this setting allows the acquisition of one position in around 45 s. Since there is a delay due to position changing, it is recommended to set a maximum of 12 positions in these conditions.

7. Image analysis

1. Process the movies on the software Fiji, using the plug-in Orthogonal view and manually track the nuclei.

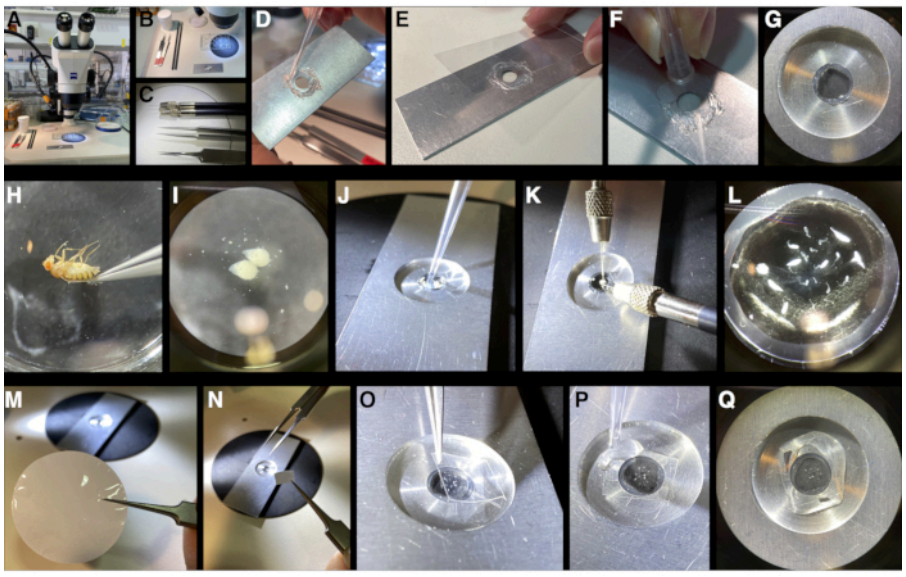

Figure 4: Step by step micro-chamber mounting pictures. (**A,B,C**) Preparation of the needed tools: dissecting well plate, forceps, needles, imaging media, silicon grease, permeable membrane, and the aluminum slide. (**D**) Application of the silicon grease at the back of the aluminum slide with a pipette tip. (**E**) A glass coverslip is glued on the silicon grease to create the bottom of the chamber. (**F,G**) Pressure application on the coverslip with the wider extremity of a pipette tip to create a joint inside the chamber. (**H,I**) Dissection of the fly ovaries in the imaging media. (**J**) Pipetting of a drop of imaging media in the micro-chamber. (**K,L**) Separation of the ovarioles in the micro-chamber using needles. (**M,N,O**) Permeable membrane cut into a 10 x 10 mm square and placing over the drop of the medium in the micro-chamber. (**P,Q**) Sealing of the micro-chamber with halocarbon oil. The samples are ready to be imaged. Please click here to view a larger version of this figure.

Representative Results

Before migration, the nucleus is dynamic and oscillates around a central position during a period defined as pre-migration. These small movements reflect a balance of pushing and pulling forces that maintain equilibrium in the middle of the oocyte. By quantifying the trajectories of the nuclei, we have shown that the APM and LPM trajectories had similar proportions. We define the nature of the trajectory by the first contact between the nucleus and the plasma membrane[6]. Thus, the nucleus reaches either the APM or the LPM before sliding along it, to reach its final position at the intersection of the two plasma membranes **(Figure 5,Movies 1-2**). Furthermore, we have shown that distinct cues favor each of the trajectories. For example, the centrosomes clustered between the nucleus and the posterior membrane of the oocyte enable the APM trajectory. Conversely, the microtubule-associated-protein (MAP) Mushroom Body Defect (Mud), which is located asymmetrically to the nuclear envelope, supports a trajectory along the LPM[6]. Moreover, the depletion of either centrosomes or Mud affects the migration speed of the nucleus compared to the wild type context[6].

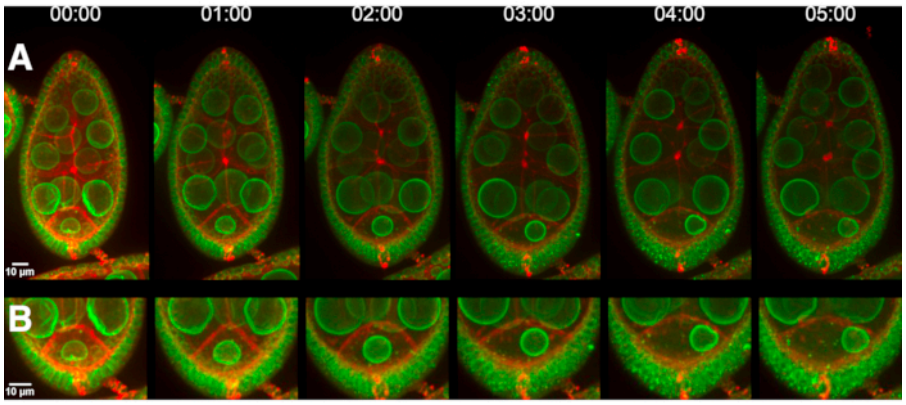

Figure 5: Representative images of the migration of the oocyte nucleus by live-imaging microscopy. (**A**) Selected frames extracted from time-lapse **Movie 1** showing the nuclear migration of the oocyte nucleus of a wild-type egg chamber expressing the nuclear envelope marker (*Fs(2)KetGFP*) and the plasma membrane marker (*ubi-PH-RFP*). (**B**) Selected frames from **Movie 2** (the cropped version of **Movie 1**) focusing on the oocyte. Time (in h:min) relative to the beginning of the time-lapse is indicated on the top of each selected frame. Please click here to view a larger version of this figure.

The oocyte and egg chamber growths are signs of correct development, which are easily visible in time-lapse recordings (**Figure 5**). On the contrary, membrane deformities disorganized follicular cells, stunted cells, and shrunken nuclei are the first signs of dying egg chambers (**Figure 6**, **Movie 3-4**). Upon the observation of these degenerative egg chambers, the nuclei movements are no longer exploitable for analysis. Usually, we do not observe any degenerated oocyte before 8 h of imaging (**Figure 6A**) and the rare cases of early degeneration are due to problems during the dissection or mounting steps (**Figure 6B**). We consider that 50% of oocytes are still alive after 10 h of imaging.

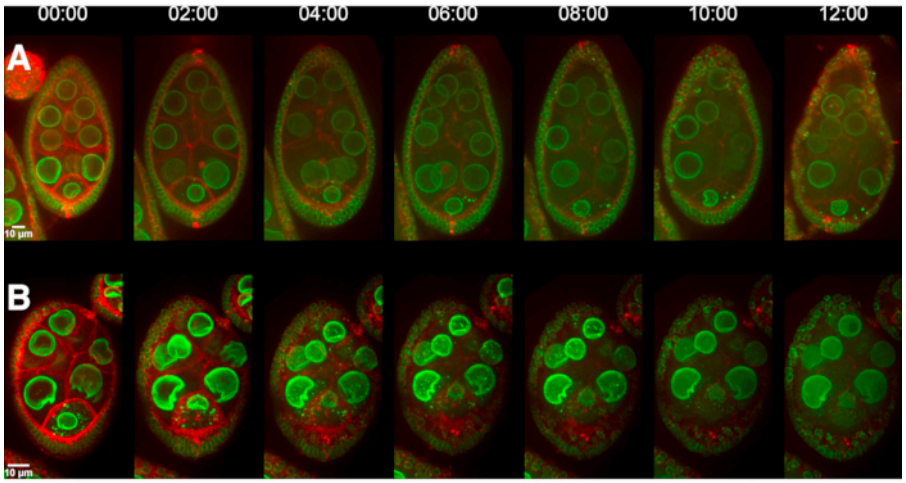

Figure 6: Representative images of the degeneration of an egg chamber during live imaging. (**A**) Selected frames extracted from time-lapse **Movie 3** showing the degeneration of a wild type egg chamber after 8 h, expressing the nuclear envelope marker (*Fs(2)KetGFP*) and the plasma membrane marker (*ubi-PH-RFP*). (**B**) Selected frames extracted from **Movie 4** showing the rapid degeneration of a wild type egg chamber. Such early degeneration is characteristic of a problem during the dissection or mounting steps. Time (in h:min) relative to the beginning of the time-lapse is indicated on the top of each selected frame. Please click here to view a larger version of this figure.

Excessive movements could be an additional issue resulting in unusable data and further analysis, as the egg chambers will not remain in the imaged frame. To circumvent this problem, we use a 40x objective that provides an adequate frame of observation and allows movements of the egg chambers along the x-y plane while providing enough resolution for a qualitative assessment of migratory path taken by the oocyte nucleus. In addition, to limit the effects of excessive movements in the z-axis and in order to keep the oocyte within the range of the z-stack, we perform z-sections over 40 µm stack (41 sections 1 µm apart), while stage-6 oocyte has a size of 20 µm.

Movie 1: Representative movie of a wild-type egg chamber expressing both the nuclear envelope marker (*Fs(2)Ket-GFP*) and the plasma membrane marker (*ubi-PH-RFP*). In this example, the oocyte nucleus contacts the anterior membrane first and slides along it to reach the antero-dorsal corner. The elapsed time of the time-lapse is indicated in h:min in the upper-left corner of the video. Please click here to download this Movie.

Movie 2: Cropped version of Movie 1, focusing on the oocyte. The elapsed time of the time-lapse is indicated in h:min in the upper-left corner of the video. Please click here to download this Movie.

Movie 3: Representative movie of a wild-type egg chamber expressing both the nuclear envelope marker (*Fs(2)Ket-GFP*) and the plasma membrane marker (*ubi-PH-RFP*). In this example, the egg chamber starts to degenerate at 8:45 h before completion of nucleus migration. The elapsed time of the time-lapse is indicated in h:min in the upper-left corner of the video. Please click here to download this Movie.

Movie 4: Representative movie of early degeneration of a wild-type egg chamber expressing both the nuclear envelope marker (*Fs(2)Ket-GFP*) and the plasma membrane marker (*ubi-PH-RFP*). The elapsed time of the time-lapse is indicated in h:min in the upper-left corner of the video. Please click here to download this Movie.

Discussion

Other protocols describe how to prepare and culture Drosophila egg chambers *ex vivo* for live-imaging assay[12,13]. The novelty of this protocol is the use of an imaging chamber constructed using a hollowed aluminum slide, a coverslip, and an O_2/CO_2 permeable membrane. The main advantage of this set-up is to limit the movement in Z without exerting pressure on the sample. Thus, the oocyte can still move freely, and this is why first, the 40x objective is used and second, z-stacks are acquired along 40 µm, while the oocyte is around 20 µm height at stage 6.

Although this protocol is relatively simple, each step is critical for the assay. The preparation of the micro-chamber, the permeable membrane, and the sealing of the chamber are essential to allow gas exchange and prevent drying of the imaging medium and, therefore, the samples. Damaging the egg chamber compromises its survival, so delicate and precise dissection techniques are paramount. Additionally, the muscular sheath must be completely removed as remaining pieces of this structure will result in unwanted egg chamber movement.

Aluminum, in addition to its safety for the sample, has been chosen for its strength, durability, and the ease of cleaning. Other materials have not been yet investigated under these conditions. The use of plastic with the development of 3D printer is tempting; however, one must be very precise with creating a hole with a height of 150 µm.

Recently, Huynh and colleagues have developed an imaging technique adapted to *Drosophila* germarium based on hydrogel[14]. Whether or not this can be adapted to stage 6 in oogenesis remains to be tested. Specifically, it is not known whether movements such as rotation of the follicle can occur in the hydrogel system. These rotation movements are essential for the elongation of the egg chamber and hence, normal development.

Other protocols have used halocarbon oil to follow oocyte nucleus migration[15,16]. The optical properties of oil and the imaging medium used in our protocol are very different. Especially, the Schneider medium has a maximum of light absorption for wavelengths around 450 nm. Therefore, we observe a higher signal/noise ratio with oil. However, the halocarbon oil greatly reduces the oocyte survival to 1-2 h, which limits the ability to follow the entire migration of the nucleus, particularly in genetic contexts where this migration is disturbed. With this present protocol, the imaging medium allows a long survival of egg chamber allowing us to perform time-lapse recording up to 12 h. Thus, we maximize our chance to capture the entire migration process.

Using our current parameters, we can only perform a maximum of 12 positions for the time-lapse. On average, one third of the imaged nuclei are viable and can be analyzed. To

improve the efficiency, a spinning-disk microscope equipped with a dual camera system, which would allow acquisitions of both wavelengths at the same time, can be used to speed up the acquisition time and thus, increase the number of positions.

Furthermore, as this micro-chamber allows to culture the dissected egg chambers for a relatively long period of time, its use can be extended to the study of other dynamic mechanisms of drosophila oogenesis that need to be assessed *ex vivo* (e.g., cytoplasmic streaming in the oocyte, follicle rotation, follicle cells morphogenesis, etc.).

Disclosures

The authors declare no competing interests.

Acknowledgments

We are extremely grateful to Jean-Antoine Lepesant and Nicolas Tissot who originally developed the protocol and shared some graphical elements of Figure 3 with us. We thank Fanny Roland-Gosselin who took the photos of Figure 4. We also thank other lab members for helpful discussions that contributed to the amelioration of this technique and Nathaniel Henneman for his comments that helped to improve this manuscript. We acknowledge the ImagoSeine core facility of the Institute Jacques Monod, member of France-BioImaging (ANR-10-INBS-04). Maëlys Loh is supported by a PhD fellowship from the French Ministry of Research (MESRI). Antoine Guichet and Fred Bernard were supported by the ARC (Grant PJA20181208148), the Association des Entreprises contre le Cancer (Grant Gefluc 2020 #221366) and by an Emergence grant from IdEx Université de Paris (ANR-18-IDEX-0001).

References

1. Merkle, J. A., Wittes, J., Schüpbach, T. Signaling between somatic follicle cells and the germline patterns the egg and embryo of Drosophila. *Current Topics in Developmental Biology.* **140**, 55-86 (2020).
2. Roth, S., Lynch, J. A. Symmetry breaking during drosophila oogenesis. *Cold Spring Harbor Perspectives in Biology.* **1** (2), a001891-a001891 (2009).
3. Bernard, F., Lepesant, J.-A., Guichet, A. Nucleus positioning within Drosophila egg chamber. *Seminars in Cell and Developmental Biology.* **82**, 25-33 (2017).
4. Koch, E. A., Spitzer, R. H. Multiple effects of colchicine on oogenesis in Drosophila: Induced sterility and switch of potential oocyte to nurse-cell developmental pathway. *Cell and Tissue Research.* **228** (1), 21-32 (1983).
5. Januschke, J. et al. The centrosome-nucleus complex and microtubule organization in the Drosophila oocyte. *Development (Cambridge, England).* **133**, 129-139 (2006).
6. Tissot, N. et al. Distinct molecular cues ensure a robust microtubule-dependent nuclear positioning in the Drosophila oocyte. *Nature Communications.* **8**, 15168 (2017).
7. Cetera, M., Horne-Badovinac, S. Round and round gets you somewhere: collective cell migration and planar polarity in elongating Drosophila egg chambers. *Current Opinion in Genetics & Development.* **32**, 10-15 (2015).
8. Hudson, A. M., Petrella, L. N., Tanaka, A. J., Cooley, L. Mononuclear muscle cells in Drosophila ovaries revealed by GFP protein traps. *Developmental Biology.* **314**, 329-340 (2008).
9. Gervais, L., Claret, S., Januschke, J., Roth, S., Guichet, A. PIP5K-dependent production of PIP2 sustains

microtubule organization to establish polarized transport in the Drosophila oocyte. *Development.* **135** (23), 3829-3838 (2008).

10. Villányi, Z., Debec, A., Timinszky, G., Tirián, L., Szabad, J. Long persistence of importin- b explains extended survival of cells and zygotes that lack the encoding gene ´ n Villa. *Mechanisms of Development.* **3**- **4** (125), 196-206 (2008).
11. Schindelin, J. et al. Fiji: An open-source platform for biological-image analysis. *Nature Methods.* **9** (7), 676-682 (2012).
12. Prasad, M., Jang, A. C. C., Starz-Gaiano, M., Melani, M., Montell, D. J. A protocol for culturing drosophila melanogaster stage 9 egg chambers for live imaging. *Nature Protocols.* **2** (10), 2467-2473 (2007).
13. Weil, T. T., Parton, R. M., Davis, I. Preparing individual Drosophila egg chambers for live imaging. *Journal of Visualized Experiments: JoVE.* (60) (2012).
14. Chanet, S., Huynh, J. R. Collective cell sorting requires contractile cortical waves in germline cells. *Current Biology.* **30** (21), 4213-4226.e4 (2020).
15. Zhao, T., Graham, O. S., Raposo, A., St Johnston, D. Growing microtubules push the oocyte nucleus to polarize the drosophila dorsal-ventral axis. *Science (New York, N.Y.).* **336** (6084), 999-1003 (2012).
16. Legent, K., Tissot, N., Guichet, A. Chapter 7 Oogenesis using fixed and live imaging. *Drosophila Oogenesis: Methods and Protocols.* **1328**, 99-112 (2015).

b) Mud asymmetry is not necessary for the regulation of the nuclear trajectories

Using this method, I investigated the importance of Mud asymmetry for Mud function in the nuclear trajectory regulation. To analyze the nuclear trajectories, I used the transgene *Fs(2)Ket-GFP* to label nuclei and the ubiquitous transgene Pleckstrin Homology domain (PH) of the Phospholipase C ∂1 (PLC∂1) fused to RFP (*PH-RFP*) to label plasma membranes. I recorded nuclear migrations in *mud* null mutant (*mud*^{4}) living egg chambers expressing two copies of transgenic *mud* tagged GFP: inserted at locus 65B2 and at locus 50E1, in order to have the normal allelic copies. For example, GFP-Mud control was assessed in flies of the following genotype: *mud*^{4} *; GFP-mud*^{50E1} *, Fs(2)Ket-GFP / II ; GFP-mud*^{65B2} *, ubi-PH-RFP / III*. First, I validated the functionality of the transgene *GFP-mud* expressed in *mud* mutant context (fig I. 12), as it rescued the WT trajectory proportions observed in (Tissot et al., 2017).

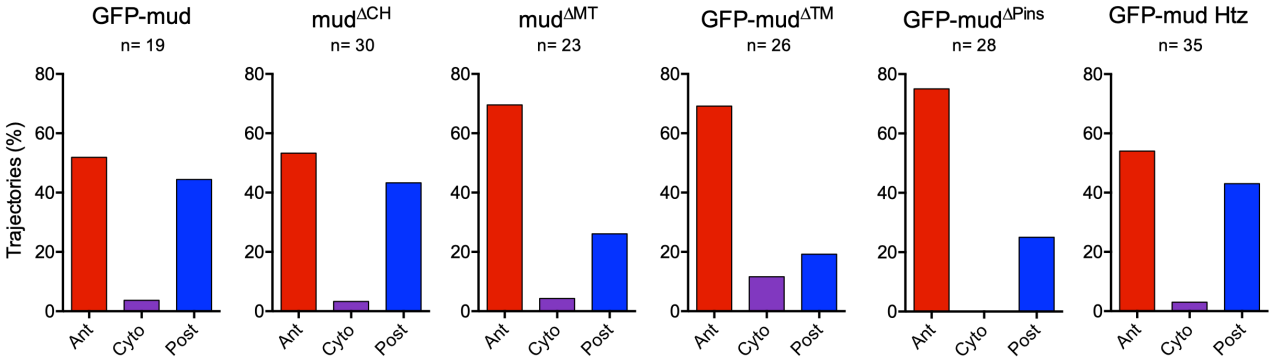

Figure I. 12: Mud asymmetry is not necessary for Mud regulation of the nuclear trajectories. Graphs presenting the nuclear trajectory proportions in the different genetic contexts expressing Mud deleted for its different domains.

The deletion of the CH domain, which affects Mud asymmetry, did not affect the trajectories as they were similar to control (fig I. 12.mud$^{\Delta CH}$). Deletion of the MT domain (fig I. 12.mud$^{\Delta MT}$) as well as the TM domains (fig I. 12.GFP-mud$^{\Delta TM}$), which induce partial delocalization of nuclear Mud, phenocopied *mud* mutant trajectories with a decrease of trajectories along the posterior plasma membrane of the oocyte. The deletion of Pins domain, which does not affect Mud asymmetry, phenocopied *mud* mutant nuclear trajectories (fig I. 12.GFP-mud$^{\Delta Pins}$). Due to genetic difficulties, only one copy of *GFP-mud*$^{\Delta Pins}$ was expressed in *GFP-mud*$^{\Delta Pins}$ flies to rescue *mud*^{4} context, while for the other conditions two copies of Mud were expressed. Therefore, I wondered if the heterozygous (Htz) expression of Mud affected functionality of the protein. To test this, I performed the same experiment on egg chambers expressing only one copy of GFP-Mud^{65B2} in a *mud* null context (fig I. 12.GFP-mud Htz), and observed that the trajectories of the nuclei were similar to the WT, indicating that one copy of Mud is sufficient for its functionality. To assess the role of Pins on Mud function, I investigated Pins localization in egg chambers expressing Pins::GFP (CRISPR Knock-IN) (fig I. 13). Pins localization was not associated with the oocyte nucleus or in its vicinity, but rather associated with the plasma membranes, which was not in favor of an interaction with Mud at the oocyte NE and a subsequent role in the nuclear migration trajectory.

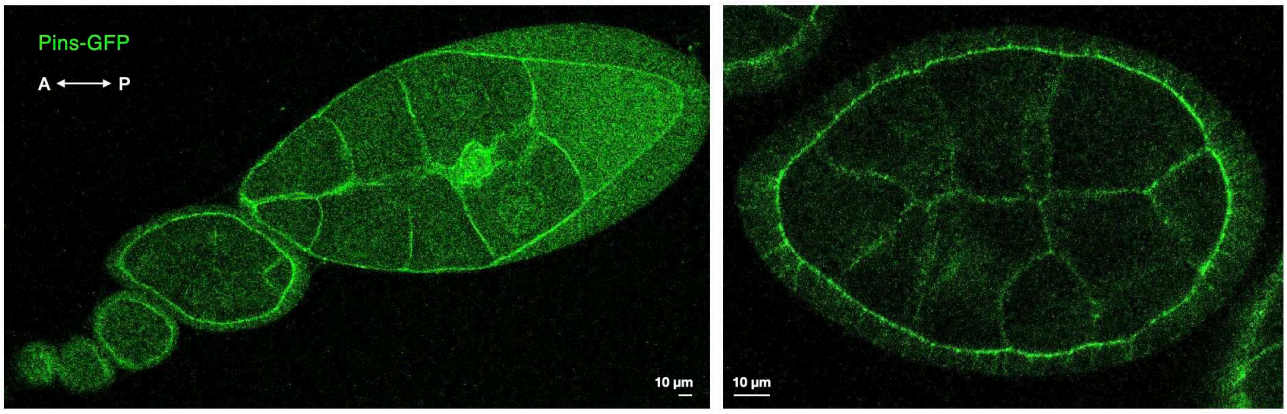

Figure I. 13: Pins localization in the Drosophila egg chamber. Acquisitions of egg chambers expressing Pins-GFP. (Left panel) Ovariole oriented along the antero-posterior axis (A-P), (Right panel) Stage 6 egg chamber displaying an accumulation of Pins signal associated with the plasma membranes. The orientation of the egg chamber is indicated by the arrow A (anterior), P (posterior). Bars, 10µm.

One explanation regarding the effect of Pins domain deletion is that this deletion also affects the MT domain (fig I. 1). Therefore, the posterior trajectory decrease could reflect the perturbation of the MT binding site, which is consistent with the trajectory proportions observed in *mud*$^{\Delta MT}$ (fig I. 12.mud$^{\Delta MT}$). Altogether, these results highlight that Mud asymmetry is not necessary for its function, as its loss does not affect the trajectories during the oocyte nucleus migration. However, these data indicate that the MT and TM domains, which both display a perinuclear delocalization of Mud, are important for trajectory regulation. Therefore, I hypothesized that Mud localization needs to be restricted at the oocyte NE for the control of the posterior trajectory. I next aimed to identify by which mechanisms Mud localizes at the oocyte NE.

CHAPTER II : MUD LOCALIZATION AT THE OOCYTE NUCLEAR ENVELOPE

1) Mud localization dynamics to the oocyte nuclear envelope

a) Mud localization dynamic is a rather slow process

In a first approach to understand how Mud localizes at the NE, and to understand if this is an active or passive diffusion process, I analyzed Mud dynamics by Fluorescence Recovery After Photobleaching (FRAP). To do so, I photobleached the GFP of GFP-Mud on a region at the posterior nuclear hemisphere where Mud is the most enriched, and recorded the fluorescence recovery in this region (fig II. 1.A-A'). As comparison, I used the *Fs(2)Ket-GFP* strain (fig II. 1.B-B'), and observed that Fs(2)Ket-GFP fluorescence recovery was at 80% in 2min, while Mud recovery was at 40% in 30min (fig II. 1.C-C'). These results show that the dynamics of Mud is slower compared to Fs(2)Ket, which does not seem to involve molecular diffusion, but rather longer processes, such as microtubule polymerization/depolymerization for example.

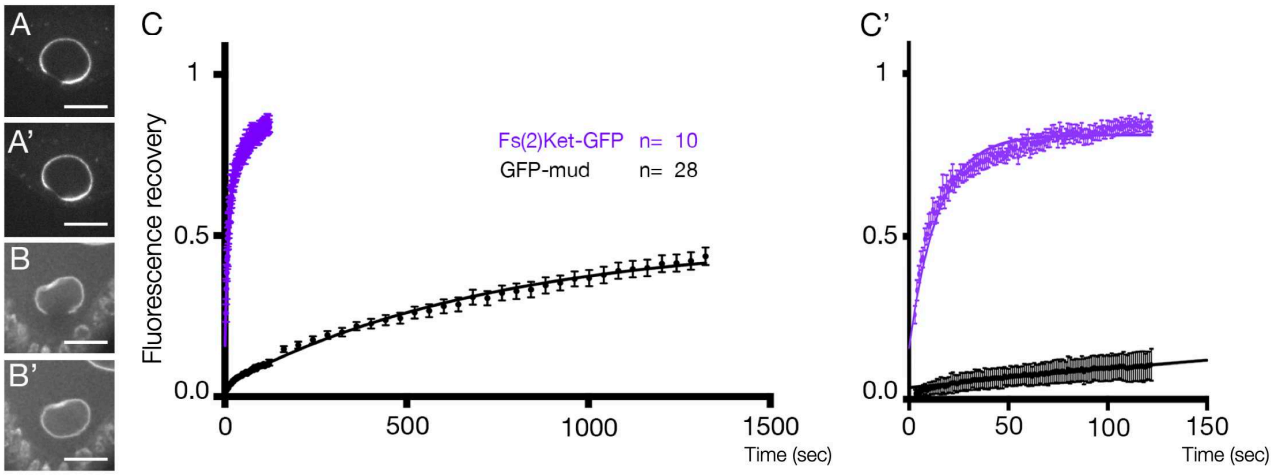

Figure II. 1: Localization dynamics of Mud at the oocyte NE is a rather slow process. (A-B') Acquisitions showing the fluorescence recovery of GFP-Mud after photobleaching at t=0s (A) and at t=120s (A'), and of Fs(2)KetGFP at t=0s (B) and at t=120s (B'). (C) FRAP graph presenting the GFP recovery of GFP-Mud (in black) and Fs(2)KetGFP (in purple). (C') Zoom of the (C) curve showing the fluorescence recovery of the first two minutes of the experiment.

b) MT are involved in Mud localization dynamics

To test if microtubules were involved in the dynamic of Mud at the NE, I performed FRAP experiments on GFP-Mud-expressing fly ovaries that were incubated with 1µg.mL^{-1} Colcemid to depolymerize the microtubules. For control condition, ovaries were treated with EtOH (fig II. 2). Lower fluorescence recovery is observed when the ovaries were treated with Colcemid compared to those treated with EtOH. Indeed, 30min after photobleaching, fluorescence recovery was at 35% for the control and 25% for Colcemid treated ovaries. These results do not indicate a direct involvement of microtubules in Mud oocyte NE localization and dynamics, but suggest that Mud dynamics at the NE do not require polymerizing microtubules.

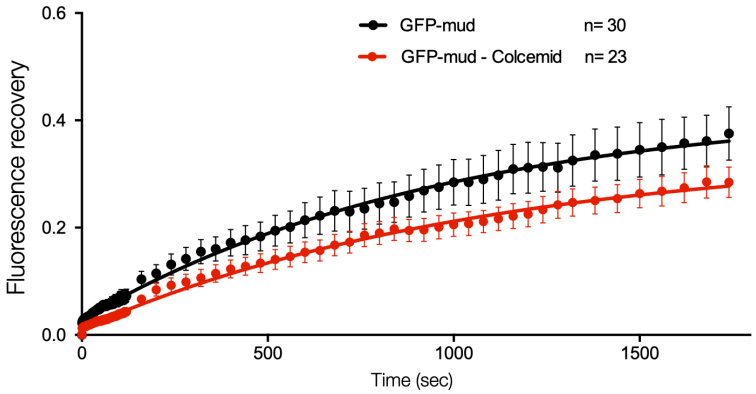

Figure II. 2: Graph representing the Fluorescence Recovery of GFP-Mud Control (ovary incubation in EtOH) (black curve) and GFP-Mud-Colcemid (ovary incubation with Colcemid) (red curve) after photobleaching of the GFP at t=0 sec.

c) The TM domains are involved in Mud localization dynamics

In the aim of testing the importance of putative TM domains, I assessed the dynamics of GFP-Mud$^{\Delta TM}$ (fig II. 3). GFP-Mud$^{\Delta TM}$ fluorescence recovery was not higher than the control GFP-Mud, but quicker. Indeed, the same threshold at 40% was reached in the two conditions by the end of the experiment, however, GFP-Mud$^{\Delta TM}$ recovery reached this threshold at 15min, while it was reached at 25min for GFP-Mud recovery. These results indicate that the deletion of TM domains gives Mud more mobility at the NE, and reinforce the hypothesis that Mud is a transmembrane protein at the oocyte NE.

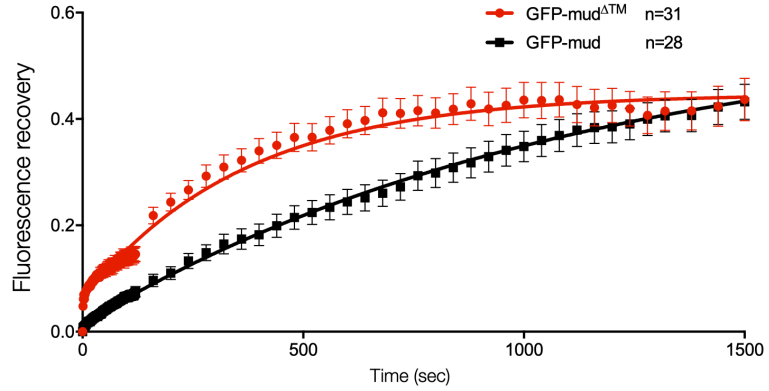

Figure II. 3: Graph representing the Fluorescence Recovery of GFP-Mud (black curve) and GFP-Mud$^{\Delta TM}$ (red curve) after photobleaching of the GFP at t=0 sec.

Altogether, these experiments show that Mud is not very mobile at the oocyte NE as the maximum fluorescence recovery threshold was only 40%. This suggest that Mud localization at the oocyte NE is rather well maintained. Next, I aimed to look for protein partners of Mud that could give a better understanding of its functionality at the oocyte NE.

2) Mud interacts with Fs(2)Ket potentially via its putative Nuclear Localization Signals

a) Mud interacts with Fs(2)Ket in the Drosophila ovaries

As NuMA nuclear localization, during interphase, relies on its NLS (Gueth-Hallonet et al., 1996), and as it has been shown that Mud interacts with Fs(2)Ket in cultured *Drosophila* cells (Wee et al., 2011), I wondered if Mud interacts with Fs(2)Ket in our model. To do so, I tested the interaction from ovary lysates by co-immunoprecipitating Fs(2)Ket with Mud, and confirmed the interaction in the fly ovaries (fig II. 4).

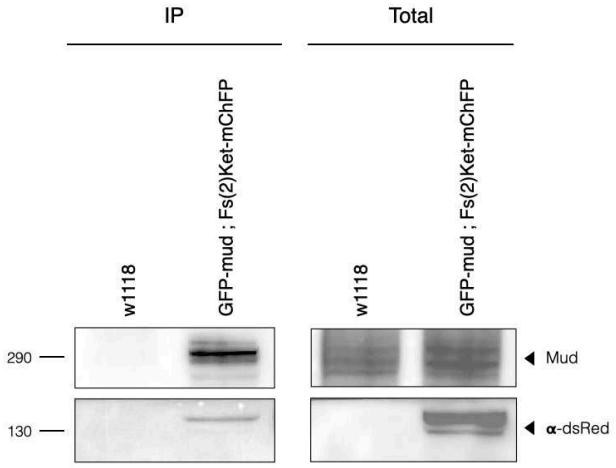

Figure II. 4: Mud interacts with Ketel in the *Drosophila* ovaries. Immunoblot against Mud and against dsRed after co-immunoprecipitation (IP) using beads anti-GFP in ovary lysates from control (*w*^{1118}), and *GFP-mud ; Fs(2)Ket-mChFP strain*. Total of loaded lysates for the corresponding conditions is on the right of the gel. The GFP-IP allows to precipitate GFP-Mud, and the detection using an antibody against dsRed allows to reveal the interaction with Fs(2)Ket-mChFP (mCherry Fluorescent Protein).

b) Mud has two putative Nuclear Localization Signals

Next, I wonder if Mud and Fs(2)Ket interaction relies on NLS recognition and therefore I searched for NLS motifs on Mud sequence. Using two NLS mapping softwares (**NLStradamus** (Nguyen Ba et al., 2009) and **cNLS Mapper** *http://nls-mapper.iab.keio.ac.jp/cgi-bin/NLS_Mapper_form.cgi*), I performed *in silico* analysis to identify NLS sequences on the different isoforms of Mud. We identified two putative NLS sequences on Mud protein sequence (fig II. 5). These NLS motifs correspond to exon 7 and exon 12. Interestingly, we noticed that the putative NLS sequences are both deleted in the construct Mud$^{\Delta MT}$ in which Mud displays a partial delocalization at the periphery of the nucleus. The NLS presence varies depending on the isoforms and interestingly, these differences correlated with the categories of isoforms we defined (fig II. 5). Indeed, isoforms of the first and second categories shared two NLS. The isoforms of the third category have only one NLS, while in the second category only -PJ isoform has one NLS. The identification of putative NLS on Mud and the interaction between Mud and Fs(2)Ket are first cues explaining how Mud localizes at the oocyte NE.

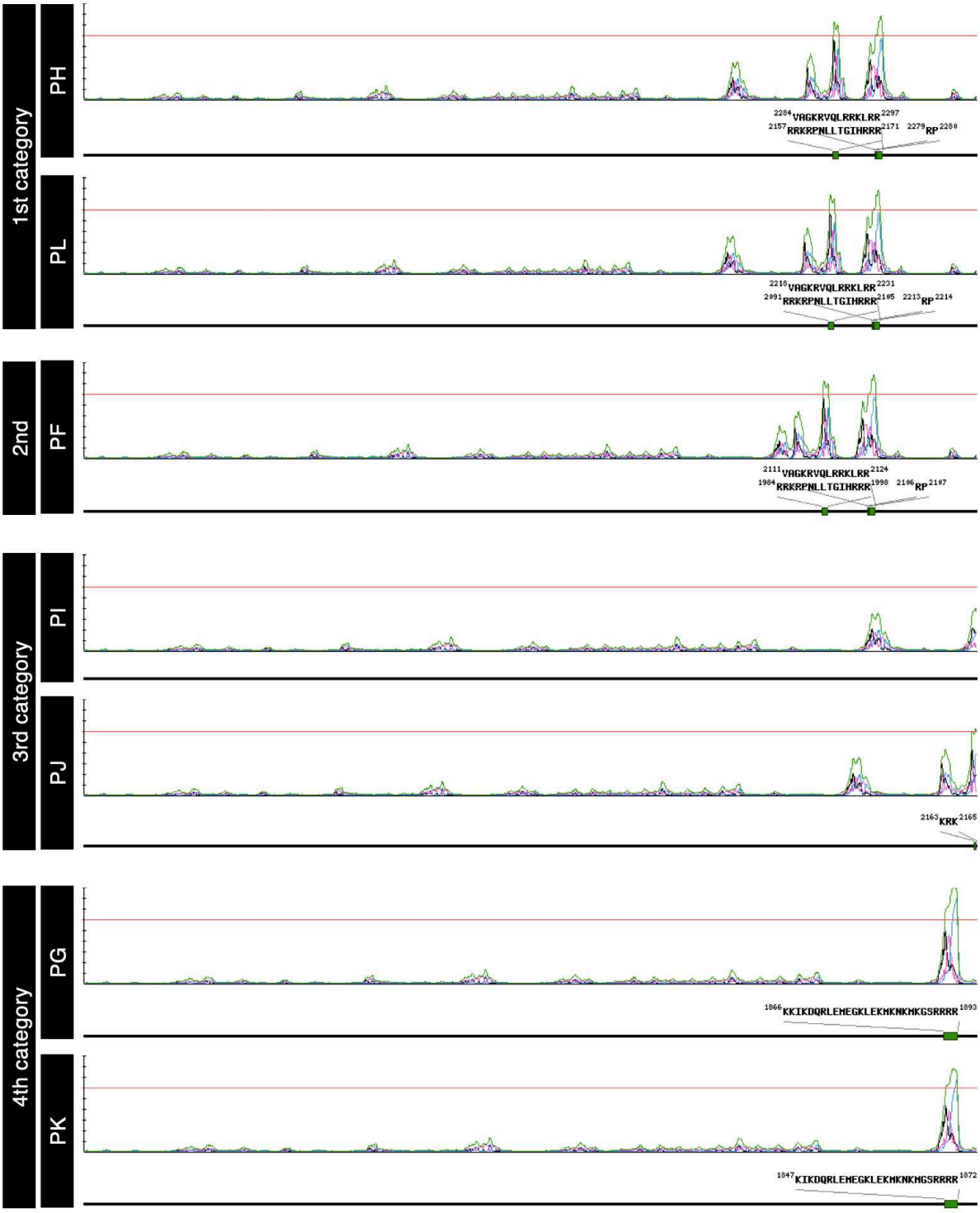

Isoform	Putative NLS sequences		
PH	2157 - RRKRPNLLTGIHRRR - 2171	2279 - RP - 2280	2284 - VAGKRVQLRRKLRR - 2297
PL	2091 - RRKRPNLLTGIHRRR - 2105	2213 - RP - 2214	2218 - VAGKRVQLRRKLRR - 2231
PF	1984 - RRKRPNLLTGIHRRR - 1998	2106 - RP - 2107	2111 - VAGKRVQLRRKLRR - 2124
PI			
PJ	2163 - KRK - 2165		
PG	1866 - KKIKDQRLEMEGKLEKMKNKMKGSRRRR - 1893		
PK	1847 - KIKDQRLEMEGKLEKMKNKMGSRRRR - 1872		

— : Mud protein sequence

■ : putative NLS motif

Figure II. 5: Mud has one or two NLS. Graphs representing the prediction of NLS motifs on Mud protein sequence, obtained on NLStradamus. The different isoforms do not all display the same NLS motifs. The PH, PL and PF isoforms are predicted to have two NLS. The PI isoform NLS prediction did not result in the identification of such sequence. The PJ isoform is predicted to have one NLS. The PG and PK isoforms are predicted to have on NLS. (Bottom) Table of the predicted NLS motifs by NLStradamus.

3) Generation of the transgenic flies putative NLS deleted Mud

Next, I wanted to validate these two predicted NLS motifs on exon 7 and exon 12. We generated *GFP-mud$^{\Delta Ex7}$ (exon7)* and *GFP-mud$^{\Delta Ex12}$ (exon12)* using CRISPR-Cas9 technique. Egg chambers expressing GFP-Mud$^{\Delta Ex7}$ and GFP-Mud$^{\Delta Ex12}$ respectively did not show an impairment of Mud localization at the oocyte NE nor asymmetry, compared to the control GFP-Mud (fig II. 6). However, there was partial delocalization of Mud in the perinuclear region.

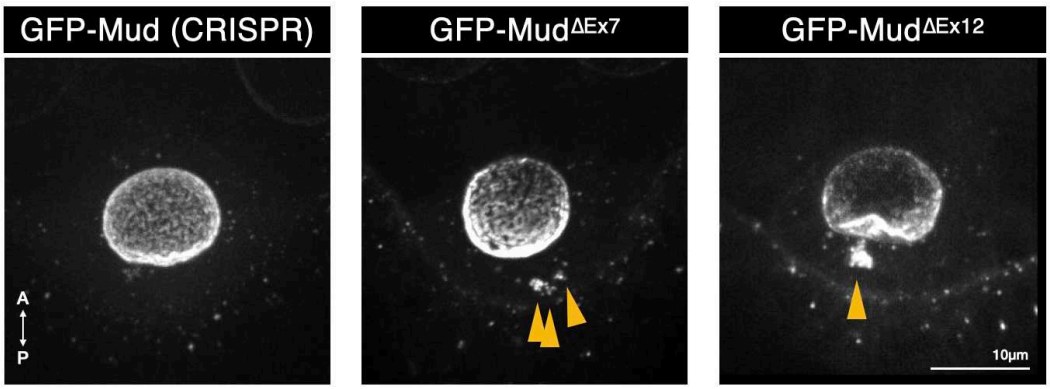

Figure II. 6: Perinuclear delocalization of Mud deleted of the putative NLS. Z-projections of living egg chambers from *GFP-mud (CRISPR)* flies, *GFP-mud$^{\Delta Ex7}$* flies, and *GFP-mud$^{\Delta Ex12}$* flies. The yellow arrows show the partial perinuclear delocalization of Mud at the posterior of the oocyte, in addition of its localization around the oocyte NE. The orientation of the egg chamber is indicated by the arrow A (anterior), P (posterior). Bar, 10µm.

To investigate if the interaction between Mud and Fs(2)Ket occurs via the typical mechanism based on NLS recognition, I tested the interaction between Fs(2)Ket and GFP-Mud$^{\Delta Ex7}$ or GFP-Mud$^{\Delta Ex12}$. To do so, I immunoprecipitated GFP-Mud$^{\Delta Ex7}$ or GFP-Mud$^{\Delta Ex12}$ using anti-GFP beads, and probed for anti-dsRed to detect Fs(2)Ket-mCherry. Fs(2)Ket and Mud still interact when either putative NLS from exon7 or from exon12 was deleted (n=4) (fig II. 7). This result show that none of the identified NLS motif is sufficient by itself to drive the interaction between Mud and Fs(2)Ket. Indeed, these two motifs could be redundant so as to ensure the protein interaction.

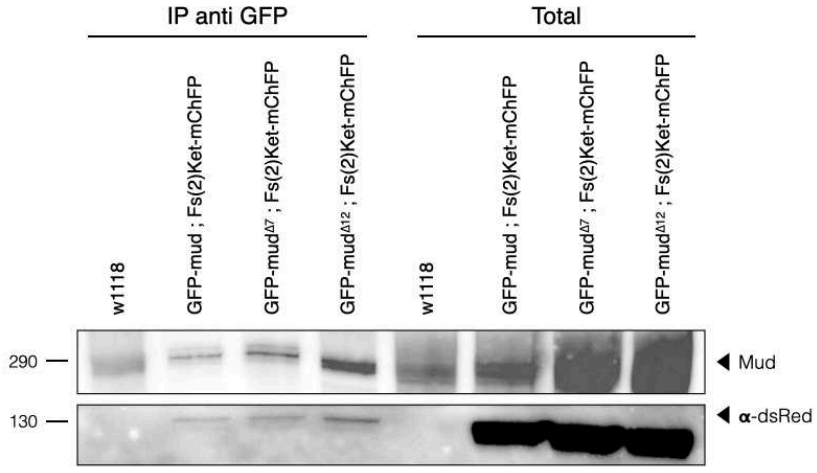

Figure II. 7: Mud deleted of either exon 7, or exon 12, still interacts with Fs(2)Ket. Immunoblot against Mud and against dsRed after co-immunoprecipitation (IP) using beads anti-GFP in ovary lysates from control (*w^{1118}*), *GFP-mud ; Fs(2)Ket-mChFP* strain, *GFP-mud$^{\Delta Ex7}$; Fs(2)Ket-mChFP* strain, and *GFP-mud$^{\Delta Ex12}$; Fs(2)Ket-mChFP* strain. Total of loaded lysates for the corresponding conditions is on the right of the gel. Detection using an antibody against dsRed allows to reveal the interaction with Fs(2)Ket-mChFP.

4) Fs(2)Ket and RanBP2 localize Mud at the oocyte nuclear envelope

a) Mud interacts with nucleoporin RanBP2

Next, I aimed to identify other partner proteins associated with the oocyte NE that could be involved in the localization of Mud, such as the nucleoporin Nup107 and the NPC cytoplasmic filament nucleoporin Nup358/RanBP2. Nup107 co-localizes with Mud at the oocyte NE (Tissot et al., 2017). RanBP2 has been shown to control NPC assembly in the *Drosophila* oocyte (Hampoelz et al., 2019), and has been identified as an Fs(2)Ket partner in *Drosophila* cultured cells (Guruharsha et al., 2011). RanBP2-GFP localizes around the NE of the germline cells and the somatic cells (fig II. 8). Its localization is punctate only around the oocyte NE while it is uniform at the nurse cell NE. By co-immunoprecipitation from ovary lysates, Mud interacts with RanBP2 (fig II. 9). Nup107 was also detectable in *GFP-mud* immunoprecipitation. Therefore, I identified a new partner for Mud: RanBP2. Next, I assessed the role of Fs(2)Ket and RanBP2 on Mud localization at the oocyte NE.

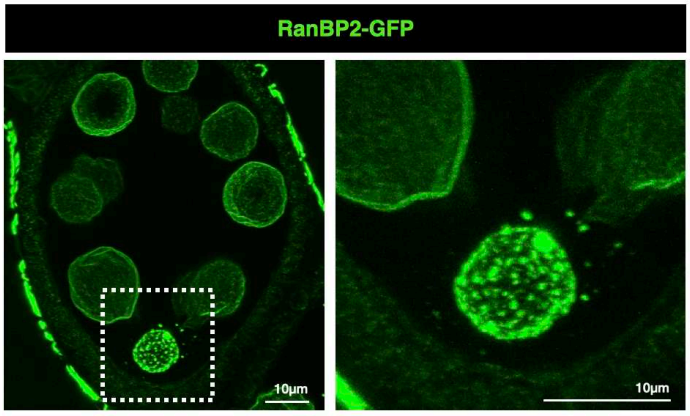

Figure II. 8: RanBP2 localization in the *Drosophila* egg chamber. Early chamber (stage 6A) expressing RanBP2-GFP. The GFP signal is uniform around the nuclei of the nurse cells, while it is punctuate around the oocyte nucleus. Moreover, the intensity is higher around the oocyte nucleus compared to the nurse cell nucleus. Bars, 10µm.

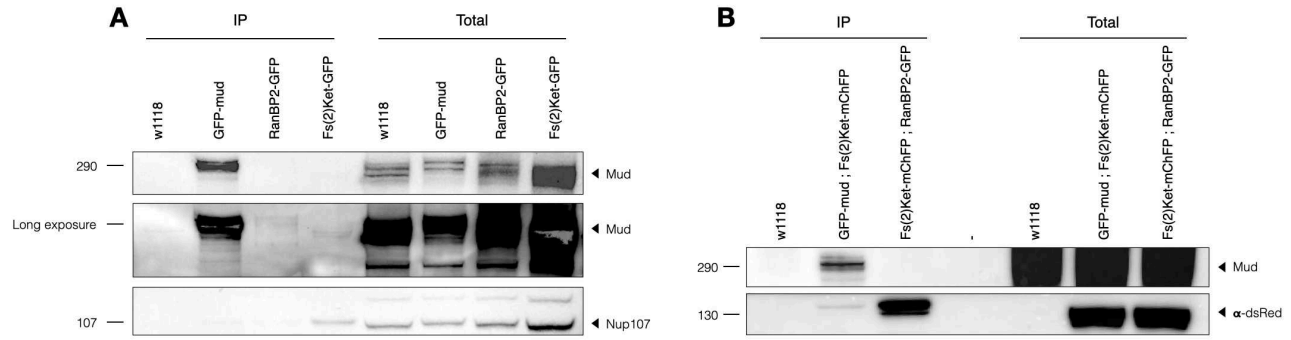

Figure II. 9: Mud interacts with RanBP2. (A) Immunoblot against Mud and Nup107 on immunoprecipitation (IP) using anti-GFP beads performed in ovary lysates from different strains: control strain *w*^{1118}, and in *GFP-mud* strain, *RanBP2-GFP* strain, and *Fs(2)Ket-GFP* strain. Total lysate are on the right of the gel. (B) Immunoblot against Mud and ds-Red on immunoprecipitations using anti-GFP beads performed in ovary lysates from different strains: control strain *w*^{1118}, and in *GFP-mud ; Fs(2)Ket-mChFP* strain, and in *Fs(2)Ket-mChFP ; RanBP2-GFP* strain.

b) Fs(2)Ket is necessary for the localization of Mud at the oocyte nucleus

To test the role of Fs(2)Ket on Mud localization at the oocyte NE, I used two different RNAi against Fs(2)Ket expressed in the germ cells (fig II. 10). I validated the use of *Fs(2)Ket-RNAi*^{Val20} as Fs(2)Ket-GFP was not detectable in germ cells compared to *Fs(2)Ket-RNAi*^{Val22} in which Fs(2)Ket-GFP was partially affected. Moreover, in *Fs(2)Ket-RNAi*^{Val20} context, Mud localization at the oocyte NE is abolished. This result indicates that Fs(2)Ket is required to localize Mud at the oocyte NE.

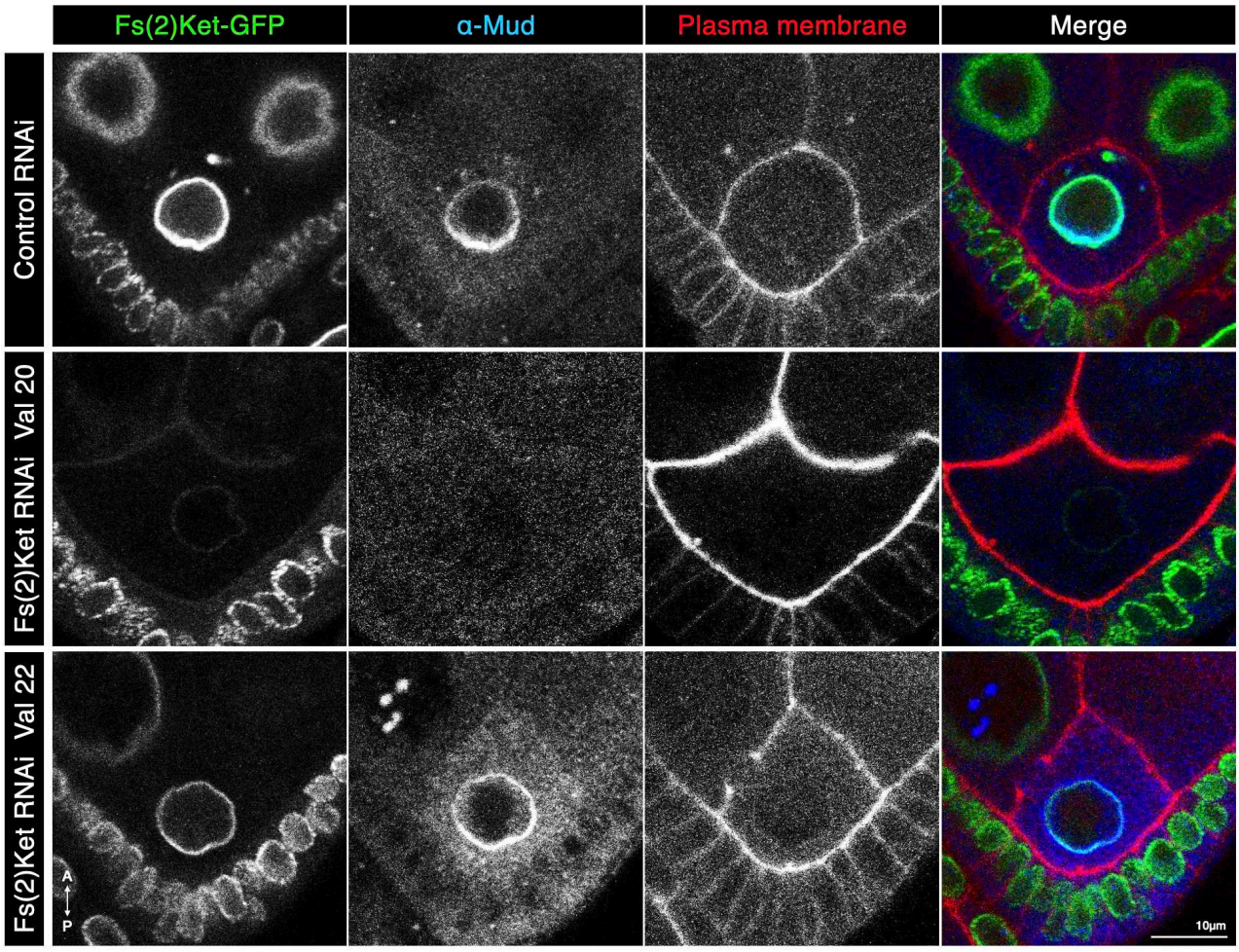

Figure II. 10: Fs(2)Ket is required to localize Mud at the oocyte NE. Immunofluorescence against Mud on egg chambers expressing RNAi driving the depletion of *Fs(2)ket* Valium 20 or Valium 22. These RNAi are only expressed in the germline cells, and therefore do not affect the follicular cells. The plasma membrane is visible via the expression of PH-RFP in these strains as well. The orientation of the egg chamber is indicated by the arrow A (anterior), P (posterior). Bars, 10µm.

c) RanBP2 contributes to Mud and Fs(2)Ket maintenance at the nuclear envelope

I then investigated the role of RanBP2 on the localization of Mud at the oocyte NE, using an RNAi against RanBP2 expressed in the germ cells (fig II. 11). Immunofluorescence using anti-Mud antibody shows that Mud asymmetry was not affected in this context, however there was partial delocalization of Mud at the posterior periphery of the oocyte nucleus. Moreover, Fs(2)Ket-GFP co-localized with Mud delocalization. These results show that RanBP2 is involved in proper localization of both Mud and Fs(2)Ket at the oocyte NE, and suggests a role in the retention of these two proteins at the NE. In addition of Mud localization, there was an effect of Fs(2)Ket depletion and RanBP2 depletion respectively on the development of the egg chambers and the positioning of the nucleus.

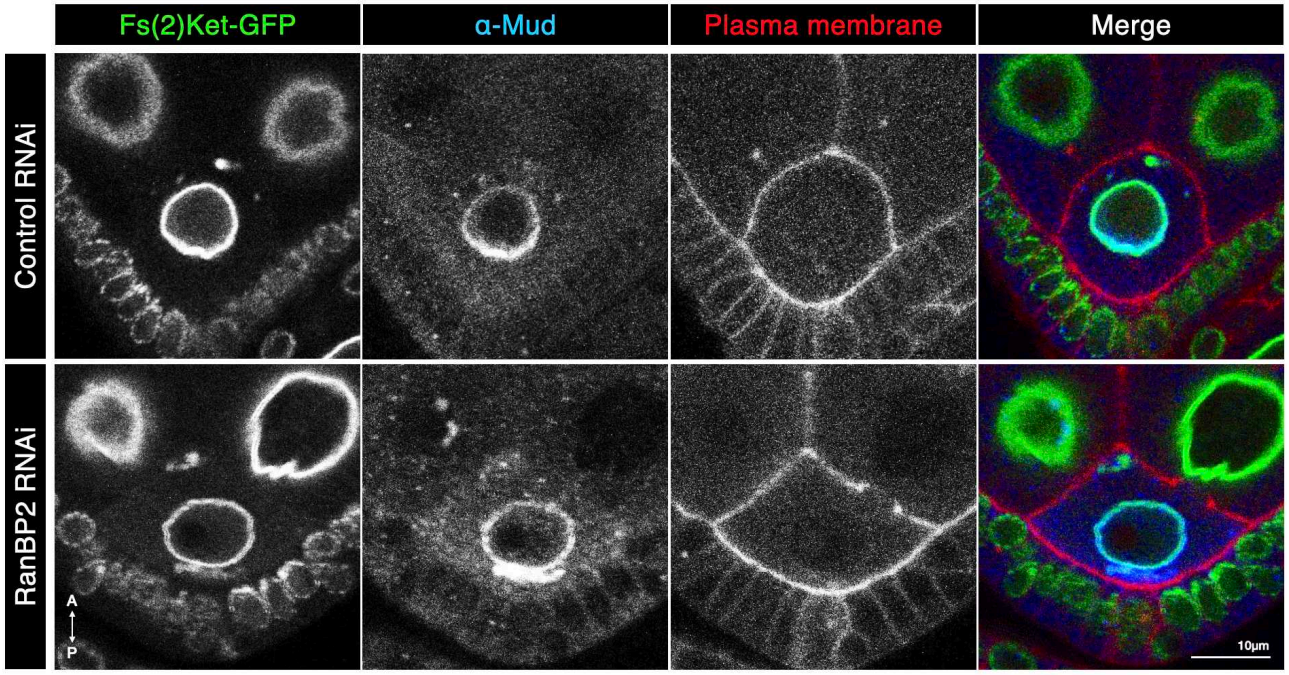

Figure II. 11: RanBP2 is required for correct localization of Mud and Fs(2)Ket at the oocyte NE. Egg chambers expressing Fs(2)KetGFP labeling the nuclei, PH-RFP labeling the plasma membrane and *RanBP2-RNAi* in the germline cells. Mud is detected by immunofluorescence using an antibody. The orientation of the egg chamber is indicated by the arrow A (anterior), P (posterior). Bars, 10µm.

d) Fs(2)Ket and RanBP2 are required in oogenesis

When using RNAi against *Fs(2)Ket* or *RanBP2* expressed in the germline cells, the aspect of the egg chambers was severely affected on the most matured egg chambers of the ovarioles compared to control ovariole (fig II. 12). Additionally, the development of *Fs(2)Ket*-depleted egg chambers was correct until stage 7-8, after which the nurse cells as well as the follicular cells show signs of disorganization and degenerescence. This difference between the early-oogenesis and late-oogenesis could reflect the force of the RNAi driver. Indeed, before stage 5-6, Fs(2)Ket-GFP signal is still detectable in the germline cells, while it is not when the egg chambers show signs of degenerescence.

Similarly, development of RanBP2-depleted egg chambers was affected but at later stage of oogenesis. The nucleus positioning was correct at stage 7-8, but at later stages the egg chambers were smaller and disorganized as well.

Altogether, these results indicate that 1) Mud is localized at the oocyte NE by Fs(2)Ket and that 2) RanBP2 is also involved in the restriction at the NE of Mud and Fs(2)Ket. Moreover, Fs(2)Ket is indispensable for oogenesis, and RanBP2 is required at later stages of oogenesis.

These observations also suggest that nucleus migration was affected in *Fs(2)Ket-RNAi* context. Therefore, I wanted to assess oocyte nuclear migration in this condition where Mud is delocalized from the oocyte nucleus. This would allow me to investigate the necessity of Mud restriction at the oocyte NE. To do so, I performed live imaging microscopy on *Fs(2)Ket-RNAi* expressing egg chambers. However, due to the degenerescence of the egg chambers and their morphology defects, I did not observe a proper nuclear migration.

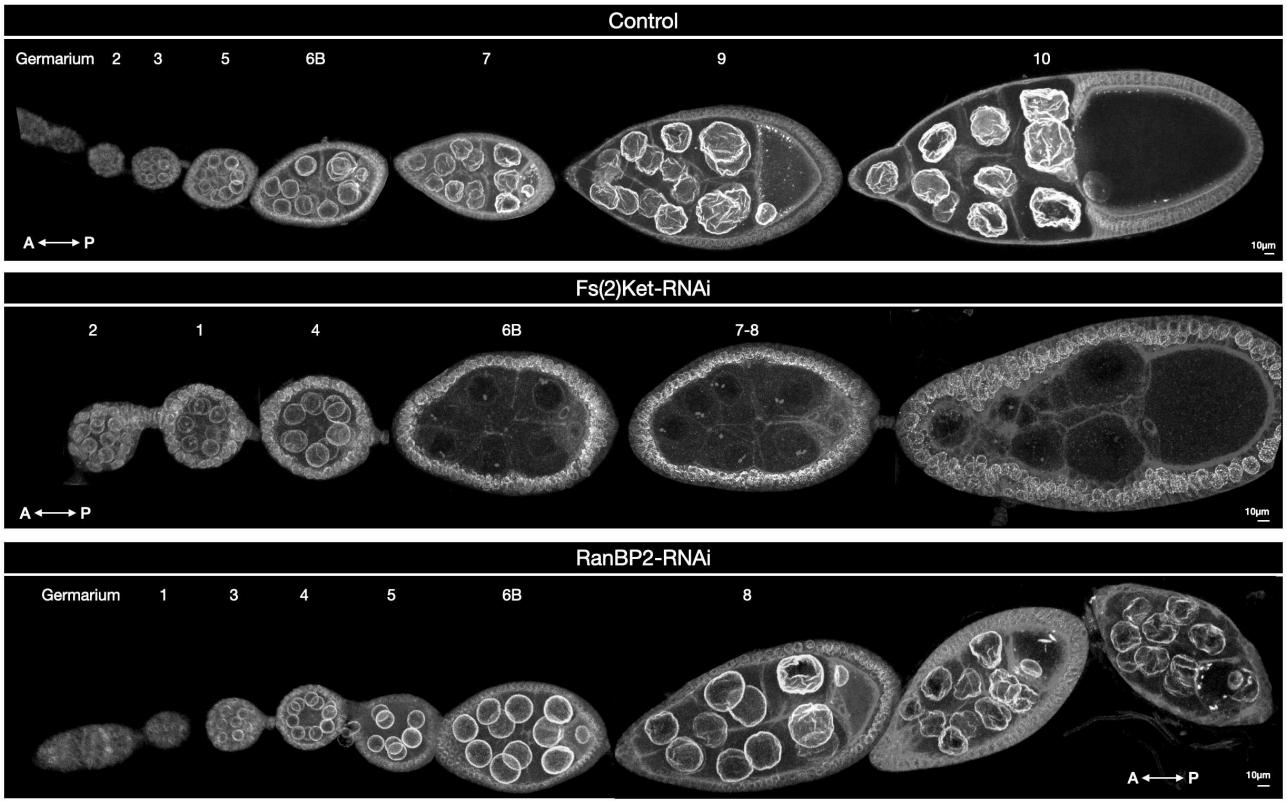

Figure II. 12: Fs(2)Ket and RanBP2 are required for oogenesis. Z-projection of representative ovarioles from a Control strain (Top panel), *Fs(2)Ket-RNAi* (Valium 20) expressing flies (Middle panel), and *RanBP2-RNAi* expressing flies (Bottom panel). The expression of the transgenes Fs(2)Ket-GFP and PH-RFP allow to visualize the nuclei and the plasma membranes of the egg chambers respectively. The stages of the egg chambers are indicated. The orientation of the egg chamber is indicated by the arrow A (anterior), P (posterior). Bar, 10µm.

5) Perinuclear delocalization of Mud

As I identified several contexts inducing a perinuclear delocalization of Mud at the oocyte, either in domain mutants, or in absence of one of its protein partner, I aimed to characterize this accumulation at the posterior of the nucleus. Although the deletion of the MT or TM domains, or putative NLS domains, or deletion of Fs(2)Ket or RanBP2 all cause a partial perinuclear delocalization of Mud at the posterior of the oocyte nucleus, these delocalizations differ (fig II. 13). Interestingly, delocalization of Mud deleted from its putative TM or NLS domains, in (fig II. 13.C) *GFP-mud$^{\Delta TM}$* , (fig II. 13.D) *GFP-mud$^{\Delta Ex7}$* or (fig II. 13.E) *GFP-mud$^{\Delta Ex12}$*, showed defined punctuates whereas it has stronger accumulation of signal in (fig II. 13.F) *mud$^{\Delta MT}$*, in (fig II. 13.G-G') *RanBP2-RNAi* or in (fig II. 13.H-I') *Fs(2)Ket-RNAi* context.

To determine the nature of perinuclear delocalization of Mud$^{\Delta MT}$, previous experiments of co-localization have been performed in my lab, between Mud and Lamin, WGA (Wheat Germ Agglutinin), KDEL (lys-asp-glu-leu, which is a C-terminal motif found on proteins involved in endoplasmic reticulum retention system), Shot (the only Spektraplakin in Drosophila) and Nup133. None of these association displayed a co-localization.

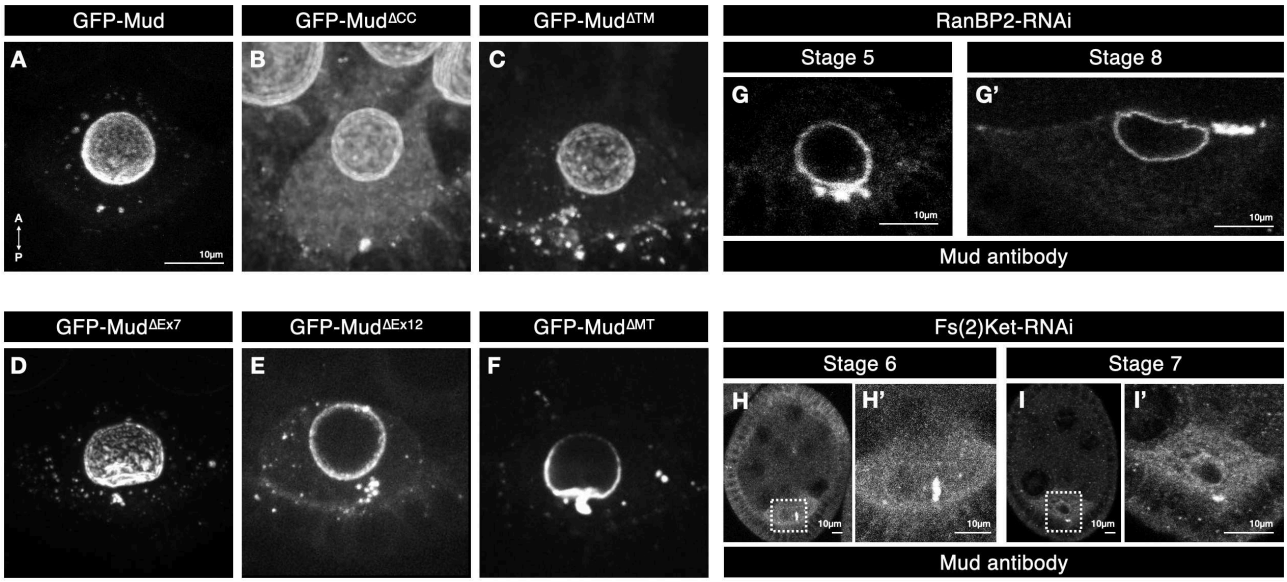

Figure II. 13: Mud perinuclear delocalization. Acquisitions of egg chambers from different strains in which Mud displays a partial delocalization at the posterior periphery of the nucleus. (A-F) Z-projection of imaged stacks to show Mud signal in oocytes expressing (A) GFP-Mud (CRISPR), (B) GFP-Mud$^{\Delta CC}$ 65B2, (C) GFP-Mud$^{\Delta TM}$, (D) GFP-Mud$^{\Delta Ex7}$, (E) GFP-Mud$^{\Delta Ex12}$, or (F) GFP-Mud$^{\Delta MT}$ (CRISPR). (G-G') Immunofluorescence against Mud of stage 5 and stage 8 egg chambers expressing *RanBP2-RNAi* in the germline cells. (H-I) Immunofluorescence against Mud of stage 6 and stage 7 egg chambers expressing *Fs(2)Ket-RNAi* Valium 20 in the germline cells, with the corresponding zoom (H'-I'). The orientation of the egg chamber is indicated by the arrow A (anterior), P (posterior). Bar, 10µm.

As GFP-Mud$^{\Delta Ex7}$ and GFP-Mud$^{\Delta Ex12}$ displayed partial delocalization in punctuates at the posterior of the nucleus where the centrosomes localize, I aimed to test co-localization between Mud and the centrosomes in these contexts. In living samples expressing both GFP-Mud (control or GFP-Mud$^{\Delta Ex7}$ or GFP-Mud$^{\Delta Ex12}$) and Asl-tomato to label the centrosomes, I observed co-localization of the two proteins only when Mud was deleted from its putative NLS motifs (fig II. 14). Mud seems to decorate and surround Asl. These results show that when Mud lacks its putative NLS domains, it is partially localized to the centrosomes, and therefore reinforces the hypothesis of the need for Mud retention at the oocyte NE. This could be a strategy to prevent Mud intervention on the dynamic or behavior of the oocyte centrosomes, or to ensure the organization of the ncMTOC at the oocyte nucleus.

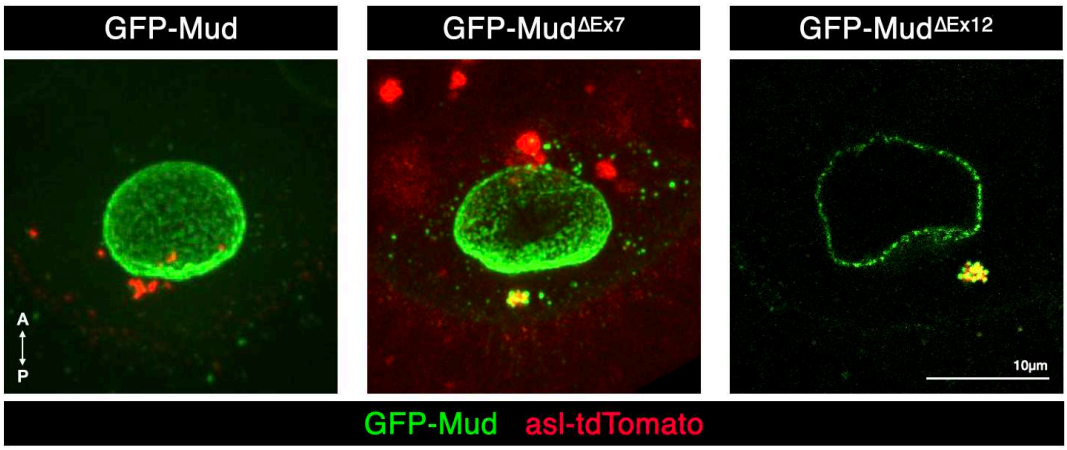

Figure II. 14: Mud$^{\Delta NLS}$ perinuclear delocalization co-localizes with the centrosomes. Acquisitions of egg chambers expressing GFP-Mud ; asl-tdTomato (left panel) GFP-Mud$^{\Delta Ex7}$; asl-tdTomato (middle panel), and GFP-Mud$^{\Delta Ex12}$; asl-tdTomato (right panel). The centrosomes are clustered and decorated by dots of GFP-Mud$^{\Delta NLS}$. The left and middle panel images are Z-projections of several imaged stacks, while the right panel image is one imaged stack only. The orientation of the egg chamber is indicated by the arrow A (anterior), P (posterior). Bar, 10µm.

Previously, my lab has shown that ɣ-tubulin localized around the oocyte NE, and therefore hypothesized that the microtubules emanating from NE were nucleated there (Januschke et al., 2006). It was shown that this nucleation was asymmetrically distributed around the NE with an enrichment on the nuclear posterior hemispheres where Mud is enriched (Tissot et al., 2017). We hypothesized that Mud was involved in microtubule nucleation and its asymmetry and could serve as a scaffold protein recruiting the proteins necessary to form the nuclear ncMTOC in the oocyte. Therefore, we wanted to identity protein partner candidates, validate their interaction with Mud and investigate their role on Mud localization and on the nucleus migration. First, we aimed to assess Mud role in the microtubule nucleation asymmetry at the oocyte NE.

1) Mud in microtubule nucleation at the oocyte nuclear envelope

Colcemid has been previously used to depolymerize the microtubules and observe the asters which emanate from the oocyte NE (Tissot et al., 2017). When optimizing the experimental conditions, I observed microtubule re-polymerization after 15 to 20min in the mounting oil after treatment with Colcemid (*Results - Part II. I. 3.a*). This amount of time is therefore challenging while considering the time it takes for mounting live ovaries followed by multiple position acquisitions by Spinning Disk microscopy. To optimize the experiment efficiency, I tried to fixe ovaries after Colcemid ovary incubation, so as to equally stop microtubule dynamics and obtain better reproducibility (fig III. 1.A). Although it seemed that the microtubule signal around the oocyte NE was weaker in fixed samples compared to living samples, as the asymmetry of nucleation at the posterior of the plasma membrane was correctly visible, I analyzed nucleation asymmetry at the NE in fixed samples (fig III. 1.B). Using the asymmetry semi-automated macro, quantification of the nucleation site distribution at the oocyte NE did not show an asymmetry under these conditions (fig III. 1.B) which differ from the conditions used in (Tissot et al., 2017). Therefore, we did not pursue our investigation regarding the role of Mud in the asymmetry of microtubule nucleation at the oocyte NE. Next, to investigate Mud's role in forming the nuclear ncMTOC, we aimed to identify some protein partners.

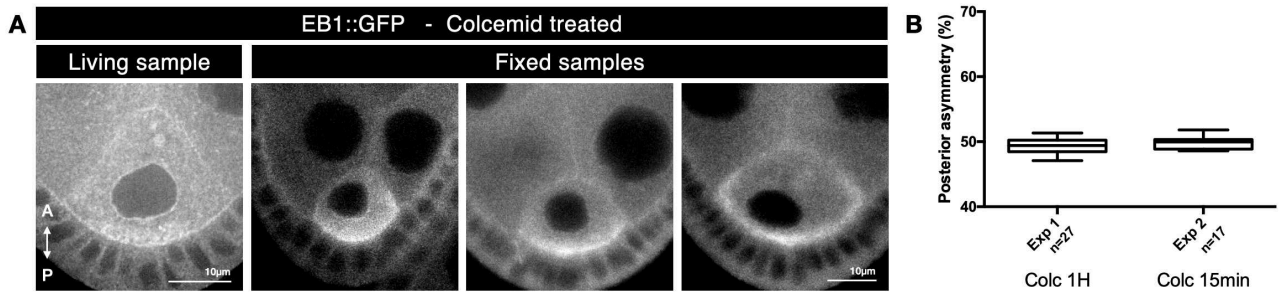

Figure III. 1: Microtubule nucleation at the oocyte NE in fixed samples. (A-C) Acquisitions of egg chambers, expressing EB1::GFP, treated with Colcemid to depolymerize the microtubules and measure the asymmetry of microtubule nucleation sites at the oocyte nucleus. (D) Graph presenting the quantifications of the asymmetry of the asters a the oocyte NE. 50% of asymmetry corresponds to no difference of signal intensity on both hemispheres. Under 50%: anterior asymmetry. Above 50%: posterior asymmetry.

2) Protein partner research

To identify protein partners which could be involved in Mud localization or in microtubule nucleation at the oocyte NE, I performed GFP-Trap of GFP-Mud from ovary lysates of the different transgenic strains. The aim was to of identify the domains of interaction that were involved in potential interactions. The following *mud* strains were used: GFP-Mud ; GFP-Mud$^{\Delta CC}$; GFP-Mud$^{\Delta Pins}$; GFP-Mud$^{\Delta TM}$. From these results, we established a list of 24 potential candidates for which the p-value was less than 0,05 (based on the candidate enrichment in the *GFP-mud* condition compared to the negative control condition) (fig III. 2). Mud was among one of the most enriched proteins identified, confirming the direct immunoprecipitation. Among the candidates, a few proteins were proteins that display a domain of RNA binding, some have post-translational modification functions, and some other have microtubule associated functions. To pursue our investigation, we decided to focus on proteins that were associated with microtubules, and notably: Tao and Otefin.

Enrichment Mud IP // Control IP	Name	Known informations	Mud	ΔCC	ΔPins	ΔTM	Colc
Infinity	dribble	RNA Binding					
Infinity	otefin	NE protein. Interacts with γ-tub					
190,51	CG3499	AAA-protease					
157,66	kurz protein	Helicase activity					
46,32	CG11586	Zinc Finger protein					
41,87	CG13531						
37,66	exuperantia	SAM domain, RNA binding					
20,28	MIP16750p	Aspartic peptidase					
18,69	RH47312p	Glutathione S-transferase					
18,20	**Mud**						
18,06	ubiquitin carboxy-terminal hydrolase	Peptidase - Found in MT interactome					
8,78	eIF5B	Translation initiation factor					
6,36	Tao	Set/Thr Kinase - MT dynamics regulation					
4,13	CG2246	Phosphoribosyl transferase					
3,37	larval serum protein 1 beta						
3,36	sec3	Exocyst					
2,78	CG10932	ActeylCoA acetyltransferase					
2,65	female-specific independent of transformer						
2,62	CG13126	Methyl-transferase activity					
2,59	CG12729						
2,32	ovarian tumor	MT organization, early oogenesis					
2,06	regulatory particle non-ATPase 1						
1,73	CG3061	Chaperonne					
1,68	FI06040p	mRNA Binding					
1,51	mitochondrial ribosomal protein S25	Ribosomal component					

Figure III. 2: Mud potential partner candidates co-immunoprecipitated with Mud and identified by Mass Spectrometry. Table presenting the potential partner of Mud based on their significant enrichment in *GFP-mud* condition compared to negative control condition *w^{1118}*. Identification of proteins in the other conditions is represented with the color code green (present) and red (absent).

3) Tao and Otefin: two potential candidates

a) Tao: a microtubule-associated kinase

Tao is a microtubule-associated kinase involved in the regulation of microtubule dynamics, as it plays a role in the stabilization of the plus ends in *Drosophila* cultured cells (Liu et al., 2010). Moreover, Tao's role on microtubule dynamics has been reported to be necessary for correct development of the mushroom body (King et al., 2011). First, I investigated the localization of Tao in the *Drosophila* egg chamber, using a strain generated by CRISPR/Cas9-mediated transgene integration which expresses Tao-Venus-GFP (Poon et al., 2016). Tao was associated with the plasma membranes of the egg chambers (fig III. 3).

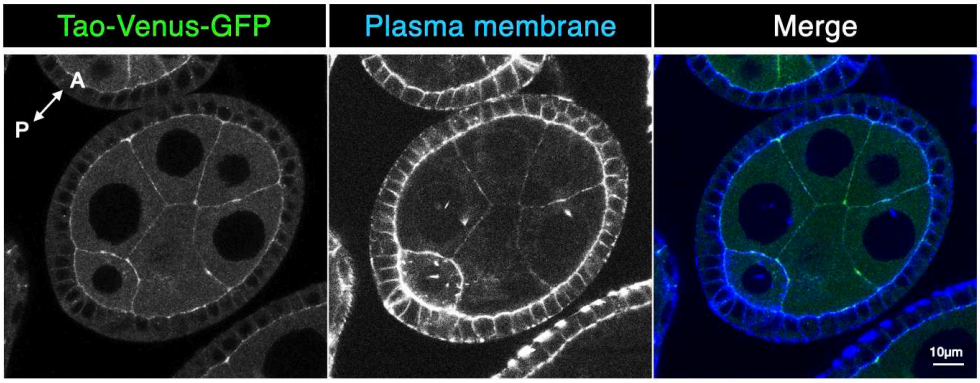

Figure III. 3: Tao localizes at the plasma membranes in the fly egg chambers. Immunofluorescence of Tao-Venus-GFP, labeling the plasma membrane. Orientation of the egg chamber is indicated with the arrow, (A: anterior. P: posterior). Bars, 10µm.

In the aim of confirming the interaction between Mud and Tao, I wanted to immunoprecipitate Tao-Venus-GFP using beads anti-GFP. In these experimental conditions, I could not immunoprecipitate Tao. So as to assess a potential role of Tao in Mud localization or nucleus positioning, I next depleted Tao in the germline cells, using RNAi lines, and observed that its depletion did not disturb Mud asymmetry (fig III. 4.A), nor the nucleus positioning and maintenance after nuclear migration (fig III. 4.B).

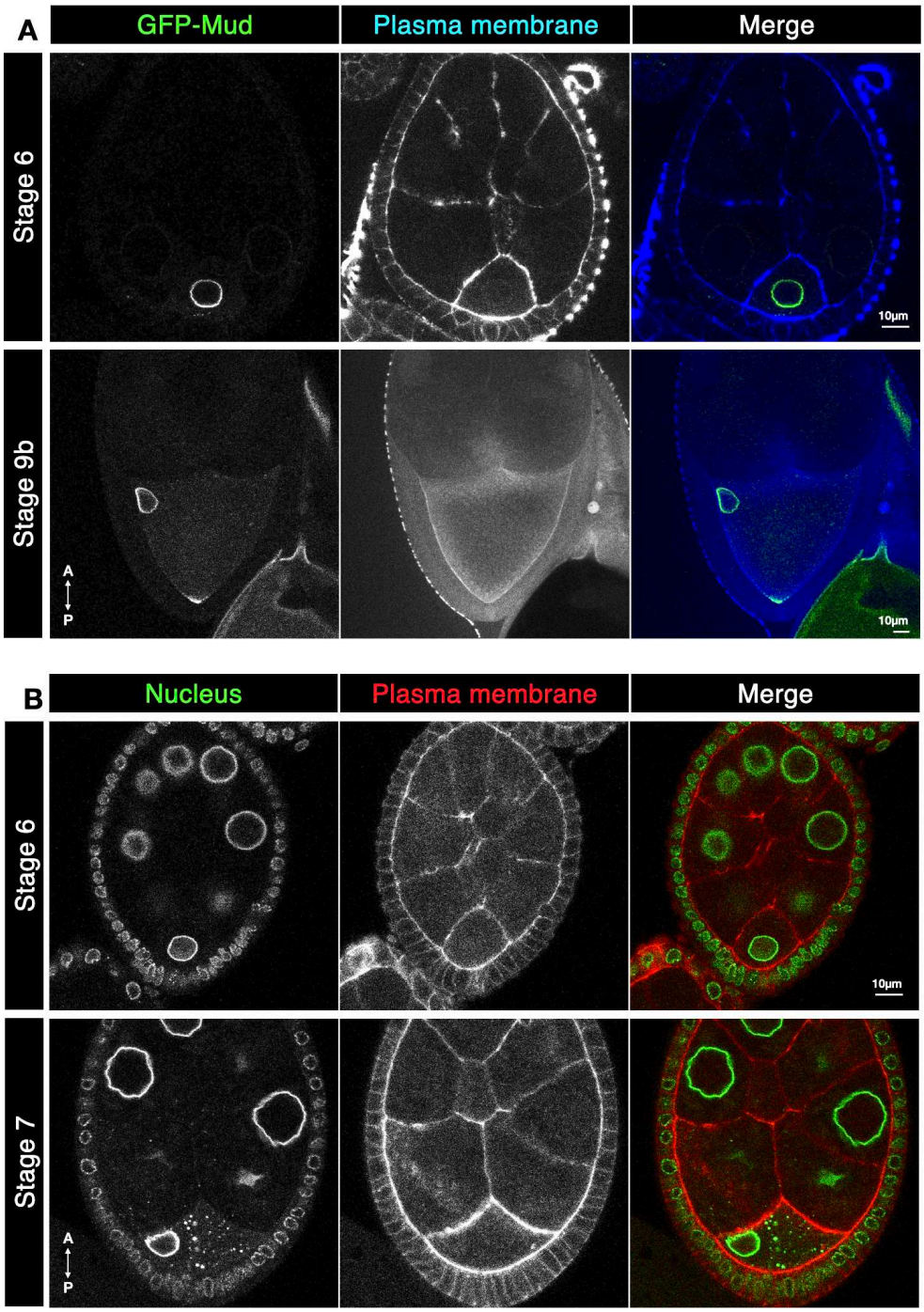

Figure III. 4: Tao is not involved in Mud asymmetry nor nucleus positioning in the Drosophila oogenesis. (A) Immunofluorescence of Stage 6 and 9b egg chambers expressing Tao-RNAi and GFP-Mud, the plasma membrane is labeled. (B) Acquisitions of Stage 6 and 7 egg chambers expressing Tao-RNAi in the germline cells. The nuclei are visualized by the detection of Fs(2)KetGFP, and the plasma membrane by the detection of PH-RFP. The orientation of the egg chamber is indicated by the arrow A (anterior), P (posterior). Bar, 10µm.

b) Otefin: the Emerin homolog

Otefin is a LEM-binding protein that localizes at the inner nuclear membrane and binds the lamina (Goldberg et al., 1998). In *Drosophila*, there are three LEM-domain proteins: dMAN1 the homolog of LEM2 (Wagner and Krohne, 2007), and, Otefin and Bocksbeutel (Bocks) the functional homologs of Emerin (Barton et al., 2014). In the female germ stem cells, mutation of Emerin impairs the nuclear lamina integrity, causing defective chromosomal segregation upon mitosis (Duan et al., 2021). As it is required for the viability of germ stem cells, Otefin depletion also affects the development of *Drosophila* ovaries (Barton et al., 2013; Jiang et al., 2008). From *Drosophila* cultured cell lysates, Otefin has been shown to co-precipitate with α- and ɣ-tubulin (Habermann et al., 2012). Moreover, the mutation of Emerin, in *Drosophila* female germ stem cells, induces a mislocalization of the centrosomes and their retention of the PCM, which therefore nucleate astral microtubules, causing a defect of the chromosomal segregation during mitosis in the cyst (Duan et al., 2021). These results suggest a role of Emerin in centrosome structure and maturation. Altogether, these informations make Otefin an interesting partner candidate for Mud. In order to confirm the interaction between Mud and Otefin, I immunoprecipitated Mud with Otefin, validating their interaction in the *Drosophila* ovaries (n=4) (fig III. 5). Then, I assessed the localization of Otefin in the egg chamber by immunofluorescence (fig III. 6). Otefin localizes at the nuclear rim of follicular cells and at the nuclear rim of oocyte nucleus and the two adjacent nurse cell nuclei. I observed a co-localization between Mud, Otefin and the lamin at the oocyte NE. Otefin was distributed in an isotropic manner around the NE (fig III. 6).

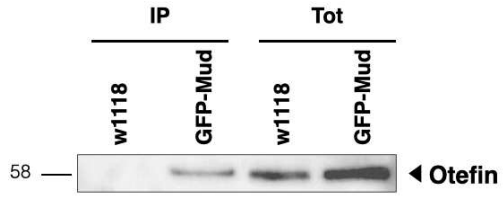

Figure III. 5: Mud interacts with Otefin in the Drosophila ovaries. Immunoprecipitation of GFP-Mud followed by immunoblot probing against Otefin reveals the interaction between the two proteins (n=4).

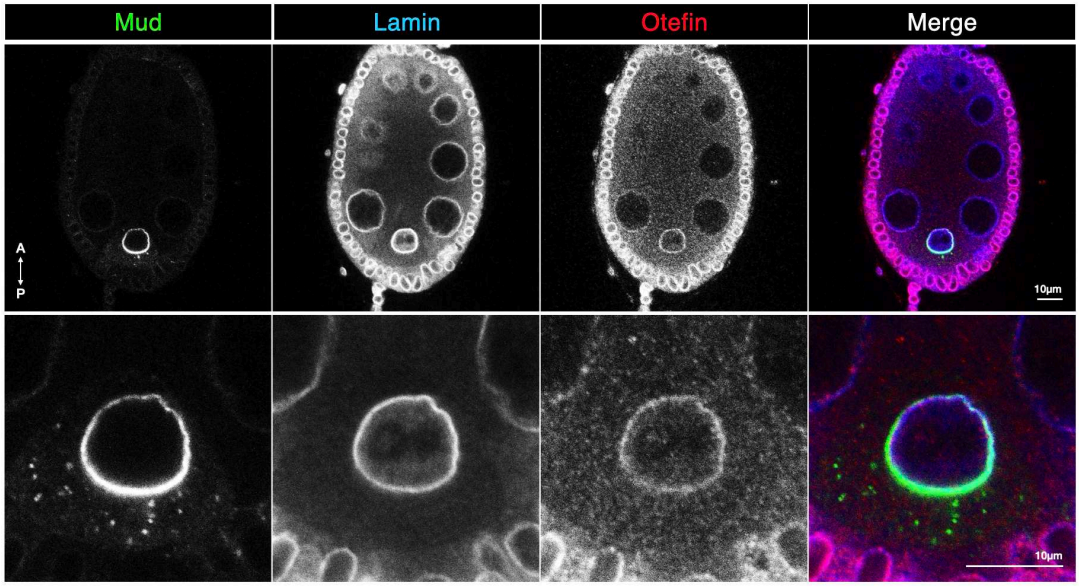

Figure III. 6: Otefin co-localizes with Mud and Lamin at the oocyte nucleus. Immunofluorescences of GFP-Mud expressing fly ovaries, labeling Lamin and Otefin. The bottom panel is a zoom of of the oocyte nucleus of the top panel. Bars, 10µm.

Next, I investigated Otefin's role on Mud localization and nuclear positioning. Otefin depletion using RNAi expressed in germ cells did not affect Mud asymmetry (fig III. 7.A), or nuclear asymmetrical positioning (fig III. 7.B). Altogether, these results allowed us to confirm at least one protein partner of Mud, Otefin. However, as we did not observe any effect of Otefin depletion, we did not pursue our research on Mud and Otefin in the context of the oocyte nuclear migration.

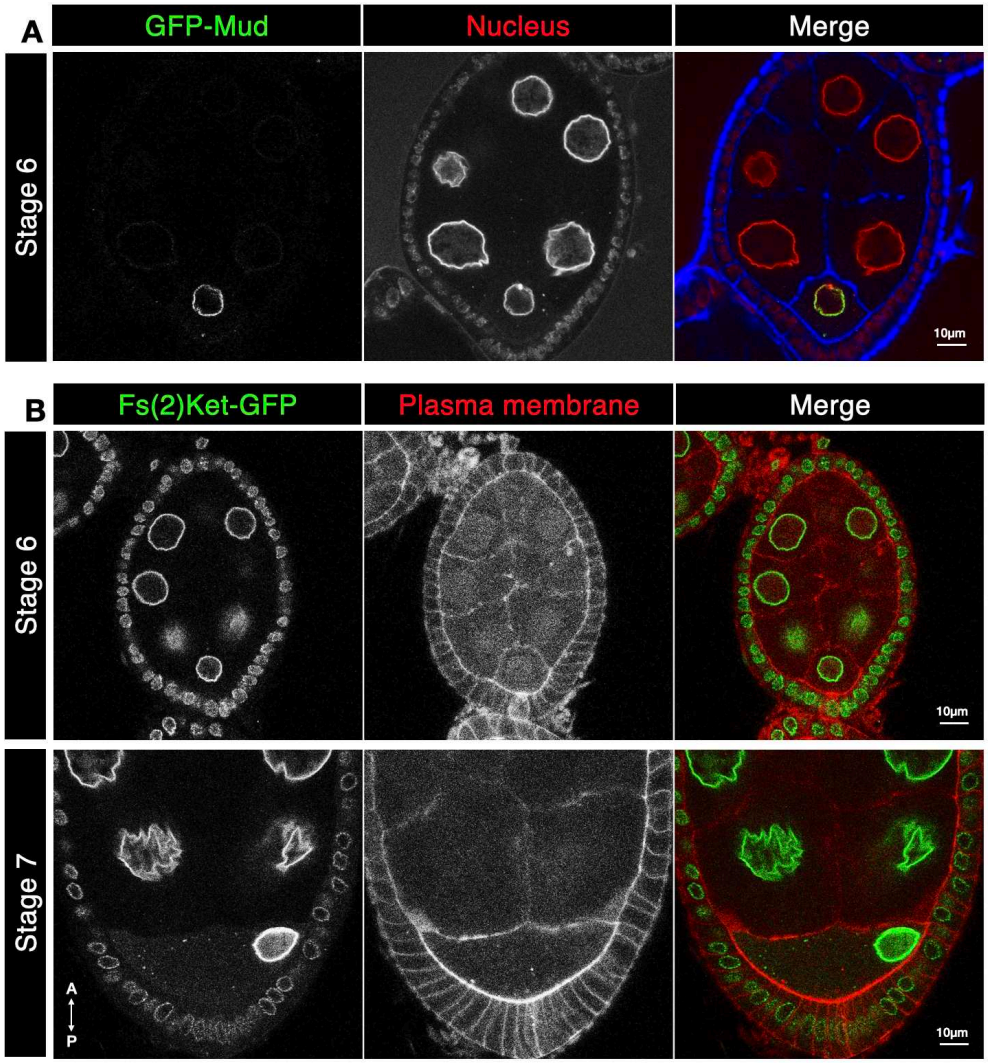

Figure III. 7: Otefin is not involved in Mud asymmetry nor nucleus positioning in the Drosophila oogenesis. (A) Immunofluorescence of Stage 6 egg chamber expressing GFP-Mud and Otefin-RNAi in the germline cells, to label the nucleus (using WGA) and the plasma membrane.
(B) Acquisitions of stage 6 and 7 egg chambers expressing Otefin-RNAi in the germline cells. The nuclei are visualized by the detection of Fs(2)KetGFP and the plasma membrane by the detection of PH-RFP. Orientation of the egg chamber is indicated by the arrow A (anterior), P (posterior). Bar, 10µm.

Thus, we now know that Mud localization at the oocyte NE is dependent on Fs(2)Ket. Moreover, RanBP2, a newly identified Mud partner, participates in the restriction of Mud and Fs(2)Ket at the oocyte NE. My results show that Mud C-terminal region; notably newly identified NLS domains, MT binding site, and TM domains, seem to contribute in Mud restriction from the centrosomes, which partial delocalization correlates with a decrease of the posterior trajectory of the nuclear migration. To confirm this, it will be important to assess oocyte nuclear trajectory in *GFP-mud*$^{\Delta Ex7}$ and *GFP-mud*$^{\Delta Ex12}$.

PART 2 : CENTROSOMES IN THE OOCYTE NUCLEAR MIGRATION

In this part, I will present my results investigating the mechanisms by which centrosomes act on nuclear migration. This work has been submitted and is currently under revision (Loh et al., 2022).

CHAPTER I : CENTROSOME CLUSTERING PRIOR TO MIGRATION

As to better understand the mechanisms by which the centrosomes regulate the nuclear migration in the oocyte, I aimed to better characterize their clustering behavior, and investigate the importance of this process regarding the positioning of the nucleus and its migration. First, I proposed a revision of our staging method, and observed that it correlates with the centrosome behavior and the nucleus positioning prior to migration. Finally, trying to understand by which mechanism centrosome clustering is regulated, I investigated the role of Kinesin-1.

1. Oogenesis stage refinement

In the literature, oogenesis can be classified into early-, mid-, and late oogenesis. Early oogenesis represents stages from 1 to 6, mid-oogenesis represents stages from 7 to 10a, and the following stages are considered as late oogenesis (Fedorova et al., 2019; Jia et al., 2016; King et al., 1956; Lin and Spradling, 1993). Indeed, oogenesis stages are notably defined on the base of morphological criteria, nucleus positioning, division state of the follicular cells, or other cytoplasmic events within the egg chamber. The inconvenient of staging egg chambers regarding their morphology appears while studying specific processes in mutant contexts in which development delays or morphology defects are induced. Staging egg chambers on the base of particular event, such as nucleus positioning, is also not suitable when studying the oocyte nuclear migration. For example, we define stage 6 egg chamber as as an oval shaped egg chamber, which displays a non migrated oocyte nucleus (*i.e* in contact with the anterior and lateral plasma membranes). However, I noticed that nucleus position, as well as oocyte shape and egg chamber length, varied in WT egg chambers that we would classified as stage 6 (fig I. 1).

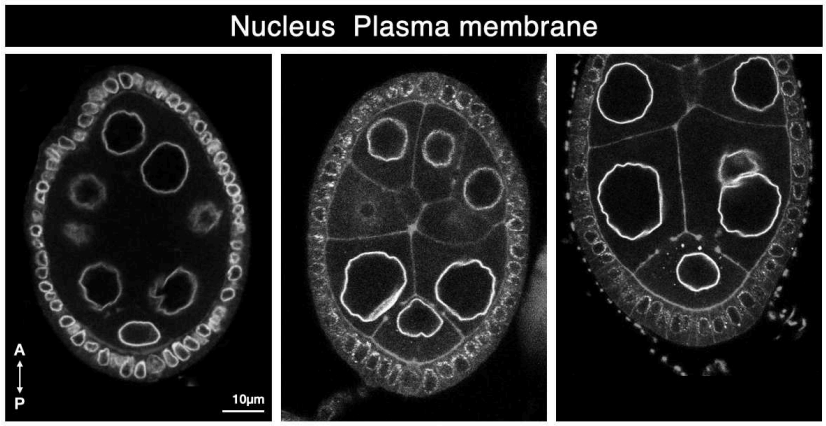

Figure I. 1: Oogenesis stage 6 prior to stage refinement. Immunofluorescences of control egg chambers to label nuclei and plasma membrane. Egg chambers identified such as stage 6 egg chambers prior to stage refinement, on the base of the egg chamber oval shape. The oocyte nucleus of left and right panels are rather centered in the oocyte, while the middle panel oocyte nucleus is in contact with the anterior plasma membrane. The two first egg chambers are smaller than the right panel egg chamber. Bar, 10µm.

Moreover, over the years and depending on the field, authors do not always refer to the same oogenesis stage for a given event. For example, nowadays the oocyte nuclear migration process is referred to occur between stages 6 and 7 of oogenesis (Tissot et al., 2017), while it was described to occur between stage 7 and stage 8 (Duncan and Warrior, 2002; Januschke et al., 2002), or in between stages 7 and 9 (Roth and Lynch, 2009; Theurkauf et al., 1992). Finally, early and mid-oogenesis stages are less well characterized than the late stages. Therefore, for this study, I aimed to refine our staging definition and characterize the nucleus positioning in WT background, before investigating it in mutant contexts. Recently, Chen et al., proposed a refined classification of stages 4 to 8 based on different parameters: egg chamber morphology, mitotic cycle state of the egg chamber different cells, somatic cell number, egg chamber aspect ratio and volume, and nurse cell diameter (Chen et al., 2019). Interestingly, the authors distinguished stage 6 egg chambers into two stages: 6A and 6B (fig I. 2). However, on morphological aspects, we would classify their representative stage 7 egg chamber as a stage 6 egg chamber, as the oocyte shape of their stage 7 egg chamber is typical of a stage where the nuclear migration has not started yet. Similarly, we would classify their representative stage 8 egg chambers as a stage 7 egg chamber, as the oocyte shape and volume are typical of a stage 7 egg chamber.

stage	6A	6B	7	8
morphology	increased follicle aspect ratio; equal nurse cell ploidy	more follicle cells and bigger nurse cell nuclei; follicle cells cease mitosis at the end of 6B	increased follicle aspect ratio; no mitotic follicle cells; higher nurse cell ploidy at posterior; no oocyte yolk visible	yolk in oocyte visible; anterior squamous cell morphogenesis not yet initiated
duration (h)	1.5	1.5	6	6
representative confocal image DNA membrane GFP F-actin	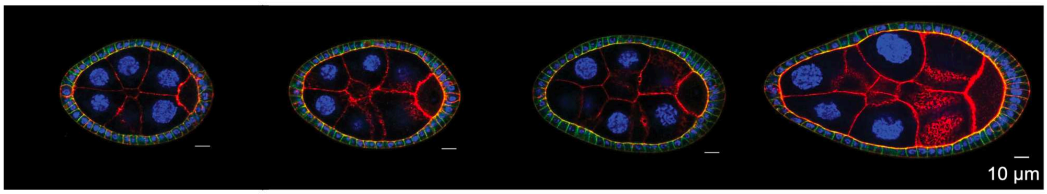			
number of cells	550 ± 44	751 ± 66	887 ± 33	862 ± 28
aspect ratio	1.42 ± 0.12	1.54 ± 0.12	1.82 ± 0.09	1.91 ± 0.07
volume (µm³)	131,636 ± 32,104	219,000 ± 8,0991	334062 ± 49880	552705 ± 91295
nurse cell nuclear diameter (µm)	14.28 ± 1.95	15.59 ± 2.61	19.86 ± 3.05	23.64 ± 1.66

Figure I. 2: Staging egg chambers in *Drosophila* oogenesis, adapted from (Chen et al., 2019). Representative images of WT egg chambers of stage 6A to 8 and corresponding morphological description. Stage durations in hour (h) according to (Lin and Spradling, 1993), measures of the number of follicular cells, egg chamber aspect ratio, egg chamber volume, and nurse cell diameter. Values shown are average ± standard deviation (s.d.) Bars, 10 µm.

a) Cut and Hindsight as staging markers

To decipher correctly oogenesis stages to further study the asymmetrical position of the oocyte nucleus in mutant contexts, my lab had previously used Cut and Hindsight (Hnt) as markers. Cut and Hnt are two transcription factors which expressions have the particularity to depend on the somatic follicular cell division cycle (Sun and Deng, 2007). Indeed, follicular cells divide until mid-oogenesis, after which they go through endocycles. Thus, Cut is expressed in somatic follicular cell nuclei in early oogenesis egg chambers, while Hnt is expressed in the follicular cell nuclei of mid- and late oogenesis egg chambers. By using these two markers in WT contexts, my lab was able to validate the use of this method to distinguish stage 7 egg chambers from earlier egg chambers, and confirm that oocyte nucleus migration was complete at stage 7. Indeed, analyzing

these previously taken images, I observed that follicular cells were Cut positive and Hnt negative in stage 5 egg chambers (fig I. 3.A). Conversely, in stage 7 egg chambers, follicular cells were Cut negative and Hnt positive. However, when studying the active process of nuclear migration at stage 6 rather than asymmetrical positioning at stage 7, I noticed that stage 6 egg chambers were Hnt negative, but Cut marker was either positive or negative. Moreover, I noticed that stage 6 Cut positive egg chambers were smaller than stage 6 Cut negative egg chambers (fig I. 3.B) similarly to the morphological differences observed by Chen and colleagues between stage 6A and 6B (fig I. 2). As Cut and Hnt staging method is not compatible with live imaging, and is not sufficient to distinguish precisely between stage 6A and 6B, I aimed to use Chen et al. method to decipher in between Cut positive and Cut negative stage 6 egg chambers.

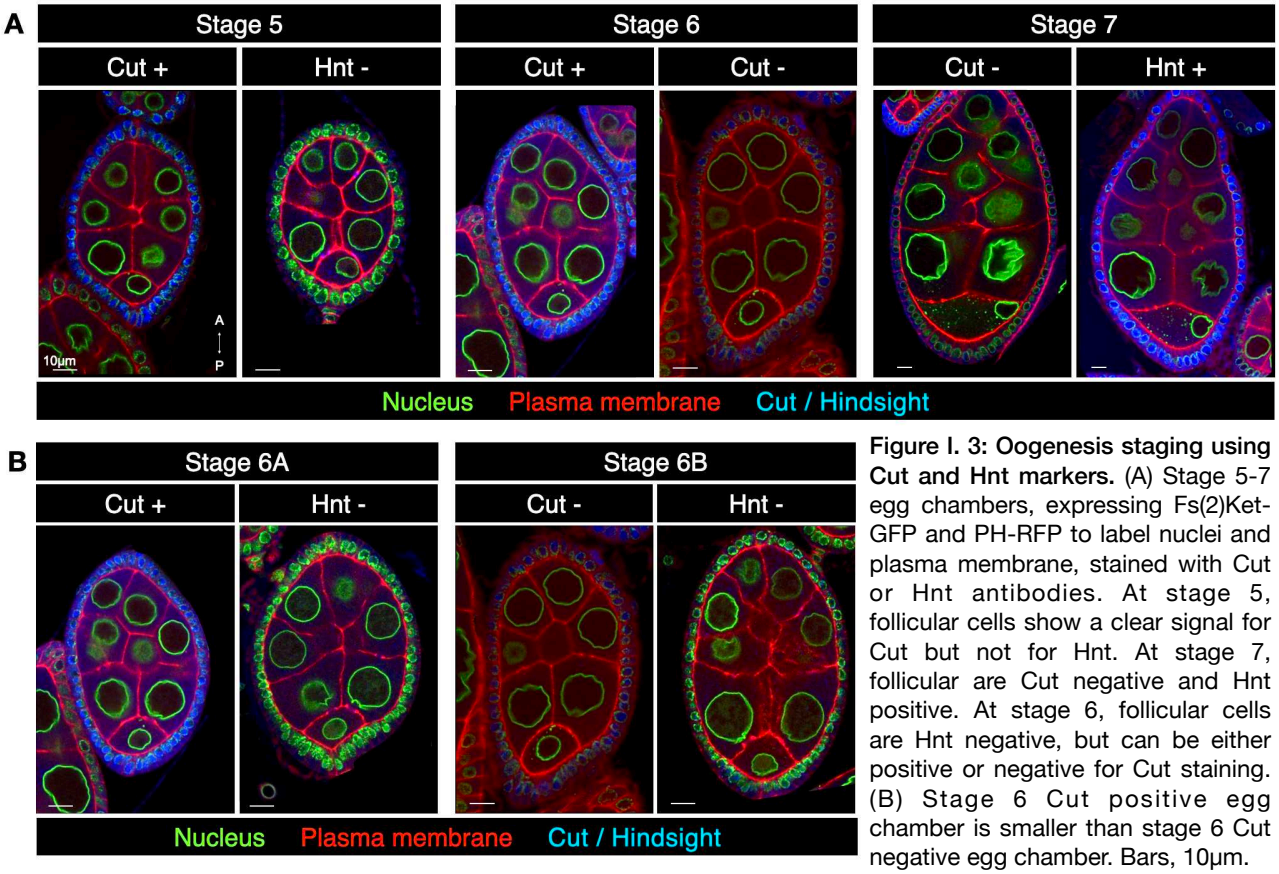

Figure I. 3: Oogenesis staging using Cut and Hnt markers. (A) Stage 5-7 egg chambers, expressing Fs(2)Ket-GFP and PH-RFP to label nuclei and plasma membrane, stained with Cut or Hnt antibodies. At stage 5, follicular cells show a clear signal for Cut but not for Hnt. At stage 7, follicular are Cut negative and Hnt positive. At stage 6, follicular cells are Hnt negative, but can be either positive or negative for Cut staining. (B) Stage 6 Cut positive egg chamber is smaller than stage 6 Cut negative egg chamber. Bars, 10µm.

b) Refinement of oogenesis stages using morphological and quantitative parameters

By measuring egg chamber aspect ratio (length/width) and the two oocyte adjacent nurse cell diameters (fig I. 4.A), on the previously taken acquisitions using Cut and Hnt, I found very similar results than Chen et al. (fig I. 4.B-C). Adapting their classification to our morphological definition of stage 6 and 7, I proposed that their stage 6A corresponds to our 5, their 6B to our 6A, their 7 to our 6B, and their 8 to our 7. Using this method on control egg chambers, I observed a progressive increase of nurse cell diameters (fig I. 5). However, as standard error of the means were overlapping from one stage to another, the nurse cell diameter can not be used by itself to stage egg chambers. I proposed that a combination of criteria, such as nurse cell diameter, oocyte shape, and egg chamber aspect ratio, are required to correctly stage the egg chambers.

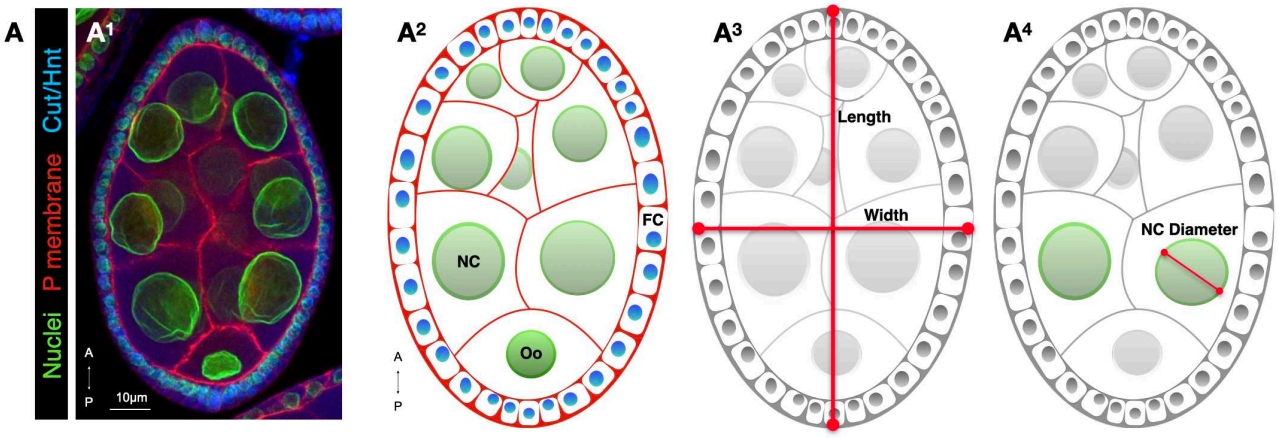

B

Criteria / Nucleus	Non migrated nucleus	Migrated nucleus
Egg chamber aspect ratio	1.54 ± 0.16	1.76 ± 0.13
Nurse cell diameter (µm)	17.28 ± 3.4	23.69 ± 2.95

C

Criteria / Nucleus	Non migrated nucleus		Migrated nucleus	
Cut/Hindsight label	Cut +	Hnt-	Cut -	Hnt +
Egg chamber aspect ratio	1.58 ± 0.16	1.43 ± 0.12	1.73 ± 1.04	1.80 ± 0.12
Nurse cell diameter (µm)	15.6 ± 1.93	20.1 ± 3.62	23.13 ± 3.31	23 ± 3.72

Figure I. 4: Oogenesis staging method refinement of egg chambers surrounding the oocyte nuclear migration. (A) (A[1]) Stage 6 egg chamber, expressing Fs(2)Ket-GFP to label nuclei (green) and PH-RFP to label plasma membrane (red), stained with Cut antibody (blue). (A[2]) Corresponding scheme showing the nuclei of different cell types: the follicular cells (FC) in blue, the nurse cells (NC) in light green, and the oocyte (Oo) in dark green. (A[3]) Corresponding schematic diagram showing the definition of the egg chamber length and width to determine the aspect ratio. (A[4]) Corresponding schematic diagram showing the definition of the two NC diameters that are adjacent to the oocyte. The orientation of the egg chamber is indicated by the arrow A (anterior), P (posterior). Bar, 10µm. (B-C) Table presenting the data obtained when measuring the aspect ratio and NC diameters of egg chambers stained for Cut and Hnt.

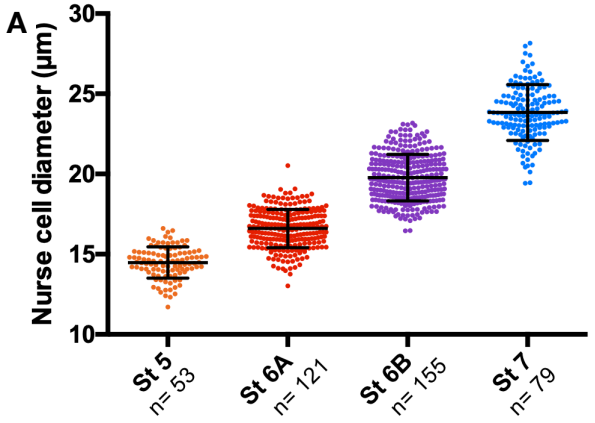

B

Stage	Nurse cell diameter (µm)
St 5	14,6 ± 0,78
St 6A	16,6 ± 1,37
St 6B	19,2 ± 1,43
St 7	23,5 ± 1,98

Figure I. 5: Oocyte adjacent nurse cell diameter measurement to stage egg chambers. (A) Distribution of nurse cell diameters, from WT egg chambers, showing a progressive increase in size allowing categorization of 4 different stages: 5, 6A, 6B, 7. (n indicates the number of analyzed egg chambers but dots corresponds to each measured nuclei). Means ± s.e.m for each stage are indicated in (E).

c) Nucleus positioning along the newly defined stages

Using this method to stage egg chambers, I next aimed to characterize egg chamber morphology prior to migration. Therefore, I characterized living control egg chambers expressing markers to label the nuclei and plasma membranes (fig I. 6.A-top). Stage 5 egg chamber is rather round, compared to stage 6A and 6B egg chambers which progressively elongate and display an oval shape. Stage 7 egg chamber is longer and larger. The oocyte shape and volume also progress along these stages (fig I. 6.A-bottom). Indeed, at stage 5, the oocyte anterior plasma membrane is a croissant shape, and the nucleus mainly occupies the oocyte volume. At stage 6A, the oocyte volume is bigger around the nucleus. At stage 6B, the oocyte volume is even bigger and the anterior and posterior plasma membrane intersections are further apart. At stage 7, the oocyte volume is bigger and the anterior plasma membrane more linear than curved. The quantifications of the oocyte nucleus positioning along these stages shows an evolution as well (fig I. 6.B). At stage 5 and 6A, the nuclei are mainly positioned at the anterior of the oocyte, in contact or proximity with the anterior plasma membrane of the oocyte. At stage 6B, just prior to nuclear migration, the oocyte nuclei are mostly centered in the cell, indicating of a centering movement of the nucleus in between stage 6A and 6B. The oocyte nuclear migration occurs between stage 6B and 7, at which the nucleus is asymmetrically positioned within the oocyte in contact with the anterior and plasma membranes. After the refinement of our staging criteria and the characterization of the associated morphology and nucleus positions, I aimed to characterized the oocyte centrosome clustering.

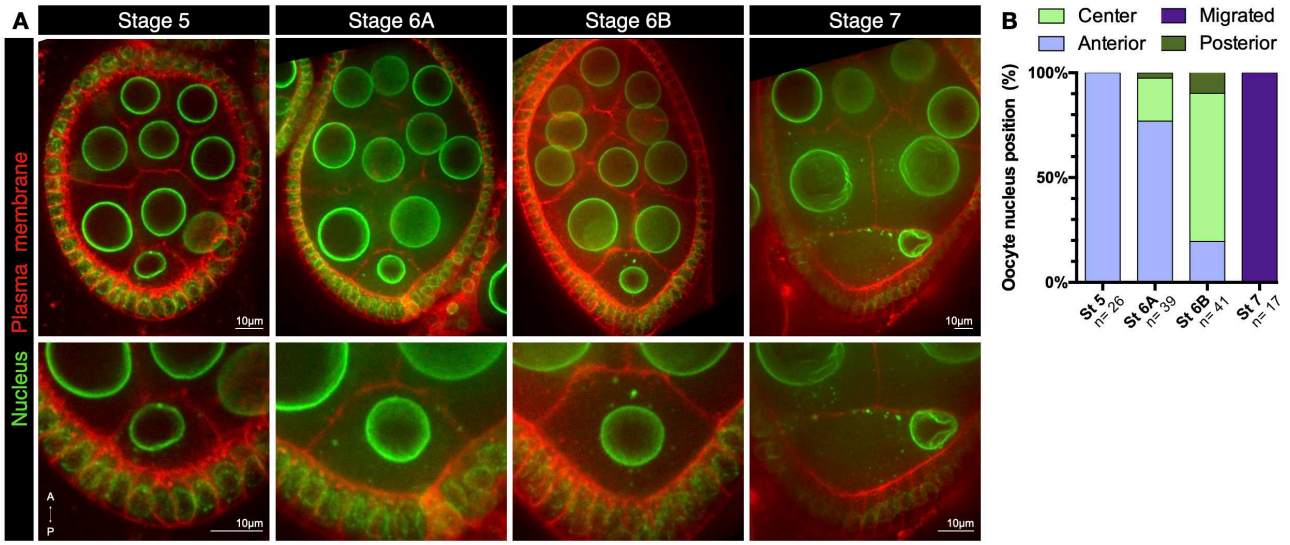

Figure I. 6: Characterization of the nucleus positioning prior to migration. (A) Z-projections of Stage 5 to 7 living egg chambers, expressing Fs(2)Ket-GFP to label nuclei (green) stained with Cellmask to reveal plasma membranes (red). Representative examples of the different morphology of the egg chambers at stages 5, 6A, 6B and 7 (top panel) and magnification of their nuclear positions (bottom panel). The orientation of the egg chamber is indicated by the arrow A (anterior), P (posterior). Bars, 10µm. (B) Distribution of nucleus positions at the different stages. Positions have been categorized and color-coded as anterior in pale blue, center in pale green, posterior in dark green and migrated in purple. n indicates the number of analyzed egg chambers.

2. Centrosome clustering prior to migration

Studies have investigated oocyte centrosome migration from nurse cells to oocyte in the germarium (Bolívar et al., 2001; Mahowald and Strassheim, 1970), their role during nuclear migration by exerting pushing forces and regulating the anterior trajectory (Tissot et al., 2017), as well as their elimination at late-oogenesis (Pimenta-Marques et al., 2016). Although, studies agree to describe that centrosomes migrate in association with the nucleus to the antero-lateral cortex at mid-oogenesis (Januschke et al., 2006), they differ when describing their behaviors. Indeed, centrosomes have been reported to coalesce into a compact structure (Tissot et al., 2017), or large cluster (Bolívar et al., 2001), or dynamic dense cluster that also displays sparse distribution (Zhao et al., 2012). Thus, I aimed to characterize their clustering along the developmental stages preceding the nuclear migration.

a) Progressive clustering of the oocyte centrosomes prior to migration

To characterize centrosome clustering in the oocyte, I imaged control living egg chambers expressing the transgenes Fs(2)Ket-GFP and asl-td-Tomato to label the nuclei and centrosomes respectively (fig I. 7.A). To determine centrosome clustering or scattering aspect, I took two parameters in account: centrosome number (considered as scattered when >10 centrosomes were distinguishable) and spatial distribution (considered as scattered if sparse distribution in the oocyte volume). Based on this qualitative quantification, I observed that at stage 5 and 6A, when the nucleus is anteriorly positioned in the oocyte, centrosomes are mainly scattered (fig I. 7.B). At stage 6B, prior to migration, when the nucleus is centered in the oocyte, centrosomes are clustered. They remain clustered at the completion of oocyte nuclear migration at stage 7. Moreover, at stage 7 centrosome number was decreased compared to previous stages. These results show that centrosome clustering is a progressive process occurring prior to oocyte nuclear migration. Additionally, centrosome clustering correlates with nucleus centering within the oocyte.

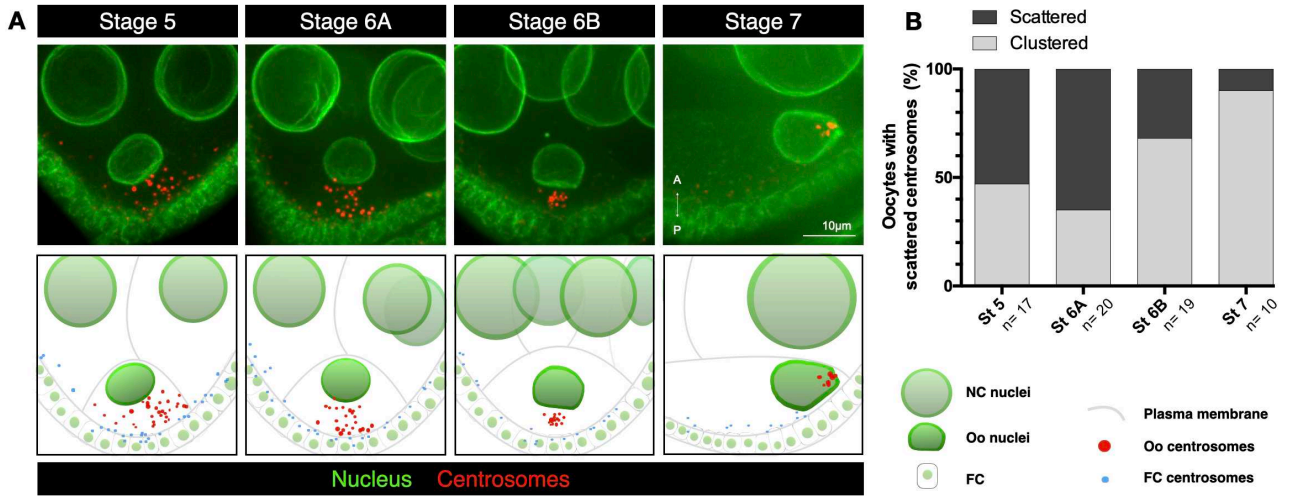

Figure I. 7: Progressive centrosome clustering prior to the oocyte nucleus migration. (A) (Top panel) Representative Z-projection images of stage 5 to 7 egg chambers, expressing Fs(2)Ket-GFP to label nuclei (green), asl-tdTomato to label centrosomes (red). The orientation of the egg chamber is indicated by the arrow A (anterior), P (posterior). Bar, 10µm. (Bottom panel) Schematic diagrams of the image above, with oocyte centrosomes in red and follicular cell centrosomes in blue. (B) Quantification of oocytes categorized as scattered (black) and clustered (gray) depending on centrosome distributions at the different stages. n indicates the number of analyzed egg chambers.

In order to follow centrosome dynamic at the onset and during nuclear migration, I also performed live imaging in this control condition in which Fs(2)Ket-GFP and asl-td-Tomato are expressed to label the nuclei and the centrosomes (fig I. 8). The time-lapses show that the centrosomes are indeed very dynamic but remain tightly associated with the movements of the oocyte nucleus. They become tightly clustered once the nucleus has started its migratory trajectory. At the completion of nuclear migration, they are positioned in between the nucleus and the plasma membrane, and they are less numerous compared as in earlier stage. Altogether, these results show that oocyte nucleus centering concomitantly occurs with centrosome clustering, and explain the previous reported differences regarding their compact or scattered distribution.

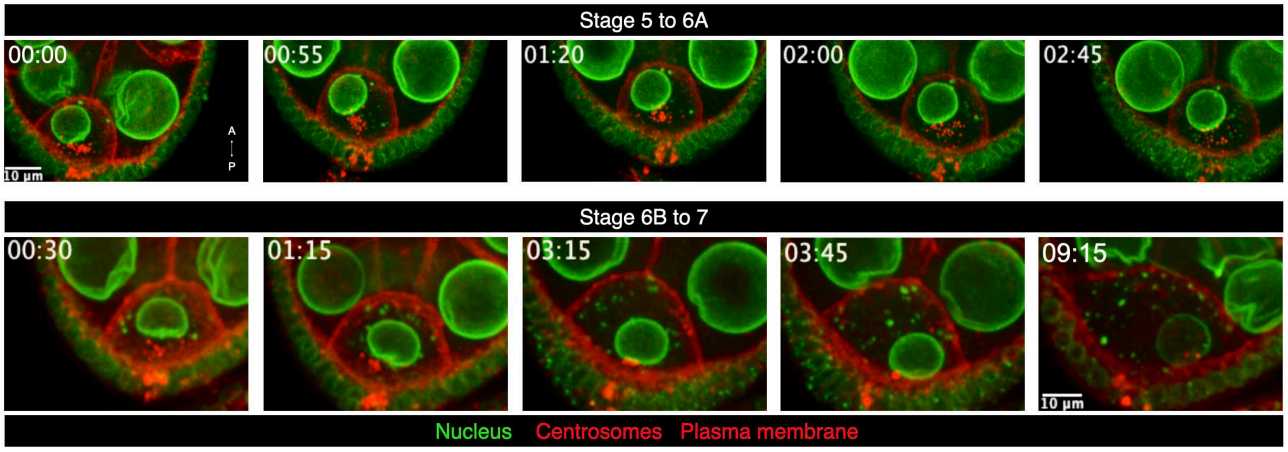

Figure I. 8: Progressive centrosome clustering prior to the oocyte nucleus migration. (Top panel) Selected frames extracted from time-lapse movie of developing egg chamber from stage 5 to 6A expressing Fs(2)Ket-GFP labeling nuclei, PH-RFP labeling plasma membrane, and asl-tdTomato labeling centrosomes. Oocyte nucleus is anteriorly positioned and centrosomes are scattered between the nucleus and posterior membrane. (Bottom panel) Selected frames from time-lapse movie of developing egg chamber from stage 6B to 7 expressing Fs(2)Ket-GFP labeling nuclei, PH-RFP labeling plasma membrane, and asl-tdTomato labeling centrosomes. The centrosomes aggregate at the posterior of centered nucleus, and follow the migrating nucleus from the oocyte center to cortex antero-lateral. The orientation of the egg chamber is indicated by the arrow A (anterior), P (posterior). Time is indicated (h:min). Bars, 10µm.

b) Kinesin-1 Heavy Chain co-localizes with the oocyte centrosomes

Next, we wondered by which mechanism oocyte centrosome clustering was regulated. As microtubule motors can slide microtubules and organize them, we aimed to investigate their contribution in centrosome clustering. While minus end directed motors are more likely investigated in the gathering of cellular components as they can pull on microtubules, it has been observed that oocyte centrosome were more dispersed under Kinesin-1 light chain (Klc) depletion context (Hayashi et al., 2014). Moreover, preliminary experiments in my lab suggested a similar dispersion under the depletion of Kinesin-1 heavy chain (Khc). Therefore, we hypothesized that Kinesin-1 regulates the oocyte centrosome clustering. First, I aimed to assess the distribution of Kinesin-1 in the *Drosophila* oocyte. Using a transgenic strain expressing GFP-tagged Klc, I observed that Klc localized in an even manner in the oocyte cytoplasm (fig I. 9.A). Using a recombinant strain expressing GFP-tagged Khc in a *khc* null mutant *khc*^{27}, Khc displays an enrichment in the oocyte compared to the nurse cells (fig I. 9.B). This localization difference in the germ cells is consistent with microtubule enrichment in the oocyte compared to nurse cells

(Theurkauf et al., 1992). In addition, I observed that Khc localizes around oocyte nucleus and accumulates in posterior perinuclear region where the centrosomes reside. I next aimed to assess co-localization between Khc and centrosomes (fig I. 10). By performing immunofuorescences against Khc on control egg chambers expressing asl-td-Tomato to label centrosomes, I observed a co-localization. These results show that Khc and Klc have different localization in the fruit fly oocyte, and the localization of Khc at the centrosomes led reinforced our interest to investigate the role of Kinesin-1 on oocyte centrosome clustering.

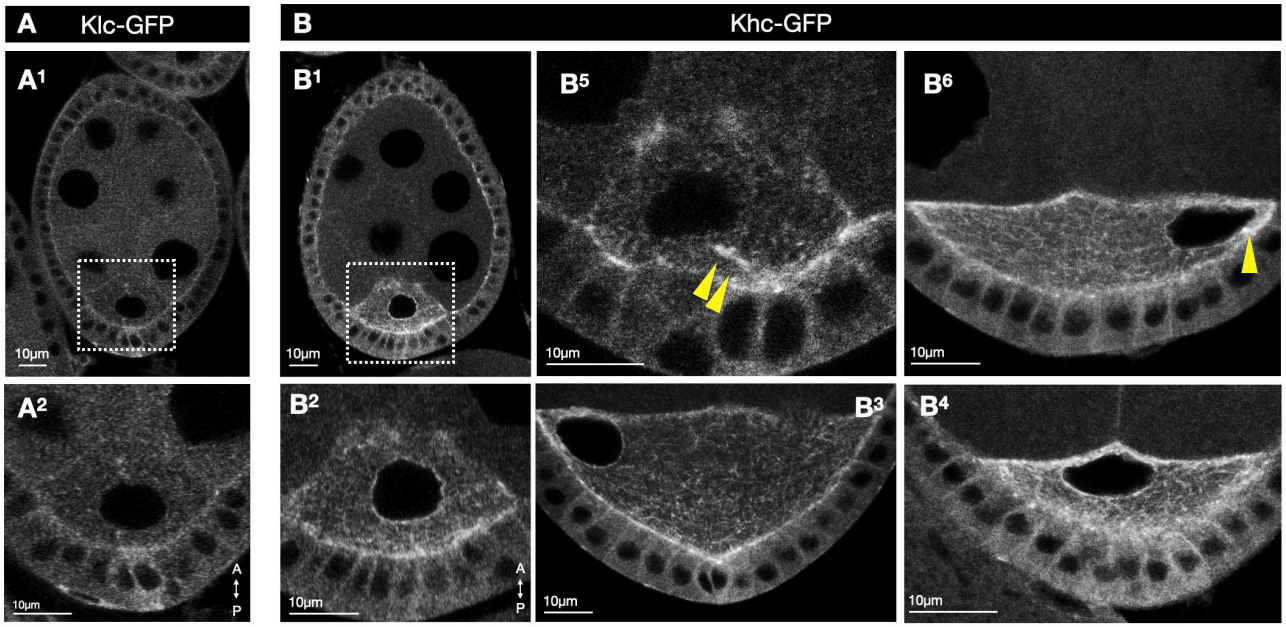

Figure I. 9: Kinesin-1 localization in the *Drosophila* oocyte. (A[1]) Stage 6B egg chamber expressing Klc-GFP, and higher magnification corresponding to the square (A[2]). (B) Egg chambers of different stages expressing Khc-GFP in a *Khc*^{27} homozygous background. (B[1]) Stage 6B egg chamber, and higher magnification corresponding to the square (B[2]). (B[3-4]) Stage 8 and 7 egg chambers showing an enrichment of Khc around the oocyte nucleus, (B[5-6]) stage 6 and 8 egg chambers showing the localization of Khc at the centrosomes (indicated by the yellow arrow head). The orientation of the egg chamber is indicated by the arrow A (anterior), P (posterior). Bars : 10µm.

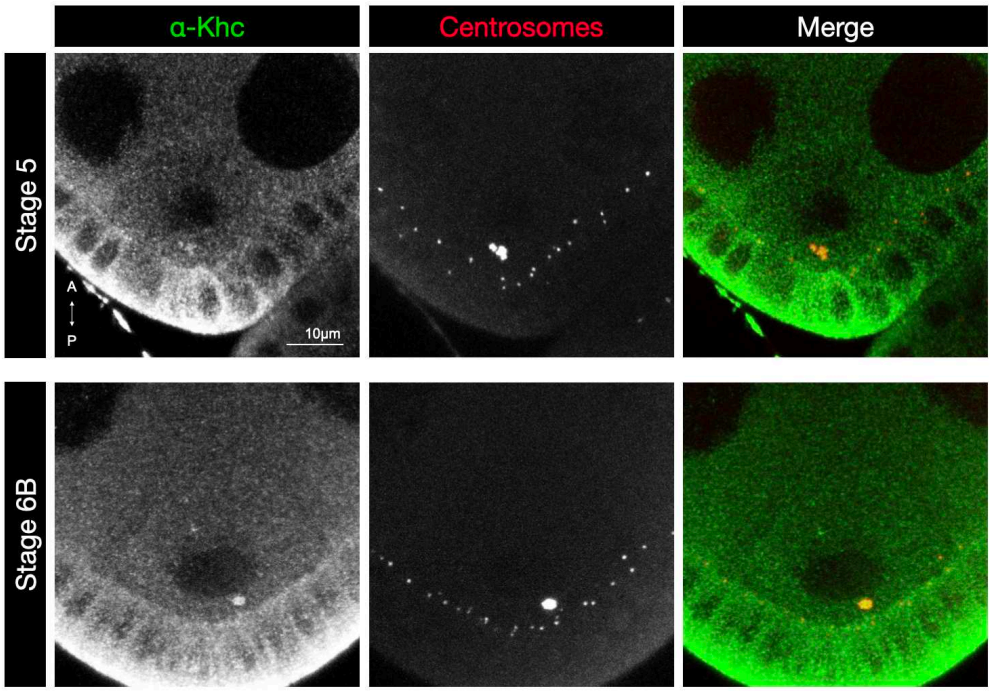

Figure I. 10: Khc co-localizes with the oocyte centrosomes. Immunofluorescences against Khc on control egg chambers expressing asl-td-Tomato to label the centrosomes. At stage 5 (top panel) and at stage 6B (bottom panel), Khc signal co-localizes with the centrosomes at the posterior of the oocyte. The orientation of the egg chamber is indicated by the arrow A (anterior), P (posterior). Bar : 10µm.

c) Centrosome clustering is Kinesin-1 dependent

Thus, I investigated Kinesin-1 role on centrosome clustering at stages surrounding the oocyte nuclear migration. As control, I used an RNAi against a gene that is not expressed in the *Drosophila* ovaries (Parisi et al., 2004). For depleting Khc or Klc, I used two different RNAi specifically expressed in the egg chamber germ cells (fig I. 11). The depletion of either Khc or Klc caused a clustering defect at every stages compared to control RNAi. These results show that Kinesin-1 is required for centrosome clustering. Moreover, I also observed a mislocalization of the oocyte nucleus. Indeed, not only nuclear migration was affected at stage 7, but the nucleus was always anteriorly positioned, and nuclear indentation which correlates with centrosome position was not facing the posterior plasma membrane. Therefore, I next aimed to assess more precisely Kinesin-1 role on nucleus positioning and migration during oogenesis.

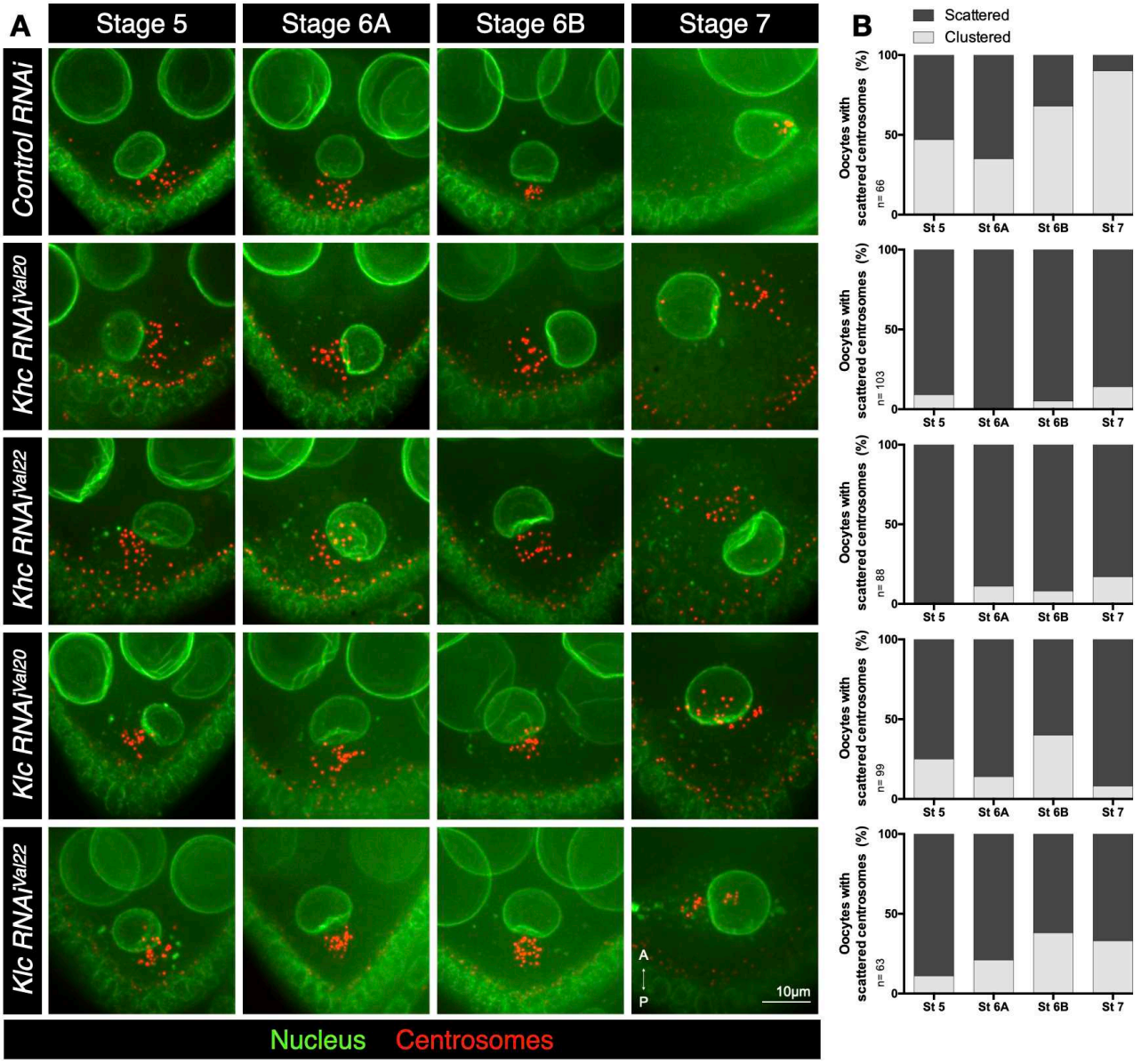

Figure I. 11: Khc and Klc are required for centrosome clustering in the *Drosophila* oocyte. (A) Representative images of stage 5 to 7 egg chambers, expressing Fs(2)Ket-GFP to label nuclei (green), asl-tdTomato to label centrosomes (red) and the indicated RNAi under the control of the mat-αtub-Gal4 driver which is specific of the germ cells. The orientation of the egg chamber is indicated by the arrow A (anterior), P (posterior). Bar : 10µm. (B) Corresponding quantification of oocyte centrosomes categorized as scattered (black) and aggregate (gray) at the different stages for each genotype.

CHAPTER II : NUCLEUS MIGRATION IS DEPENDENT ON KINESIN-1

Investigation of Kinesin-1 role on nucleus asymmetrical positioning, during *Drosophila* oogenesis, have reported that the motor was not required for nucleus migration but that Khc was necessary for nuclear positioning maintenance at late stage of oogenesis, while Klc was dispensable (Duncan and Warrior, 2002; Januschke et al., 2002; Palacios and St Johnston, 2002). These experiments were performed using different genetic tools than the RNAi that we express in the germ cells and which are efficient early in oogenesis. Indeed, in these previous experiments, to deplete Kinesin-1, they generated heat-inducible germline clones which effect might not be as strong at stage 6-7. Moreover, they studied nuclear position at later-oogenesis stages around 8-9. These two factors could be reasons explaining why we obtained different results regarding Kinesin-1 role in nuclear migration and in nuclear positioning prior to migration. As we previously observed a nuclear mis-positioning prior to migration in Kinesin-1 depleted contexts, I investigated Kinesin-1 role in nuclear migration and positioning prior to migration.

1. Nucleus positioning and migration is Kinesin-1 dependent

To characterize Kinesin-1 contribution in oocyte nucleus positioning, I used flies expressing RNAi against Khc (fig II. 1.B-C) or Klc (fig II. 1.D-E) in germ cells, as well as Fs(2)Ket-GFP and PH-RFP labeling the nuclei and plasma membranes. At stage 7 in Khc-RNAi contexts (fig II. 1.B-C), nuclei were not correctly positioned in the antero-lateral cortex (referred as migrated), but rather at the anterior. In Klc-RNAi conditions, nucleus migration was not abolished but reduced, suggesting different contribution of Khc and Klc in the oocyte nuclear migration (fig II. 1.D-E). Moreover, these results confirm that Kinesin-1 depletion causes nuclear mis-positioning prior to nuclear migration, as they are mainly anteriorly positioned at stage 5-6B. Therefore, this experiment show that Khc is necessary for the oocyte nuclear migration, and that Kinesin-1 is required for nuclear positioning prior to migration, which is consistent with its importance in centrosome clustering.
Additionally, I confirmed these results by analyzing experiments that were previously performed in my lab using germline mitotic clones. Induction of GFP/FRT clones of Khc^{27} mutant allele, a *Khc* null allele (Januschke et al., 2002) shows that the oocyte nucleus is mostly anteriorly positioned until stage 10b at least compared to control (fig II. 2.A-B). Induction of GFP/FRT clones of two distinct *Klc* null alleles: Klc^{8ex94} (Gindhart et al., 1998) and Klc^{Saturn} (Hayashi et al., 2014) confirmed Klc importance for nucleus positioning prior to stage 7 compared to control (fig II. 2.C-E). In these contexts, I observed that nuclei were correctly positioned around stage 9, indicating that the nuclear asymmetric position is only delayed in *Klc* mutants. This result is consistent with previous work showing that Khc can function independently of Klc in the *Drosophila* oocyte, notably in mRNA transport and Dynein localization (Palacios and St Johnston, 2002). Therefore, these results suggest that Khc and Klc are differently required regarding the oocyte nuclear migration.

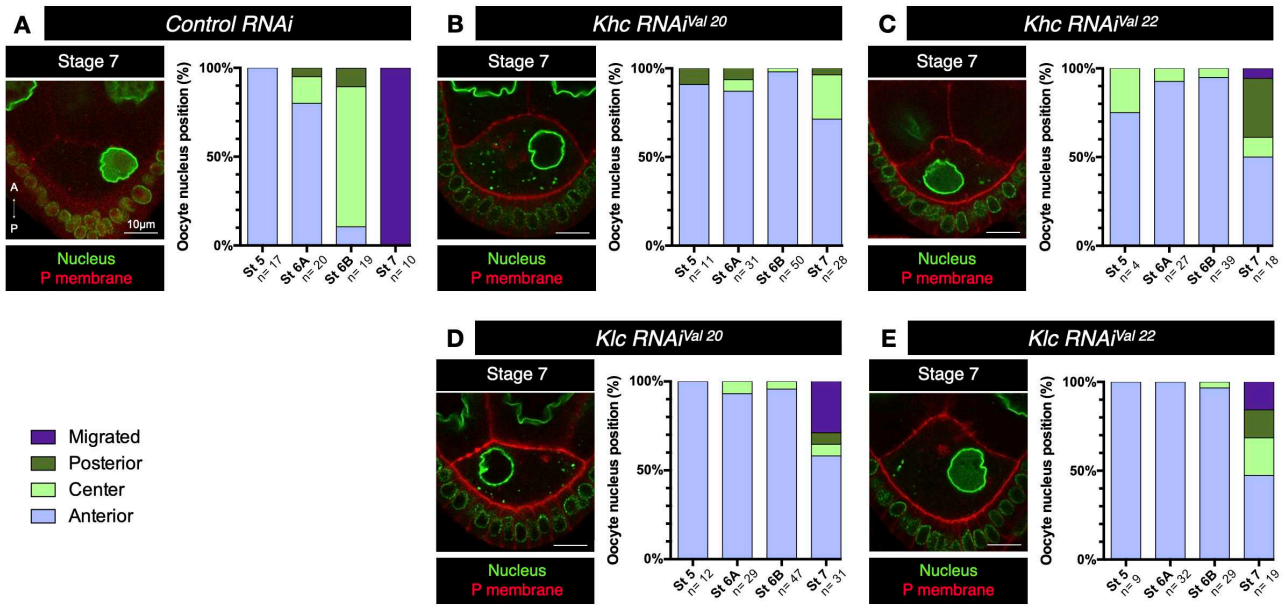

Figure II. 1: Khc and Klc are required for nucleus positioning and migration. RNAi-mediated analysis of nucleus positioning in egg chambers expressing (A) *control-RNAi* (UASp-CG12699-RNAi), (B) *Khc-RNAi*^{Val20}, (C) *Khc-RNAi*^{Val22}, (D) *Klc-RNAi*^{Val20}, or (E) *Klc-RNAi*^{Val22} in the germ cells, as well as Fs(2)Ket-GFP and PH-RFP labeling the nuclei and plasma membrane. Representative image of stage 7 egg chamber and distribution of nucleus positions at the different stages. Bars : 10µm. Positions have been categorized and color-coded as anterior in pale blue, center in pale green, posterior in dark green and migrated in purple. n indicates the number of analyzed egg chambers.

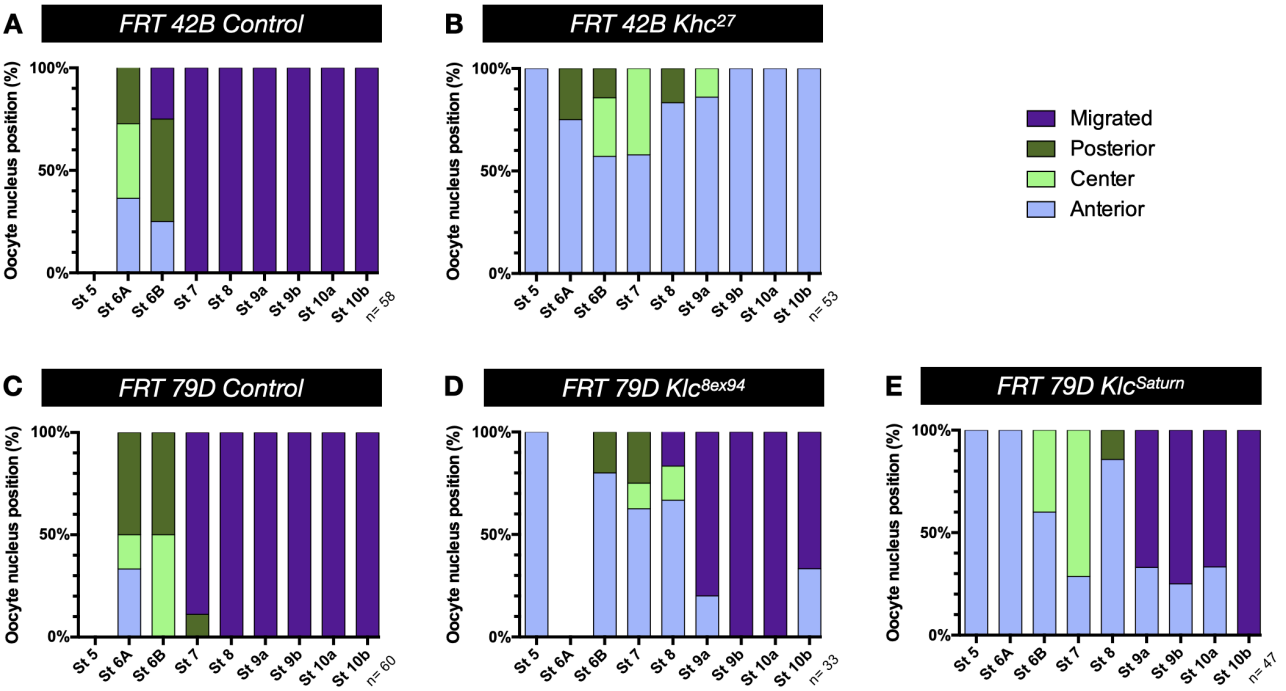

Figure II. 2: Khc and Klc are differently required for the oocyte nuclear migration. (A-E) Distributions of nucleus positions at the different stages. Positions have been categorized and color-coded as anterior in pale blue, center in pale green, posterior in dark green and migrated in purple. n indicates the number of analyzed egg chambers. GFP/FRT clonal analysis of nucleus positions in control egg chambers *Khc*^{27} heterozygous (A) and *Khc*^{27} mutant (B), *Klc* heterozygous (C), *Klc*^{8ex94} mutant (D) and *Klc*^{Saturn} (E) mutant egg chambers.

2. Different contribution of Khc and Klc in microtubule organization

Next, to understand how Kinesin-1 regulates nuclear migration, we hypothesized that Kinesin-1 acts on microtubule organization and stability. To test this, I quantified microtubule density in *control-RNAi*, *Khc-RNAi*^{Val20} and *Klc-RNAi*^{Val22} expressing living egg chambers, by quantifying Jupiter-GFP signal, a MAP which localizes along microtubules (Baffet et al., 2012). In control condition, I observed a progressive decrease of microtubule density in the oocyte along the stages (fig II. 3). Klc depletion did not cause significant difference compared to control, while Khc depletion induced a significant decrease of microtubule density in the oocyte at stage 6B and 7 compared to control. This difference could explain nuclear migration inhibition in absence of Khc.

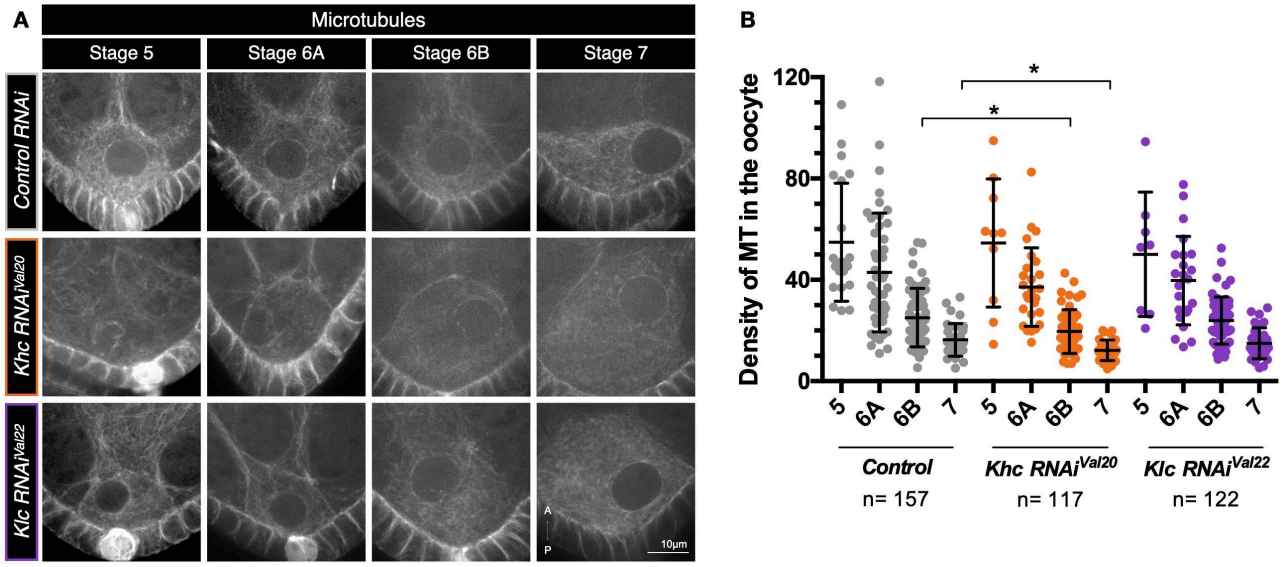

Figure II. 3: Khc and Klc impact differently the microtubules. (A) Representative examples of oocyte Z-projection of stage 5 to 7 egg chambers expressing Jupiter-GFP labeling microtubules, and *control RNAi* (*UASp-CG12699 RNAi*), *Khc-RNAi*^{Val20} and *Klc RNAi*^{Val22} in the germ cells. The orientation of the egg chamber is indicated by the arrow A (anterior), P (posterior). Bar, 10µm. (B) Quantification of microtubule (MT) density in oocytes of the indicated stages and genotypes. Microtubule signal intensity of the entire oocyte was measured on a Sum slices-projection. Mann-Whitney test, *p < 0.05. n indicates the number of analyzed egg chambers.

In C-terminal region of Khc, tail domain contains an MT binding motif that gives Khc its capacity to cross-link microtubules and subsequently organize them, independently of Klc (Lu et al., 2016). Therefore, we hypothesized that Khc effect on microtubule density could require its function in microtubule cross-linking. To investigate if this function of Khc was responsible of further nuclear positioning defects, I assessed nuclear positioning in *khc* null egg chambers expressing *Khc*^{mutA}. *Khc*^{mutA} corresponds to mutated Khc MT-binding motif in tail domain, in which C-terminal binding site affinity to microtubules is strongly decreased (Lu et al., 2016). As control, I used flies expressing *khc*^{WT} in a *khc* null mutant background (fig II. 4.A). It is important to note that in this condition, at stage 6B nuclei were more posteriorly positioned compared to previous controls. In *khc*^{mutA} context, nuclear migration was delayed compared to control (fig II. 4.B), and in a similar manner than in *Klc* mutants. Although I observed a difference in nuclear positioning prior to migration in *khc*^{mutA} compared to *khc*^{WT}, the number of analyzed egg chambers are insufficient to conclude. However, regarding stage 6B and 7, these results suggest that Khc microtubule cross-linking function, although not necessary, is involved during oocyte nuclear migration.

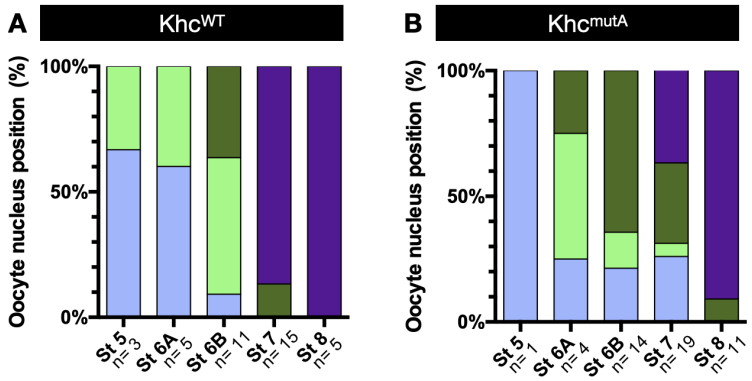

Figure II. 4: Khc microtubule cross-linking fonction is not essential for nuclear migration. Distribution of the nucleus position at the different stages in (A) *Khc^{WT}* (control condition) and in (B) *Khc^{mutA}*. Positions have been categorized and color-coded as anterior in pale blue, center in pale green, posterior in dark green and migrated in purple. n indicates the number of analyzed egg chambers.

Altogether these results show that Kinesin-1 is necessary for centrosome clustering and for nuclear positioning prior to and for migration. As Khc microtubule cross-linking function is involved during oocyte nuclear migration, we next wondered if constitutively active Kinesin-1 would cause a precocious nuclear migration. Kinesin-1 can auto-inhibit through the folding of Khc which requires Hinge2 domain of Khc (fig II. 5). Khc Hinge2 domain deletion, prevents Khc folding, and is therefore proposed to induce constitutively active Kinesin-1 (Kelliher et al., 2018).

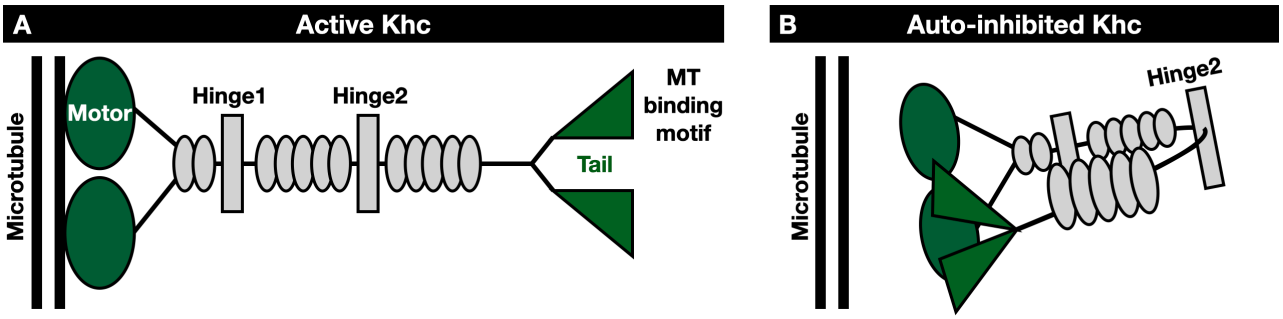

Figure II. 5: Hinge2 domain mediates Khc auto-inhibition. (A) Scheme representing Khc domains: the motor domains in the N-terminal region bind the microtubules, the Hinge domains are separated by coiled-coil domains (gray ovals), and at the C-terminal region the tail domain is responsible of cargo binding and contains the MT binding site (which is mutated in *khc^{mutA}*). (B) The auto-inhibition of Khc requires Hinge2 domain which allows Khc to fold on itself. These schemes are inspired by (Verhey et al., 2011; Wong-Riley and Besharse, 2012).

To test if constitutively active Kinesin-1 could induce a precocious nuclear positioning or migration, I analyzed oocyte nuclear positions in *khc* null egg chambers expressing *Khc$^{\Delta Hinge2}$*. Surprisingly, the results show that nuclei of *Khc$^{\Delta Hinge2}$* egg chambers were anteriorly positioned prior to migration compared to control (fig II. 6.A-B). Moreover, nuclear migration was negatively affected as well compared to control at stage 7 and 8. Although Hinge2 deletion is a gain of function mutation, these nuclear positioning were similar to the ones observed in absence of Khc, we therefore wondered if the transgene *khc* still carried the mutation for Hinge2. To confirm Hinge2 domain deletion, I performed genomic PCR from a *control* fly lysate (*Khc^{WT}*) and a *Khc$^{\Delta Hinge2}$* fly (fig II. 6.C), and validated the use of this strain. Overall, this result indicates that a regulation of Kinesin-1 is required for the correct positioning and migration of the oocyte nucleus.

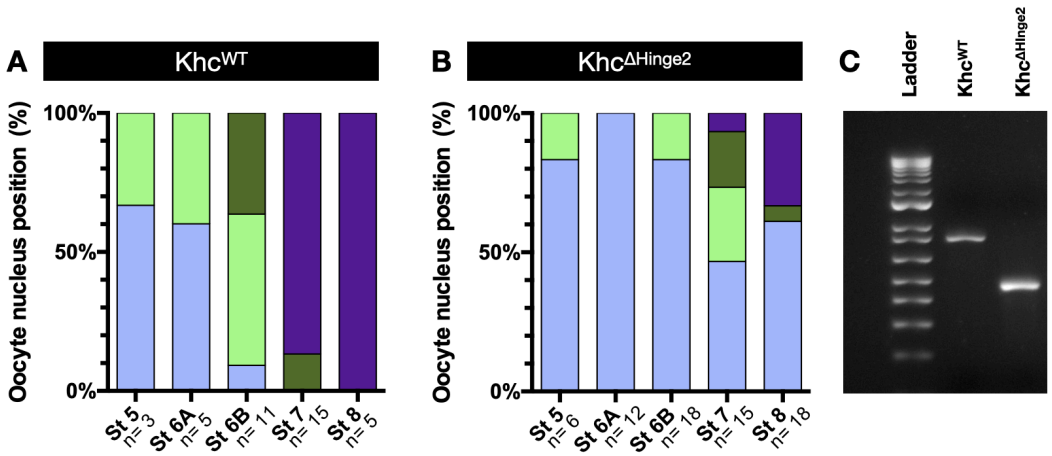

Figure II. 6: Constitutively active Khc phenocopies Klc mutant. (A-B) Distribution of nucleus position at different stages in (A) *Khc^{WT}* (control condition) and in (B) *Khc$^{\Delta Hinge2}$*. Positions have been categorized and color-coded as anterior in pale blue, center in pale green, posterior in dark green and migrated in purple. n indicates the number of analyzed egg chambers. (C) Genomic PCR to test Hinge2 deletion in *Khc$^{\Delta Hinge2}$* compared to the control *Khc^{WT}*.

3. Kinesin-1 is not involved in Mud localization at the oocyte NE

Next, I aimed to investigate Kinesin-1 potential role on Mud localization at the oocyte NE. Indeed, as I previously observed the partial delocalization of Mud at the centrosomes in some mutant contexts, I wondered if in absence of Kinesin-1, Mud distribution was affected. I found that Mud localization at the oocyte NE was not altered when Khc or Klc were depleted (fig II. 7.A), as well as Mud asymmetry was not different compared to the control (fig II. 7.B).

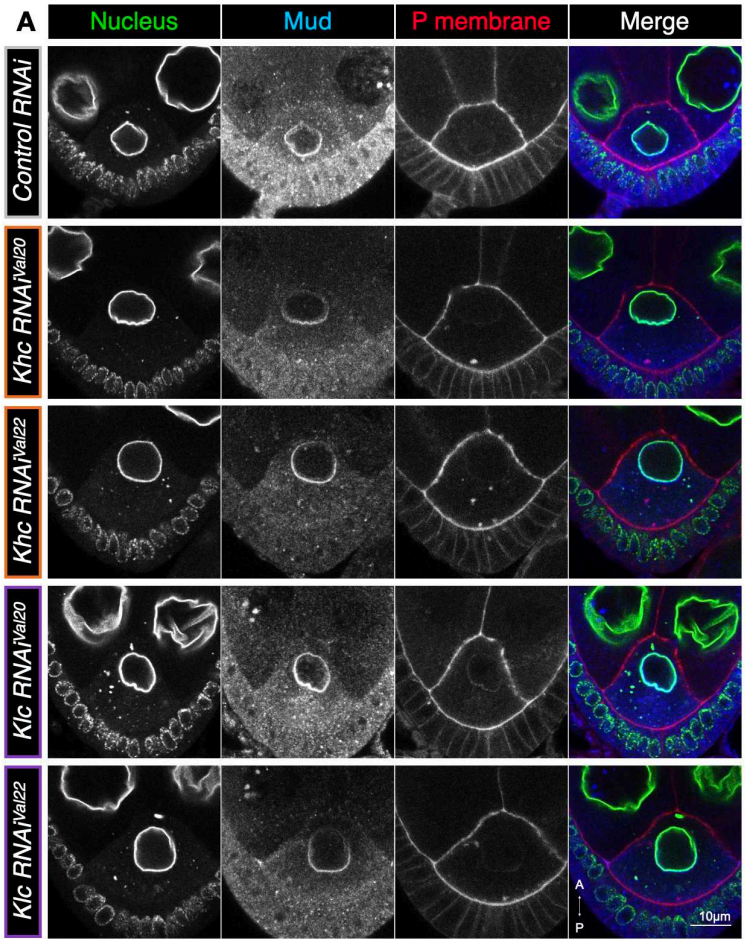

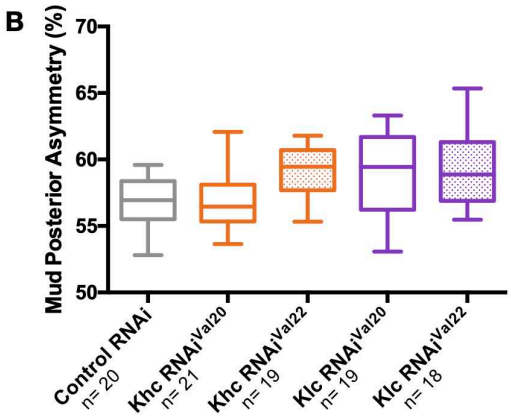

Figure II. 7: Kinesin-1 is not involved in Mud distribution or asymmetry at the oocyte NE. (A) Representative images of stage 6B egg chambers, expressing Fs(2)Ket-GFP to label nuclei (green) and PH-RFP to label plasma membrane (red) and the indicated RNAi stained with Mud antibodies (blue). Bar : 10µm. (B) Quantification of Mud asymmetry at the posterior of the nucleus in the indicated genotypes. n indicates the number of analyzed egg chambers.

4. Kinesin-1 does not remove Dynein from the oocyte centrosomes

It is surprising to observe Kinesin-1 involved in centrosome clustering, as this process often requires minus-end directed motors (such as Dynein or Kinesin-14 for example). The microtubule minus end directed Kinesin-14 KIFC1/HSET, Nonclaret disjunctional (Ncd) in the flies, has been identified, in *Drosophila* cultured cells and neuroblasts, as an important regulator of centrosome clustering by cross-linking the anti-parallel microtubules emanating from different centrosomes (Basto et al., 2008; Kwon et al., 2008). Previously, my lab has reported the interdependence of Kinesin-1 and Dynein to localize each other in the *Drosophila* oocyte (Januschke et al., 2002). We then wondered if the effect of Kinesin-1 depletion on centrosome clustering could be the consequence of a mis-localization of Dynein at the oocyte centrosomes. To test this, I imaged egg chambers expressing ubi-DLic-GFP or Tub-Dmn-GFP in the germ cells to localize Dynein and dynactin subunits in the oocyte, as well as asl-td-Tomato to label the centrosomes, as well as germ cell specific RNAi against against Khc or Klc (fig II. 8). The results show that Kinesin-1 depletion did not remove Dlic nor Dmn from the centrosomes. However, in most of the cases, we noticed an enrichment of Dlic-GFP and Dmn-GFP in the vicinity of the centrosomes when Khc or Klc were depleted. As the centrosomes are active these stages (Tissot et al., 2017) and are therefore surrounded by PCM, we wondered if Kinesin-1 was involved in the activity of the centrosomes.

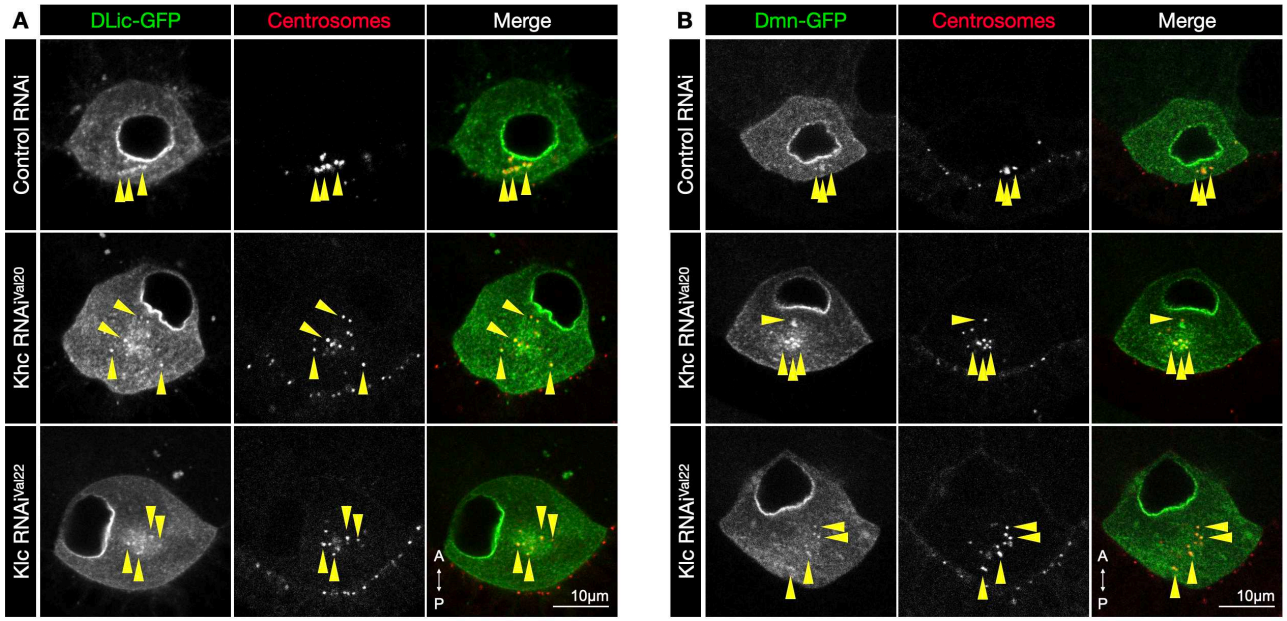

Figure II. 8: Kinesin-1 depletion does not affect centrosomal distribution of Dynein. (A-B) Oocytes from stage 6B egg chambers expressing ubi-DLiC-GFP (A) or UAS-Dynamitin-GFP (B, Dmn-GFP), ubi-asl-tdTomato to label centrosomes (red) and control RNAi (UASp-Him RNAi – See Methods) (top row), Khc RNAiVal20 (middle row) and Klc RNAival22 (bottom row) under the control of the mat-αtub-Gal4 driver. The yellow arrowheads indicate the centrosomes. Scale bars : 10µm.

Altogether, these results show that Khc and Klc are required for nuclear positioning prior to migration and for migration. However, experiments on microtubule density or organization did not inform us on the mechanism by which Kinesin-1 proceeds to ensure correct centrosome clustering and nuclear positioning. Previously, my lab has shown that the centrosomes of the oocyte are active along the nuclear migration, as PCM component co-localized with centrioles, and that they exert pushing forces on the nucleus (Tissot et al., 2017). Moreover, it is known that centrosomes progressively lose their activity after the migration until a complete elimination by the end of oogenesis. Notably, the elimination process at mid- to late oogenesis, around stage 9, has been described and shows the importance of Polo-like kinase 1 (PLK1, Polo in *Drosophila*) (Pimenta-Marques et al., 2016). Indeed, a decrease of Polo from the centrosomes correlates with a decrease of centrosomal activity. As the centrosomes are scattered at early stages and are tightly clustered at late degradation stages, we hypothesized that centrosome clustering at stage 6B reflected a decrease of centrosomal activity. Therefore, we hypothesized that centrosome clustering was a cause of a down-regulation of centrosomal activity at stage 6B.

1. Centrosome clustering and activity

In order to establish a link between centrosome behavior and activity, I used a tool developed by Pimenta-Marques et al., to over-express Polo in the oocyte and target it at the centrosomes due to its fusion with a Pericentrin - AKAP450 Centrosomal Targeting (PACT) sequence (Pimenta-Marques et al., 2016). Pimenta et al., have shown in this context, that oocyte centrosomal activity down regulation is inhibited along oogenesis and that centrosomes are not degraded. Thus, I imaged and analyzed centrosome clustering and nucleus positioning at stages 5, 6A, 6B, and 7 in egg chambers expressing Polo-PACT and compared to control egg chambers (fig III. 1). In Polo-PACT condition, centrosomes display a significant clustering defect at stage 7 compared to control, as well as a defect in asymmetrical nucleus positioning at stage 7. Thus, these results indicate that centrosomal activity maintenance prevents centrosome clustering, and suggest that clustered centrosomes are less active centrosomes than when scattered. Furthermore, these results show that a decrease of centrosomal activity is required for a correct asymmetrical nuclear positioning at stage 7. As centrosome clustering is Kinesin-1 dependent, and as the maintenance of centrosomal activity impairs centrosome clustering, we hypothesized that Kinesin-1 could be involved in the down-regulation of oocyte centrosomal activity.

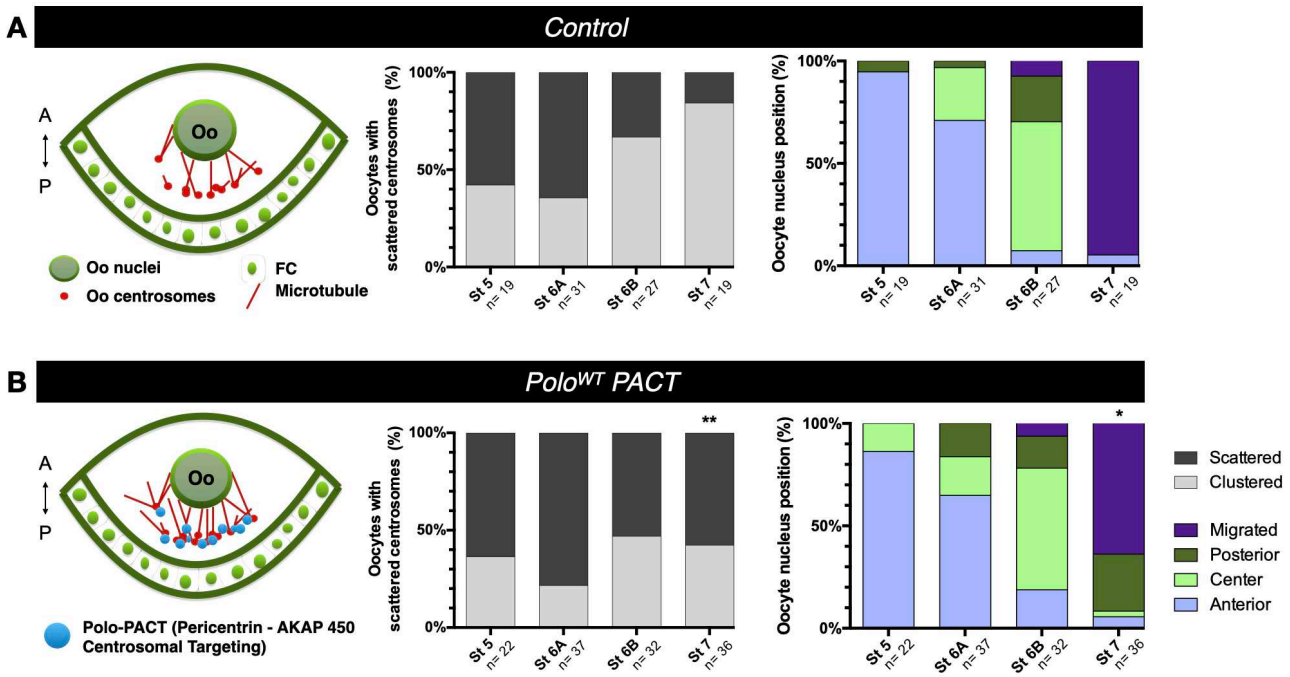

Figure III. 1: Preventing centrosome activity decay impairs centrosome clustering and nucleus positioning. (A-B left panel scheme) Scheme representing (A) control condition, and (B) *PoloWT-PACT* condition in which Polo is over-expressed in the germ cells and targeted at the centrosomes as it is fused to PACT sequence (Pericentrin - AKAP450 Centrosomal Targeting). (A-B middle panel) Quantification of oocyte centrosome clustering categorized as scattered (black) and clustered (gray) at the different stages in *control* and *PoloWT-PACT*. (A-B right panel) Quantification of the nucleus position distribution at the different stages. Positions have been categorized and color-coded as anterior in pale blue, center in pale green, posterior in dark green and migrated in purple. n indicates the number of analyzed egg chambers. Chi2 test, *p < 0.05, **p = 0,005 compared to the control condition (per stage).

2. Kinesin-1 mediated centrosome activity regulation

It is rather challenging to assess centrosomal activity, i.e nucleation capacity, in the oocyte of the fruit fly. Indeed, because of their clustering at stage 6B just prior to nuclear migration, centrosomes are not easily distinguishable from one to another in control condition. Similarly, if one individualized centrosome is distinguishable from the others, its nucleating capacity might not be representative of the rest of them. For these reasons, we decided to test the centrosome activity by revealing the presence and co-localization of PCM components, such as Asl which has been shown to recruit other PCM components during centrosome maturation (Conduit et al., 2014b). As discussed previously, one way to regulate centrosome activity is the PCM component removal from the centrosomes (Muroyama et al., 2016) (*see Introduction - Chapter III. 2.a*). Therefore, we hypothesized that through its cargo function, Kinesin-1 could translocate PCM components away from the centrosomes. To test this hypothesis, I assessed the localization of Asl and Spd2, which co-localize and follow the oocyte nuclear migration (fig III. 2). I confirmed that Asl depletion, when using an Asl-RNAi expressed in the germ cells, was associated with an absence of Spd2-GFP in the oocyte (fig III. 3). Although in some cases, Asl-td-Tomato and Spd2-GFP were still detectable into a tightly dense structure in the oocyte, in most of the cases Asl-tomato and Spd2-GFP were not detectable in the oocyte anymore. This experiment is consistent with what has been reported regarding the recruitment of Spd2 by Asl at the centrosomes (Conduit et al., 2014b).

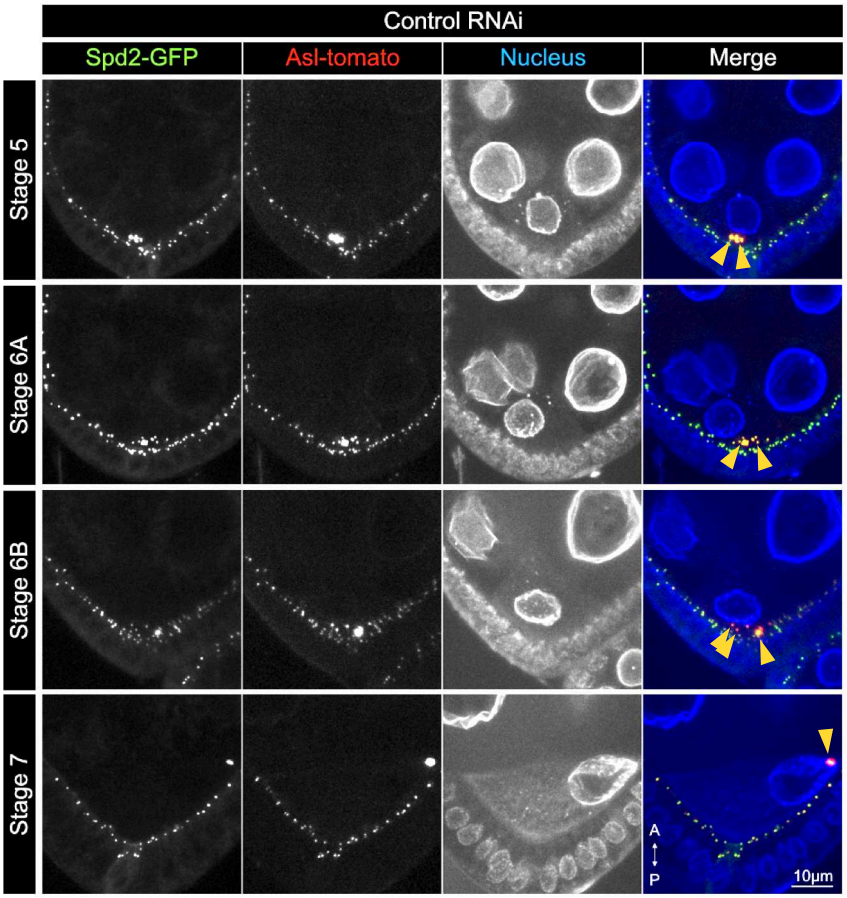

Figure III. 2: Oocyte centrosomal activity seen via the co-localization of Asl and Spd2. Representative Z-projection of stage 5, 6A, 6B, and 7 egg chambers expressing *control-RNAi* in the germ cells, as well as Spd2-GFP and Asl-td-Tomato labeling centrosomes (indicated by yellow arrow heads). The nuclei were stained using WGA. In the control condition, Spd2-GFP and Asl-td-Tomato signals co-localize and show the progressive centrosome clustering as well as the nuclear associated migration of centrosomes.The orientation of the egg chamber is indicated by the arrow A (anterior), P (posterior). Bars : 10µm. (B)

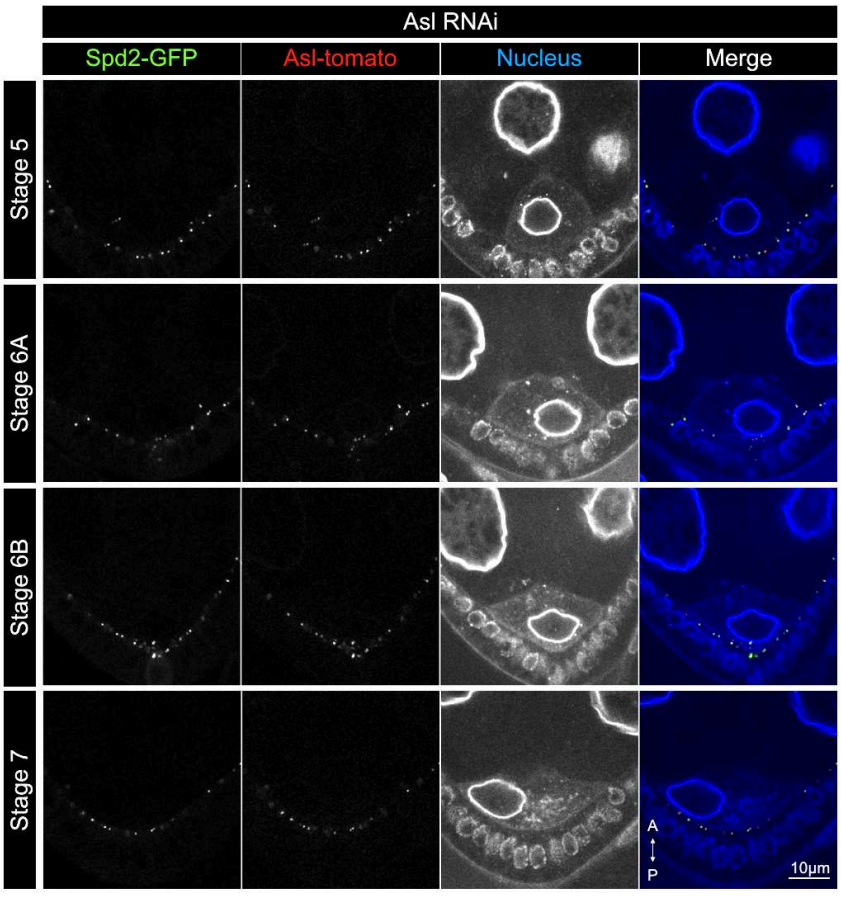

Figure III. 3: Centrosome inactivation validation. Representative images of stage 5, 6A, 6B, and 7 egg chambers expressing *asl-RNAi* in the germ cells, as well as Spd2-GFP and Asl-td-Tomato labeling the centrosomes. The nuclei were stained using WGA. In most of the cases, Spd2-GFP and Asl-td-Tomato signals were no longer detectable in the oocyte, showing that Spd2 is recruited at the centrosomes by Asl. The orientation of the egg chamber is indicated by the arrow A (anterior), P (posterior). Bar : 10µm. (B)

Next, to assess the contribution of Kinesin-1 on centrosomal activity, I performed the same experiment on egg chambers expressing either *Khc-RNAi*^{Val20} or *Klc-RNAi*^{Val22} (fig III. 4) in the germ cells. These observations require further quantifications of Asl-td-Tomato and Spd2-GFP signal intensity. Nonetheless, it seems that in control condition (fig III. 2), at stage 6B and 7, Spd2-GFP punctuates are smaller than Asl-td-Tomato punctuates, compared to stage 5 and 6A where Spd2 and Asl completely co-localize. Moreover, in Khc-depleted context, Asl-td-Tomato seems more intense in the oocyte on an individualized centrosomes compared to follicular cell individualized centrosome. In Klc-depleted context, Asl-td-Tomato and Spd2-GFP on individualized oocyte centrosomes seem similar than on individualized centrosomes in the follicular cells. These results are consistent with a role of Khc in the decrease of Asl levels from the centrosomes and subsequent role in the down-regulation of centrosomal activity. Altogether, these experiments show that oocyte centrosomal activity starts to decrease at stage 6B which allow the centrosomes to cluster, and the subsequent nuclear centering within the oocyte before the nucleus migration. Furthermore, Khc regulates centrosomal activity by a decay of Asl levels at the oocyte centrosomes.

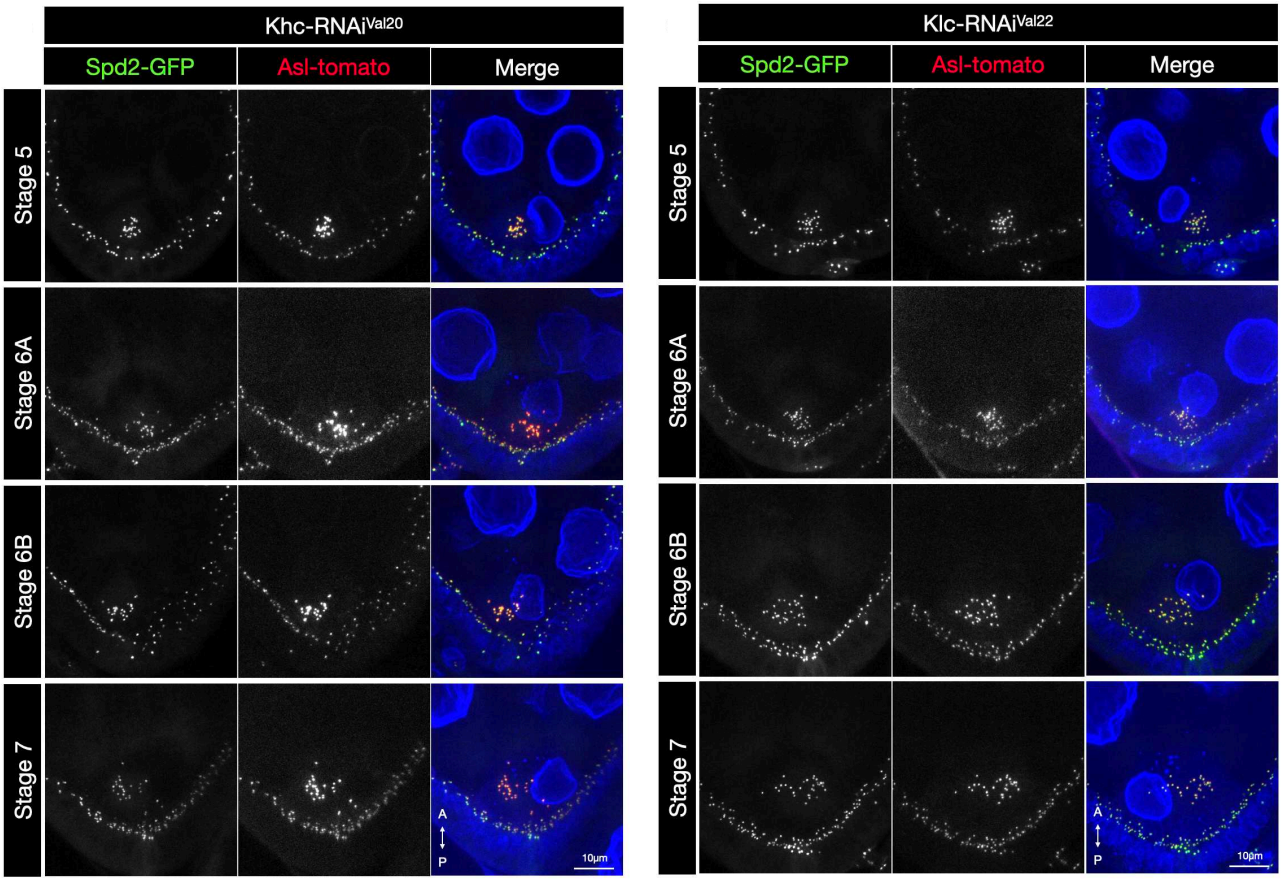

Figure III. 4: Khc-mediated Asl down-regulation at the oocyte centrosomes. Representative Z-projection of stage 5, 6A, 6B, and 7 egg chambers expressing *Khc-RNAi*^{Val20} (left panel), or *Klc-RNAi*^{Val22} (right panel) in the germ cells, as well as Spd2-GFP and Asl-td-Tomato labeling centrosomes. The nuclei were stained using WGA. For further quantifications, the signal detected at the oocyte centrosomes should be normalized compared to the follicular cell centrosome signals. The orientation of the egg chamber is indicated by the arrow A (anterior), P (posterior). Bars : 10µm. (B)

3. Requirement of fine tune of the forces to migrate

Although these experiments are consistent with a function of Kinesin-1 associated with the down-regulation of centrosomal activity in the oocyte, centrosome inactivation caused by Asl depletion (fig III. 3) did not affect nuclear positioning such as Kinesin-1 depletion, suggesting that a very fine regulation of this activity is required in order to correctly position the nucleus. Thus, we wondered if the inactivation of oocyte centrosomes could rescue the lack of regulation by Kinesin-1. To test this, I imaged double mutant egg chambers in which the centrosomes and Khc or Klc were depleted, using RNAi expressed in the germ cells (fig III. 4). When depleting Khc or Klc and inactivating the centrosomes at the same time, the oocyte nuclear migration was partially rescued at stage 7 and almost completely at stage 8 (fig III. 4.B,C,E). These results are consistent with the need of centrosomal activity down-regulation for the correct positioning of the oocyte nucleus prior to its migration and for its migration.

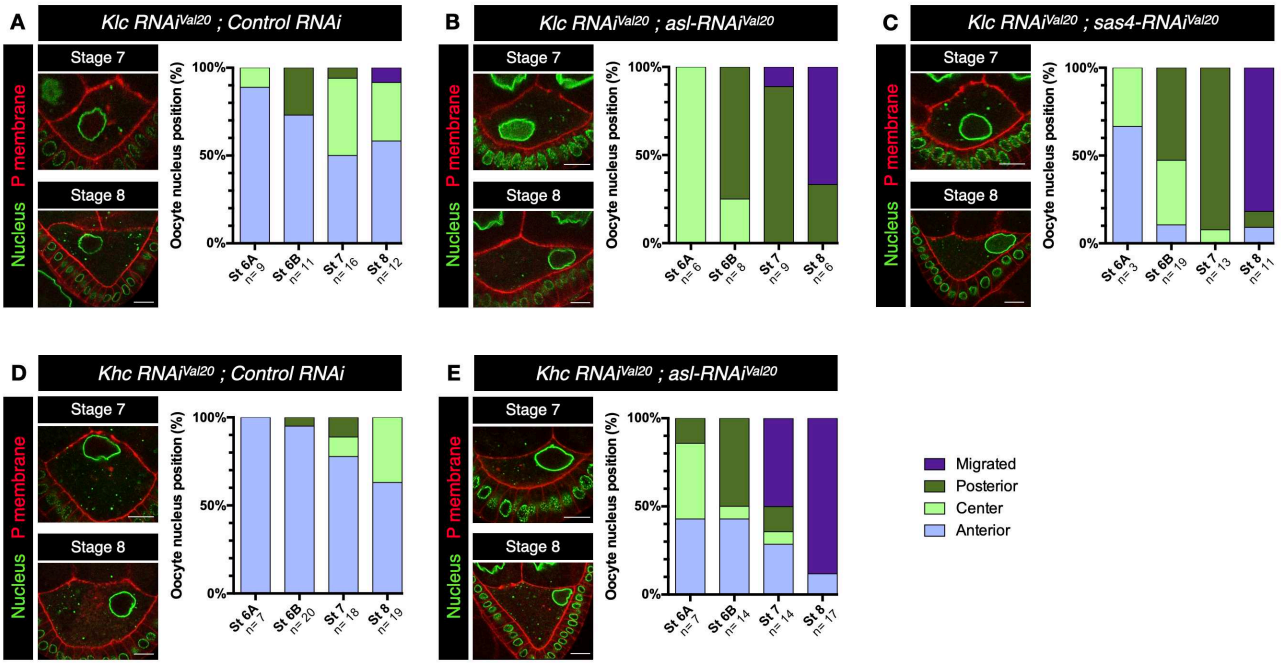

Figure III. 2: Centrosome inhibition and Kinesin-1 depletion restore oocyte nuclear migration. (A-E) Representative images of stage 7 and 8 egg-chambers and distribution of nucleus positions at the different stages. Positions have been categorized and color-coded as anterior in pale blue, center in pale green, posterior in dark green and migrated in purple. n indicates the number of analyzed egg chambers. (A-C) Expression of *Klc-RNAi*^{Val20} in combination with *control RNAi* (*UASp-Ap-RNAi*) (A), or *UASp-asl-RNAi*^{Val20} (B), and *UASp-sas4-RNAi*^{Val20} (C). (D-E) Expression of *Khc-RNAi*^{Val20} in combination with *control RNAi* (*UASp-Ap-RNAi*) (D), or *UASp-asl-RNAi*^{Val20} (E). The RNAi were expressed in the germ cells, and combined with Fs(2)Ket-GFP to label nuclei (green) and PH-RFP to label plasma membrane (red). The orientation of the egg chamber is indicated by the arrow A (anterior), P (posterior). Bars : 10µm.

Altogether, these experiments allowed me to characterize the oocyte centrosome clustering, which is a progressive event that occurs prior to nuclear migration and concomitantly to the centering of the nucleus within the cell. These results show that centrosome clustering is dependent on Kinesin-1, which is down-regulates centrosomal activity, most likely by removing PCM components from the centrosomes.

DISCUSSION

The nucleus migration in *Drosophila* oocyte is a critical event required to asymmetrically position the nucleus and further specify the dorso-ventral axis of the future embryo. This movement is therefore finely controlled and highly robust, and relies on different but redundant molecular actors, such as the centrosomes and the MAP Mud (Tissot et al., 2017). During my PhD, I aimed to understand more precisely by which mechanisms these two actors are involved in the positioning and migration of the *Drosophila* oocyte nucleus. To refine our view of the migratory process, I propose a new distinction of the stages that precede nuclear migration. This distinction allowed me to characterize the nuclear position prior to migration that I have correlated with centrosome clustering. We identified Kinesin-1 requirement in centrosome clustering, nuclear positioning, and nucleus migration. My results suggest a role of Kinesin-1 in the down-regulation of centrosomal activity, notably by affecting Asl levels at the centrosomes. On the other hand, we identified NLS motifs on Mud and the necessity of Fs(2)Ket, to localize Mud at the oocyte NE. I showed that Mud asymmetry is not necessary for nuclear trajectory regulation. However, the deletion of different domains of Mud or the depletion of RanBP2 induce a partial delocalization of Mud in posterior perinuclear region. In $mud^{\Delta MT}$, Mud strongly delocalizes in the perinuclear region and the nuclear trajectories phenocopy *mud* mutant, suggesting a role and importance of Mud maintenance at the oocyte NE.

1. Centrosome clustering: an evolutive adaptation for Kinesin-1 regulation ?

In the light of my results, we now know that the *Drosophila* oocyte nuclear positioning relies on centrosome clustering, which is a sign of decreased centrosomal activity, dependent on Kinesin-1; notably Khc. I must address a few important questions to delve further into these data. Why do oocyte centrosomes cluster ? Does centrosome clustering occur as a consequence of down-regulation of microtubule nucleation capacity, or does centrosome clustering occur to facilitate a common degradation of the centrosomes ? Generally, cells do not tolerate extra centrosomes as they impair cellular integrity by affecting the correct establishment of spindles and subsequent chromosome segregation (Ganem et al., 2009). Therefore, cells with supernumerary centrosomes adopt mechanisms to either remove, inactivate or cluster them. The phenomenon of centrosome clustering and the molecular actors involved in this process are well described in the cancer field. In many cancer types, such as breast, lung, colon, prostate, and brain cancers, centrosomes display aberrations and abnormalities: either in their number or physical defects (Bettencourt-Dias et al., 2011; Godinho and Pellman, 2014). In terms of physical defects, they are often enlarged in cancers compared to physiological contexts, and their nucleating capacity is either enhanced or reduced. Regarding centrosome number, supernumerary centrosomes are a sign of tumorigenesis in human (Fukasawa, 2007; Godinho et al., 2014). A hypothesis is that oocyte centrosome clustering in *Drosophila* could be an evolutionary adaptation of the oocyte to allow Khc to efficiently down-regulate centrosomal activity until complete elimination of the centrosomes prior to the end of oogenesis. Kinesin-1 could translocate PCM components away from the centrosomes and redistribute them at ncMTOCs of the oocyte, notably at the nucleus where Khc also localizes. Furthermore, it would be interesting to verify the functional interaction by co-immunoprecipitation between Khc and Asl, as well as with other PCM components and regulators, such as Cnn, Spd2, and Polo kinase.

2. Centrosome clustering: the triggering event for nuclear migration ?

Another question regarding centrosome clustering relates to its requirement in nuclear migration beforehand. While my lab has identified Mud and centrosome involvement in the regulation of the nuclear migration trajectories (Tissot et al., 2017), the key event triggering this nuclear migration is still not known. In the *Drosophila* oogenesis field, the oocyte nucleus is thought, since many years, to be positioned at the posterior of the cell until its migration to the antero-lateral cortex. Nuclear migration is proposed to be induced by an « unknown signal » or « back signaling » emanating from the posterior follicular cells in response to their own stimulation by Gurken signaling, which occurs in early oogenesis in the germarium when the antero-posterior axis is defined (González-Reyes and St Johnston, 1994; Peri and Roth, 2000; Riechmann and Ephrussi, 2001; Roth, 2003; Theurkauf et al., 1992). This « back signaling » is proposed to induce reorganization of the oocyte microtubule network at mid-oogenesis, which shifts oocyte microtubule network polarity and concomitantly the nucleus migrates towards the anterior plasma membrane. Nonetheless, no molecular cues have been identified as such an upstream signal so far (*reviewed in* (Milas and Telley, 2022). Therefore, the key event inducing nuclear migration has not yet been identified. In the light of our results, we can hypothesize that centrosome clustering is the first step required to induce oocyte nucleus migration, as it allows centering of the nucleus in the oocyte and prevents migration when altered. Indeed, we now propose that the oocyte nuclear migration is a three steps process: 1) centering from stage 5 to 6A: the centrosomes cluster, which allows the nucleus to move from the oocyte anterior to the center, 2) oscillations from stage 6A to 6B: the nucleus oscillates under the pushing forces exerted by the different sources of the oocyte microtubules, 3) trajectory from stage 6B to 7: proper migration along the routes favored by either Mud or centrosomes. To test if centrosome clustering is sufficient for the oocyte nucleus centering and further migration, we could treat the fly ovaries with the drug Griseofulvin. Griseofulvin has been shown to interfere with the microtubule network by inhibiting the polymerization and resulting in centrosome de-clustering in several cases of cancer cell lines, when used at concentration that are non toxic for normal cells (Bramann et al., 2013; Raab et al., 2012; Rebacz et al., 2007; Rhys and Godinho, 2017). Conversely, if centrosome clustering is the key element required for nuclear migration, a precocious clustering of centrosomes, prior to stage 6B, should induce nucleus migration at earlier stage than 6B. As we have shown the requirement of Kinesin-1 to cluster the centrosomes, we could try to enhance Kinesin-1 activity to induce a precocious clustering, notably by overexpressing Ensconcin (MAP7) in the germ cells. Importantly, Ensconsin has been shown to recruit Kinesin-1 at microtubules in *Drosophila* oocyte (Sung et al., 2008) and boost the activity of Kinesin-1 in *Drosophila* neuroblasts without affecting its stability (Metivier et al., 2019). Moreover, *ensconcin* mutants show defect in nucleus positioning at late-oogenesis stages (Sung et al., 2008).

3. Which isoforms of Mud are present in the *Drosophila* oocyte ?

Mud asymmetry is established from the germarium and remains so until completion of the nucleus migration. The difficulty of studying Mud domain contribution in the *Drosophila* oocyte is that *mud* gene encodes for 7 isoforms. The longest isoform of Mud protein has 2501 amino acids. The isoforms are similar in their N-terminal and vary in their C-terminal regions (Guan et al., 2000). Additionally, all of the isoforms possess the CH domains, while their CC, MT and TM domains vary (fig D. 1). Interestingly, regarding their size and their domains, I observed that we could classify them into four categories, as shown in the table below (fig D. 2).

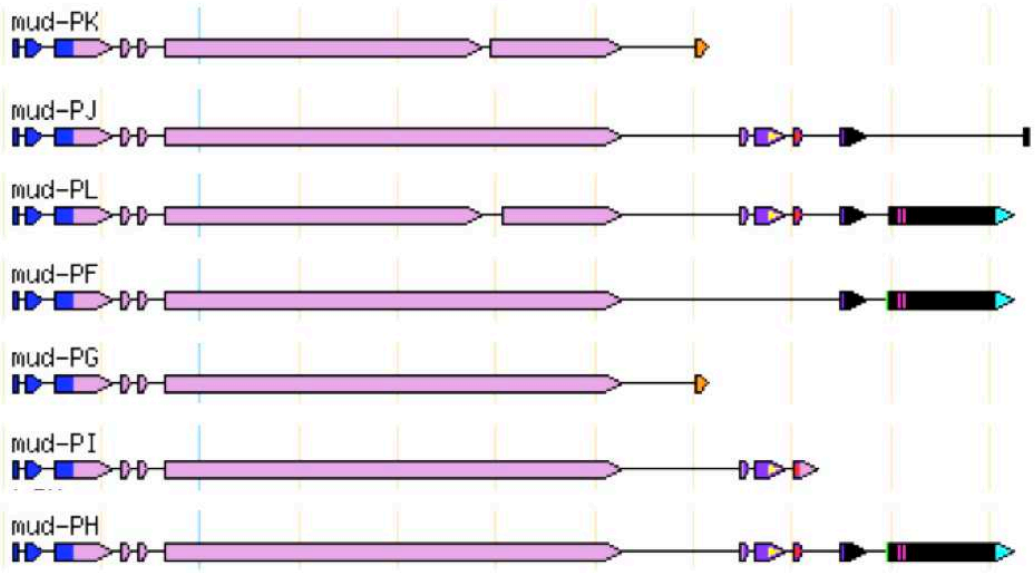

Figure D. 1: Mud gene encodes for 7 isoforms, adapted from Flybase - Mud and (Guan et al., 2000)**.** Color-coded representation of the predicted domains by analysis of the polypeptide products (P) encoded by *mud* transcripts.
■: CH domain ■: CC domain ■: MT binding domain ■: NLM (NuMA/LIN-5/Mud) domain ■: Pins binding domain ■ ■ : putative TM domains ■: putative PIP2 binding domain

	Mud isoforms	Size (kDa)	CH	CC *	NLM	Pins	MT	TM
1st Category	Mud PH	249,1	✓	✓	✓	✓	✓	✓
	Mud PL	286,5	✓	✓	✓	✓	✓	✓
2nd Category	Mud PF	274,5	✓	✓	✗	✗	✓	✓
3rd Category	Mud PI	242,8	✓	✓	✓	✓	✓	✗
	Mud PJ	248,9	✓	✓	✓	✓	✓	✗
4th Category	Mud PG	223,3	✓	✓	✗	✗	✗	✓
	Mud PK	220,8	✓	✓	✗	✗	✗	✓

Figure D. 2: Classification of Mud isoforms in three categories depending on their size and their domains. Table representing the size (kDa) and the presence (✓) or absence (✗) of the different domains depending on the isoform. Depending on these parameters, we can categorize the isoforms in four classes. (*) Although all the isoforms possess a CC domain, there are some variabilities.

The temporal and spatial expression of Mud isoforms in the *Drosophila* oocyte has not yet been studied. However, I observed distinct sized bands via SDS-page gel followed by western blotting Mud in ovary protein lysates (fig D. 3). These results indicate that several Mud isoforms are present in the ovaries of the fruit fly.

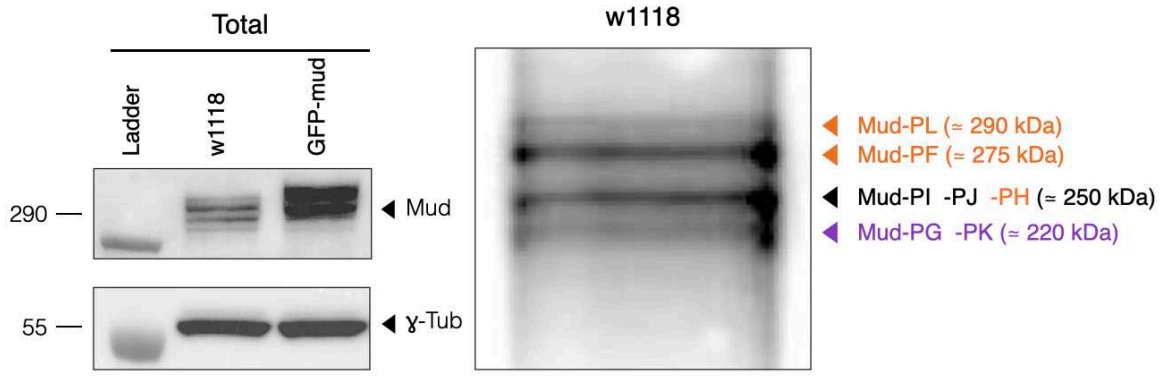

Figure D. 3: Several categories are Mud isoforms are present in the Drosophila ovaries. (Left panel) Immunoblot from ovary lysate of WT flies (*w*^{1118}) or *GFP-mud* flies, against Mud and ɣ-tub (as loading control). Mud antibody recognizes a sequence in CC domain that is common to the isoforms (Izumi et al., 2006). (Right panel) Magnification of the proteins revealed by Mud antibody in the *w*^{1118} line shows 4 different sized bands, that could correspond to the different isoforms.

Altogether, the presence of Mud isoforms and the variability between different domains could explain why we never observed complete delocalization from the oocyte nucleus using our different tools of *mud* domain mutants. Indeed, the domain variance makes it difficult to confirm the necessity of the TM or NLS domains for example, even though the phenotypes, when deleted, are promising in the investigation of a role in Mud distribution and function. Although not mention ed in the results, the study of TM domain was particularly surprising, as I observed differences in Mud asymmetry depending on if analyzed in fixed or living egg chambers. Thus, there was a marked difference in Mud$^{\Delta TM}$ asymmetry between living egg chambers versus fixed egg chambers. Asymmetrical Mud signal intensity was decreased in fixed versus living egg chambers. Egg chamber treatment with Phosphate Buffer Saline (PBS) or Paraformaldehyde (PFA) can disturb microtubule stability (Legent et al., 2015). Furthermore, I observed that microtubule were not involved in Mud asymmetry and as this shift did not occur with other strains, it is unlikely that the microtubules are responsible of this difference. Another hypothesis could be that an interaction with a protein partner through the TM domains is destabilized under egg chamber fixation and affects Mud$^{\Delta TM}$ asymmetry.

4. What is the purpose of Mud asymmetry ?

The observation of GFP-Mud reveals that the protein localization evolves throughout oogenesis. From the germarium until mid-oogenesis stages, Mud is asymmetrically distributed around the oocyte NE. After the oocyte nuclear migration at stage 7, Mud is isotropically distributed. Then at stage 8-9, orientation of the asymmetry shifts for being enriched on the anterior nuclear hemisphere. Moreover, the fact that Mud posterior asymmetry is maintained from the germarium until the completion of the nuclear migration could reflect an importance of the asymmetry for the migration or the associated mechanisms. Regarding Mud asymmetry, the deletion of CH domains, common to all isoforms, did not affect the nuclear trajectory proportions. This result indicates that Mud asymmetry is not required for its function in the control of posterior nuclear trajectory. Nonetheless, it seems unlikely that this feature is not associated with a specific function of the protein, as Mud is no longer asymmetrical after nuclear migration completion in WT oocytes.

Although, under my experimental conditions, I did not observe microtubule nucleation asymmetry at the oocyte NE, Mud's role in this nucleation or distribution remains to be further characterized. To test if Mud is responsible for the asymmetrical distribution of microtubule nucleation sites at the NE, we could perform FRET (Fluorescence Resonance Energy Transfert) in the oocyte between Mud and ɣ-tubulin, or with EB1. By doing so, we could understand the localization of their interaction surrounding the nucleus, which would occur predominantly on the posterior compared to the anterior nuclear hemisphere. Other oocyte MAPs display an asymmetrical distribution around the nucleus, such as Dynein, Cam, and Asp (Yu et al., 2006). Asp depletion has been shown to induce the loss of Mud asymmetry and nuclear trajectories by phenocopying *mud* mutant (Tissot et al., 2017). Mud, together with Asp, Cam and Dynein, could be a conserved complex (van der Voet et al., 2009) in the *Drosophila* oocyte and act on the organization of nuclear ncMTOC-associated microtubules or centrosomal microtubules. Another hypothesis regarding the asymmetrical co-localization of Mud and Dynein could be that together they participate in the nuclear migration, or in centrosomes-nucleus coupling. Dynein could bind the free plus end of microtubules emanating from the centrosomes and exert pulling forces to maintain their association with the nucleus during its migration. Using co-immunoprecipitation, I confirmed the interaction between Mud and Dynein Heavy Chain (Dhc) in the *Drosophila* ovaries (fig D. 4).

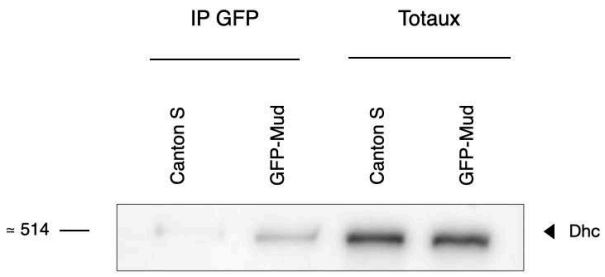

Figure D. 4: Mud interacts with Dynein Heavy Chain (Dhc) in the Drosophila ovaries. Immunoprecipitation of GFP-Mud in ovary lysates from the WT strain (Canton S) and GFP-mud strain shows co-IP with Dhc. .

Interestingly, Nup358/RanBP2 recruits BicD2 (*Drosophila* Bicaudal homolog) which in turn recruits Dynein and dynactin to the NPCs to maintain the centrosomes close to the nucleus prior to mitotic entry in dividing cells and for apical nuclear migration in neural stem cells (Baffet et al., 2015; Splinter et al., 2010). Furthermore, in these cells, BicD2 regulates Dynein and Kinesin-1 prior to mitotic entry which are involved in the positioning of centrosomes and nucleus displacement. I have shown that Mud interacts with RanBP2, and that nucleoporin is involved in Mud localization at the oocyte NE. It is therefore interesting to assess the role of Bicaudal (BicD) in *Drosophila* oocyte nucleus migration in association with Mud. Using transgenic strains developed by (Lu et al., 2022) which express RNAi against BicD or DLiC, I assessed the role of Dynein on Mud asymmetry and nucleus positioning. In the few cases that I observed, *BicD*- and *Dlic-RNAi* did not abolish nuclear asymmetric position or Mud asymmetry at mid-oogenesis. However, at late-oogenesis stages (around stage 9) the nucleus was mispositioned, and Mud was not always detectable or asymmetric at the oocyte NE (fig D. 5). Conversely, Mud could be necessary for the recruitment of Dynein at the oocyte NE and its asymmetry. It would be therefore interesting to test the asymmetry of Dynein, Asp, and Cam in a *mud* mutant. Perhaps more important than the asymmetry itself, my results are consistent with the importance of Mud restriction at the nucleus for correct posterior nuclear trajectory regulation.

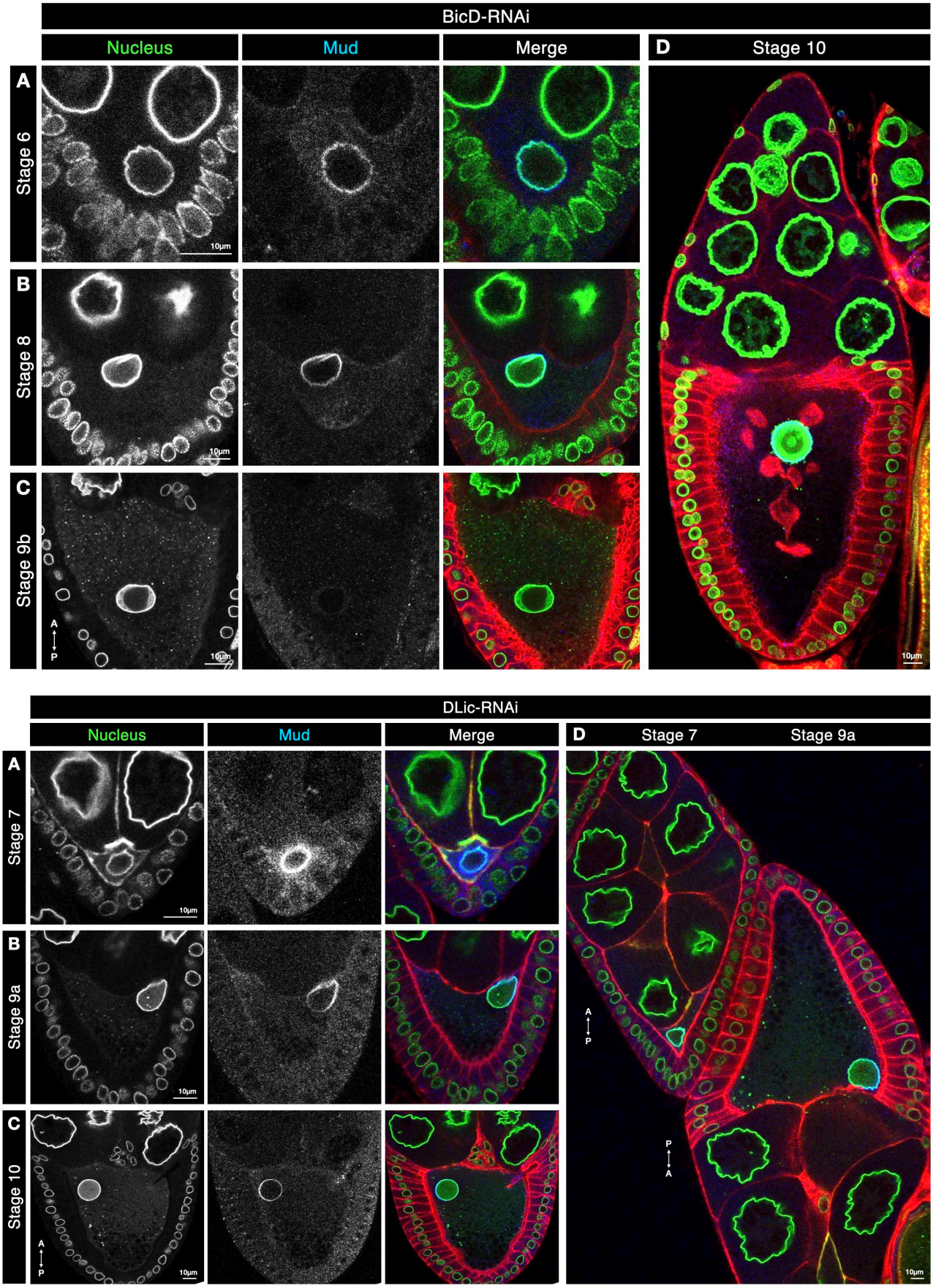

Figure D. 5: Preliminary data regarding the effect of BicD (top panel) and Dlic (bottom panel) on Mud localization and nucleus positioning. Immunofluorescences against Mud on egg chambers expressing BicD-RNAi or Dlic-RNAi in the germline cells. The transgenes *Fs(2)Ket-GFP* and *PH-RFP* are expressed to label nuclei and the plasma membrane respectively. The orientation of the egg chamber is indicated by the arrow A (anterior), P (posterior). Bars, 10µm. (Nota Bene: The orientation of the two egg chambers are different in (D)).

5. What is Mud's role at the oocyte nuclear enveloppe ?

Mud has been proposed to have a role in nuclear integrity, as experiments in *Drosophila* germ cells show that Mud depletion causes Lamin Dm0 absence at the oocyte NE and a diffusion of DNA in the cytoplasm (Christophorou et al., 2015). It is important to note that, at mid- (stage 6) and late oogenesis (stage 9a), we did not observe an absence of Lamin Dm0 labeling or Fs(2)Ket at the oocyte NE in *mud* mutant context (fig D. 6.A-B) and electronic microscopy of *mud*^{4} egg chambers did not show any oocyte NE disruption (fig D. 6.C). However, as Mud asymmetry is enriched on nuclear hemisphere facing centrosomes and plasma membrane which are two other ncMTOC of the oocyte, an exciting hypothesis could be that Mud is required to strengthen the NE and counteract pushing forces exerted on the nucleus. Nevertheless, depletion of centrosomes (Tissot et al., 2017) or microtubule depolymerization do not abolish Mud asymmetry.

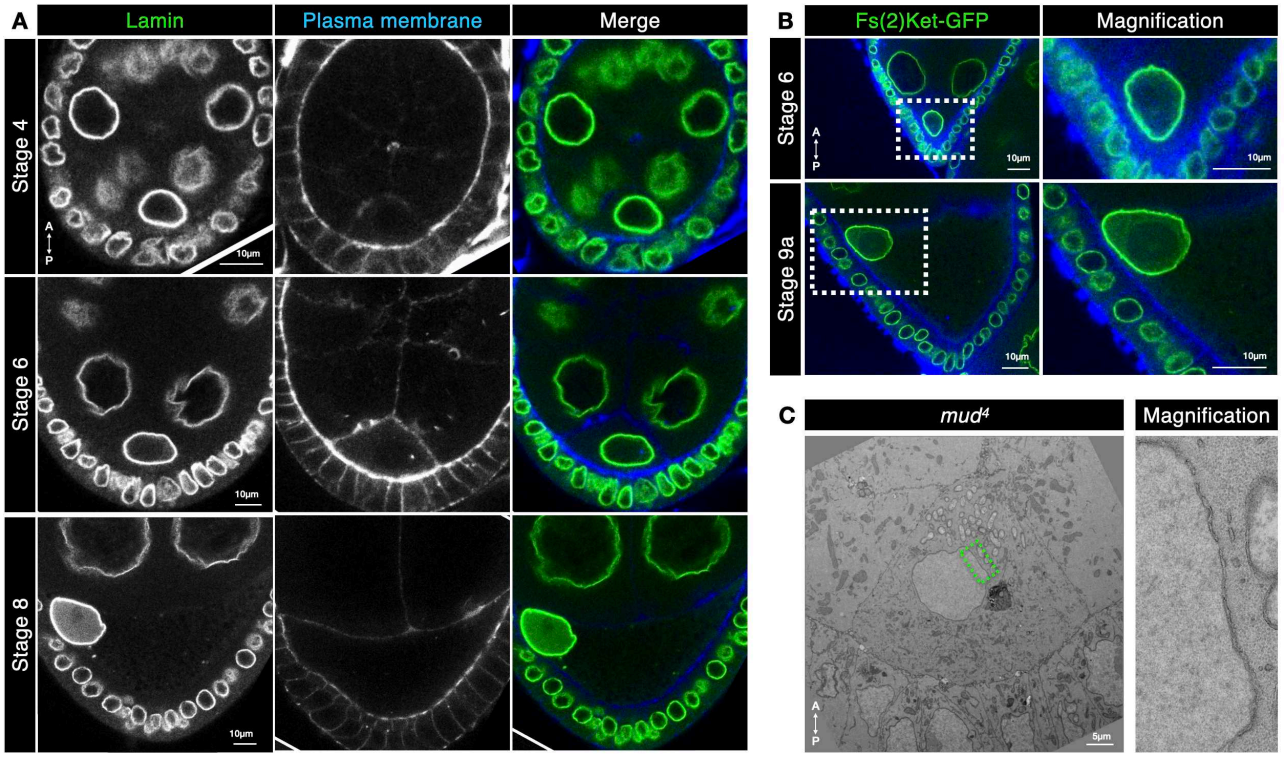

Figure D. 6: Mud mutation does not affect oocyte NE at mid- or late oogenesis. Immunofluorescence in *mud* null mutant (*mud*^{4}) egg chambers against Lamin Dm0 (A) or expressing Fs(2)Ket-GFP (B), phalloidin labeling plasma membrane. Bars, 10µm. (C) Fred Bernard data - Electron microscopy of *mud*^{4} oocyte (right panel) and magnification of a region of the NE (left panel). Bar, 5µm.

RanBP2 is a key player in the formation of pre-NPC granules. It serves as platform to recruit nucleoporins such as Nup107. (Hampoelz et al., 2019). These granules are synthesized in the oocyte cytoplasm and passed on to the early embryo, in which nuclei rapidly grow and require membranes and NPCs. As the oocyte nucleus grows concomitantly with the egg chamber (fig D. 7), we can assume that new material is required to ensure NE integrity. Moreover, electronic microscopy experiments conducted in my lab, show that Mud localizes on the outer nuclear membrane of the oocyte NE and is closely associated with NPCs (Bernard et al., 2021). Mud, together with Fs(2)Ket, RanBP2 and Nup107 could participate in oocyte NE growth by providing new NPCs. It would be interesting to test if RanBP2 recruitment at the oocyte NE is dependent on Mud.

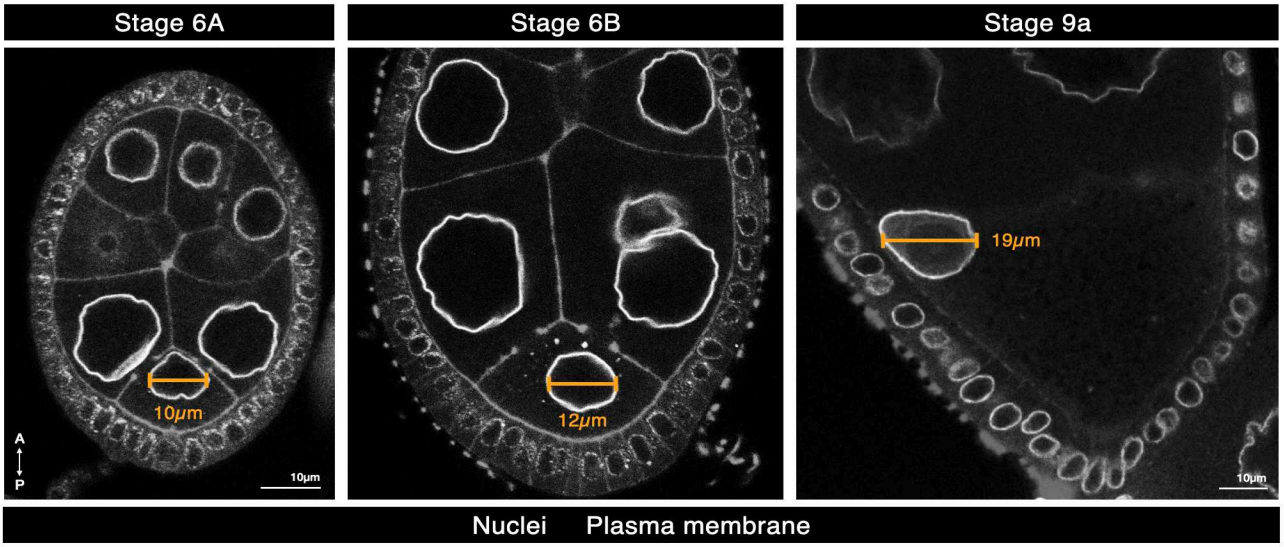

Figure D. 7: Oocyte nucleus growth along oogenesis. Immunofluorescence of WT egg chambers of stage 6A, 6B, and 9a, to label the nuclei and the plasma membrane. The orange line and associated measurement is the oocyte nucleus diameter. The orientation of the egg chamber is indicated by the arrow A (anterior), P (posterior). Bar, 10µm.

Reinforcing my interest for a role of Mud associated with the oocyte NE, studies have reported that NuMA can self-assemble and be part of a larger filamentous network in the nucleus: the nuclear matrix (*see Chapter I 1.c*) (Abad et al., 2007; Gueth-Hallonet et al., 1998; Merdes and Cleveland, 1998; Razin et al., 2014; Saredi et al., 1996). Two hypothetical models explain the post-mitotic nuclear localization of NuMA: 1) NuMA is sequestered in the nucleus in order to prevent its interaction with cytoplasmic microtubules and subsequent spindle organization function. 2) NuMA plays a role in chromatin reorganization and NE reformation by participating in the establishment of the nuclear matrix (Radulescu and Cleveland, 2010). NuMA C-terminal region is required for oligomerization and its coiled-coil domain is responsible for the architecture of this higher-level structure. Indeed, NuMA forms hexagonal multi-arm structures that decorate the nucleus interior (Harborth et al., 1999). The addition or deletion of the coiled-coil domain causes a change in the hexagons spacing, suggesting that this region defines the lattice architecture. Furthermore, NuMA oligomerization participates in nuclear matrix establishment which has an important role in the maintenance of nuclear shape, organization and architecture (Compton and Cleveland, 1993; Gueth-Hallonet et al., 1998; Harborth et al., 1999; Rajeevan et al., 2020; Saredi et al., 1996). When NuMA NLS are deleted (NuMA$^{\Delta NLS}$), it accumulates in the cytoplasm and forms a filamentous mass with larger cables compared to WT NuMA (23nm diameter and 5nm respectively) (Figure D. 8.A) (Saredi et al., 1996). Altogether these studies show that NuMA is important and necessary for nucleus integrity. The filamentous mass formed by NuMA$^{\Delta NLS}$ is particularly interesting as it bears resemblance to the structure formed by Mud$^{\Delta MT}$. Indeed, my lab has previously observed Mud$^{\Delta MT}$ structure by electronic microscopy, which forms a dense mass in the cytoplasm (fig D. 8.B). Identification of the structure observed in *mud$^{\Delta MT}$* remains to be identified. Although I observed that Mud$^{\Delta Ex7}$ and Mud$^{\Delta Ex12}$ partially delocalize to centrosomes, due to genetic setbacks I could not assess if GFP-Mud$^{\Delta MT}$ co-localizes with centrosomes as well. The structure in Mud$^{\Delta MT}$ is bigger and more dense than the delocalization of Mud$^{\Delta Ex7 \text{ or } \Delta Ex12}$, suggesting the recruitment of additional proteins. Tubulin could be an interesting component candidate to test, as NuMA$^{\Delta NLS}$ structure stained positive for tubulin (Saredi et al., 1996).

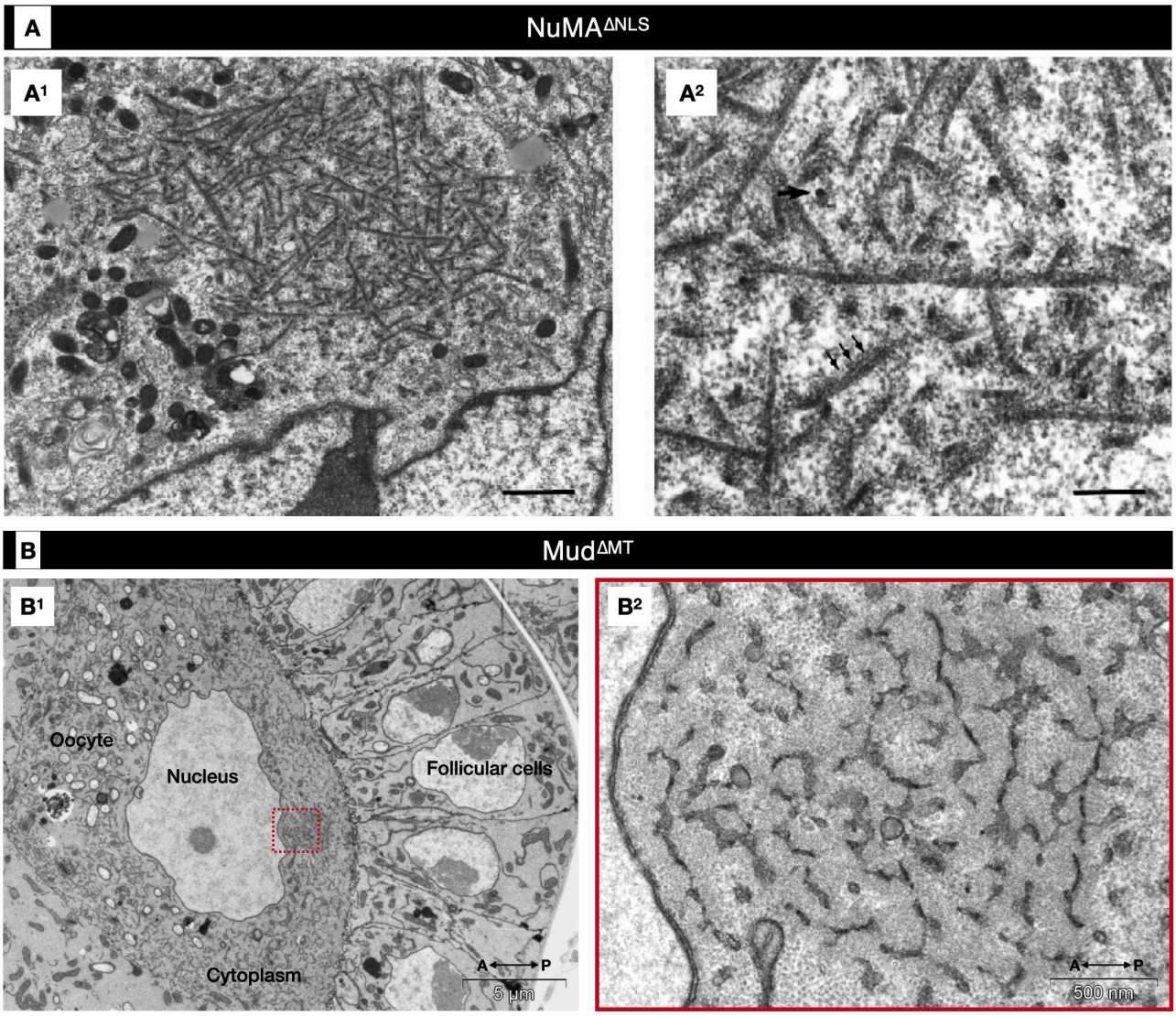

Figure D. 8: NuMA$^{\Delta NLS}$ self-assembles and forms a filamentous structure in the cytoplasm similarly to Mud$^{\Delta MT}$. (A) Adapted from (Saredi et al., 1996), Electron microscopy of the cytoplasm of BHK-21 cells transfected with NuMA$^{\Delta NLS}$. Bars 1µm (A^1) and 200nm (A^2). NuMA$^{\Delta NLS}$ forms filamentous structure containing 23nm diameter cables in the cytoplasm. (B) Data from Fred Bernard, Electronic microscopy of oocyte from *mud$^{\Delta MT}$* flies. The follicular cells, oocyte cytoplasm, and oocyte nucleus are annotated. (B^2) Magnification of the red square region defined in (B^1) corresponds to the perinuclear structure in which Mud$^{\Delta MT}$ partially delocalizes from the NE. Orientation of the egg chamber is indicated by the arrow A (anterior), P (posterior). Bars 5µm (B^1) and 500nm (B^2).

6. Is Mud restricted to the NE to avoid centrosomal localization ?

NuMA localization in the nucleus during interphase is a proposed mechanism to sequester its microtubule-associated function to not disturb, enhance or organize centrosomes or microtubules (Gueth-Hallonet et al., 1996; Merdes and Cleveland, 1998). In *mud$^{\Delta MT}$* context, the nuclear migration phenocopies the trajectories observed in *mud* depleted context with a decrease of the posterior route. This result led us hypothesize that proper localization of Mud and its restriction at the oocyte NE are required for Mud function to regulate nuclear migration. We now know that the oocyte nuclear migration, although a robust event, requires a very fine tuned balance of microtubule forces. Indeed, it has been shown that Mud can promote microtubule polymerization (Bowman et al., 2006), and NuMA can affect the clustering of the centrosomes in cancer cells that display supernumerary centrosomes (Quintyne et al., 2005).

It has been proposed that Mud is necessary for completion of meiosis at the end of oogenesis prior to fertilization, which proceeds in absence of centrosomes (Yu et al., 2006). It is possible that Mud does not have a main role in nuclear migration at mid-oogenesis, but has to be stored in the oocyte until it is required at the end of oogenesis. As Mud$^{\Delta Ex7}$ and Mud$^{\Delta Ex12}$ co-localize in part at the centrosomes, I hypothesize that Mud has to be restricted at the nucleus away from the centrosomes to avoid a potential additional action on the centrosomes. The nuclear migration trajectories have to therefore be assessed in the *mud$^{\Delta Ex7}$* and *mud$^{\Delta Ex12}$* contexts. In addition, it would be interesting to investigate the role of Mud on centrosome clustering in these contexts. I hypothesize that Mud$^{\Delta Ex7}$ and Mud$^{\Delta Ex12}$ could enhance centrosome clustering in a Dynein-dependent fashion which could affect the timing for nuclear migration. It could also modulate nucleation capacity as Mud is capable of promoting microtubule polymerization (Bowman et al., 2006). The potential role of Mud at the centrosomes might subsequently affect the trajectories.

7. What is actin's role in the Drosophila oocyte nuclear positioning and migration ?

Although *Drosophila* oocyte nuclear migration depends on microtubules, the role of actin has to be addressed, as it could bring precision support microtubule network as well as the nucleus itself. More studies show that cytoskeletal elements are interconnected, and suggest that these different elements should not be considered individuals actors but rather a unified system in which components rely on the others (Dogterom and Koenderink, 2019). Interestingly, it has been shown that actin can regulate microtubule growth at the centrosome but also organize and stabilize microtubules (Inoue et al., 2019). Moreover, in addition of their role as microtubule organizing center, it has been shown that the centrosomes can organize actin by serving as platform for the recruitment of actin nucleating factors (Farina et al., 2016). Furthermore, centrosomal actin filaments have been shown to regulate the coupling centrosome/nucleus via the LINC complex (Obino et al., 2016). Interestingly, the *Drosophila* oocyte nucleus, which constitutes a microtubule ncMTOC, is surrounded by a cage of actin filaments (Januschke et al., 2002). It is therefore interesting to investigate the role of actin in the positioning and migration of the oocyte nucleus. When depleting the two identified actors of the nuclear trajectory Mud and centrosomes, 50% of nuclei still migrate (Tissot et al., 2017), suggesting that other important players are involved in the regulation of this robust event. Although 1) the plasma membrane ncMTOC importance has not been assessed in the oocyte nuclear migration yet, and 2) depolymerization of the microtubules by Colcemid treatment abolishes the migration, the investigation of actin's role remains to be elucidated. Even though actin might not be as critical as the microtubules for the oocyte nuclear migration, it could play a role in the regulation of the different ncMTOC and in nuclear trajectories. Unpublished data in my lab from experiments using Latrunculin drug to depolymerize actin filaments have been performed to assess its role in the nuclear migration. In drug concentrations that were sufficient to abolish phalloidin signal in the oocyte, while allowing a correct development of the egg chambers, the nucleus was asymmetrically localized at later stages of oogenesis, suggesting that actin is not necessary for the migration. In the light of our new results, it would be interesting to pursue these experiments

and analyze the nuclear position prior to migration, as well as the behavior of the centrosomes. Furthermore, I have shown that the CH domain of Mud was required for its asymmetry at the oocyte nucleus, and that microtubules themselves were not necessary for Mud distribution. The CH domains are domains of interactions with the cytoskeleton elements. Therefore, the role of actin on Mud localization has to be assessed.

Finally, many studies highlight the importance of the cytoplasm viscosity in the context of organelle positioning, notably in the mouse oocyte and the sea urchin zygote in which the actin cytoskeleton is an important player (Almonacid et al., 2019a; Xie et al., 2022). In the sea urchin zygote, the viscoelastic properties of the cytoplasm have been shown to regulate the positioning of the mitotic spindle and centrosomes and be sufficient to move objects back to their original places after manipulation with optical tweezers (Xie et al., 2022). It was shown that F-actin filaments constitute 40-50% of the crowding agents of the cytoplasm, giving elastic and viscous properties to the cytoplasm. During mouse oocyte growth, the nucleus moves from an asymmetrical to a center position within the oocyte, which is necessary for the success of the meiotic divisions (Almonacid et al., 2018, 2019b). This nuclear migration is actin-dependent, but does not require microtubules nor centrosomes. A gradient of actin filaments and associated propulsion forces are established from the cortex to the oocyte center which impacts the viscosity of the cytoplasm and promotes the nucleus centering. In the understanding of the precise role of the microtubules in the oocyte nuclear migration, it will be interesting to investigate the viscosity properties that they confer to the *Drosophila* oocyte cytoplasm. Conversely, it has been shown that depending on the physical properties of the cytoplasm, the microtubule dynamics was modulated, notably the more viscosity the slower the microtubule depolymerization and polymerization are (Molines et al., 2022). Viscosity properties could vary in the oocyte cytoplasm from the anterior to the posterior, or from the cortexes compared to the center, and thus influence the trajectories as well.

Altogether, this work allowed me to better characterize the two actors of the oocyte nuclear migration trajectory in *Drosophila*. Further investigations on the different ncMTOC contribution in oocyte nuclear positioning and migration, as well as the characterization of their associated microtubule forces, will bring a deeper comprehension to the system. The precise characterization of the nuclear ncMTOC will be essential to decipher of a potential microtubule organization role of Mud.

▪ Microscopy

a) Acquisitions of fixed samples

1 day old females were collected and put with fresh media for 30-48 hours at 25°C prior to dissection. Ovaries were dissected in PBS-Tween20 0,1%, fixed in 4% paraformaldehyde diluted in PBS-TritonX-100 0,3% and directly mount in Citifluor™ (EMS) on a coverslip if no additional markers were required, otherwise Immunofluorescence was performed by an overnight incubation at 4°C with primary antibodies in 1X PBS -TritonX-100 0,1% supplemented with 0,3% BSA, and a 2h incubation with secondary antibodies in 1X PBS -TritonX-100 0,1% supplemented with 0,3% BSA at room temperature. After washes, ovaries were mounted in Citifluor™ (EMS).

Images were captured using Zen software on a Zeiss 710 confocal microscope (488, 561, 640 nm lasers and the x40 or x63 objectives).

The primary and secondary antibodies used are listed below.

Antibodies	Host species	Dilution	Reference
Primary antibodies			
anti Mud	rabbit	1:1000	Izumi et al., 2006
anti Otefin	goat	1:500	Barton et al., 2014
anti Lamin Dm0	mouse	1:10	DSHB
anti Nup107	rabbit	1:500	Belgareh et al., 2001
anti Nup 133	rabbit	1:500	Belgareh et al., 2001
anti Khc	rabbit	1:250	Cytoskeleton TM #AKIN01
anti alpha tubulin DM1A	mouse	1:250	Sigma #T6199
anti alpha tubulin B-5-1-2	mouse	1:100	Sigma
anti gamma-tubulin GTU-88	mouse	1:100	Sigma
anti Cut	mouse	1:50	DSHB #2B10
anti Hindsight	mouse	1:100	DSHB #1G9
Secondary antibodies			
anti mouse Alexa647	chicken	1:100	Invitrogen #A21463
anti rabbit Alexa647	goat	1:200	Immunoresearch #111-605-144
Labels			
SiR-actin		1:150	Cytsokeleton TM
Phalloidin-rhodamin		1:200	LifeTech
Wheat Germ Agglutinin (WGA)		1:200	Molecular Probes

b) Acquisitions of living samples

1 day old females were collected and put with fresh media for 30-48 hours at 25°C prior to dissection. Ovaries were dissected in Schneider medium and directly mount in halocarbon oil (Voltalef 10S) on a coverslip. Images were captured using Metamorph software on a Zeiss Axio Observer Z1 confocal microscope coupled with a spinning disk module CSU-X1 and a sCMOS camera PRIME 95 (488, 561, 640 nm lasers and a x63 oil immersion objective).
For egg chambers that did not express a plasma membrane marker, ovaries were first incubated with live-cell CellMask Deep Red (Invitrogen, #C10046) at 1:1000 diluted in Schneider medium room temperature for 10min.
In order to image the whole nucleus, 21 stacks along the z axis of a 1µm range were taken for each egg chamber.

c) Nuclear migration time-lapse

To perform live-imaging time-lapse, refer to the protocol: (Loh et al., 2021).

▪ Fluorescence Recovery After Photobleaching

1-2 day old female ovaries were dissected in Schneider media and mount in halocarbon oil (Voltalef 10S) on a coverslip. For each egg chamber, a round ROI of 2,9μm diameter was determined on the oocyte posterior hemisphere of the nucleus. The GFP of this zone was photo-bleached by 3 repetitions of 1ms with the 488nm laser at maximum intensity. To measure the fluorescence recovery, images were acquired for 30min following different steps :

- Pre-photobleaching : acquisitions every seconds for 20 sec
- Post-photobleaching : acquisitions every seconds for 2min, then every 40 seconds for 20min, finally every minute for 7,5min.

Images were captured using Metamorph software on a Zeiss Axio Observer Z1 confocal microscope coupled with a spinning disk module CSU-X1 and a sCMOS camera PRIME 95 (488nm lasers and a x63 oil immersion objective). Quantifications were done in Fiji using a macro developed in the lab to normalize the recovering fluorescence with the background signal.

▪ Co-immunoprecipitation

Protein extracts were obtained from 30 ovary pairs of 2 day old females, dissected in 1X PBS supplemented with 1X protease inhibitors(cOmplete™, EDTA-free, Sigma). The ovaries were then lysate at 4°C in Lysis Buffer (10mM Tris/Cl pH7.5; 150mM NaCL; 0,5mM EDTA; 0,5% NP-40) supplemented with 1X protease inhibitors. The samples were then centrifuged at 4°C at 13000rpm for 10min. The supernatants were incubated with 15μl of GFP-Trap_MA or RFP-Trap_MA beads (ChromoTek) at 4°C for 1h.

The samples were analyzed by Western-Blot consisting in protein migration by electrophoresis on a 4-12% polyacrylamid gel (Invitrogen), followed by a liquid transfer on a PolyVinyliDene Fluoride (PVDF) membrane, which was saturated with 5% milk 1X PBS. The membrane was the incubated overnight with primary antibodies at 4°C and incubation with HRP-coupled secondary antibodies at room temperature for 2h, before revealing with ChemiDoc MP Imaging (BioRad) using West femto chemiluminescent reagents (ThermoScientific).

▪ Genotyping

DNA was extracted from a whole fly in Squishing Buffer (10mMTris-HCl pH8,2 ,1mM EDTA, 25mM NaCl, 200μg/ml Proteinase K). The amplification procedure consisted of a denaturation of 2min at 94°C followed by 30 cycles of denaturation 30sec at 94°C, annealing 40sec at 60°C, elongation 50sec at 72°C, and a finale extension of 10min at 72°C. PCR reaction mixture were prepared in 25μl volumes including 0,8mM primers, 200μM dNTPs, 0,5X GoTaq buffer, GoTaq Flexi DNA polymerase (Promega) (5 U/lL), and DNase and RNase free ddH2O.The PCR products were visualized on 0,5X TBE diluted 1,5% agarose gel supplemented in SYBR Safe (Invitrogen) at 1:10000, and imaged with

The primers for testing the deletion of Khc Hinge2 domain were :

- Forward : 5'ACAAGGATGAGGAGATCAATCAGC 3'
- Reverse : 5'GTAGCTCGTCCATCTGAGAATC 3'

▪ Graphs and statistical analysis

All images were processed using the software Fiji (Schindelin et al., 2012).

Statistics : Graphs as well as statistical tests were carried out with GraphPad Prism6.

ANNEX: ARTICLE

Kinesin-1 promotes centrosome clustering and nuclear migration in the *Drosophila* oocyte

Maëlys Loh1, Déborah Dauvet1, Frida Sanchez-Garrido1, Kahina Sadaouli1, Fred Bernard1,* and Antoine Guichet1,*

Kinesin-1 promotes centrosome clustering and nuclear migration in the *Drosophila* oocyte

Maëlys Loh[1], Déborah Dauvet[1], Frida Sanchez-Garrido[1], Kahina Sadaouli[1], Fred Bernard[1,*] and Antoine Guichet[1,*]

[1]: University of Paris, Institut Jacques Monod, CNRS, UMR 7592, France - Polarity and Morphogenesis Team
[*]: Co-corresponding authors (frederic.bernard@ijm.fr; antoine.guichet@ijm.fr)

Key words

Kinesin, nucleus, centrosomes, microtubules, Drosophila, oocyte

Summary statement

In this study, we identified a crucial role of Kinesin-1 in centrosome clustering required for nuclear positioning and migration in the *Drosophila* oocyte.

Abstract

Accurate positioning of the nucleus is essential in many cellular contexts. Microtubules and their associated motors are important players in this process. Although nuclear migration in *Drosophila* oocytes is controlled by microtubule-generated forces, a role for microtubule-associated molecular motors in nuclear positioning has yet to be reported. In this study, we first characterize novel landmarks that allow a precise description of the pre-migratory stages. Using these newly defined stages, we report that, prior to migration, the nucleus moves from the anterior side of the oocyte toward the center and concomitantly the centrosomes cluster at the posterior of the nucleus. In absence of Kinesin-1, centrosome clustering is impaired and the nucleus fails to position and migrate properly. In addition, we show that maintaining a high level of Polo-kinase at centrosomes prevents centrosome clustering and impairs nuclear positioning, suggesting that Kinesin-1 associated defects result from a failure to reduce centrosome activity. Consistently, depleting centrosomes rescues the nuclear migration defects induced by Kinesin-1 inactivation. In summary, our results suggest that Kinesin-1 controls nuclear migration in the oocyte by modulating centrosome activity.

Introduction

The cytoskeleton plays a central role in nuclear positioning, which regulates many cellular and developmental systems, including zygote formation, cell division, cell polarity and motility, and in this process. Actin filaments, microtubules (MTs), as well as associated motor proteins are instrumental in the underlying mechanisms of this positioning. In many cases, MTs participate to localize the nucleus in close association with a centrosome, acting as MT organizing center.

The MT plus-end directed motor, Kinesin-1, plays an essential function in the nuclear positioning in several cellular contexts (Duncan and Warrior, 2002; Folker et al., 2013; Fridolfsson and Starr, 2010; Januschke et al., 2002; Metzger et al., 2012; Meyerzon et al., 2009; Roux et al., 2009; Splinter et al., 2010; Williams et al., 2014; Wilson and Holzbaur, 2012; Wilson and Holzbaur, 2015). Kinesin-1 is a hetero-tetramer, composed of a dimerized Kinesin heavy chains (Khc) and two regulatory Kinesin light chains (Klc) (Verhey et al., 2011). Kinesin-1 can affect nuclear positioning via different mechanisms. For example, Kinesin-1 can transport the nucleus as cargo and drive its displacement along MTs towards their plus ends via an interaction between Klc and nuclear envelope (NE) associated proteins

such as Nesprins (Meyerzon et al., 2009; Roux et al., 2009). Alternatively, Khc can control nuclear positioning independently of Klc by crosslinking MTs via a C-terminal MT binding site or indirectly through an association with the MT associated protein (MAP) Ensconsin/Map7 (Metzger et al., 2012). In the *Drosophila* oocyte, asymmetric positioning of the nucleus is crucial for the organization of MT-based transport which controls, among other things, the asymmetric localization of mRNAs that encode determinants of the polarity axes of the future embryo (González-Reyes et al., 1995; Guichet et al., 2001; Januschke et al., 2006; Roth et al., 1995; Swan et al., 1999).

During the 14-stage process of oogenesis, the oocyte is specified from a group of 16 interconnected germ cells, while the remaining 15 cells differentiate into nurse cells (NCs) (Huynh and St Johnston, 2004). This germline cyst of 16 cells is surrounded by epithelial follicle cells forming an egg chamber. The oocyte is positioned at the posterior of the egg chamber in contact with the follicle cells. (Fig; 1B) (Huynh and St Johnston, 2004). During development, MT organization evolves several times through complex and not yet fully understood mechanisms. In early oogenesis, MT minus-ends located at the posterior of the oocyte organize a network towards the ring canals (Grieder et al., 2000; Nashchekin et al., 2021). Then, at mid-oogenesis, concomitantly with nuclear migration, the MT network is progressively reorganized to result in the formation of a dense network with a weak anterior to posterior bias of MT plus-ends. At stage 10, MTs are further reorganized as bundles that are parallel to the cell cortex and generate a cytoplasmic flow (Drechsler et al., 2020; Januschke et al., 2006; Lu et al., 2016; Nashchekin et al., 2016; Parton et al., 2011; Theurkauf et al., 1993; Trong et al., 2015). Throughout oocyte development, MT polymerization occurs from several sources (Januschke et al., 2006; Lu et al., 2021; Nashchekin et al., 2016; Nashchekin et al., 2021) including the centrosomes that are active from the beginning of oogenesis until stage 11 (Pimenta-Marques et al., 2016).

The oocyte contains at least 16 centrosomes, as in early oogenesis the centrosomes of the 15 NCs migrate through the ring canals into the oocyte to eventually form a cluster located between the nucleus and the posterior plasma membrane of the oocyte (Bolívar et al., 2001; Mahowald and Strassheim, 1970; Nashchekin et al., 2021; Pimenta-Marques et al., 2016). During mid-oogenesis, this cluster co-migrates with the nucleus and remains asymmetrically localized in close vicinity to the nucleus (Januschke et al., 2006; Tissot et al., 2017; Zhao et al., 2012). Then, the centrosomes gradually lose their pericentriolar materials (PCM), leading to their elimination during late oogenesis (Pimenta-Marques et al., 2016).

Pioneering studies have revealed that the movement of the *Drosophila* oocyte nucleus is mediated by MTs (Koch and Spitzer, 1983). More recent work further showed that a dual relationship exists between the nucleus and the MTs within the oocyte. Nuclear positioning influences the MT network organization in the oocyte. Additionally, the MTs are instrumental in the nuclear migration (Januschke et al., 2006; Tissot et al., 2017; Zhao et al., 2012). Between stages 6 to 7, the oocyte nucleus migrates from the center to the anterior side of the oocyte and is subsequently maintained at the boundary between the plasma membrane of the anterior margin and the lateral membrane (Bernard et al., 2018). This asymmetric nuclear positioning will subsequently specify the identity of the dorsal cortex and initiates the establishment of dorsal-ventral polarity of the egg chamber and the future embryo (González-Reyes et al., 1995; Guichet et al., 2001; Roth et al., 1995). Then, as the oocyte size increases, a MT-dependent process maintains the nucleus at that position until completion of oogenesis (Roth and Lynch, 2009). Migration of the nucleus is achieved by MTs pushing forces exerted on the NE (Tissot et al., 2017; Zhao et al., 2012). We have further reported that distinct molecular cues act in complementary fashion during this process (Tissot et al., 2017). One is associated with the MAP Mushroom-body defect (Mud), which is asymmetrically located at the NE of oocyte nucleus. The second cue corresponds to the centrosomes.

However, the mechanisms ensuring the nuclear migration onset remain unknown. Furthermore, although MT involvement has been clearly demonstrated, the potential involvement of MT-associated motors, particularly Kinesin-1 has not been identified in the oocyte nuclear migration. Kinesin-1 has been reported to be necessary only for the positioning maintenance of the nucleus after its asymmetric migration. Moreover, only Khc but not Klc is required for this process (Duncan and Warrior, 2002; Januschke et al., 2002; Loiseau et al., 2010; Palacios and St Johnston, 2002; Williams et al., 2014).

In this study, by improving our ability to identify the developmental stages preceding the migration of the nucleus in the *Drosophila* oocyte, we have further characterized the mechanisms controlling the onset of nuclear migration and reveal a role for Kinesin-1. We found, despite differences in function, that both subunits of Kinesin-1, Khc and Klc, are involved for nuclear positioning and migration. We further show that Kinesin-1 is required for centrosome clustering at the onset of the nuclear migration and that the two processes are correlated. We propose that Kinesin-1 controls oocyte nuclear migration by modulating MT organizing activity of centrosomes.

Results

Novel landmarks to define nuclear positioning prior to migration

The nature of mechanisms ensuring nuclear migration onset remain unknown, particularly because of the lack of precise description of pre-migratory stages independently of the nuclear positioning itself. Therefore, we sought to better characterize the development of the oocyte and egg chamber from stages 5 to 7, which precede and overlap with nuclear migration, respectively. In a first attempt, we took advantage of a cell cycle switch that occurs in the surrounding follicular epithelium (Rowe et al., 2020) simultaneously to the nuclear migration in the oocyte. Cut and Hindsight (Hnt) are two transcription factors typically used as specific markers of the mitotic and endocycle cycles, respectively (Sun and Deng, 2005; Sun and Deng, 2007). Accordingly, before oocyte nuclear migration (stage 6), the follicular cells express Cut, and after completion of nuclear migration (stage 7) they express Hnt (Sup Fig 1). However, there are intermediate cases where Cut and Hnt are not expressed, therefore these criteria are not sufficient to define nuclear migration onset in the oocyte. Furthermore, staging the egg chambers by assessing the level of Cut and Hnt expression requires immunodetection in follicular cells and is consequently not compatible with live imaging.

More recently the Bilder lab reported that NC diameter provides another landmark of egg chamber development (Chen et al., 2019). We found that applying this criterion to two NCs in contact with the oocyte allowed us to better describe the period of nuclear pre-migration (Fig. 1A, B). The measurement of the NC diameter (Fig. 1 C, D) together with the egg chamber aspect ratio and the oocyte shape (see methods) allowed us to distinguish four steps, refining this developmental phase through the stages 5, 6A, 6B and 7.

At stage 5 the nucleus is always anteriorly positioned in the oocyte, in contact with or in close vicinity of the anterior membrane of the oocyte. At stage 6A, most of oocytes exhibit a nucleus in the anterior part of the oocyte, even if there are some instances of central positioning. At stage 6B, the nucleus is mostly found in a central position and at stage 7 the migration is complete, and the nucleus is in contact with both the anterior and the lateral plasma membranes of the oocyte (Fig. 1 E, F).

Khc and Klc subunits are differentially required for nuclear positioning

Using these criteria to stage the egg chambers, we looked for factors that are required for nuclear migration onset. We found that RNAi mediated inactivation of *Khc* in the oocyte impairs the position of the nucleus. In this context, the nucleus remains anteriorly positioned at stages 6A and 6B and subsequently fails to migrate at stage 7 (Fig. 2A-B). Similar results

were obtained with a second RNAi line directed against *Khc* (Fig. 2C). We confirm our results by generating germline mitotic clones. Induction of GFP/FRT clones of the Khc^{27} mutant allele, a *Khc* null allele (Januschke et al., 2002), revealed similar phenotypes to the RNAi knockdown conditions, thus confirming that Khc is necessary for nuclear migration and that its loss results in non-centered nucleus at stage 6B (Fig. 2 D, E).

Subsequently, we decided to test the role of Klc, the non-motor subunit of Kinesin-1 in nuclear positioning and migration. Similarly to *Khc* down-regulation, RNAi mediated knockdown of *Klc* in the oocyte leads to mispositioned nuclei that remain at the anterior of the oocyte at stages 6A and 6B. In this genetic background, stage 7 egg chambers display non-migrated nuclei (Fig.3 A-C). This indicates that Klc is involved in early nucleus positioning but also required for the nuclear migration. Furthermore, a GFP/FRT-mediated clonal analysis with two distinct *Klc* alleles confirmed these results (Fig.3 D-F). However, in mutant contexts for *Klc*, we noted that the nuclei eventually migrate, as we can detect some correctly positioned nuclei at stage 9 and beyond (Sup. Fig. 2 C-E), consistent with previously published studies (Palacios and St Johnston, 2002). The latter result contrasts with *Khc* mutant oocytes that still display nuclear positioning defects at stage 9 and beyond (Sup. Fig. 2 A, B). This difference underlines different requirements for both subunits that could reflect different subcellular distributions of Khc and Klc. Indeed, when we assessed their respective intracellular location using GFP-fusion proteins, we found that both subunits are evenly distributed in the oocyte cytoplasm but Khc is additionally enriched around the nucleus, while Klc is not (Sup Fig. 3 A, B).

Altogether, these results show that both Kinesin-1 subunits are required for migration onset between stages 6 and 7, but then at stage 9 and beyond, only Khc is required to maintain the nucleus position in an asymmetric manner. This further indicates that in absence of Klc, a Khc-dependent process, although less efficient, is sufficient to ensure the nuclear migration and lead to delayed asymmetric positioning.

Khc and Klc subunits differentially affect the MTs

Kinesin-1 has been shown to interfere directly with MT organization (Daire et al., 2009; Drechsler et al., 2020; Nieuwburg et al., 2017), especially through its ability to crosslink MTs (Lu et al., 2016; Metzger et al., 2012). Hence, we wondered if the nuclear migration defects observed in absence of Khc and Klc could be explained by defects in MT organization. We therefore decided to quantify MT density from stage 5 to 7, in *Khc* and *Klc* knockdown contexts. To do so, we assessed MT organization by quantifying the signal of

Jupiter-GFP, a MAP along the length of MTs (Baffet et al., 2012). In the control condition, we noticed that the density of MTs in the oocyte decreases from stage 5 to 7 (Fig. 4 A-B). Furthermore, in *Khc* RNAi-mediated depletion, the MT density is significantly smaller than the control at stages 6B and 7. However, no significant difference could be detected between the control condition and the *Klc* RNAi-mediated depletion at any stage (Fig. 4 A-B). These results indicate that Khc, but not Klc, is required for proper MT stability. The effect of Khc upon MT organization at stages 6B and 7 may explain the failure of the nucleus to properly migrate in absence of Khc. However, this would not explain the requirement of Klc for nuclear migration onset prior to stage 7, as MT density is not affected by the absence of Klc. Therefore, it is unlikely that the role of Kinesin-1 in nuclear migration is limited to its effect on MT stability.

Khc and Klc subunit are required for centrosomes clustering

Since we have previously reported two different and complementary cues involved in the migration of the *Drosophila* oocyte nucleus, i.e the MAP Mud and the centrosomes (Tissot et al., 2017), we wondered whether Kinesin-1 affects either of these elements. When we quantified Mud asymmetry at the NE, we did not find any difference between the control condition and RNAi-mediated depletion of either *Khc* or *Klc* (Sup. Fig. 4). We next investigated a putative effect of Kinesin-1 on centrosomes. After oocyte specification, the centrosomes of the 15 NCs migrate through the ring canals into the oocyte, forming a cluster of at least 16 centrosomes (Pimenta-Marques et al., 2016). Prior to nuclear migration, this cluster frequently coalesces in a compact structure in proximity of the nuclear side facing the oocyte posterior (Tissot et al., 2017; Zhao et al., 2012). We first monitored centrosome distribution by following the centrosomal protein Asterless (Asl) fused to RFP which allowed live imaging of the centrosomes in the developing oocyte (Tissot et al., 2017). A precise analysis in control oocytes, using our newly defined stages, revealed a switch in centrosome dispersion between stages 6A and 6B, when the nucleus centers itself in the oocyte. Whereas most centrosomes are scattered at stages 5 and 6A, most are clustered at stages 6B and 7 (Fig 5 A-A'). Live imaging experiments confirmed that the centrosomes, although in the vicinity of the nucleus, are dynamic and dispersed at early stages (Movies 1, 2). Then, while the nucleus centers itself in the oocyte, the centrosomes aggregate and remain clustered during migration (Movies 3, 4). We next investigated the requirement for Khc and Klc subunits in centrosome clustering and found that both *Khc* and *Klc* RNAi-mediated depletions, impair centrosome clustering at stage 6B compared to control (Fig 5 B-B' and Sup. Fig. 5). These

results indicate that both subunits are required for centrosome clustering. Interestingly, a previous study has also reported this lack of clustering in absence of Klc (Hayashi et al., 2014). This Kinesin-1 effect upon centrosome clustering result is surprising, since plus-end directed MT-associated motors are involved in centrosome separation (Métivier et al., 2019), whereas centrosome clustering is usually ensured by minus-end directed MT-associated motors (Basto et al., 2008; Robinson et al., 1999). As Kinesin-1 often functions cooperatively with Dynein and as both motors are known to have interdependent functions (Duncan and Warrior, 2002; Januschke et al., 2002; Splinter et al., 2010), we then investigated if Kinesin-1 was required for Dynein localization at the centrosome. However, *Khc* RNAi-mediated depletion did not affect Dynein location at the centrosomes (Sup. Fig 6). This indicates that Kinesin-1 involvement in centrosome clustering is not connected to the Dynein transport towards the centrosomes.

Kinesin-1 mediated centrosome clustering is needed for nuclear migration

As centrosome clustering and nuclear centration occur concomitantly and in addition both processes are affected by the loss of function of Kinesin-1, we wondered if the two processes were linked. Previous studies have reported that during the stages 5 to 7, all centrosomes, scattered or aggregated, are surrounded by pericentriolar material (PCM) and are therefore considered active i.e. they can organize microtubules (Januschke et al., 2006; Pimenta-Marques et al., 2016; Tissot et al., 2017; Zhao et al., 2012). Moreover, it has been shown that centrosome elimination is a progressive process that starts at stage 6-7 with a decrease in PCM – centrosome association (Pimenta-Marques et al., 2016). Furthermore, it has been demonstrated that PCM decline is the consequence of Polo-like kinase 1 (Polo) decay from the centrosome. Hence, the ectopic tethering of an active form of Polo to centrioles, with a Pericentrin – AKAP450 Centrosomal Targeting (PACT) domain, is sufficient to prevent PCM loss and maintain active centrosomes (Pimenta-Marques et al., 2016).

We hypothesized that centrosome clustering observed in stage 6B could be a result of decreased centrosomal activity. Accordingly, we found that Polo-PACT expression reduces the level of centrosome clustering, particularly at stage 7 (Fig 6 A, B). Interestingly, these defects are similar to those observed when both *Klc* and *Khc* are inactivated by RNAi at the stages 6B and 7 (Fig 5B'). To further investigate if nucleus position defects observed in Kinesin-1 mutant background are a consequence of defects in centrosome clustering, we assessed oocyte nucleus positioning when expressing Polo-PACT. In this context, we found

that nuclear migration is significantly reduced compared to control at stage 7 (Fig. 6 C, D). This result points to a link between the persistence of centrosome scattering and a defect in nuclear migration. These results further suggest that a function of the Kinesin-1, with its two subunits Khc and Klc, is to promote centrosome clustering by promoting PCM removal but also that clustered centrosomes with reduced activity are needed to allow the migration of the nucleus

Centrosome suppression and Kinesin-1 inactivation restore nuclear migration

Since nuclear migration defects in Kinesin-1 inactivation context may be related to excessive centrosome activity, we next asked whether the inactivation of Kinesin-1 together with centrosome inactivation could restore the migratory capacity of the nucleus. In order to test this possibility, we induced inactivation through RNAi-mediated depletion of *Asl* or *Sas-4*, two essential components for centrosome biogenesis (Blachon et al., 2008; Stevens et al., 2007), and analyzed the effect in combination with the inactivation of *Klc*. In *Klc-RNAi ; asl-RNAi* double knockdown, as well as, *Klc-RNAi ; sas4-RNAi* double knockdown, the positioning of the nucleus prior to its migration is shifted to the center and the posterior in comparison to the *Klc-RNAi* knockdown. In addition, the nuclear migration, although delayed, is significantly rescued at stage 8 (Fig. 7 A-C). Similarly, in *Khc-RNAi ; asl-RNAi* double knockdown, the positioning of the nucleus at stage 6 is shifted to the center and the posterior compared to *Khc-RNAi* knockdown. Nuclear migration is also significantly rescued at stage 7 (Fig. 7 D-E). Altogether, these results indicate that centrosome inactivation restores the ability of the nucleus to center and to migrate when Kinesin-1 is inactivated. This further indicates, that the Kinesin-1, with the involvement of its two subunits Klc and Khc, is essential for the migration of the nucleus by controlling the level of centrosome activity and clustering.

Discussion

The *Drosophila* oocyte is a valuable model system to study the molecular mechanisms required for MT-dependent asymmetric nuclear positioning. In this developmental context, MTs are the main cytoskeletal elements required. In *Drosophila* oocyte, the MTs exert pushing forces required for nuclear migration (Tissot et al., 2017; Zhao et al., 2012). Previously, it was proposed that Kinesin-1 is not required for the nuclear migration in the oocyte but only for its maintenance in an asymmetrical position (Duncan and Warrior, 2002; Januschke et al., 2002; Palacios and St Johnston, 2002). In this study, we clearly show that Kinesin-1 is required for nuclear migration. All previous studies that reported that Khc and

Klc are dispensable for nuclear migration did so on the basis of ovoD/FRT-mediated clonal analysis that did not show any positional defect of the nucleus at stages 6/7. We believe that it is possible that the ovoD dominant effect triggering oocyte degeneration (Chou and Perrimon, 1996), is not fully penetrant at stage 6/7 and thus the potential involvement of Khc and Klc subunits for nuclear migration has been overlooked (Duncan and Warrior, 2002; Januschke et al., 2002; Palacios and St Johnston, 2002). Importantly, with our RNAi-mediated analysis, as well as our GFP/FRT-mediated clonal analysis we have similar results to those previously published at stage 9 and beyond (Sup. Fig. 2).

Our results indicate that prior to its migration the nucleus moves from an anterior position to the center of the oocyte between the stages 5 and 6B. This suggests that, to migrate, the nucleus has to be centered in the oocyte. In addition, we report that Kinesin-1 controls this nuclear displacement, at least in part, by promoting centrosome clustering. This effect was not expected based on existing literature, as Kinesins and plus-end directed motors are generally involved in centrosome separation (Métivier et al., 2019) and instead minus-end directed motors bring the centrosomes closer (Robinson et al., 1999). We ruled out the possibility of an indirect effect on the location of Dynein, therefore a direct role of Kinesin-1 could be considered. In this regard, we also observed that in the *Drosophila* oocyte, increasing centrosome activity by over-expression of Polo kinase led to an impairment of centrosome clustering, hence suggesting that Kinesin-1 could have a role in PCM removal. Indeed, it has been previously shown that the decrease in Polo at the centrosome is responsible for the loss of PCM and the subsequent decrease in centrosome activity and disappearance (Pimenta-Marques et al., 2016). Accordingly, Kinesin-1 could either transport Polo or some PCM components away from active centrosomes. In this regard and interestingly, a recent work has reported that in *Drosophila* neuroblasts and squamous epithelial cells, Khc interacts directly with the PCM organizer Pericentrin-like protein (Plp) but also that Kinesin-1 is required for a differential distribution of Polo between the two centrosomes of a mitotic spindle (Hannaford et al., 2022). An attractive model would be that the PCM removed by Kinesin at the centrosomes is recycled to the previously described non-centrosomal MT sources in the oocyte, i.e the nucleus (Tissot et al., 2017) and the anterior cortex (Nashchekin et al., 2016). It is also interesting to note that the link between Kinesin-1 and centrosome activity has been previously suggested in the early *Drosophila* embryo where Kinesin-1 reduces centrosome motility (Winkler et al., 2015) and in the *C. elegans* zygote where Kinesin-1 prevents premature centrosome maturation (McNally et al., 2012).

In addition, our data revealed different requirements for the two Kinesin-1 subunits, Khc and Klc. While both proteins are required for nuclear centering and centrosome clustering, the nuclear positioning defect observed in the absence of Klc, but not Khc, is rescued at stage 9. This indicates that Khc independently of Klc can fulfill an additional function for nuclear positioning. It is quite striking that the delay for nuclear migration does not gradually appear after stage 7, as we would expect from a simple slowing down of the process, but is sharply occurring at stage 9. We and others have previously shown that the MT network in the oocyte undergoes dramatic rearrangement at stage 9 to organize bundles at the cell cortex (Drechsler et al., 2020; Januschke et al., 2006; Lu et al., 2016; Nashchekin et al., 2016; Parton et al., 2011; Trong et al., 2015). At this stage, the MTs generate a cytoplasmic flow which sustains an advection-based transport corresponding to an active transport induced by fluid flow (Drechsler et al., 2017; Drechsler et al., 2020; Ganguly et al., 2012; Loiseau et al., 2010; Williams et al., 2014). This process requires Khc activity, but not Klc, as in absence of Klc the cytoplasmic streaming is unaffected (Loiseau et al., 2010; Palacios and St Johnston, 2002; Williams et al., 2014). More recently, it has been identified that the origin of the cytoplasmic flow is generated by sliding of MT bundles against each other. Khc triggers the sliding by binding one MT with a C-terminal MT-binding site while walking along a second MT using its motor domain (Lu et al., 2016). This hypothesis does not exclude the alternative possibility that Khc has a different partner to perform its roles at a later stage, including the maintenance of the asymmetric position of the nucleus. Notably it was observed that the nucleus of egg chambers mutant for *ensconsin*, was not maintained in an asymmetric position (Metzger et al., 2012; Sung et al., 2008).

Previous works have highlighted the role of centrosomes as a cue to sustain the nuclear migration in the oocyte (Tissot et al., 2017; Zhao et al., 2012), even if centrosome inhibition does not prevent it (Stevens et al., 2007). Here, our results suggest that very active and scattered centrosomes do not allow the oocyte nuclear migration, meaning that centrosomes would negatively regulate the nucleus migration. The seemingly contradiction of this results may simply underline the necessity of fine-tuning centrosome activity for nucleus migration. One possibility is that scattered centrosomes may exert uncoordinated forces on the nucleus that results to prevent nucleus migration. Therefore, a decrease in their activity would allow the centrosomes to cluster at the posterior of the NE and participate to the MT associated pushing forces required for nuclear migration.

Materials and Methods

Drosophila stocks and culture conditions

Drosophila stocks and crosses were maintained under standard conditions at 25°C.
The following fly strains were used :
w^{1118} BL#3605, *CantonS*, *mat-αtub-Gal4* BL#7062, *Fs(2)Ket-GFP* (Villányi et al., 2008), *ubi-PH-RFP* (Claret et al., 2014), *ubi-asl td-Tomato* (Gopalakrishnan et al., 2011), *ubi-Khc-GFP* (Sung et al., 2008), *Klc-GFP* (Sarov et al., 2016), *UASp-polo^{WT}-PACT* (Pimenta-Marques et al., 2016), *ubi-DLic-GFP* (Baumbach et al., 2015), *mat-αtub-GFP-Dmn* (Januschke et al., 2002), *hsp-flp ; FRT 42B ubi-GFP*, *hsp-flp ; FRT 79D ubi-GFP* (gift from JR Huynh), *FRT 42B Khc^{27}* (Januschke et al., 2002), *FRT 79D Klc^{8ex94}* (Gindhart et al., 1998), *FRT 79D Klc^{Saturn}* (Hayashi et al., 2014), *Jupiter-GFP* (Baffet et al., 2012).

RNAi crosses

The following fly lines, generated from the TRIP project (Perkins et al., 2015) and obtained from the BDSC, have been used in this study :
UASp-Khc RNAi^{Val20} (attP2, Valium 20) BL #35770, *UASp-Khc RNAi^{Val22}* (attP2, Valium 22) BL #35409, *UASp-Klc RNAi$^{Val20\text{-}attP2}$* (attP2, Valium 20) BL #33934, *UASp Klc RNAi^{Val22}* (attP40, Valium 22) BL #36795, *UASp-Klc RNAi$^{Val20\text{-}attP40}$* (attP40, Valium 20) BL #42957, *UASp-Ap RNAi^{Val20}* (attP2, Valium 20) BL #41673, *UASp-Him RNAi^{Val22}* (attP2, Valium 22) BL #42809, *UASp-CG12699 RNAi^{Val20}* (attP40, Valium20) BL#44111, *UASp-asl RNAi^{Val20}* (attP2, Valium 20) BL #35039, *UASp-asl RNAi^{Val22}* (attP40, Valium 22) BL #38220, *UASp-sas4 RNAi^{Val20}* (attP2, Valium 20) BL#35049
RNAi crosses were all performed using females from RNAi lines and maintained under standard conditions at 25°C. As control RNAi, we used lines expressing RNAi directed against genes not expressed in ovary, i.e *CG12699*, *Apterous* (Ap) and *Holes in Muscle* (Him) (Brown et al., 2014; Parisi et al., 2004). In addition the lines were selected and used regarding the Valium plasmid used as well as the insertion point in the genome (attP2 or attP40).

Heat-Shock Treatment for clonal analysis

Heat-shocks were carried out for 1 hr in a water bath at 37°C, 3 days in a row from L1 larvae.

Immunostaining of the fly ovaries

1day old females were collected and put with fresh media for 30-48 hours at 25°C prior to dissection. Ovaries were dissected, fixed in PBS with 4% paraformaldehyde and incubated overnight at 4°C with primary antibodies in PBS with 0,1% Tween. Primary antibodies include : mouse α-Cut (DSHB #2B10, supernatant) at 1:50 ; mouse α-Hindsight (DSHB #1G9, supernatant) at 1:100 ; rabbit α-Mud (Izumi et al., 2006) at 1:1000. Ovaries were then incubated with secondary antibodies at room temperature for 2 hours. Secondary antibodies include : chicken α-mouse Alexa647 (Invitrogen, #A21463) at 1:100 and goat α-rabbit Alexa647 (Jackson Immunoresearch #111-605-144) at 1:200. For egg chambers that did not express a plasma membrane marker nor a nucleus marker, ovaries were respectively incubated with SiR-actin (Cytoskeleton TM) at 1:150 and with Wheat Germ Agglutinin (WGA) (Molecular Probes) at 1:200, at 4°C overnight.
After washes, ovaries were mounted in Citifluor^{TM} (EMS). Images were captured using Zen software on a Zeiss 710 confocal microscope (488, 561, 640 nm lasers and the x40 or x63 objectives).

Live imaging of egg chambers

To assess nucleus position, 1day old females were collected and put with fresh media for 30-48 hours at 25°C prior to dissection. Ovaries were dissected in Schneider medium and directly mount in halocarbon oil (Voltalef 10S) on a coverslip.

For egg chambers that did not express a plasma membrane marker, ovaries were first incubated with live-cell CellMask Deep Red (Invitrogen, #C10046) at 1:1000 diluted in Schneider medium room temperature for 10min.

To image the centrosome clustering, time-lapses of 4 hours (acquisition intervals of 5min) on living egg chambers have been performed, following previously described protocol (Loh et al., 2021).

Images were captured using Metamorph software on a Zeiss Axio Observer Z1 confocal microscope coupled with a spinning disk module CSU-X1 and a sCMOS camera PRIME 95

(488, 561, 640 nm lasers and a x63 oil immersion objective). In order to image the whole nucleus, 21 stacks along the z axis of a 1µm range were taken for each egg chamber.

Image analysis, quantification and statistical analysis

All images were processed using the software Fiji (Schindelin et al., 2012).

Egg chamber staging : To stage the egg chambers, we measured nucleus diameters of the two closest nurse cells of the oocyte, using the z-section corresponding to the larger diameter of the considered nurse cells. These diameters were measured using the « Straight, segmented lines » tool on Fiji. In case the two nurse cells show diameters that can be categorized in different stages, we then took in account the shape and the size of the oocyte and the egg chamber aspect ratio as suggested by (Chen et al., 2019).

Distribution of the centrosomes :

To determine the distribution of the centrosome, we relied our qualitative analysis on two parameters : the number and the general spatial spreading in the oocyte. Centrosomes were considered as dispersed when either 10 centrosomes at least were clearly distinct or were spread over more than 5 µm.

Measure of MT density : The MT signal intensity of the entire oocyte was measured on a Sum slices -projection and the contour of the oocyte was delimited with the tool « Freehand selections ».

Statistics : Bar plots as well as statistical tests were carried out with GraphPad Prism6.

Acknowledgements

We would like to thank the ImagoSeine core facility of the Institut Jacques Monod, member of IBiSA and the France-BioImaging (ANR-10-INBS-04) infrastructure at the Institut Jacques Monod for their help and support. Monica Bettencourt-Dias, David Ish-Horowicz, Rippei Hayashi, Jean-René Huynh, Isabelle Palacios, the Bloomington Drosophila Stock Center, Vienna Drosophila Research Center and the Developmental Studies Hybridoma Bank for fly stocks and reagents. We are grateful to Véronique Brodu, Paul Conduit, Nathaniel Henneman, Jean-Antoine Lepesant, Lionel Pintard for critical comments on the manuscript. We are grateful to the laboratory members for helpful discussions.

Competing interests

The authors declare no competing or financial interests.

Author contributions

The project was conceived by F. Bernard and A. Guichet. F. Bernard. and A. Guichet designed the experiments that were subsequently performed by M. Loh, D. Dauvet, F. Sanchez-Garrido, K. Sadaouli and F. Bernard. The data were analyzed by M. Loh, F. Bernard and A. Guichet. The project funding, administration, and supervision were provided by F. Bernard and A. Guichet. M. Loh prepared the figures. A. Guichet and F. Bernard wrote the manuscript, which was edited and reviewed by M. Loh.

Fundings

This work was funded by the Fondation ARC (PJA-20181208148) pour la Recherche sur le Cancer, the Ligue Contre le Cancer Comité de Paris (RS20/75-17), the Association des Entreprises contre le Cancer (Grant Gefluc 2020 #221366) and by an Emergence grant from IdEx Université de Paris (ANR-18-IDEX-0001). M.L was supported by a fellowship from “Ministère de l’Education Nationale, de la Recherche et de la Technologie” (MENRT) obtained from the BioSPC doctoral school. F.B is supported by Université de Paris. A.G is supported by the CNRS.

References

Baffet, A. D. D., Benoit, B., Januschke, J., Audo, J., Gourhand, V., Roth, S. and Guichet, A. (2012). Drosophila tubulin-binding cofactor B is required for microtubule network formation and for cell polarity. *Mol. Biol. Cell* **23**, 3591–3601.

Basto, R., Brunk, K. and Vinadogrova, T. (2008). Centrosome amplification can initiate tumorigenesis in flies. *Chemtracts* **21**, 111–113.

Baumbach, J., Novak, Z. A., Raff, J. W. and Wainman, A. (2015). Dissecting the Function and Assembly of Acentriolar Microtubule Organizing Centers in Drosophila Cells In Vivo. *PLoS Genet.* **11**, e1005261.

Bernard, F., Lepesant, J.-A. J.-A. J. A. and Guichet, A. (2018). Nucleus positioning within Drosophila egg chamber. *Semin. Cell Dev. Biol.* **82**, 25–33.

Blachon, S., Gopalakrishnan, J., Omori, Y., Polyanovsky, A., Church, A., Nicastro, D., Malicki, J. and Avidor-Reiss, T. (2008). Drosophila asterless and vertebrate Cep152 are orthologs essential for centriole duplication. *Genetics* **180**, 2081–2094.

Bolívar, J., Huynh, J.-R., López-Schier, H., González, C., St Johnston, D. and González-Reyes, A. (2001). Centrosome migration into the Drosophila oocyte is independent of BicD and egl, and of the organisation of the microtubule cytoskeleton. *Development* **1909**, 1889–1909.

Brown, J. B., Boley, N., Eisman, R., May, G. E., Stoiber, M. H., Duff, M. O., Booth, B. W., Wen, J., Park, S., Suzuki, A. M., et al. (2014). Diversity and dynamics of the Drosophila transcriptome. *Nature* **512**, 393–399.

Chen, D. Y., Crest, J., Streichan, S. J. and Bilder, D. (2019). Extracellular matrix stiffness cues junctional remodeling for 3D tissue elongation. *Nat. Commun.* **10**, 1–15.

Chou, T. Bin and Perrimon, N. (1996). The autosomal FLP-DFS technique for generating germline mosaics in Drosophila melanogaster. *Genetics* **144**, 1673–1679.

Claret, S., Jouette, J., Benoit, B., Legent, K. and Guichet, A. (2014). PI(4,5)P2 Produced by the PI4P5K SKTL Controls Apical Size by Tethering PAR-3 in Drosophila Epithelial Cells. *Curr. Biol.* **24**, 1071–1079.

Daire, V., Giustiniani, J., Leroy-Gori, I., Quesnoit, M., Drevensek, S., Dimitrov, A., Perez, F. and Poüs, C. (2009). Kinesin-1 regulates microtubule dynamics via a c-Jun N-terminal kinase-dependent mechanism. *J. Biol. Chem.* **284**, 31992–32001.

Drechsler, M., Giavazzi, F., Cerbino, R. and Palacios, I. M. (2017). Active diffusion and advection in Drosophila oocytes result from the interplay of actin and microtubules. *Nat.*

Commun. **8**,.

Drechsler, M., Lang, L. F., Al-Khatib, L., Dirks, H., Burger, M., Schönlieb, C.-B. and Palacios, I. M. (2020). Optical flow analysis reveals that Kinesin-mediated advection impacts the orientation of microtubules in the Drosophila oocyte. *Mol. Biol. Cell* **31**, 1246–1258.

Duncan, J. E. and Warrior, R. (2002). The cytoplasmic dynein and kinesin motors have interdependent roles in patterning the Drosophila oocyte. *Curr. Biol.* **12**, 1982–1991.

Folker, E. S., Schulman, V. K. and Baylies, M. K. (2013). Translocating myonuclei have distinct leading and lagging edges that require Kinesin and Dynein. *Development*.

Fridolfsson, H. N. and Starr, D. A. (2010). Kinesin-1 and dynein at the nuclear envelope mediate the bidirectional migrations of nuclei. *J. Cell Biol.* **191**, 115–128.

Ganguly, S., Williams, L. S., Palacios, I. M. and Goldstein, R. E. (2012). Cytoplasmic streaming in Drosophila oocytes varies with kinesin activity and correlates with the microtubule cytoskeleton architecture. *Proc. Natl. Acad. Sci. U. S. A.* **109**, 15109–15114.

Gindhart, J. G., Desai, C. J., Beushausen, S., Zinn, K. and Goldstein, L. S. B. (1998). Kinesin light chains are essential for axonal transport in Drosophila. *J. Cell Biol.* **141**, 443–454.

González-Reyes, A., Elliott, H., St Johnston, D., Gonzalez-Reyes, A., Elliott, H. and St Johnston, D. (1995). Polarization of both major body axes in Drosophila by gurken-torpedo signalling. *Nature* **375**, 654–658.

Gopalakrishnan, J., Mennella, V., Blachon, S., Zhai, B., Smith, A. H., Megraw, T. L., Nicastro, D., Gygi, S. P., Agard, D. A. and Avidor-Reiss, T. (2011). Sas-4 provides a scaffold for cytoplasmic complexes and tethers them in a centrosome. *Nat. Commun.* **2**, 359.

Grieder, N. C., de Cuevas, M. and Spradling, A. C. (2000). The fusome organizes the microtubule network during oocyte differentiation in Drosophila. *Development* 4253–4264.

Guichet, A., Peri, F. and Roth, S. (2001). Stable anterior anchoring of the oocyte nucleus is required to establish dorsoventral polarity of the drosophila egg. *Dev. Biol.* **237**, 93–106.

Hannaford, M. R., Liu, R., Billington, N., Swider, Z. T. and Galletta, B. J. (2022). Pericentrin is a Kinesin-1 Activator that Drives Centriole Motility. *bioRxiv*.

Hayashi, R., Wainwright, S. M., Liddell, S. J., Pinchin, S. M., Horswell, S. and Ish-Horowicz, D. (2014). A genetic screen based on in vivo RNA imaging reveals centrosome-independent mechanisms for localizing gurken transcripts in Drosophila. *G3*

Genes, Genomes, Genet. **4**, 749–760.

Huynh, J. R. and St Johnston, D. (2004). The origin of asymmetry: Early polarisation of the Drosophila germline cyst and oocyte. *Curr. Biol.* **14**, 438–449.

Izumi, Y., Ohta, N., Hisata, K., Raabe, T. and Matsuzaki, F. (2006). Drosophila Pins-binding protein Mud regulates spindle-polarity coupling and centrosome organization. *Nat. Cell Biol.* **8**, 586–593.

Januschke, J., Gervais, L., Dass, S., Kaltschmidt, J. A., Lopez-Schier, H., St. Johnston, D., Brand, A. H., Roth, S. and Guichet, A. (2002). Polar transport in the Drosophila oocyte requires Dynein and Kinesin I cooperation. *Curr. Biol.* **12**, 1971–1981.

Januschke, J., Gervais, L., Gillet, L., Keryer, G., Bornens, M. and Guichet, A. (2006). The centrosome-nucleus complex and microtubule organization in the Drosophila oocyte. *Development* **133**, 129–139.

Koch, E. A. and Spitzer, R. H. (1983). Multiple effects of colchicine on oogenesis in Drosophila: Induced sterility and switch of potential oocyte to nurse-cell developmental pathway. *Cell Tissue Res.* **228**, 21–32.

Loh, M., Guichet, A. and Bernard, F. (2021). Nuclear migration in the drosophila oocyte. *J. Vis. Exp.* **2021**, 1–12.

Loiseau, P., Davies, T., Williams, L. S., Mishima, M. and Palacios, I. M. (2010). Drosophila PAT1 is required for Kinesin-1 to transport cargo and to maximize its motility. *Development* **137**, 2763–2772.

Lu, W., Winding, M., Lakonishok, M., Wildonger, J. and Gelfand, V. I. (2016). Microtubule–microtubule sliding by kinesin-1 is essential for normal cytoplasmic streaming in *Drosophila* oocytes. *Proc. Natl. Acad. Sci.* **113**, E4995–E5004.

Lu, W., Lakonishok, M. and Gelfand, V. I. (2021). Gatekeeper function for Short stop at the ring canals of the Drosophila ovary. *Curr. Biol.* **31**, 3207–3219.e5.

Mahowald, A. P. and Strassheim, J. M. (1970). Intercellular migration of centrioles in the germarium of Drosophila melanogaster. An electron microscopic study. *J. Cell Biol.* **45**, 306–320.

McNally, K. L. P., Fabritius, A. S., Ellefson, M. L., Flynn, J. R., Milan, J. A. and McNally, F. J. (2012). Kinesin-1 Prevents Capture of the Oocyte Meiotic Spindle by the Sperm Aster. *Dev. Cell* **22**, 788–798.

Métivier, M., Monroy, B. Y., Gallaud, E., Caous, R., Pascal, A., Richard-Parpaillon, L., Guichet, A., Ori-McKenney, K. M. and Giet, R. (2019). Dual control of Kinesin-1 recruitment to microtubules by Ensconsin in Drosophila neuroblasts and oocytes.

Development **146**,.

Metzger, T., Gache, V., Xu, M., Cadot, B., Folker, E. S., Richardson, B. E., Gomes, E. R. and Baylies, M. K. (2012). MAP and kinesin-dependent nuclear positioning is required for skeletal muscle function. *Nature* **484**, 120–124.

Meyerzon, M., Fridolfsson, H. N., Ly, N., McNally, F. J. and Starr, D. A. (2009). UNC-83 is a nuclear-specific cargo adaptor for kinesin-1-mediated nuclear migration. *Development* **136**,.

Nashchekin, D., Fernandes, A. R., St Johnston, D. and Johnston, D. S. (2016). Patronin/Shot Cortical Foci Assemble the Noncentrosomal Microtubule Array that Specifies the Drosophila Anterior-Posterior Axis. *Dev. Cell* **38**, 61–72.

Nashchekin, D., Busby, L., Jakobs, M., Squires, I. and St. Johnston, D. (2021). Symmetry breaking in the female germline cyst. *Science (80-.).* **374**, 874–879.

Nieuwburg, R., Nashchekin, D., Jakobs, M., Carter, A. P., Khuc Trong, P., Goldstein, R. E. and St Johnston, D. (2017). Localised dynactin protects growing microtubules to deliver oskar mRNA to the posterior cortex of the Drosophila oocyte. *Elife* **6**,.

Palacios, I. M. and St Johnston, D. (2002). Kinesin light chain-independent function of the Kinesin heavy chain in cytoplasmic streaming and posterior localisation in the Drosophila oocyte. *Development* **129**, 5473–5485.

Parisi, M., Nuttall, R., Edwards, P., Minor, J., Naiman, D., Lü, J., Doctolero, M., Vainer, M., Chan, C., Malley, J., et al. (2004). A survey of ovary-, testis-, and soma-biased gene expression in Drosophila melanogaster adults. *Genome Biol.* **5**,.

Parton, R. M., Hamilton, R. S., Ball, G., Yang, L., Cullen, C. F., Lu, W., Ohkura, H. and Davis, I. (2011). A PAR-1-dependent orientation gradient of dynamic microtubules directs posterior cargo transport in the Drosophila oocyte. *J. Cell Biol.* **194**, 121–135.

Perkins, L. A., Holderbaum, L., Tao, R., Hu, Y., Sopko, R., McCall, K., Yang-Zhou, D., Flockhart, I., Binari, R., Shim, H. S., et al. (2015). The transgenic RNAi project at Harvard medical school: Resources and validation. *Genetics* **201**, 843–852.

Pimenta-Marques, A., Bento, I., Lopes, C. A. M., Duarte, P., Jana, S. C. and Bettencourt-Dias, M. (2016). A mechanism for the elimination of the female gamete centrosome in Drosophila melanogaster. *Science* **4866**, 1–16.

Robinson, J. T., Wojcik, E. J., Sanders, M. A., McGrail, M. and Hays, T. S. (1999). Cytoplasmic dynein is required for the nuclear attachment and migration of centrosomes during mitosis in Drosophila. *J. Cell Biol.* **146**, 597–608.

Roth, S. and Lynch, J. A. (2009). Symmetry breaking during Drosophila oogenesis. *Cold*

Spring Harb. Perspect. Biol. **1**, a001891.

Roth, S., Neuman-Silberberg, F. S., Barcelo, G., Schüpbach, T. and Schupbach, T. (1995). cornichon and the EGF receptor signaling process are necessary for both anterior-posterior and dorsal-ventral pattern formation in Drosophila. *Cell* **81**, 967–978.

Roux, K. J., Crisp, M. L., Liu, Q., Kim, D., Kozlov, S., Stewart, C. L. and Burke, B. (2009). Nesprin 4 is an outer nuclear membrane protein that can induce kinesin-mediated cell polarization. *Proc. Natl. Acad. Sci. U. S. A.* **106**, 2194–2199.

Rowe, M., Paculis, L., Tapia, F., Xu, Q., Xie, Q., Liu, M., Jevitt, A. and Jia, D. (2020). Analysis of the Temporal Patterning of Notch Downstream Targets during Drosophila melanogaster Egg Chamber Development. *Sci. Rep.* **10**, 7370–7378.

Sarov, M., Barz, C., Jambor, H., Hein, M. Y., Schmied, C., Suchold, D., Stender, B., Janosch, S., Vinay Vikas, K. J., Krishnan, R. T., et al. (2016). A genome-wide resource for the analysis of protein localisation in Drosophila. *Elife* **5**, 1–38.

Schindelin, J., Arganda-Carreras, I., Frise, E., Kaynig, V., Longair, M., Pietzsch, T., Preibisch, S., Rueden, C., Saalfeld, S., Schmid, B., et al. (2012). Fiji: An open-source platform for biological-image analysis. *Nat. Methods* **9**, 676–682.

Splinter, D., Tanenbaum, M. E., Lindqvist, A., Jaarsma, D., Flotho, A., Yu, K. Lou, Grigoriev, I., Engelsma, D., Haasdijk, E. D., Keijzer, N., et al. (2010). Bicaudal D2, dynein, and kinesin-1 associate with nuclear pore complexes and regulate centrosome and nuclear positioning during mitotic entry. *PLoS Biol.* **8**, e1000350.

Stevens, N. R., Raposo, A. A. S. F., Basto, R., St Johnston, D. and Raff, J. W. W. (2007). From Stem Cell to Embryo without Centrioles. *Curr. Biol.* **17**, 1498–1503.

Sun, J. and Deng, W. M. (2005). Notch-dependent downregulation of the homeodomain gene cut is required for the mitotic cycle/endocycle switch and cell differentiation in Drosophila follicle cells. *Development* **132**, 4299–4308.

Sun, J. and Deng, W.-M. M. (2007). Hindsight Mediates the Role of Notch in Suppressing Hedgehog Signaling and Cell Proliferation. *Dev. Cell* **12**, 431–442.

Sung, H. H., Telley, I. A., Papadaki, P., Ephrussi, A., Surrey, T. and Rørth, P. (2008). Drosophila Ensconsin Promotes Productive Recruitment of Kinesin-1 to Microtubules. *Dev. Cell* **15**, 866–876.

Swan, A., Nguyen, T. and Suter, B. (1999). Drosophila Lissencephaly-1 functions with Bic-D and dynein in oocyte determination and nuclear positioning. *Nat. Cell Biol.* **1**, 444–449.

Theurkauf, W. E., Alberts, B. M., Nung Jan, Y., Jongens, T. A., Jan, Y. N. and Jongens,

T. A. (1993). A central role for microtubules in the differentiation of Drosophila oocytes. *Development* 1169–1180.

Tissot, N., Lepesant, J.-A. A., Bernard, F., Legent, K., Bosveld, F., Martin, C., Faklaris, O., Bellaïche, Y., Coppey, M. and Guichet, A. (2017). Distinct molecular cues ensure a robust microtubule-dependent nuclear positioning in the Drosophila oocyte. *Nat. Commun.* **8**, 15168.

Trong, P. K., Doerflinger, H., Dunkel, J., St Johnston, D. and Goldstein, R. E. (2015). Cortical microtubule nucleation can organise the cytoskeleton of drosophila oocytes to define the anteroposterior axis. *Elife* **4**, 1–31.

Verhey, K. J., Kaul, N. and Soppina, V. (2011). Kinesin assembly and movement in cells. *Annu. Rev. Biophys.* **40**, 267–288.

Villányi, Z., Debec, A., Timinszky, G., Tirián, L. and Szabad, J. (2008). Long persistence of importin-β explains extended survival of cells and zygotes that lack the encoding gene. *Mech. Dev.* **125**, 196–206.

Williams, L. S., Ganguly, S., Loiseau, P., Ng, B. F. and Palacios, I. M. (2014). The auto-inhibitory domain and ATP-independent microtubulebinding region of Kinesin heavy chain are major functional domains for transport in the Drosophila germline. *Development* **141**, 176–186.

Wilson, M. H. and Holzbaur, E. L. F. (2012). Opposing microtubule motors drive robust nuclear dynamics in developing muscle cells. *J. Cell Sci.* **125**, 4158–4169.

Wilson, M. H. and Holzbaur, E. L. F. (2015). Nesprins anchor kinesin-1 motors to the nucleus to drive nuclear distribution in muscle cells. *Development* **142**, 218–228.

Winkler, F., Gummalla, M., Künneke, L., Lv, Z., Zippelius, A., Aspelmeier, T. and Grosshans, J. (2015). Fluctuation Analysis of Centrosomes Reveals a Cortical Function of Kinesin-1. *Biophysj* **109**, 856–868.

Zhao, T., Graham, O. S., Raposo, A. and St Johnston, D. (2012). Growing Microtubules Push the Oocyte Nucleus to Polarize the Drosophila Dorsal-Ventral Axis. *Science* **336**, 999–1003.

Figure legends

Figure 1. Oocyte staging and characterization of the nucleus positioning prior to migration.

(A-B) Stage 6 egg chamber oriented with anterior (A) at the top and posterior (P) at the bottom, expressing *Fs(2)Ket-GFP* to label nuclei (green) and *ubi-PH$^{PLC\partial 1}$-RFP* to label plasma membrane (red), stained with Cut antibody (blue) (A) and schematic diagram highlighting the nuclei of the different cell types : the follicular cells (FC) in blue, the nurse cells (NC) in light green and the oocyte (Oo) in dark green (B). Scale bar: 10µm. **(C)** Distribution of NC diameters shows a progressive increase in size and allows the categorization of 4 different stages (n indicates the number of analyzed egg chambers but dots corresponds to each measured nuclei). Means ± s.e.m for each stage are indicated in D. **(E)** Stage 5 to 7 egg chambers, expressing *Fs(2)Ket-GFP* to label nuclei (green) stained with Cellmask to reveal plasma membranes (red). Representative examples of the different nuclear positions at stages 5, 6A, 6B and 7. The oocytes are oriented with anterior (A) at the top and posterior (P) at the bottom. Scale bar : 10µm. **(F)** Distribution of nucleus positions at the different stages. Positions have been categorized and color-coded as anterior in pale blue, center in pale green, posterior in dark green and migrated in purple. n indicates the number of analyzed egg chambers. See Sup Table 1 for detailed values of the quantifications.

Figure 2. Khc is required for nucleus positioning and migration.

Representative image of stage 7 egg-chambers and distribution of nucleus positions at the different stages. Positions have been categorized and color-coded as anterior in pale blue, center in pale green, posterior in dark green and migrated in purple. n indicates the number of analyzed egg chambers. **(A-C)** RNAi mediated analysis of nucleus positions where control RNAi (*UASp-CG12699-RNAi – See Methods*) (A) *Khc-RNAi^{Val20}* (B) and *Khc-RNAi^{Val22}* (C) have been expressed using the *mat-αtub-Gal4* driver combined with *Fs(2)Ket-GFP* to label nuclei (green) and *ubi-PH$^{PLC\partial 1}$-RFP* to label plasma membrane (red). **(D-E)** GFP/FRT clonal analysis of nucleus positions in control egg chambers (*Khc^{27}* heterozygous) (D) and *Khc^{27}* mutant egg chambers revealed by the absence of GFP in germline nuclei (E). Nuclei and plasma membranes are revealed by WGA and SiR-actin staining, respectively. See Sup Table 1 for detailed values of the quantifications.

Figure 3. Klc is required for the nucleus positioning and efficient migration.

Representative image of stage 7 egg-chambers and distribution of nucleus positions at the different stages. Positions have been categorized and color-coded as anterior in pale blue, center in pale green, posterior in dark green and migrated in purple. n indicates the number of analyzed egg chambers. **(A-C)** RNAi mediated analysis of nucleus positions where control RNAi (*UASp-CG12699-RNAi – See Methods,* identical panel to Figure 2A) (A) *Klc-RNAi*^{Val20} (B) and *Klc-RNAi*^{Val22} (C) have been expressed using the *mat-αtub-Gal4* driver combined with *Fs(2)Ket-GFP* to label nuclei (green) and *ubi-PH*$^{PLC\delta 1}$*-RFP* to label plasma membrane (red). **(D-F)** GFP/FRT clonal analysis of nucleus positions in control egg chambers (*Klc* heterozygous) (D), *Klc*^{8ex94} (E) and *Klc*^{Saturn} (F) mutant egg chambers revealed by the absence of GFP in germline nuclei. Nuclei and plasma membranes are revealed by WGA and SiR-actin staining, respectively. See Sup Table 1 for detailed values of the quantifications.

Figure 4. Khc and Klc impact differently the MTs.

(A) Representative examples of oocytes of stage 5 to 7 egg chambers expressing *Jupiter-GFP,* to label the MTs, and control RNAi (*UASp-CG12699 RNAi – See Methods*) (top row), *Khc RNAi*^{Val20} (middle row) and *Klc RNAi*^{val22} (bottom row) under the control of the *mat-αtub-Gal4* driver. The oocytes are oriented with anterior (A) at the top and posterior (P) at the bottom. Scale bar : 10µm. **(B)** Quantification of MT density in oocytes of the indicated stages and genotypes. Mann-Whitney test, *$p < 0.05$. n indicates the number of analyzed egg chambers. See Sup Table 1 for detailed values of the quantifications.

Figure 5. Khc and Klc are required for centrosome clustering at stage 6B.

(A-B) (*Top row*) Representative Z-projection images of stage 5 to 7 egg chambers (A) and stage 6B (B), expressing *Fs(2)Ket-GFP* to label nuclei (green), *ubi-asl-tdTomato* to label centrosomes (red) and control RNAi (*UASp-CG12699 RNAi – See Methods*) (A) or the indicated RNAi (B) under the control of the *mat-αtub-Gal4* driver. The oocytes are oriented with anterior (A) at the top and posterior (P) at the bottom. Scale bar : 10µm. (*Bottom row*) Schematic diagrams of the image above, with oocyte centrosomes in red and follicular cell centrosomes in blue. **(A'-B')** Quantification of oocytes categorized as scattered (black) and aggregate (gray) depending on centrosome distributions, at the different stages and for the different genotypes. n indicates the number of analyzed egg chambers. See Sup Table 1 for detailed values of the quantifications.

Figure 6. Preventing centrosome decay affects their clustering and nucleus positioning.
(A-B) Quantification of oocytes categorized as scattered (black) and aggregate (gray) depending on centrosome distributions, at the different stages of control (*identical panel to Figure 5A*) and *Polo^{WT}-PACT* over-expressing egg chambers under the control of the *mat-αtub-Gal4* driver. **(C-D)** Distribution of nucleus positions at the different stages has been quantified in the egg chambers quantified in A and B. Positions have been categorized and color-coded as anterior in pale blue, center in pale green, posterior in dark green and migrated in purple. n indicates the number of analyzed egg chambers. Chi2 test, *p < 0.05, **p = 0,005 compared to the control condition (per stage). See Sup Table 1 for detailed values of the quantifications.

Figure 7. Centrosome inhibition and Kinesin-1 inactivation restore nuclear migration
Representative image of stage 7 and 8 egg-chambers and distribution of nucleus positions at the different stages. Positions have been categorized and color-coded as anterior in pale blue, center in pale green, posterior in dark green and migrated in purple. n indicates the number of analyzed egg chambers. **(A-E)** Expression of *Klc-RNAi^{Val20}* (A-C) in combination with control RNAi (*UASp-Ap-RNAi – See Methods*) (A) *UASp-asl-RNAi^{Val20}* (B) and *UASp-sas4-RNAi^{Val20}* (C) or *Khc-RNAi^{Val20}* in combination with control RNAi (*UASp-Ap-RNAi – See Methods*) (D) *UASp-asl-RNAi^{Val20}* (E) using the *mat-αtub-Gal4* driver combined with *Fs(2)Ket-GFP* to label nuclei (green) and *ubi-PH$^{PLC\delta1}$-RFP* to label plasma membrane (red). See Sup Table 1 for detailed values of the quantifications.

Movie 1. Time-lapse movie of developing egg chamber from stage 5 to 6A expressing *Fs(2)Ket-GFP* to label nuclei (green), *ubi-PH$^{PLC\delta1}$-RFP* to label plasma membrane (red) and *ubi-asl-tdTomato* to label centrosomes (red). The nucleus is anteriorly positioned in the oocyte and the centrosomes are scattered between the nucleus and the posterior membrane of the oocyte. Scale bar : 10µm. Time is indicated (h :min)
Movie 2. Crop of Movie 1 focusing on the oocyte region of the egg chamber. Scale bar : 10µm. Time is indicated (h :min).

Movie 3. Time-lapse movie of developing egg chamber from stage 6B to 7 expressing *Fs(2)Ket-GFP* to label nuclei (green), *ubi-PH$^{PLC\delta1}$-RFP* to label plasma membrane (red) and

ubi-asl-tdTomato to label centrosomes (red). The centrosomes aggregate at the posterior of the centered nucleus, and follow the nucleus during its migration from the center of the oocyte to the cortex antero-lateral of the oocyte. Scale bar : 10µm. Time is indicated (h :min).

Movie 4. Crop of Movie 3 focusing on the oocyte region of the egg chamber. Scale bar : 10µm. Time is indicated (h :min).

Figure 1

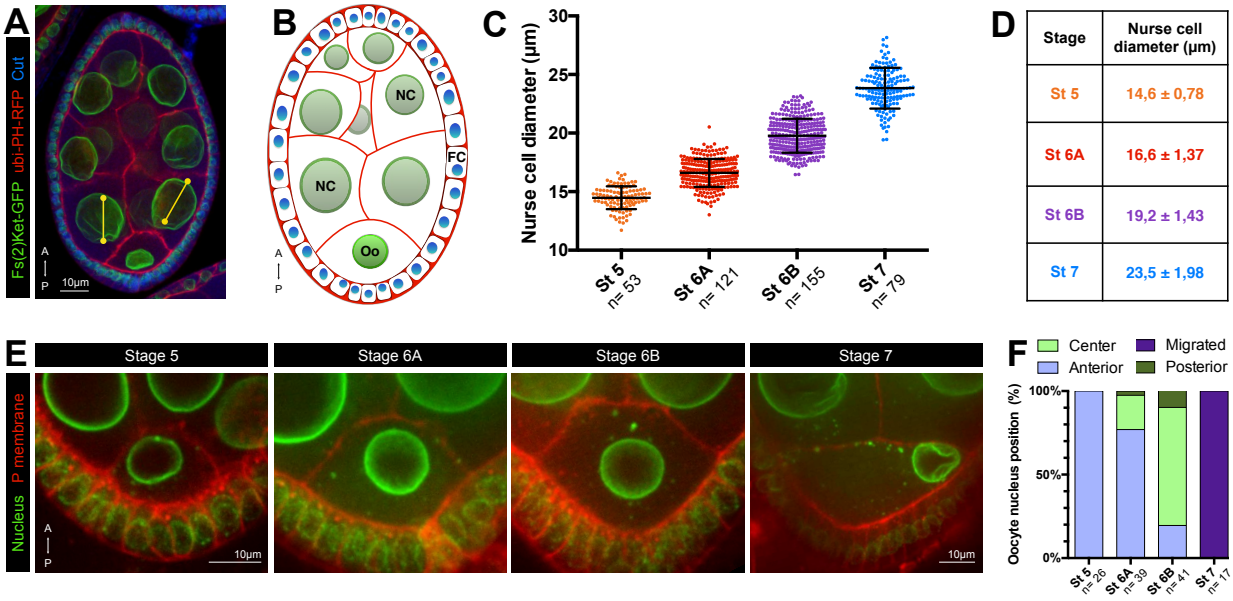

Stage	Nurse cell diameter (µm)
St 5	14,6 ± 0,78
St 6A	16,6 ± 1,37
St 6B	19,2 ± 1,43
St 7	23,5 ± 1,98

Figure 2

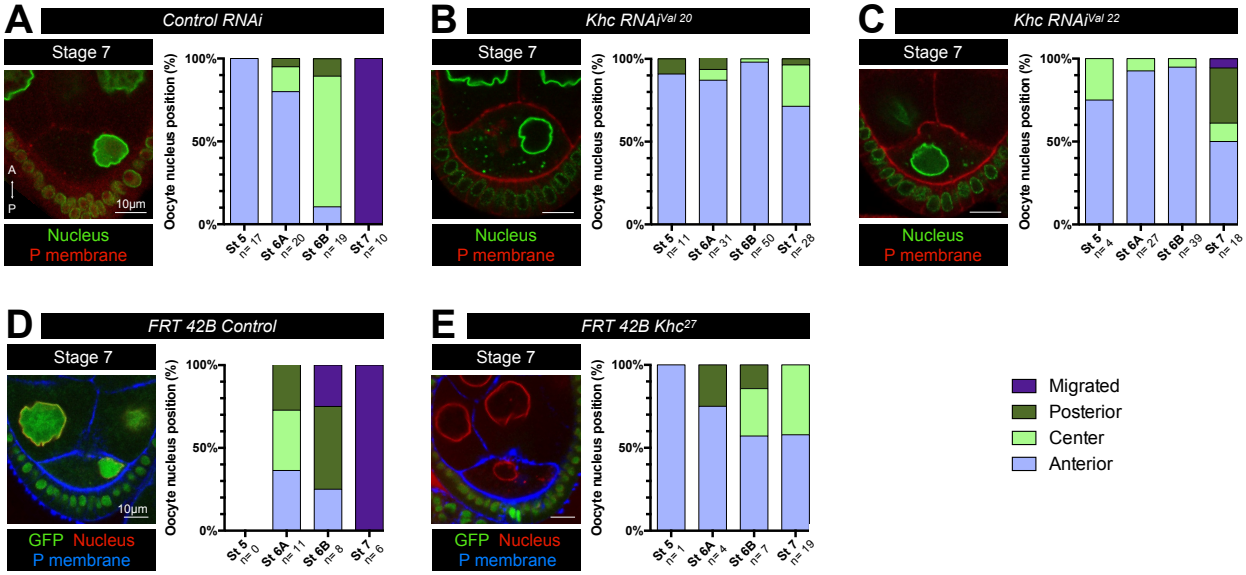

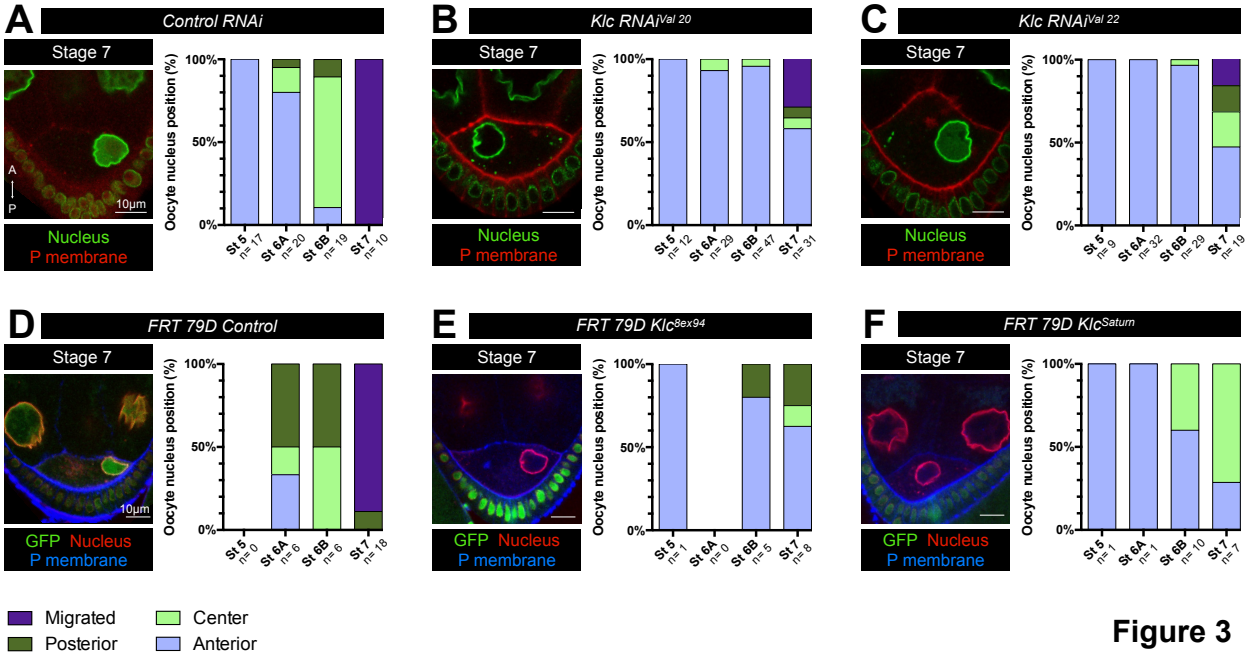

Figure 3

Figure 4

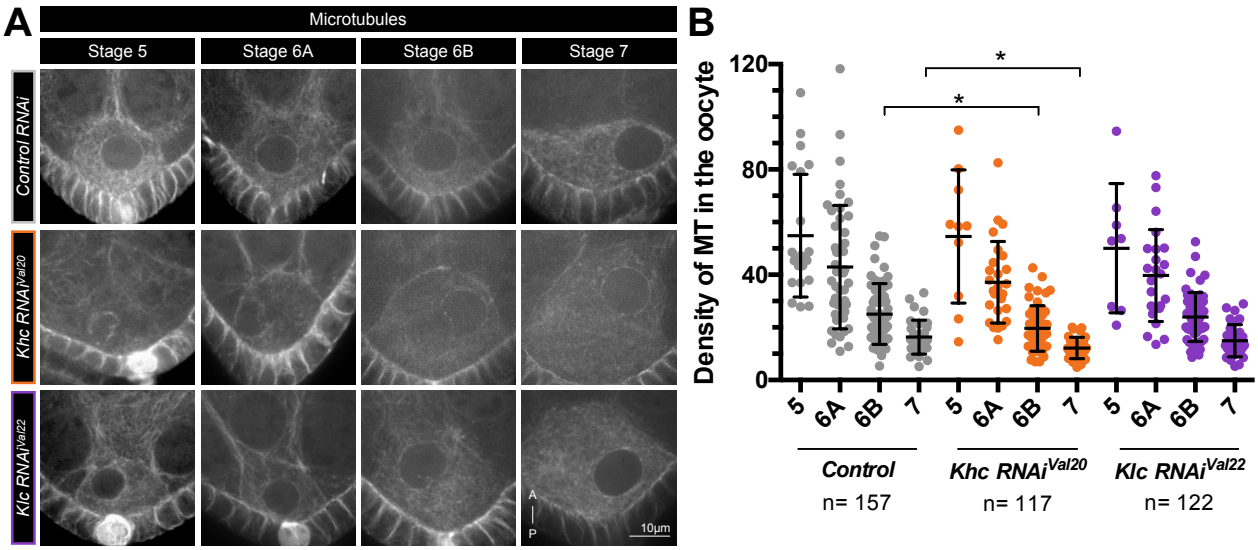
A
Microtubules
Stage 5
Stage 6A
Stage 6B
Stage 7
Control RNAi
Khc RNAiVal20
Klc RNAiVal22
A
P
10µm
B
Density of MT in the oocyte
120
80
40
0
*
*
5
6A
6B
7
Control
n= 157
Khc RNAiVal20
n= 117
Klc RNAiVal22
n= 122

Figure 5

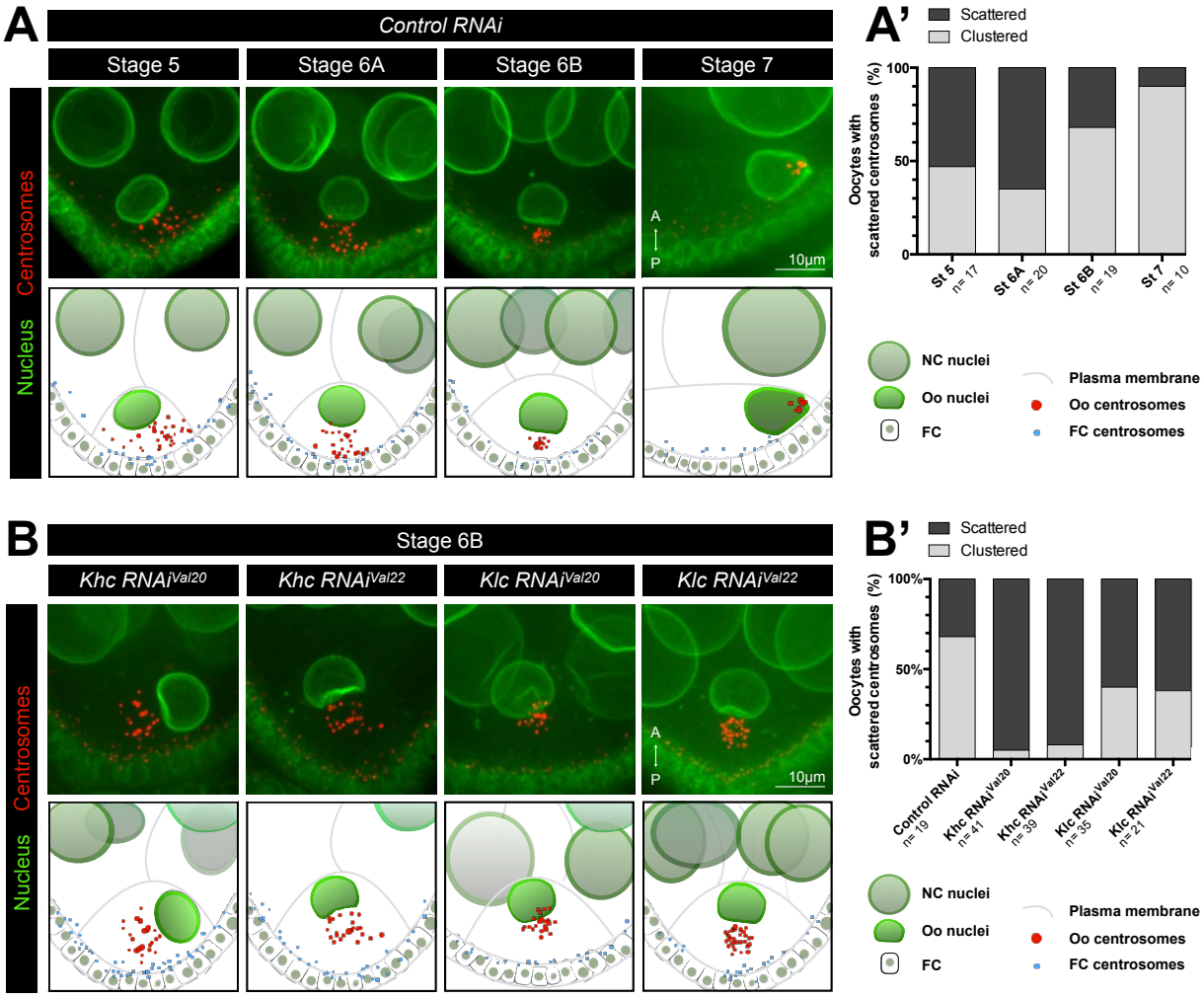
A
Control RNAi
Stage 5
Stage 6A
Stage 6B
Stage 7
Centrosomes
Nucleus
A
P
10µm
A'
Scattered
Clustered
Oocytes with scattered centrosomes (%)
100
50
0
St 5 n= 17
St 6A n= 20
St 6B n= 19
St 7 n= 10
NC nuclei
Oo nuclei
FC
Plasma membrane
Oo centrosomes
FC centrosomes
B
Stage 6B
Khc RNAi Val20
Khc RNAi Val22
Klc RNAi Val20
Klc RNAi Val22
Centrosomes
Nucleus
A
P
10µm
B'
Scattered
Clustered
Oocytes with scattered centrosomes (%)
100%
50%
0%
Control RNAi n= 19
Khc RNAi Val20 n= 41
Khc RNAi Val22 n= 39
Klc RNAi Val20 n= 35
Klc RNAi Val22 n= 21
NC nuclei
Oo nuclei
FC
Plasma membrane
Oo centrosomes
FC centrosomes

Figure 6

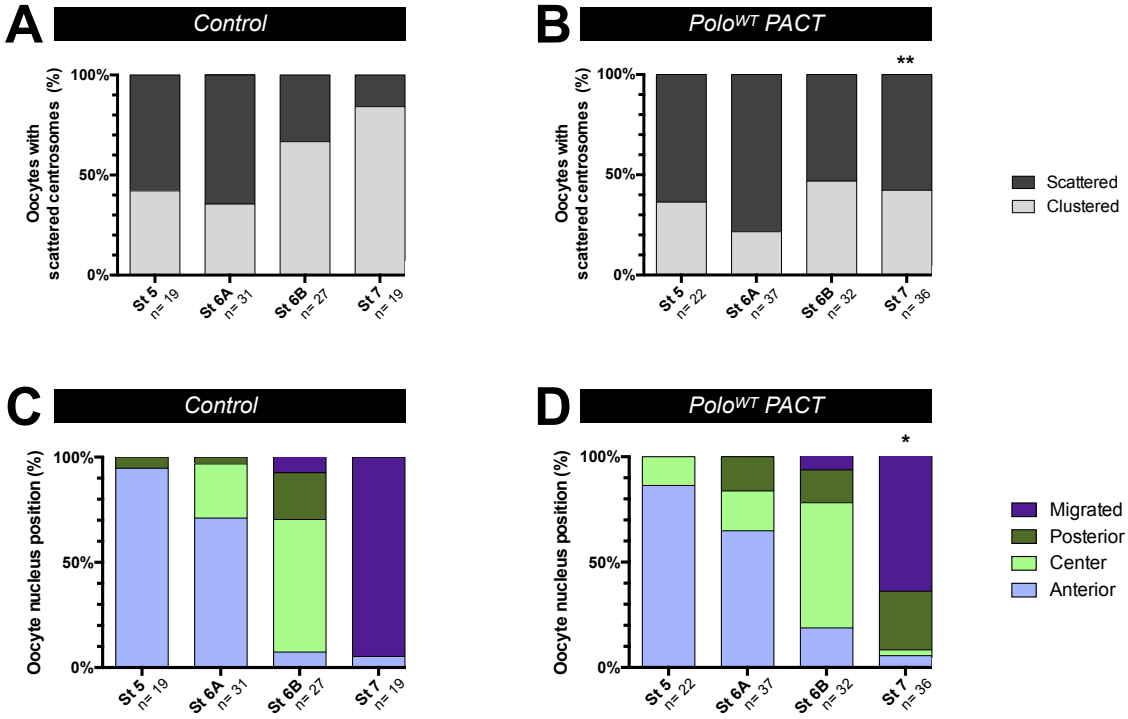

Figure 7

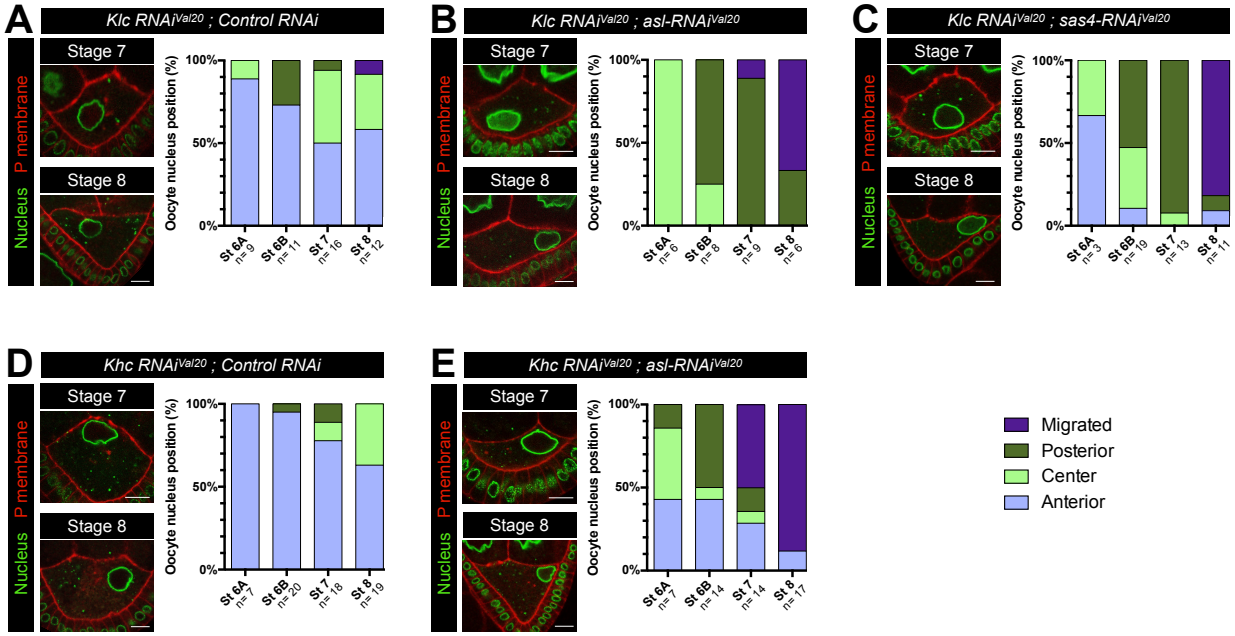

BIBLIOGRAPHIE

Abad, P.C., Lewis, J., Mian, I.S., Knowles, D.W., Sturgis, J., Badve, S., Xie, J., Lelièvre, S.A., 2007. NuMA influences higher order chromatin organization in human mammary epithelium. Mol Biol Cell 18, 348-361.

Adam, S.A., Lobl, T.J., Mitchell, M.A., Gerace, L., 1989. Identification of specific binding proteins for a nuclear location sequence. Nature 337, 276-279.

Agrawal, R., Gillies, J.P., Zang, J.L., Zhang, J., Garrott, S.R., Shibuya, H., Nandakumar, J., DeSantis, M.E., 2022. The KASH5 protein involved in meiotic chromosomal movements is a novel dynein activating adaptor. Elife 11.

Akhmanova, A., Kapitein, L.C., 2022. Mechanisms of microtubule organization in differentiated animal cells. Nat Rev Mol Cell Biol 23, 541-558.

Allan, V., 2014. Cell biology. One, two, three, cytoplasmic dynein is go! Science 345, 271-272.

Allan, V.J., 2011. Cytoplasmic dynein. Biochem Soc Trans 39, 1169-1178.

Almonacid, M., Al Jord, A., El-Hayek, S., Othmani, A., Coulpier, F., Lemoine, S., Miyamoto, K., Grosse, R., Klein, C., Piolot, T., Mailly, P., Voituriez, R., Genovesio, A., Verlhac, M.H., 2019a. Active Fluctuations of the Nuclear Envelope Shape the Transcriptional Dynamics in Oocytes. Dev Cell 51, 145-157 e110.

Almonacid, M., Terret, M.E., Verlhac, M.H., 2018. Control of nucleus positioning in mouse oocytes. Semin Cell Dev Biol 82, 34-40.

Almonacid, M., Terret, M.E., Verlhac, M.H., 2019b. Nuclear positioning as an integrator of cell fate. Curr Opin Cell Biol 56, 122-129.

Avidor-Reiss, T., Fishman, E.L., 2019. It takes two (centrioles) to tango. Reproduction 157, R33-r51.

Azimzadeh, J., Bornens, M., 2007. Structure and duplication of the centrosome. J Cell Sci 120, 2139-2142.

Baffet, A.D., Benoit, B., Januschke, J., Audo, J., Gourhand, V., Roth, S., Guichet, A., 2012. Drosophila tubulin-binding cofactor B is required for microtubule network formation and for cell polarity. Mol Biol Cell 23, 3591-3601.

Baffet, A.D., Hu, D.J., Vallee, R.B., 2015. Cdk1 Activates Pre-mitotic Nuclear Envelope Dynein Recruitment and Apical Nuclear Migration in Neural Stem Cells. Dev Cell 33, 703-716.

Barton, L.J., Pinto, B.S., Wallrath, L.L., Geyer, P.K., 2013. The Drosophila nuclear lamina protein otefin is required for germline stem cell survival. Dev Cell 25, 645-654.

Barton, L.J., Wilmington, S.R., Martin, M.J., Skopec, H.M., Lovander, K.E., Pinto, B.S., Geyer, P.K., 2014. Unique and shared functions of nuclear lamina LEM domain proteins in Drosophila. Genetics 197, 653-665.

Basto, R., Brunk, K., Vinadogrova, T., Peel, N., Franz, A., Khodjakov, A., Raff, J.W., 2008. Centrosome amplification can initiate tumorigenesis in flies. Cell 133, 1032-1042.

Basto, R., Lau, J., Vinogradova, T., Gardiol, A., Woods, C.G., Khodjakov, A., Raff, J.W., 2006. Flies without centrioles. Cell 125, 1375-1386.

Bastock, R., St Johnston, D., 2008. Drosophila oogenesis. Curr Biol 18, R1082-1087.

Batzenschlager, M., Herzog, E., Houlné, G., Schmit, A.C., Chabouté, M.E., 2014. GIP/MZT1 proteins orchestrate nuclear shaping. Front Plant Sci 5, 29.
Batzenschlager, M., Masoud, K., Janski, N., Houlné, G., Herzog, E., Evrard, J.L., Baumberger, N., Erhardt, M., Nominé, Y., Kieffer, B., Schmit, A.C., Chabouté, M.E., 2013. The GIP gamma-tubulin complex-associated proteins are involved in nuclear architecture in Arabidopsis thaliana. Front Plant Sci 4, 480.
Bergstralh, D.T., Dawney, N.S., St Johnston, D., 2017. Spindle orientation: a question of complex positioning. Development 144, 1137-1145.
Berleth, T., Burri, M., Thoma, G., Bopp, D., Richstein, S., Frigerio, G., Noll, M., Nüsslein-Volhard, C., 1988. The role of localization of bicoid RNA in organizing the anterior pattern of the Drosophila embryo. Embo j 7, 1749-1756.
Bernard, F., Jouette, J., Durieu, C., Le Borgne, R., Guichet, A., Claret, S., 2021. GFP-Tagged Protein Detection by Electron Microscopy Using a GBP-APEX Tool in Drosophila. Front Cell Dev Biol 9, 719582.
Bernard, F., Lepesant, J.A., Guichet, A., 2018. Nucleus positioning within Drosophila egg chamber. Semin Cell Dev Biol 82, 25-33.
Bettencourt-Dias, M., Hildebrandt, F., Pellman, D., Woods, G., Godinho, S.A., 2011. Centrosomes and cilia in human disease. Trends Genet 27, 307-315.
Bolívar, J., Huynh, J.R., López-Schier, H., González, C., St Johnston, D., González-Reyes, A., 2001. Centrosome migration into the Drosophila oocyte is independent of BicD and egl, and of the organisation of the microtubule cytoskeleton. Development 128, 1889-1897.
Bone, C.R., Tapley, E.C., Gorjánácz, M., Starr, D.A., 2014. The Caenorhabditis elegans SUN protein UNC-84 interacts with lamin to transfer forces from the cytoplasm to the nucleoskeleton during nuclear migration. Mol Biol Cell 25, 2853-2865.
Bornens, M., 2008. Organelle positioning and cell polarity. Nat Rev Mol Cell Biol 9, 874-886.
Bornens, M., 2021. Centrosome organization and functions. Curr Opin Struct Biol 66, 199-206.
Bosveld, F., Markova, O., Guirao, B., Martin, C., Wang, Z., Pierre, A., Balakireva, M., Gaugue, I., Ainslie, A., Christophorou, N., Lubensky, D.K., Minc, N., Bellaïche, Y., 2016. Epithelial tricellular junctions act as interphase cell shape sensors to orient mitosis. Nature 530, 495-498.
Bowman, S.K., Neumüller, R.A., Novatchkova, M., Du, Q., Knoblich, J.A., 2006. The Drosophila NuMA Homolog Mud regulates spindle orientation in asymmetric cell division. Dev Cell 10, 731-742.
Bramann, E.L., Willenberg, H.S., Hildebrandt, B., Müller-Mattheis, V., Schott, M., Scherbaum, W.A., Haase, M., 2013. Griseofulvin inhibits the growth of adrenocortical cancer cells in vitro. Horm Metab Res 45, 297-300.
Brendza, R.P., Serbus, L.R., Saxton, W.M., Duffy, J.B., 2002. Posterior localization of dynein and dorsal-ventral axis formation depend on kinesin in Drosophila oocytes. Curr Biol 12, 1541-1545.
Brodu, V., Baffet, A.D., Le Droguen, P.M., Casanova, J., Guichet, A., 2010. A developmentally regulated two-step process generates a noncentrosomal microtubule network in Drosophila tracheal cells. Dev Cell 18, 790-801.
Brohawn, S.G., Partridge, J.R., Whittle, J.R., Schwartz, T.U., 2009. The nuclear pore complex has entered the atomic age. Structure 17, 1156-1168.

Brown, E.H., King, R.C., 1964. STUDIES ON THE EVENTS RESULTING IN THE FORMATION OF AN EGG CHAMBER IN DROSOPHILA MELANOGASTER. Growth 28, 41-81.
Bugnard, E., Zaal, K.J., Ralston, E., 2005. Reorganization of microtubule nucleation during muscle differentiation. Cell Motil Cytoskeleton 60, 1-13.
Cadot, B., Gache, V., Gomes, E.R., 2015. Moving and positioning the nucleus in skeletal muscle - one step at a time. Nucleus 6, 373-381.
Cadot, B., Gache, V., Vasyutina, E., Falcone, S., Birchmeier, C., Gomes, E.R., 2012. Nuclear movement during myotube formation is microtubule and dynein dependent and is regulated by Cdc42, Par6 and Par3. EMBO Rep 13, 741-749.
Callaini, G., Whitfield, W.G., Riparbelli, M.G., 1997. Centriole and centrosome dynamics during the embryonic cell cycles that follow the formation of the cellular blastoderm in Drosophila. Exp Cell Res 234, 183-190.
Canty, J.T., Tan, R., Kusakci, E., Fernandes, J., Yildiz, A., 2021. Structure and Mechanics of Dynein Motors. Annu Rev Biophys 50, 549-574.
Cau, P., Navarro, C., Harhouri, K., Roll, P., Sigaudy, S., Kaspi, E., Perrin, S., De Sandre-Giovannoli, A., Lévy, N., 2014. Nuclear matrix, nuclear envelope and premature aging syndromes in a translational research perspective. Semin Cell Dev Biol 29, 125-147.
Cha, B.J., Serbus, L.R., Koppetsch, B.S., Theurkauf, W.E., 2002. Kinesin I-dependent cortical exclusion restricts pole plasm to the oocyte posterior. Nat Cell Biol 4, 592-598.
Charrier, E.E., Janmey, P.A., 2016. Mechanical Properties of Intermediate Filament Proteins. Methods Enzymol 568, 35-57.
Chen, D.Y., Crest, J., Streichan, S.J., Bilder, D., 2019. Extracellular matrix stiffness cues junctional remodeling for 3D tissue elongation. Nat Commun 10, 3339.
Chen, J.W., Barker, A.R., Wakefield, J.G., 2015. The Ran Pathway in Drosophila melanogaster Mitosis. Front Cell Dev Biol 3, 74.
Cho, A., Kato, M., Whitwam, T., Kim, J.H., Montell, D.J., 2016. An Atypical Tropomyosin in Drosophila with Intermediate Filament-like Properties. Cell Rep 16, 928-938.
Christophorou, N., Rubin, T., Bonnet, I., Piolot, T., Arnaud, M., Huynh, J.R., 2015. Microtubule-driven nuclear rotations promote meiotic chromosome dynamics. Nat Cell Biol 17, 1388-1400.
Clark, T.G., Rosenbaum, J.L., 1979. An actin filament matrix in hand-isolated nuclei of X. laevis oocytes. Cell 18, 1101-1108.
Compton, D.A., Cleveland, D.W., 1993. NuMA is required for the proper completion of mitosis. J Cell Biol 120, 947-957.
Compton, D.A., Luo, C., 1995. Mutation of the predicted p34cdc2 phosphorylation sites in NuMA impair the assembly of the mitotic spindle and block mitosis. J Cell Sci 108 (Pt 2), 621-633.
Compton, D.A., Szilak, I., Cleveland, D.W., 1992. Primary structure of NuMA, an intranuclear protein that defines a novel pathway for segregation of proteins at mitosis. J Cell Biol 116, 1395-1408.
Conduit, P.T., Brunk, K., Dobbelaere, J., Dix, C.I., Lucas, E.P., Raff, J.W., 2010. Centrioles regulate centrosome size by controlling the rate of Cnn incorporation into the PCM. Curr Biol 20, 2178-2186.

Conduit, P.T., Feng, Z., Richens, J.H., Baumbach, J., Wainman, A., Bakshi, S.D., Dobbelaere, J., Johnson, S., Lea, S.M., Raff, J.W., 2014a. The centrosome-specific phosphorylation of Cnn by Polo/Plk1 drives Cnn scaffold assembly and centrosome maturation. Dev Cell 28, 659-669.
Conduit, P.T., Richens, J.H., Wainman, A., Holder, J., Vicente, C.C., Pratt, M.B., Dix, C.I., Novak, Z.A., Dobbie, I.M., Schermelleh, L., Raff, J.W., 2014b. A molecular mechanism of mitotic centrosome assembly in Drosophila. Elife 3, e03399.
Crisp, M., Liu, Q., Roux, K., Rattner, J.B., Shanahan, C., Burke, B., Stahl, P.D., Hodzic, D., 2006. Coupling of the nucleus and cytoplasm: role of the LINC complex. J Cell Biol 172, 41-53.
D'Angelo, M.A., Anderson, D.J., Richard, E., Hetzer, M.W., 2006. Nuclear pores form de novo from both sides of the nuclear envelope. Science 312, 440-443.
Dagenbach, E.M., Endow, S.A., 2004. A new kinesin tree. J Cell Sci 117, 3-7.
Dammermann, A., Desai, A., Oegema, K., 2003. The minus end in sight. Curr Biol 13, R614-624.
de Anda, F.C., Pollarolo, G., Da Silva, J.S., Camoletto, P.G., Feiguin, F., Dotti, C.G., 2005. Centrosome localization determines neuronal polarity. Nature 436, 704-708.
de Belle, J.S., Heisenberg, M., 1996. Expression of Drosophila mushroom body mutations in alternative genetic backgrounds: a case study of the mushroom body miniature gene (mbm). Proc Natl Acad Sci U S A 93, 9875-9880.
Dechat, T., Pfleghaar, K., Sengupta, K., Shimi, T., Shumaker, D.K., Solimando, L., Goldman, R.D., 2008. Nuclear lamins: major factors in the structural organization and function of the nucleus and chromatin. Genes Dev 22, 832-853.
Dogterom, M., Koenderink, G.H., 2019. Actin-microtubule crosstalk in cell biology. Nat Rev Mol Cell Biol 20, 38-54.
Doxsey, S., 2001. Re-evaluating centrosome function. Nat Rev Mol Cell Biol 2, 688-698.
Du, Q., Stukenberg, P.T., Macara, I.G., 2001. A mammalian Partner of inscuteable binds NuMA and regulates mitotic spindle organization. Nat Cell Biol 3, 1069-1075.
Du, Q., Taylor, L., Compton, D.A., Macara, I.G., 2002. LGN blocks the ability of NuMA to bind and stabilize microtubules. A mechanism for mitotic spindle assembly regulation. Curr Biol 12, 1928-1933.
Duan, T., Cupp, R., Geyer, P.K., 2021. Drosophila female germline stem cells undergo mitosis without nuclear breakdown. Curr Biol 31, 1450-1462.e1453.
Duncan, J.E., Warrior, R., 2002. The cytoplasmic dynein and kinesin motors have interdependent roles in patterning the Drosophila oocyte. Curr Biol 12, 1982-1991.
Dupin, I., Camand, E., Etienne-Manneville, S., 2009. Classical cadherins control nucleus and centrosome position and cell polarity. J Cell Biol 185, 779-786.
Dupin, I., Sakamoto, Y., Etienne-Manneville, S., 2011. Cytoplasmic intermediate filaments mediate actin-driven positioning of the nucleus. J Cell Sci 124, 865-872.
Ephrussi, A., Dickinson, L.K., Lehmann, R., 1991. Oskar organizes the germ plasm and directs localization of the posterior determinant nanos. Cell 66, 37-50.
Esue, O., Carson, A.A., Tseng, Y., Wirtz, D., 2006. A direct interaction between actin and vimentin filaments mediated by the tail domain of vimentin. J Biol Chem 281, 30393-30399.
Farina, F., Gaillard, J., Guérin, C., Couté, Y., Sillibourne, J., Blanchoin, L., Théry, M., 2016. The centrosome is an actin-organizing centre. Nat Cell Biol 18, 65-75.

Fedorova, E.V., Dorogova, N.V., Bolobolova, E.U., Fedorova, S.A., Karagodin, D.A., Ogienko, A.A., Khruscheva, A.S., Baricheva, E.M., 2019. GAGA protein is required for multiple aspects of Drosophila oogenesis and female fertility. Genesis 57, e23269.
Fletcher, D.A., Mullins, R.D., 2010. Cell mechanics and the cytoskeleton. Nature 463, 485-492.
Folker, E.S., Schulman, V.K., Baylies, M.K., 2012. Muscle length and myonuclear position are independently regulated by distinct Dynein pathways. Development 139, 3827-3837.
Forth, S., Hsia, K.C., Shimamoto, Y., Kapoor, T.M., 2014. Asymmetric friction of nonmotor MAPs can lead to their directional motion in active microtubule networks. Cell 157, 420-432.
Fridolfsson, H.N., Starr, D.A., 2010. Kinesin-1 and dynein at the nuclear envelope mediate the bidirectional migrations of nuclei. J Cell Biol 191, 115-128.
Fry, A.M., Sampson, J., Shak, C., Shackleton, S., 2017. Recent advances in pericentriolar material organization: ordered layers and scaffolding gels. F1000Res 6, 1622.
Fukasawa, K., 2007. Oncogenes and tumour suppressors take on centrosomes. Nat Rev Cancer 7, 911-924.
Galli, M., van den Heuvel, S., 2008. Determination of the cleavage plane in early C. elegans embryos. Annu Rev Genet 42, 389-411.
Ganem, N.J., Godinho, S.A., Pellman, D., 2009. A mechanism linking extra centrosomes to chromosomal instability. Nature 460, 278-282.
Ganguly, S., Williams, L.S., Palacios, I.M., Goldstein, R.E., 2012. Cytoplasmic streaming in Drosophila oocytes varies with kinesin activity and correlates with the microtubule cytoskeleton architecture. Proc Natl Acad Sci U S A 109, 15109-15114.
Gerlitz, G., Bustin, M., 2011. The role of chromatin structure in cell migration. Trends Cell Biol 21, 6-11.
Gindhart, J.G., Jr., Desai, C.J., Beushausen, S., Zinn, K., Goldstein, L.S., 1998. Kinesin light chains are essential for axonal transport in Drosophila. J Cell Biol 141, 443-454.
Godinho, S.A., Pellman, D., 2014. Causes and consequences of centrosome abnormalities in cancer. Philos Trans R Soc Lond B Biol Sci 369.
Godinho, S.A., Picone, R., Burute, M., Dagher, R., Su, Y., Leung, C.T., Polyak, K., Brugge, J.S., Théry, M., Pellman, D., 2014. Oncogene-like induction of cellular invasion from centrosome amplification. Nature 510, 167-171.
Goldberg, M., Lu, H., Stuurman, N., Ashery-Padan, R., Weiss, A.M., Yu, J., Bhattacharyya, D., Fisher, P.A., Gruenbaum, Y., Wolfner, M.F., 1998. Interactions among Drosophila nuclear envelope proteins lamin, otefin, and YA. Mol Cell Biol 18, 4315-4323.
Goldstein, L.S., Gunawardena, S., 2000. Flying through the drosophila cytoskeletal genome. J Cell Biol 150, F63-68.
González-Reyes, A., Elliott, H., St Johnston, D., 1995. Polarization of both major body axes in Drosophila by gurken-torpedo signalling. Nature 375, 654-658.
González-Reyes, A., St Johnston, D., 1994. Role of oocyte position in establishment of anterior-posterior polarity in Drosophila. Science 266, 639-642.
Goryunov, D., Leung, C.L., Liem, R.K., 2004. Studying cytolinker proteins. Methods Cell Biol 78, 787-816.

Gratz, S.J., Cummings, A.M., Nguyen, J.N., Hamm, D.C., Donohue, L.K., Harrison, M.M., Wildonger, J., O'Connor-Giles, K.M., 2013. Genome engineering of Drosophila with the CRISPR RNA-guided Cas9 nuclease. Genetics 194, 1029-1035.
Grieder, N.C., de Cuevas, M., Spradling, A.C., 2000. The fusome organizes the microtubule network during oocyte differentiation in Drosophila. Development 127, 4253-4264.
Grill, S.W., Howard, J., Schäffer, E., Stelzer, E.H., Hyman, A.A., 2003. The distribution of active force generators controls mitotic spindle position. Science 301, 518-521.
Gros, O.J., Damstra, H.G.J., Kapitein, L.C., Akhmanova, A., Berger, F., 2021. Dynein self-organizes while translocating the centrosome in T-cells. Mol Biol Cell 32, 855-868.
Gruenbaum, Y., Margalit, A., Goldman, R.D., Shumaker, D.K., Wilson, K.L., 2005. The nuclear lamina comes of age. Nat Rev Mol Cell Biol 6, 21-31.
Guan, Z., Prado, A., Melzig, J., Heisenberg, M., Nash, H.A., Raabe, T., 2000. Mushroom body defect, a gene involved in the control of neuroblast proliferation in Drosophila, encodes a coiled-coil protein. Proc Natl Acad Sci U S A 97, 8122-8127.
Gueth-Hallonet, C., Wang, J., Harborth, J., Weber, K., Osborn, M., 1998. Induction of a regular nuclear lattice by overexpression of NuMA. Exp Cell Res 243, 434-452.
Gueth-Hallonet, C., Weber, K., Osborn, M., 1996. NuMA: a bipartite nuclear location signal and other functional properties of the tail domain. Exp Cell Res 225, 207-218.
Guha, S., Patil, A., Muralidharan, H., Baas, P.W., 2021. Mini-review: Microtubule sliding in neurons. Neurosci Lett 753, 135867.
Guichet, A., Peri, F., Roth, S., 2001. Stable anterior anchoring of the oocyte nucleus is required to establish dorsoventral polarity of the Drosophila egg. Dev Biol 237, 93-106.
Guild, G.M., Connelly, P.S., Shaw, M.K., Tilney, L.G., 1997. Actin filament cables in Drosophila nurse cells are composed of modules that slide passively past one another during dumping. J Cell Biol 138, 783-797.
Gundersen, G.G., Worman, H.J., 2013. Nuclear positioning. Cell 152, 1376-1389.
Guo, M., Ehrlicher, A.J., Mahammad, S., Fabich, H., Jensen, M.H., Moore, J.R., Fredberg, J.J., Goldman, R.D., Weitz, D.A., 2013. The role of vimentin intermediate filaments in cortical and cytoplasmic mechanics. Biophys J 105, 1562-1568.
Guruharsha, K.G., Rual, J.F., Zhai, B., Mintseris, J., Vaidya, P., Vaidya, N., Beekman, C., Wong, C., Rhee, D.Y., Cenaj, O., McKillip, E., Shah, S., Stapleton, M., Wan, K.H., Yu, C., Parsa, B., Carlson, J.W., Chen, X., Kapadia, B., VijayRaghavan, K., Gygi, S.P., Celniker, S.E., Obar, R.A., Artavanis-Tsakonas, S., 2011. A protein complex network of Drosophila melanogaster. Cell 147, 690-703.
Gutzeit, H.O., Koppa, R., 1982. Time-lapse film analysis of cytoplasmic streaming during late oogenesis of Drosophila. Development 67, 101-111.
Habermann, K., Mirgorodskaya, E., Gobom, J., Lehmann, V., Müller, H., Blümlein, K., Deery, M.J., Czogiel, I., Erdmann, C., Ralser, M., von Kries, J.P., Lange, B.M., 2012. Functional analysis of centrosomal kinase substrates in Drosophila melanogaster reveals a new function of the nuclear envelope component otefin in cell cycle progression. Mol Cell Biol 32, 3554-3569.
Hampoelz, B., Schwarz, A., Ronchi, P., Bragulat-Teixidor, H., Tischer, C., Gaspar, I., Ephrussi, A., Schwab, Y., Beck, M., 2019. Nuclear Pores Assemble from Nucleoporin Condensates During Oogenesis. Cell 179, 671-686.e617.

Harborth, J., Wang, J., Gueth-Hallonet, C., Weber, K., Osborn, M., 1999. Self assembly of NuMA: multiarm oligomers as structural units of a nuclear lattice. Embo j 18, 1689-1700.
Haren, L., Merdes, A., 2002. Direct binding of NuMA to tubulin is mediated by a novel sequence motif in the tail domain that bundles and stabilizes microtubules. J Cell Sci 115, 1815-1824.
Hayashi, R., Wainwright, S.M., Liddell, S.J., Pinchin, S.M., Horswell, S., Ish-Horowicz, D., 2014. A genetic screen based on in vivo RNA imaging reveals centrosome-independent mechanisms for localizing gurken transcripts in Drosophila. G3 (Bethesda) 4, 749-760.
He, L., Wang, X., Montell, D.J., 2011. Shining light on Drosophila oogenesis: live imaging of egg development. Curr Opin Genet Dev 21, 612-619.
Herrmann, H., Strelkov, S.V., 2011. History and phylogeny of intermediate filaments: now in insects. BMC Biol 9, 16.
Hetzer, M.W., 2010. The nuclear envelope. Cold Spring Harb Perspect Biol 2, a000539.
Hirokawa, N., Noda, Y., Tanaka, Y., Niwa, S., 2009. Kinesin superfamily motor proteins and intracellular transport. Nat Rev Mol Cell Biol 10, 682-696.
Holaska, J.M., Wilson, K.L., 2007. An emerin "proteome": purification of distinct emerin-containing complexes from HeLa cells suggests molecular basis for diverse roles including gene regulation, mRNA splicing, signaling, mechanosensing, and nuclear architecture. Biochemistry 46, 8897-8908.
Hu, D.J., Baffet, A.D., Nayak, T., Akhmanova, A., Doye, V., Vallee, R.B., 2013. Dynein recruitment to nuclear pores activates apical nuclear migration and mitotic entry in brain progenitor cells. Cell 154, 1300-1313.
Huber, F., Boire, A., López, M.P., Koenderink, G.H., 2015. Cytoskeletal crosstalk: when three different personalities team up. Curr Opin Cell Biol 32, 39-47.
Hughes, J.R., Meireles, A.M., Fisher, K.H., Garcia, A., Antrobus, P.R., Wainman, A., Zitzmann, N., Deane, C., Ohkura, H., Wakefield, J.G., 2008. A microtubule interactome: complexes with roles in cell cycle and mitosis. PLoS Biol 6, e98.
Huynh, J.R., Shulman, J.M., Benton, R., St Johnston, D., 2001. PAR-1 is required for the maintenance of oocyte fate in Drosophila. Development 128, 1201-1209.
Huynh, J.R., St Johnston, D., 2004. The origin of asymmetry: early polarisation of the Drosophila germline cyst and oocyte. Curr Biol 14, R438-449.
Inoue, D., Obino, D., Pineau, J., Farina, F., Gaillard, J., Guerin, C., Blanchoin, L., Lennon-Duménil, A.M., Théry, M., 2019. Actin filaments regulate microtubule growth at the centrosome. Embo j 38.
Izumi, Y., Ohta, N., Hisata, K., Raabe, T., Matsuzaki, F., 2006. Drosophila Pins-binding protein Mud regulates spindle-polarity coupling and centrosome organization. Nat Cell Biol 8, 586-593.
Januschke, J., Gervais, L., Dass, S., Kaltschmidt, J.A., Lopez-Schier, H., St Johnston, D., Brand, A.H., Roth, S., Guichet, A., 2002. Polar transport in the Drosophila oocyte requires Dynein and Kinesin I cooperation. Curr Biol 12, 1971-1981.
Januschke, J., Gervais, L., Gillet, L., Keryer, G., Bornens, M., Guichet, A., 2006. The centrosome-nucleus complex and microtubule organization in the Drosophila oocyte. Development 133, 129-139.

Januschke, J., Reina, J., Llamazares, S., Bertran, T., Rossi, F., Roig, J., Gonzalez, C., 2013. Centrobin controls mother-daughter centriole asymmetry in Drosophila neuroblasts. Nat Cell Biol 15, 241-248.
Jia, D., Xu, Q., Xie, Q., Mio, W., Deng, W.M., 2016. Automatic stage identification of Drosophila egg chamber based on DAPI images. Sci Rep 6, 18850.
Jiang, X., Xia, L., Chen, D., Yang, Y., Huang, H., Yang, L., Zhao, Q., Shen, L., Wang, J., Chen, D., 2008. Otefin, a nuclear membrane protein, determines the fate of germline stem cells in Drosophila via interaction with Smad complexes. Dev Cell 14, 494-506.
Jolly, A.L., Gelfand, V.I., 2010. Cytoplasmic microtubule sliding: An unconventional function of conventional kinesin. Commun Integr Biol 3, 589-591.
Katta, S.S., Smoyer, C.J., Jaspersen, S.L., 2014. Destination: inner nuclear membrane. Trends Cell Biol 24, 221-229.
Kelliher, M.T., Yue, Y., Ng, A., Kamiyama, D., Huang, B., Verhey, K.J., Wildonger, J., 2018. Autoinhibition of kinesin-1 is essential to the dendrite-specific localization of Golgi outposts. J Cell Biol 217, 2531-2547.
Ketema, M., Kreft, M., Secades, P., Janssen, H., Sonnenberg, A., 2013. Nesprin-3 connects plectin and vimentin to the nuclear envelope of Sertoli cells but is not required for Sertoli cell function in spermatogenesis. Mol Biol Cell 24, 2454-2466.
Khuc Trong, P., Doerflinger, H., Dunkel, J., St Johnston, D., Goldstein, R.E., 2015. Cortical microtubule nucleation can organise the cytoskeleton of Drosophila oocytes to define the anteroposterior axis. Elife 4.
King, I., Tsai, L.T., Pflanz, R., Voigt, A., Lee, S., Jäckle, H., Lu, B., Heberlein, U., 2011. Drosophila tao controls mushroom body development and ethanol-stimulated behavior through par-1. J Neurosci 31, 1139-1148.
King, R.C., Rubinson, A.C., Smith, R.F., 1956. Oogenesis in adult Drosophila melanogaster. Growth 20, 121-157.
Kivinen, K., Taimen, P., Kallajoki, M., 2010. Silencing of Nuclear Mitotic Apparatus protein (NuMA) accelerates the apoptotic disintegration of the nucleus. Apoptosis 15, 936-945.
Kiyomitsu, T., Boerner, S., 2021. The Nuclear Mitotic Apparatus (NuMA) Protein: A Key Player for Nuclear Formation, Spindle Assembly, and Spindle Positioning. Front Cell Dev Biol 9, 653801.
Koch, E.A., King, R.C., 1966. The origin and early differentiation of the egg chamber of Drosophila melanogaster. J Morphol 119, 283-303.
Koch, E.A., Smith, P.A., King, R.C., 1967. The division and differentiation of Drosophila cystocytes. J Morphol 121, 55-70.
Koch, E.A., Spitzer, R.H., 1983. Multiple effects of colchicine on oogenesis in Drosophila: induced sterility and switch of potential oocyte to nurse-cell developmental pathway. Cell Tissue Res 228, 21-32.
Kotak, S., 2019. Mechanisms of Spindle Positioning: Lessons from Worms and Mammalian Cells. Biomolecules 9.
Kracklauer, M.P., Banks, S.M., Xie, X., Wu, Y., Fischer, J.A., 2007. Drosophila klaroid encodes a SUN domain protein required for Klarsicht localization to the nuclear envelope and nuclear migration in the eye. Fly (Austin) 1, 75-85.

Kwon, M., Godinho, S.A., Chandhok, N.S., Ganem, N.J., Azioune, A., Thery, M., Pellman, D., 2008. Mechanisms to suppress multipolar divisions in cancer cells with extra centrosomes. Genes Dev 22, 2189-2203.
Lantz, V., Chang, J.S., Horabin, J.I., Bopp, D., Schedl, P., 1994. The Drosophila orb RNA-binding protein is required for the formation of the egg chamber and establishment of polarity. Genes Dev 8, 598-613.
Lebo, D.P.V., McCall, K., 2021. Murder on the Ovarian Express: A Tale of Non-Autonomous Cell Death in the Drosophila Ovary. Cells 10.
Legent, K., Tissot, N., Guichet, A., 2015. Visualizing Microtubule Networks During Drosophila Oogenesis Using Fixed and Live Imaging. Methods Mol Biol 1328, 99-112.
Lei, K., Zhang, X., Ding, X., Guo, X., Chen, M., Zhu, B., Xu, T., Zhuang, Y., Xu, R., Han, M., 2009. SUN1 and SUN2 play critical but partially redundant roles in anchoring nuclei in skeletal muscle cells in mice. Proc Natl Acad Sci U S A 106, 10207-10212.
Lei, K., Zhu, X., Xu, R., Shao, C., Xu, T., Zhuang, Y., Han, M., 2012. Inner nuclear envelope proteins SUN1 and SUN2 play a prominent role in the DNA damage response. Curr Biol 22, 1609-1615.
Lin, H., Spradling, A.C., 1993. Germline stem cell division and egg chamber development in transplanted Drosophila germaria. Dev Biol 159, 140-152.
Lin, H., Spradling, A.C., 1995. Fusome asymmetry and oocyte determination in Drosophila. Dev Genet 16, 6-12.
Lindeman, R.E., Pelegri, F., 2012. Localized products of futile cycle/lrmp promote centrosome-nucleus attachment in the zebrafish zygote. Curr Biol 22, 843-851.
Liu, Q., Pante, N., Misteli, T., Elsagga, M., Crisp, M., Hodzic, D., Burke, B., Roux, K.J., 2007. Functional association of Sun1 with nuclear pore complexes. J Cell Biol 178, 785-798.
Liu, T., Rohn, J.L., Picone, R., Kunda, P., Baum, B., 2010. Tao-1 is a negative regulator of microtubule plus-end growth. J Cell Sci 123, 2708-2716.
Loh, M., Dauvet, D., Sanchez-Garrido, F., Sadaouli, K., Bernard, F., Guichet, A., 2022. Kinesin-1 promotes centrosome clustering and nuclear migration in the Drosophila oocyte. bioRxiv, 2022.2002.2016.480671.
Loh, M., Guichet, A., Bernard, F., 2021. Nuclear Migration in the Drosophila Oocyte. J Vis Exp.
Lu, J., Wu, T., Zhang, B., Liu, S., Song, W., Qiao, J., Ruan, H., 2021. Types of nuclear localization signals and mechanisms of protein import into the nucleus. Cell Commun Signal 19, 60.
Lu, W., Lakonishok, M., Serpinskaya, A.S., Gelfand, V.I., 2022. A novel mechanism of bulk cytoplasmic transport by cortical dynein in Drosophila ovary. Elife 11.
Lu, W., Winding, M., Lakonishok, M., Wildonger, J., Gelfand, V.I., 2016. Microtubule-microtubule sliding by kinesin-1 is essential for normal cytoplasmic streaming in Drosophila oocytes. Proc Natl Acad Sci U S A 113, E4995-5004.
Lyakhovetsky, R., Gruenbaum, Y., 2014. Studying lamins in invertebrate models. Adv Exp Med Biol 773, 245-262.
Lydersen, B.K., Pettijohn, D.E., 1980. Human-specific nuclear protein that associates with the polar region of the mitotic apparatus: distribution in a human/hamster hybrid cell. Cell 22, 489-499.

Mahowald, A.P., Strassheim, J.M., 1970. Intercellular migration of centrioles in the germarium of Drosophila melanogaster. An electron microscopic study. J Cell Biol 45, 306-320.
Marthiens, V., Basto, R., 2020. Centrosomes: The good and the bad for brain development. Biol Cell 112, 153-172.
McDonough-Goldstein, C.E., Borziak, K., Pitnick, S., Dorus, S., 2021. Drosophila female reproductive tract gene expression reveals coordinated mating responses and rapidly evolving tissue-specific genes. G3 (Bethesda) 11.
McGrail, M., Hays, T.S., 1997. The microtubule motor cytoplasmic dynein is required for spindle orientation during germline cell divisions and oocyte differentiation in Drosophila. Development 124, 2409-2419.
McKenney, R.J., Huynh, W., Tanenbaum, M.E., Bhabha, G., Vale, R.D., 2014. Activation of cytoplasmic dynein motility by dynactin-cargo adapter complexes. Science 345, 337-341.
McNally, K.L., Martin, J.L., Ellefson, M., McNally, F.J., 2010. Kinesin-dependent transport results in polarized migration of the nucleus in oocytes and inward movement of yolk granules in meiotic embryos. Dev Biol 339, 126-140.
Megraw, T.L., Kaufman, T.C., 2000. The centrosome in Drosophila oocyte development. Curr Top Dev Biol 49, 385-407.
Meinke, P., Mattioli, E., Haque, F., Antoku, S., Columbaro, M., Straatman, K.R., Worman, H.J., Gundersen, G.G., Lattanzi, G., Wehnert, M., Shackleton, S., 2014. Muscular dystrophy-associated SUN1 and SUN2 variants disrupt nuclear-cytoskeletal connections and myonuclear organization. PLoS Genet 10, e1004605.
Mencarelli, C., Ciolfi, S., Caroti, D., Lupetti, P., Dallai, R., 2011. Isomin: a novel cytoplasmic intermediate filament protein from an arthropod species. BMC Biol 9, 17.
Merdes, A., Cleveland, D.W., 1998. The role of NuMA in the interphase nucleus. J Cell Sci 111 (Pt 1), 71-79.
Merdes, A., Ramyar, K., Vechio, J.D., Cleveland, D.W., 1996. A complex of NuMA and cytoplasmic dynein is essential for mitotic spindle assembly. Cell 87, 447-458.
Metivier, M., Monroy, B.Y., Gallaud, E., Caous, R., Pascal, A., Richard-Parpaillon, L., Guichet, A., Ori-McKenney, K.M., Giet, R., 2019. Dual control of Kinesin-1 recruitment to microtubules by Ensconsin in Drosophila neuroblasts and oocytes. Development 146.
Metzger, T., Gache, V., Xu, M., Cadot, B., Folker, E.S., Richardson, B.E., Gomes, E.R., Baylies, M.K., 2012. MAP and kinesin-dependent nuclear positioning is required for skeletal muscle function. Nature 484, 120-124.
Milas, A., Telley, I.A., 2022. Polarity Events in the Drosophila melanogaster Oocyte. Front Cell Dev Biol 10, 895876.
Mislow, J.M., Holaska, J.M., Kim, M.S., Lee, K.K., Segura-Totten, M., Wilson, K.L., McNally, E.M., 2002. Nesprin-1alpha self-associates and binds directly to emerin and lamin A in vitro. FEBS Lett 525, 135-140.
Molines, A.T., Lemière, J., Gazzola, M., Steinmark, I.E., Edrington, C.H., Hsu, C.T., Real-Calderon, P., Suhling, K., Goshima, G., Holt, L.J., Thery, M., Brouhard, G.J., Chang, F., 2022. Physical properties of the cytoplasm modulate the rates of microtubule polymerization and depolymerization. Dev Cell 57, 466-479.e466.

Morimoto, A., Shibuya, H., Zhu, X., Kim, J., Ishiguro, K., Han, M., Watanabe, Y., 2012. A conserved KASH domain protein associates with telomeres, SUN1, and dynactin during mammalian meiosis. J Cell Biol 198, 165-172.
Muroyama, A., Lechler, T., 2017. Microtubule organization, dynamics and functions in differentiated cells. Development 144, 3012-3021.
Muroyama, A., Seldin, L., Lechler, T., 2016. Divergent regulation of functionally distinct γ-tubulin complexes during differentiation. J Cell Biol 213, 679-692.
Murray, M.E., Mendez, M.G., Janmey, P.A., 2014. Substrate stiffness regulates solubility of cellular vimentin. Mol Biol Cell 25, 87-94.
Nashchekin, D., Busby, L., Jakobs, M., Squires, I., St Johnston, D., 2021. Symmetry breaking in the female germline cyst. Science 374, 874-879.
Nashchekin, D., Fernandes, A.R., St Johnston, D., 2016. Patronin/Shot Cortical Foci Assemble the Noncentrosomal Microtubule Array that Specifies the Drosophila Anterior-Posterior Axis. Dev Cell 38, 61-72.
Navarro-Costa, P., McCarthy, A., Prudencio, P., Greer, C., Guilgur, L.G., Becker, J.D., Secombe, J., Rangan, P., Martinho, R.G., 2016. Early programming of the oocyte epigenome temporally controls late prophase I transcription and chromatin remodelling. Nat Commun 7, 12331.
Neuman-Silberberg, F.S., Schupbach, T., 1994. Dorsoventral axis formation in Drosophila depends on the correct dosage of the gene gurken. Development 120, 2457-2463.
Nguyen Ba, A.N., Pogoutse, A., Provart, N., Moses, A.M., 2009. NLStradamus: a simple Hidden Markov Model for nuclear localization signal prediction. BMC Bioinformatics 10, 202.
Nüsslein-Volhard, C., Frohnhöfer, H.G., Lehmann, R., 1987. Determination of anteroposterior polarity in Drosophila. Science 238, 1675-1681.
Obino, D., Farina, F., Malbec, O., Sáez, P.J., Maurin, M., Gaillard, J., Dingli, F., Loew, D., Gautreau, A., Yuseff, M.I., Blanchoin, L., Théry, M., Lennon-Duménil, A.M., 2016. Actin nucleation at the centrosome controls lymphocyte polarity. Nat Commun 7, 10969.
Palacios, I.M., St Johnston, D., 2001. Getting the message across: the intracellular localization of mRNAs in higher eukaryotes. Annu Rev Cell Dev Biol 17, 569-614.
Palacios, I.M., St Johnston, D., 2002. Kinesin light chain-independent function of the Kinesin heavy chain in cytoplasmic streaming and posterior localisation in the Drosophila oocyte. Development 129, 5473-5485.
Pałka, M., Tomczak, A., Grabowska, K., Machowska, M., Piekarowicz, K., Rzepecka, D., Rzepecki, R., 2018. Laminopathies: what can humans learn from fruit flies. Cell Mol Biol Lett 23, 32.
Parisi, M., Nuttall, R., Edwards, P., Minor, J., Naiman, D., Lü, J., Doctolero, M., Vainer, M., Chan, C., Malley, J., Eastman, S., Oliver, B., 2004. A survey of ovary-, testis-, and soma-biased gene expression in Drosophila melanogaster adults. Genome Biol 5, R40.
Parton, R.M., Hamilton, R.S., Ball, G., Yang, L., Cullen, C.F., Lu, W., Ohkura, H., Davis, I., 2011. A PAR-1-dependent orientation gradient of dynamic microtubules directs posterior cargo transport in the Drosophila oocyte. J Cell Biol 194, 121-135.

Patterson, K., Molofsky, A.B., Robinson, C., Acosta, S., Cater, C., Fischer, J.A., 2004. The functions of Klarsicht and nuclear lamin in developmentally regulated nuclear migrations of photoreceptor cells in the Drosophila eye. Mol Biol Cell 15, 600-610.
Patteson, A.E., Vahabikashi, A., Goldman, R.D., Janmey, P.A., 2020. Mechanical and Non-Mechanical Functions of Filamentous and Non-Filamentous Vimentin. Bioessays 42, e2000078.
Patteson, A.E., Vahabikashi, A., Pogoda, K., Adam, S.A., Mandal, K., Kittisopikul, M., Sivagurunathan, S., Goldman, A., Goldman, R.D., Janmey, P.A., 2019. Vimentin protects cells against nuclear rupture and DNA damage during migration. J Cell Biol 218, 4079-4092.
Peri, F., Roth, S., 2000. Combined activities of Gurken and decapentaplegic specify dorsal chorion structures of the Drosophila egg. Development 127, 841-850.
Peter, A., Stick, R., 2012. Evolution of the lamin protein family: what introns can tell. Nucleus 3, 44-59.
Petry, S., Vale, R.D., 2015. Microtubule nucleation at the centrosome and beyond. Nat Cell Biol 17, 1089-1093.
Pimenta-Marques, A., Bento, I., Lopes, C.A., Duarte, P., Jana, S.C., Bettencourt-Dias, M., 2016. A mechanism for the elimination of the female gamete centrosome in Drosophila melanogaster. Science 353, aaf4866.
Pimenta-Marques, A., Bettencourt-Dias, M., 2020. Pericentriolar material. Curr Biol 30, R687-r689.
Pimenta-Marques, A., Perestrelo, T., Rodrigues, P., Duarte, P., Lince-Faria, M., Bettencourt-Dias, M., 2022. Ana1/CEP295 is an essential player in the centrosome maintenance program regulated by Polo kinase. bioRxiv, 2022.2004.2006.487296.
Pollard, V.W., Michael, W.M., Nakielny, S., Siomi, M.C., Wang, F., Dreyfuss, G., 1996. A novel receptor-mediated nuclear protein import pathway. Cell 86, 985-994.
Poon, C.L., Mitchell, K.A., Kondo, S., Cheng, L.Y., Harvey, K.F., 2016. The Hippo Pathway Regulates Neuroblasts and Brain Size in Drosophila melanogaster. Curr Biol 26, 1034-1042.
Prokocimer, M., Davidovich, M., Nissim-Rafinia, M., Wiesel-Motiuk, N., Bar, D.Z., Barkan, R., Meshorer, E., Gruenbaum, Y., 2009. Nuclear lamins: key regulators of nuclear structure and activities. J Cell Mol Med 13, 1059-1085.
Quan, Y., Ji, Z.L., Wang, X., Tartakoff, A.M., Tao, T., 2008. Evolutionary and transcriptional analysis of karyopherin beta superfamily proteins. Mol Cell Proteomics 7, 1254-1269.
Quintyne, N.J., Reing, J.E., Hoffelder, D.R., Gollin, S.M., Saunders, W.S., 2005. Spindle multipolarity is prevented by centrosomal clustering. Science 307, 127-129.
Raab, M.S., Breitkreutz, I., Anderhub, S., Rønnest, M.H., Leber, B., Larsen, T.O., Weiz, L., Konotop, G., Hayden, P.J., Podar, K., Fruehauf, J., Nissen, F., Mier, W., Haberkorn, U., Ho, A.D., Goldschmidt, H., Anderson, K.C., Clausen, M.H., Krämer, A., 2012. GF-15, a novel inhibitor of centrosomal clustering, suppresses tumor cell growth in vitro and in vivo. Cancer Res 72, 5374-5385.
Radulescu, A.E., Cleveland, D.W., 2010. NuMA after 30 years: the matrix revisited. Trends Cell Biol 20, 214-222.
Rajeevan, A., Keshri, R., Kapoor, S., Kotak, S., 2020. NuMA interaction with chromatin is vital for proper chromosome decondensation at the mitotic exit. Mol Biol Cell 31, 2437-2451.

Razin, S.V., Iarovaia, O.V., Vassetzky, Y.S., 2014. A requiem to the nuclear matrix: from a controversial concept to 3D organization of the nucleus. Chromosoma 123, 217-224.
Rebacz, B., Larsen, T.O., Clausen, M.H., Rønnest, M.H., Löffler, H., Ho, A.D., Krämer, A., 2007. Identification of griseofulvin as an inhibitor of centrosomal clustering in a phenotype-based screen. Cancer Res 67, 6342-6350.
Reck-Peterson, S.L., Redwine, W.B., Vale, R.D., Carter, A.P., 2018. The cytoplasmic dynein transport machinery and its many cargoes. Nat Rev Mol Cell Biol 19, 382-398.
Rhys, A.D., Godinho, S.A., 2017. Dividing with Extra Centrosomes: A Double Edged Sword for Cancer Cells. Adv Exp Med Biol 1002, 47-67.
Ribbeck, K., Görlich, D., 2001. Kinetic analysis of translocation through nuclear pore complexes. Embo j 20, 1320-1330.
Riechmann, V., Ephrussi, A., 2001. Axis formation during Drosophila oogenesis. Curr Opin Genet Dev 11, 374-383.
Riparbelli, M.G., Persico, V., Callaini, G., 2021. Early Drosophila Oogenesis: A Tale of Centriolar Asymmetry. Cells 10.
Roth, S., 2003. The origin of dorsoventral polarity in Drosophila. Philos Trans R Soc Lond B Biol Sci 358, 1317-1329; discussion 1329.
Roth, S., Jordan, P., Karess, R., 1999. Binuclear Drosophila oocytes: consequences and implications for dorsal-ventral patterning in oogenesis and embryogenesis. Development 126, 927-934.
Roth, S., Lynch, J.A., 2009. Symmetry breaking during Drosophila oogenesis. Cold Spring Harb Perspect Biol 1, a001891.
Roux, K.J., Crisp, M.L., Liu, Q., Kim, D., Kozlov, S., Stewart, C.L., Burke, B., 2009. Nesprin 4 is an outer nuclear membrane protein that can induce kinesin-mediated cell polarization. Proc Natl Acad Sci U S A 106, 2194-2199.
Rubin, G.M., Yandell, M.D., Wortman, J.R., Gabor Miklos, G.L., Nelson, C.R., Hariharan, I.K., Fortini, M.E., Li, P.W., Apweiler, R., Fleischmann, W., Cherry, J.M., Henikoff, S., Skupski, M.P., Misra, S., Ashburner, M., Birney, E., Boguski, M.S., Brody, T., Brokstein, P., Celniker, S.E., Chervitz, S.A., Coates, D., Cravchik, A., Gabrielian, A., Galle, R.F., Gelbart, W.M., George, R.A., Goldstein, L.S., Gong, F., Guan, P., Harris, N.L., Hay, B.A., Hoskins, R.A., Li, J., Li, Z., Hynes, R.O., Jones, S.J., Kuehl, P.M., Lemaitre, B., Littleton, J.T., Morrison, D.K., Mungall, C., O'Farrell, P.H., Pickeral, O.K., Shue, C., Vosshall, L.B., Zhang, J., Zhao, Q., Zheng, X.H., Lewis, S., 2000. Comparative genomics of the eukaryotes. Science 287, 2204-2215.
Salina, D., Bodoor, K., Eckley, D.M., Schroer, T.A., Rattner, J.B., Burke, B., 2002. Cytoplasmic dynein as a facilitator of nuclear envelope breakdown. Cell 108, 97-107.
Salpingidou, G., Smertenko, A., Hausmanowa-Petrucewicz, I., Hussey, P.J., Hutchison, C.J., 2007. A novel role for the nuclear membrane protein emerin in association of the centrosome to the outer nuclear membrane. J Cell Biol 178, 897-904.
Saredi, A., Howard, L., Compton, D.A., 1996. NuMA assembles into an extensive filamentous structure when expressed in the cell cytoplasm. J Cell Sci 109 (Pt 3), 619-630.
Schliwa, M., Euteneuer, U., Gräf, R., Ueda, M., 1999. Centrosomes, microtubules and cell migration. Biochem Soc Symp 65, 223-231.

Schoborg, T.A., Rusan, N.M., 2016. Taking Centrioles to the Elimination Round. Dev Cell 38, 10-12.
Schoumacher, M., Goldman, R.D., Louvard, D., Vignjevic, D.M., 2010. Actin, microtubules, and vimentin intermediate filaments cooperate for elongation of invadopodia. J Cell Biol 189, 541-556.
Schüpbach, T., 1987. Germ line and soma cooperate during oogenesis to establish the dorsoventral pattern of egg shell and embryo in Drosophila melanogaster. Cell 49, 699-707.
Serebryannyy, L., de Lanerolle, P., 2020. Nuclear actin: The new normal. Mutat Res 821, 111714.
Serra-Marques, A., Houtekamer, R., Hintzen, D., Canty, J.T., Yildiz, A., Dumont, S., 2020. The mitotic protein NuMA plays a spindle-independent role in nuclear formation and mechanics. J Cell Biol 219.
Serres, M.P., Samwer, M., Truong Quang, B.A., Lavoie, G., Perera, U., Görlich, D., Charras, G., Petronczki, M., Roux, P.P., Paluch, E.K., 2020. F-Actin Interactome Reveals Vimentin as a Key Regulator of Actin Organization and Cell Mechanics in Mitosis. Dev Cell 52, 210-222.e217.
Siegrist, S.E., Doe, C.Q., 2006. Extrinsic cues orient the cell division axis in Drosophila embryonic neuroblasts. Development 133, 529-536.
Siller, K.H., Cabernard, C., Doe, C.Q., 2006. The NuMA-related Mud protein binds Pins and regulates spindle orientation in Drosophila neuroblasts. Nat Cell Biol 8, 594-600.
Simon, D.N., Wilson, K.L., 2011. The nucleoskeleton as a genome-associated dynamic 'network of networks'. Nat Rev Mol Cell Biol 12, 695-708.
Simon, D.N., Zastrow, M.S., Wilson, K.L., 2010. Direct actin binding to A- and B-type lamin tails and actin filament bundling by the lamin A tail. Nucleus 1, 264-272.
Smith, D.E., Gruenbaum, Y., Berrios, M., Fisher, P.A., 1987. Biosynthesis and interconversion of Drosophila nuclear lamin isoforms during normal growth and in response to heat shock. J Cell Biol 105, 771-790.
Sosa, B.A., Kutay, U., Schwartz, T.U., 2013. Structural insights into LINC complexes. Curr Opin Struct Biol 23, 285-291.
Sosa, B.A., Rothballer, A., Kutay, U., Schwartz, T.U., 2012. LINC complexes form by binding of three KASH peptides to domain interfaces of trimeric SUN proteins. Cell 149, 1035-1047.
Splinter, D., Razafsky, D.S., Schlager, M.A., Serra-Marques, A., Grigoriev, I., Demmers, J., Keijzer, N., Jiang, K., Poser, I., Hyman, A.A., Hoogenraad, C.C., King, S.J., Akhmanova, A., 2012. BICD2, dynactin, and LIS1 cooperate in regulating dynein recruitment to cellular structures. Mol Biol Cell 23, 4226-4241.
Splinter, D., Tanenbaum, M.E., Lindqvist, A., Jaarsma, D., Flotho, A., Yu, K.L., Grigoriev, I., Engelsma, D., Haasdijk, E.D., Keijzer, N., Demmers, J., Fornerod, M., Melchior, F., Hoogenraad, C.C., Medema, R.H., Akhmanova, A., 2010. Bicaudal D2, dynein, and kinesin-1 associate with nuclear pore complexes and regulate centrosome and nuclear positioning during mitotic entry. PLoS Biol 8, e1000350.
Srinivasan, D.G., Fisk, R.M., Xu, H., van den Heuvel, S., 2003. A complex of LIN-5 and GPR proteins regulates G protein signaling and spindle function in C elegans. Genes Dev 17, 1225-1239.
Starr, D.A., Han, M., 2003. ANChors away: an actin based mechanism of nuclear positioning. J Cell Sci 116, 211-216.

Stevens, N.R., Raposo, A.A., Basto, R., St Johnston, D., Raff, J.W., 2007. From stem cell to embryo without centrioles. Curr Biol 17, 1498-1503.
Strambio-De-Castillia, C., Niepel, M., Rout, M.P., 2010. The nuclear pore complex: bridging nuclear transport and gene regulation. Nat Rev Mol Cell Biol 11, 490-501.
Sun, J., Deng, W.M., 2007. Hindsight mediates the role of notch in suppressing hedgehog signaling and cell proliferation. Dev Cell 12, 431-442.
Sung, H.H., Telley, I.A., Papadaki, P., Ephrussi, A., Surrey, T., Rørth, P., 2008. Drosophila ensconsin promotes productive recruitment of Kinesin-1 to microtubules. Dev Cell 15, 866-876.
Tang, T.K., Tang, C.J., Chen, Y.L., Wu, C.W., 1993. Nuclear proteins of the bovine esophageal epithelium. II. The NuMA gene gives rise to multiple mRNAs and gene products reactive with monoclonal antibody W1. J Cell Sci 104 (Pt 2), 249-260.
Tassin, A.M., Maro, B., Bornens, M., 1985. Fate of microtubule-organizing centers during myogenesis in vitro. J Cell Biol 100, 35-46.
Tavosanis, G., Llamazares, S., Goulielmos, G., Gonzalez, C., 1997. Essential role for gamma-tubulin in the acentriolar female meiotic spindle of Drosophila. Embo j 16, 1809-1819.
Technau, M., Roth, S., 2008. The Drosophila KASH domain proteins Msp-300 and Klarsicht and the SUN domain protein Klaroid have no essential function during oogenesis. Fly (Austin) 2, 82-91.
Theurkauf, W.E., Alberts, B.M., Jan, Y.N., Jongens, T.A., 1993. A central role for microtubules in the differentiation of Drosophila oocytes. Development 118, 1169-1180.
Theurkauf, W.E., Smiley, S., Wong, M.L., Alberts, B.M., 1992. Reorganization of the cytoskeleton during Drosophila oogenesis: implications for axis specification and intercellular transport. Development 115, 923-936.
Tikhonenko, I., Magidson, V., Gräf, R., Khodjakov, A., Koonce, M.P., 2013. A kinesin-mediated mechanism that couples centrosomes to nuclei. Cell Mol Life Sci 70, 1285-1296.
Tirián, L., Timinszky, G., Szabad, J., 2003. P446L-importin-beta inhibits nuclear envelope assembly by sequestering nuclear envelope assembly factors to the microtubules. Eur J Cell Biol 82, 351-359.
Tissot, N., Lepesant, J.A., Bernard, F., Legent, K., Bosveld, F., Martin, C., Faklaris, O., Bellaiche, Y., Coppey, M., Guichet, A., 2017. Distinct molecular cues ensure a robust microtubule-dependent nuclear positioning in the Drosophila oocyte. Nat Commun 8, 15168.
Tran, P.T., Marsh, L., Doye, V., Inoué, S., Chang, F., 2001. A mechanism for nuclear positioning in fission yeast based on microtubule pushing. J Cell Biol 153, 397-411.
Trieselmann, N., Wilde, A., 2002. Ran localizes around the microtubule spindle in vivo during mitosis in Drosophila embryos. Curr Biol 12, 1124-1129.
Trokter, M., Mücke, N., Surrey, T., 2012. Reconstitution of the human cytoplasmic dynein complex. Proc Natl Acad Sci U S A 109, 20895-20900.
Tsai, J.W., Lian, W.N., Kemal, S., Kriegstein, A.R., Vallee, R.B., 2010. Kinesin 3 and cytoplasmic dynein mediate interkinetic nuclear migration in neural stem cells. Nat Neurosci 13, 1463-1471.
Tsai, L.H., Gleeson, J.G., 2005. Nucleokinesis in neuronal migration. Neuron 46, 383-388.
van der Voet, M., Berends, C.W., Perreault, A., Nguyen-Ngoc, T., Gönczy, P., Vidal, M., Boxem, M., van den Heuvel, S., 2009. NuMA-related LIN-5, ASPM-1, calmodulin and dynein promote meiotic spindle rotation independently of cortical LIN-5/GPR/Galpha. Nat Cell Biol 11, 269-277.

Venken, K.J., Bellen, H.J., 2007. Transgenesis upgrades for Drosophila melanogaster. Development 134, 3571-3584.
Verhey, K.J., Kaul, N., Soppina, V., 2011. Kinesin assembly and movement in cells. Annu Rev Biophys 40, 267-288.
Vinogradova, T., Miller, P.M., Kaverina, I., 2009. Microtubule network asymmetry in motile cells: role of Golgi-derived array. Cell Cycle 8, 2168-2174.
Wagner, N., Krohne, G., 2007. LEM-Domain proteins: new insights into lamin-interacting proteins. Int Rev Cytol 261, 1-46.
Wee, B., Johnston, C.A., Prehoda, K.E., Doe, C.Q., 2011. Canoe binds RanGTP to promote Pins(TPR)/Mud-mediated spindle orientation. J Cell Biol 195, 369-376.
Wilhelmsen, K., Litjens, S.H., Kuikman, I., Tshimbalanga, N., Janssen, H., van den Bout, I., Raymond, K., Sonnenberg, A., 2005. Nesprin-3, a novel outer nuclear membrane protein, associates with the cytoskeletal linker protein plectin. J Cell Biol 171, 799-810.
Wilson, M.H., Holzbaur, E.L., 2015. Nesprins anchor kinesin-1 motors to the nucleus to drive nuclear distribution in muscle cells. Development 142, 218-228.
Wilson, P.G., Zheng, Y., Oakley, C.E., Oakley, B.R., Borisy, G.G., Fuller, M.T., 1997. Differential expression of two gamma-tubulin isoforms during gametogenesis and development in Drosophila. Dev Biol 184, 207-221.
Winding, M., Kelliher, M.T., Lu, W., Wildonger, J., Gelfand, V.I., 2016. Role of kinesin-1-based microtubule sliding in Drosophila nervous system development. Proc Natl Acad Sci U S A 113, E4985-4994.
Wong-Riley, M.T., Besharse, J.C., 2012. The kinesin superfamily protein KIF17: one protein with many functions. Biomol Concepts 3, 267-282.
Wu, J., Akhmanova, A., 2017. Microtubule-Organizing Centers. Annu Rev Cell Dev Biol 33, 51-75.
Xie, J., Najafi, J., Le Borgne, R., Verbavatz, J.M., Durieu, C., Sallé, J., Minc, N., 2022. Contribution of cytoplasm viscoelastic properties to mitotic spindle positioning. Proc Natl Acad Sci U S A 119.
Yang, C.H., Lambie, E.J., Snyder, M., 1992. NuMA: an unusually long coiled-coil related protein in the mammalian nucleus. J Cell Biol 116, 1303-1317.
Yang, R., Feldman, J.L., 2015. SPD-2/CEP192 and CDK Are Limiting for Microtubule-Organizing Center Function at the Centrosome. Curr Biol 25, 1924-1931.
Yin, L.M., Schnoor, M., Jun, C.D., 2020. Structural Characteristics, Binding Partners and Related Diseases of the Calponin Homology (CH) Domain. Front Cell Dev Biol 8, 342.
Yu, J.X., Guan, Z., Nash, H.A., 2006. The mushroom body defect gene product is an essential component of the meiosis II spindle apparatus in Drosophila oocytes. Genetics 173, 243-253.
Zeng, C., 2000. NuMA: a nuclear protein involved in mitotic centrosome function. Microsc Res Tech 49, 467-477.
Zeng, C., He, D., Brinkley, B.R., 1994. Localization of NuMA protein isoforms in the nuclear matrix of mammalian cells. Cell Motil Cytoskeleton 29, 167-176.
Zhang, Q., Ragnauth, C.D., Skepper, J.N., Worth, N.F., Warren, D.T., Roberts, R.G., Weissberg, P.L., Ellis, J.A., Shanahan, C.M., 2005. Nesprin-2 is a multi-isomeric protein that binds lamin and emerin at the nuclear envelope and forms a subcellular network in skeletal muscle. J Cell Sci 118, 673-687.

Zhang, X., Lei, K., Yuan, X., Wu, X., Zhuang, Y., Xu, T., Xu, R., Han, M., 2009. SUN1/2 and Syne/Nesprin-1/2 complexes connect centrosome to the nucleus during neurogenesis and neuronal migration in mice. Neuron 64, 173-187.
Zhao, T., Graham, O.S., Raposo, A., St Johnston, D., 2012. Growing microtubules push the oocyte nucleus to polarize the Drosophila dorsal-ventral axis. Science 336, 999-1003.
Zheng, R., Ghirlando, R., Lee, M.S., Mizuuchi, K., Krause, M., Craigie, R., 2000. Barrier-to-autointegration factor (BAF) bridges DNA in a discrete, higher-order nucleoprotein complex. Proc Natl Acad Sci U S A 97, 8997-9002.
Zheng, Y., Jung, M.K., Oakley, B.R., 1991. Gamma-tubulin is present in Drosophila melanogaster and Homo sapiens and is associated with the centrosome. Cell 65, 817-823.